The Semi-Classical Sine-Gordon Equation, Universality at the Gradient Catastrophe and the Painlevé-I Equation

by

Bingying Lu

A dissertation submitted in partial fulfillment
of the requirements for the degree of
Doctor of Philosophy
(Mathematics)
in the University of Michigan
2018

Doctoral Committee:

Professor Peter Miller, Chair
Professor Jinho Baik
Professor Charles Doering
Professor Herbert Winful
Professor Sijue Wu

Bingying Lu

bylu@umich.edu

ORCID iD: 0000-0001-6918-7211

Dedication

To Lemur[1], Lexie, Leeway and Lu Wu

[1]https://en.wikipedia.org/wiki/Lemur. A clade of strepsirrhine primates endemic to the island of Madagascar.

Acknowledgements

I want to thank everyone who made this thesis possible, in particular, my cheerful best friends, especially Wei Li, for their moral support; my gloomy best friends for listening to my existential anguish (many of them overlap); my parents for their unquestioning support of my daydreams; people I met in graduate school who taught me maths and otherwise; Mathematica for usually reliably converging to one answer after four to ten tries; Christian Klein who generously provided a Matlab code to help us visualise the solutions and pointed out that I can dive into cab driving business if mathematics ever not work out for me; Liming Ling for teaching me to find and plot rogue wave solutions; Guilherme Silva for teaching me how to generate videos in TEX; Samantha Xu who gave me a beamer template with a lemur—I left beamer but the lemur stayed; Songdi Fan for proofreading and attempting to add 500 determiners to my thesis (and th-fronting the word thesis); Wei Li (again!) for helping me with formatting; the very patient committee members for their guidance; and my advisor Peter Miller: I was convinced from the very beginning that he had worked out my thesis in the back of his mind but just wouldn't tell me the answer.

Table of Contents

Dedication ii

Acknowledgements iii

List of Figures viii

Abstract x

Chapter

1 Introduction 1

1.1 sine-Gordon equation (sG) 1

1.2 Semi-classical sine-Gordon equation 3

1.3 Universality 6

1.4 Whitham modulation system for sG 10

1.5 Results and outline of the thesis 11

2 Fluxon condensates for librational Cauchy data and Riemann-Hilbert problem 15

2.1 Lax pair and inverse scattering transform for the semi-classical sG Cauchy problem 15

2.2 Initial data and the corresponding fluxon condensate 17

2.3 The Riemann-Hilbert problem for librational fluxon condensates 21

2.4 Removing Poles of **H** 23

2.5 The equivalent Riemann-Hilbert Problem for **M** 24

2.6 Notes on small time 30

3 Asymptotic behavior of fluxon condensates before the gradient catastrophe 32

3.1 The g-function and the Deift-Zhou steepest descent method 32
3.1.1 Introducing the g-function 33
3.1.2 Desired properties of g 35
3.1.3 The scalar RH problem for $g(w)$ 38
3.1.4 Constructing the g-function 38
3.1.5 Rewriting the formula for f 40
3.1.6 Constructing the desired properties of g, introducing M, H and I . 44
3.1.7 Other properties of g 48
3.1.8 Determining $w_0(x,t)$ and $w_1(x,t)$ 49
3.1.9 Qualitative behaviour of ϕ and the solution to sine-Gordon equation, numerical examples 50
3.2 Symmetries at $x = 0$ before the gradient catastrophe 52
3.2.1 θ^0 symmetry 52
3.2.2 H symmetry 55
3.3 Parametrix construction before breaking 55
3.3.1 Global parametrix 55
3.3.2 The outer parametrix 57
3.3.3 Inner parametrix 61
3.3.4 Error 62

4 Modifying the g-function near the gradient catastrophe 64
4.1 Modifying g 66
4.1.1 Defining $\mathfrak{f}$ 67
4.1.2 Analogues of $M \equiv 0$ and $I \equiv 0$, $\mathfrak{M} \equiv 0$ and $\mathfrak{I} \equiv 0$ 68
4.1.3 Eliminating the parameters m and n 69
4.2 φ expansion 70
4.2.1 Picking branches for the square roots 71
4.2.2 Computing the expansion coefficients of φ 72
4.2.3 At the gradient catastrophe point, $C_1 = C_3 = 0$ snd $C_5 \neq 0$ 73
4.3 Theorem 0: conformal coordinates near $\mathfrak{w}_0$ and $\mathfrak{w}_1$ 75
4.3.1 Branch of ρ_k^{gc} 77
4.3.2 Differentiating with respect to x and t 78
4.3.3 Simplifying the integrals 80
4.3.4 Evaluating $\det(\mathfrak{G})$ 82
4.3.5 Evaluating $W^0_{i\mathfrak{w}_j}$ 83
4.3.6 $\det W^0_{i\mathfrak{w}_j} \neq 0$ 85

4.3.7 Computing $\partial_x s_0$, $\partial_x s_1$, $\partial_x \mathfrak{w}_0$, $\partial_x \mathfrak{w}_1$ . . . 87
4.3.8 The interchangeability of x, t derivatives . . . 88
4.3.9 Schwarz symmetry . . . 89
4.3.10 Solution at the gradient catastrophe . . . 89
4.3.11 Formal expansion . . . 90

5 Theorem 1: away from the poles **92**
5.1 Statement of theorem 1 . . . 92
5.2 Tritronquée Parametrix . . . 93
5.2.1 Standard Painlevé I Riemann–Hilbert problem . . . 93
5.2.2 Painlevé-I Riemann–Hilbert problem . . . 94
5.2.3 Diagonalizing the jump . . . 95
5.2.4 Power series expansion . . . 96
5.2.5 Ridding of the phase: constant jump Riemann-Hilbert problem . . . 97
5.2.6 Solving $\mathbf{L}$ . . . 98
5.2.7 $\mathbf{A}$ and $\mathbf{U}$ Expansions . . . 98
5.2.8 Compatibility Condition . . . 100
5.2.9 Differential Equations . . . 101
5.2.10 Hamiltonian . . . 104
5.2.11 Expansion of $\mathbf{T}$ . . . 105
5.3 First correction at the gradient catastrophe . . . 106
5.3.1 Small norm problem . . . 106
5.3.2 z-plane and symmetry . . . 106
5.3.3 Inner parametrix and the tritronquée parametrix . . . 109
5.3.4 The local behaviour of $\dot{\mathbf{O}}^{\text{out}}$ . . . 110
5.3.5 Error Parametrix . . . 111
5.3.6 Error Estimate . . . 113

6 Theorem 2: near the poles **117**
6.1 Statement of theorem 2 . . . 117
6.2 Modifying the inner parametrix . . . 118
6.2.1 Schlesinger transformation . . . 118
6.2.2 $\widetilde{\mathbf{T}}\mathbf{M}\zeta^{-3\frac{\sigma_3}{4}}$ is regular near the poles . . . 119
6.3 Bäcklund transformation, modifying the outer parametrix . . . 120
6.3.1 Error matrix . . . 120
6.3.2 Riemann–Hilbert problem for $\mathbf{G}$ . . . 123

6.3.3 Scaling near the poles . . . 123
6.3.4 Riemann–Hilbert problem for **G** . . . 124
6.3.5 Fredholm theory, vanishing lemma and the existence of the solution to Riemann–Hilbert problem 3 . . . 124
6.4 Shape of local structures, solution near the poles . . . 126
6.4.1 Solving **G**, shape of local structures . . . 126

7 Conclusion **131**
7.1 Future work . . . 131
7.1.1 Soliton solution to the sine-Gordon equation at poles of the tritronquée solution . . . 131
7.1.2 Universality of the asymptotic profile at the first breaking curve for the semi-classical sine-Gordon equation . . . 132
7.1.3 Breaking curves, asymmetrical initial data . . . 132

Bibliography **133**

List of Figures

1.1 Mechanical model for sine-Gordon equation from [4] 2
1.2 Numerical demonstration of the universality behaviour for semi-classical sine-Gordon equation with various initial conditions, $\epsilon = 0.05$. 7
1.3 Left: poles of tritronquée from [31] 11

2.1 Introducing regions Ω_+, Ω_- and contours Σ_+, Σ_- 24
2.2 Jump for l 25
2.3 Jump for m 26
2.4 Jump contour for L_N^0 26
2.5 L^0 jump contour along with the contours $\Sigma_\pm$ 28
2.6 Avoiding 1. Introducing additional regions and moving the contour to approach 1 from $\mathbb{R}$. 29
2.7 Zoom in the jump contours near 1, introducing $\Sigma_{1_\pm}$ 31

3.1 Opening a lens 36
3.2 $\mathrm{Re}(i\theta)$ sign 37
3.3 R and β 39
3.4 C_β 40
3.5 The three curves C_1, C_β and C_∞ 41
3.6 γ_0 43
3.7 Contour C 44
3.8 $g(\infty)$ contour of integration 46
3.9 $x = 0.2$, $G(x) = -\mathrm{sech}(x)$. The green region denotes $\mathrm{Re}(\phi) < 0$, while red is where $\mathrm{Re}(\phi) > 0$. 50
3.10 g breaking curve 51
3.11 $x = 0$, $G(x) = -\mathrm{sech}(x)$ 51
3.12 Initial condition $G(x)$ and $x_+(\lambda)$, $x_-(\lambda)$ 53

3.13 Picture of function $G^2(s) + 16\lambda^2 = B^2(s;\lambda)$, which has two zeros at $x_+(\lambda)$ and $x_-(\lambda)$. 53
3.14 Loop L clockwise enclosing $x_+(\lambda)$ and $x_-(\lambda)$ 53
3.15 Contour C when $x = 0$ 54
3.16 Symmetry: deformation of C overlapping β and the arc of the unit circle . 54
3.17 Riemann–Hilbert problem for the global parmetrix 56
3.18 Jump for the outer parametrix 58
3.19 The homology basis on X, loop a and b 60
3.20 Airy parametrix 62
3.21 Jumps for $\mathcal{E}$ 63

4.1 Comparing zoomed-in pictures near w_0 at a generic point and at the gradient catastrophe point 64
4.2 Branch cuts for S_0 and S_1 71
4.3 The local picture of β, the unit circle, and local sign chart of $\mathrm{Re}(\phi)$. The checkerboard region denotes positive $\mathrm{Re}(\phi)$; the green region denotes negative $\mathrm{Re}(\phi)$. 78

5.1 The Painlevé-I parametrix 93
5.2 **L** jump contour 97
5.3 The jump contours for the outer parametrix on β and $\mathbb{R}_+$ are mapped to $\tilde{\beta}$ 107
5.4 **P** jump contour 108
5.5 Inner parametrix mapped to the Painlevé variable 110
5.6 Jump for **F** 112

6.1 **F** has more significant jump on the boundary of the four disks 121

Abstract

This thesis concerns the semi-classical sine-Gordon equation with pure impulse initial data below the threshold of rotation:

$$\epsilon^2 u_{tt} - \epsilon^2 u_{xx} + \sin u = 0,$$
$$u(x,0) \equiv 0, \quad \epsilon u_t(x,0) = G(x) \leq 0, \quad \text{and} \quad |G(0)| < 2.$$

We consider a wide class of solutions that decays at infinity. A dispersively-regularized shock forms in finite time. We study the universality of the solutions near a certain catastrophe point. In accordance with a conjecture by Dubrovin et al. [26] on Hamiltonian perturbations near the gradient catastrophe point of an elliptic system, we found that the asymptotics of the sine-Gordon solution is described by the tritronquée solution to the Painlevé-I equation. Furthermore, we are able to describe the local peak-like structures corresponing to where the tritronquée solution, well-known to have singularities, fails to describe the asymptotics. Our result is universal in the sense that the local asymptotics is not sensitive to the initial conditions as long as it falls into a large class of functions; it is only the space-time location of the transition that depends on the initial data. Our main tool is the Riemann–Hilbert technique for integrable systems, in particular the Deift–Zhou steepest descent method [23]. The approach is inspired by the work of Bertola-Tovbis [8] on the focusing NLS equation.

Chapter 1

Introduction

This thesis concerns the study of universal phenomena in wave propagation. The specific aspect of this topic that is of interest to us is the formation, in certain general classes of models or in specific models but from certain general types of initial data, of *universal wave patterns*. These are mathematical descriptions of evolving waves, frequently in terms of special functions, that become relevant in certain well-defined asymptotic regimes. For instance, one may think of the wake generated by a ship, and viewed at some large distance from it, taking a universal form independent of the details of the ship generating the wake.

To use rigorous analysis to prove the existence of universal wave patterns, it is useful to work in the context of models for wave motion that are mathematically tractable. In this thesis, we work with one such model that is in the class of completely integrable nonlinear partial differential equations, namely the sine-Gordon equation.

1.1 sine-Gordon equation (sG)

The sine-Gordon equation (sG) is an important and well-known nonlinear wave model. First of all, it is a universal model for dispersive waves with periodic nonlinearity. It arises in a wide range of applications. The equation was first discovered in characteristic form [9] in the 1860s as the Gauss-Codazzi conditions for surfaces of constant negative curvature in 3-space,

$$u_{\eta\xi} = \sin u. \tag{1.1}$$

In 1939 Frenkel and Kontorova [32] studied a discrete model in the theory of crystal dislocations that can be approximated by the sG equation in space-time form,

$$u_{tt} - u_{xx} + \sin u = 0. \tag{1.2}$$

A mechanical analogue of this model by A.C. Scott has been proven extremely useful for visualization and experimental observations of its solutions. It is realized by taking the continuum limit of an array of pendulums subject to gravity and coupled to their nearest neighbors via Hooke's law (torsion-coupled pendulums), see figure 1.1.

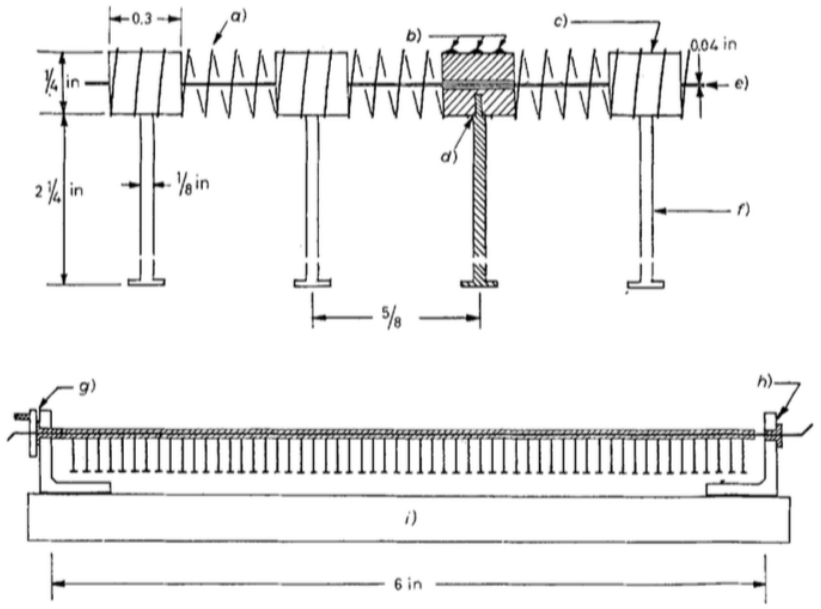

Fig. 3. – Mechanical model of the SGE: *a*) spring 0.2 diameter, *b*) solder, *c*) brass, *d*) tap and thread, *e*) piano wire, *f*) nail, *g*) and *h*) ball bearings, *i*) wooden base.

Figure 1.1: Mechanical model for sine-Gordon equation from [4]

Other appearances include modeling the transverse magnetic flux in superconducting Josephson junctions in the zero dissipation limit [43], the study of breathers, the propagation of deformation in the DNA double helix [47], the orbits of a string of stars near the inner Lindblad resonance within a galaxy, Coleman identified the solitons of sine-Gordon equation as the fundamental fermions in massive Thirring model [19], among others. For more details, we refer the readers to the 1971 classic [4], as well as more modern treatments of the topic summarised in [21].

Another reason that the sine-Gordon equation is a particularly interesting model is because of its integrability. In 1970s, the 1-D sine-Gordon model was found to be one of the very few nonlinear equations that are completely integrable in the Inverse Scattering Transform (IST) theory [2, 29]. Thus the solution to this equation can be described in great detail via the IST tools, which should be regarded as specialized analogues for nonlinear integrable equations of Fourier transform methods for linear equations. In fact, sine-Gordon, among others such as the Korteweg–de Vries (KdV) equation and cubic nonlinear-Schrödinger

(NLS) equation are the only few simple and fundamental nonlinear equations that are integrable [1]. That is not to say that the number of integrable equations is small. In fact, even the aforementioned three examples are all the first ones in a countably infinite family (or *hierarchy*) of equations. They arise as Hamiltonian flows with infinitely many conservation laws associated with infinitely many commuting symmetries. This remarkable structure is a common feature of numerous integrable systems. And there are many other known families besides the three listed here. That being said, within the class of nonlinear PDEs, integrability must be regarded as a rare phenomenon.

In this thesis, we exploit highly-specialized techniques associated with the sine-Gordon equation as a completely integrable system, leveraging them to study a certain universal wave pattern. Such techniques are generally not available for generic nonlinear wave equations, but they will allow us to obtain very precise results in the present setting. In particular, we will study the Riemann–Hilbert problem associated to the sine-Gordon equation, one of the most powerful tools to analyze the inverse scattering problem.

1.2 Semi-classical sine-Gordon equation

The terminology semi-classical in mathematical physics often refers to the Bohr correspondence principle: in the limit $\hbar \to 0$, quantum mechanics should become consistent with classical mechanics.

As mentioned above, one may expect universal wave patterns to appear in certain asymptotic limits, and as such, this thesis will be concerned with a semi-classical version of (1.2):

$$\epsilon^2 u_{tt} - \epsilon^2 u_{xx} + \sin u = 0, \tag{1.3}$$

with semi-classical initial conditions

$$u(x, 0; \epsilon) = F(x), \quad \epsilon u_t(x, 0; \epsilon) = G(x). \tag{1.4}$$

The problem we are considering is the *semi-classical Cauchy problem*, where $u(x, t; \epsilon)$ should be seen as a one-parameter family of solutions, with the initial data F, G independent of ϵ. We care most about the asymptotics of this family of solutions in the limit $\epsilon \to 0$, which is an analogue of the Bohr limit $\hbar \to 0$.

It is a well-known fact that the elementary excitations of the sine-Gordon equation are kinks, antikinks and breathers, see [2, 29, 35] for the inverse scattering theory for sG solitons. In semi-classical scaling, such solutions have width in x proportional to ϵ. In

general if $F(x) \to 2\pi n_\pm$ and $G(x) \to 0$ sufficiently fast as $x \to \pm\infty$, where $n_\pm$ are integers ($n_+ - n_-$ is the *topological charge*), the solution to the Cauchy problem (1.3)-(1.4) can be viewed (through the lens of the IST) as the combined effect of kinks, antikinks, breathers and radiation. The initial condition F and G in (1.4) being independent of ϵ suggests that approximately $1/\epsilon$ solitons of width ϵ will be excited. Before the ensemble of solitons break apart, the ones closer to each other will travel at similar speeds, thus forming a wavetrain.

One motivation to study the semi-classical limit of this equation can be found in physics. In the idealized model of long superconducting *Josephson junctions*, the parameter ϵ is the ratio of the Josephson length l_J to the transmission line length. In one such laboratory experiment, Scott, Chu, Reible [43] studied the magnetic flux in a Josephson junction of length $l_0 = 35\ cm$ with l_J approximately 10^{-4} to $10^{-3}\ m$, hence $\epsilon \approx 0.0005$. The particle-like magnetic flux corresponding to solitons in the sine-Gordon solution are called fluxons in the Josephson junctions. In accordance with the previous discussion of soliton numbers, when ϵ is small, $\mathcal{O}(1/\epsilon)$ number of fluxons will be excited. In this case, the semi-classical limit corresponds to a larger number of particles in ensembles thus resulting in a classical effect.

It is interesting to point out that in the Thirring model, the small parameter ϵ has the exact same quantum–classical interpretation as the Planck constant $\hbar$ being small. In [19], Coleman explained β^2 (same as ϵ^2 for our equation) has the same effect as $\hbar$ in the semi-classical asymptotics. Therefore small ϵ corresponds to many fundamental particles excited.

Notice that as in the Schrödinger equation, the small parameter ϵ can be scaled into the variables. If we take

$$x = \epsilon X, \quad t = \epsilon T, \tag{1.5}$$

then the initial-value problem (1.3)-(1.4) becomes

$$\begin{aligned} u_{TT} - u_{XX} + \sin u = 0, \\ u(X,0) = F(\epsilon X), \quad u_T(x,0) = G(\epsilon X). \end{aligned} \tag{1.6}$$

In this reformulation, the differential equation is again the unscaled form (1.2), but the initial data is dependent on ϵ. Taking ϵ smaller and smaller in this context means $u(X,0;\epsilon)$, $u_t(X,0;\epsilon)$ are slowly-varying in X. Equivalently, in form (1.6), the $\mathcal{O}(1/\epsilon)$ number of $\mathcal{O}(1)$ size solitons combine to form a structure of characteristic length proportional to $1/\epsilon$ across the X-axis.

A third way we can write the semi-classical initial-value problem (1.3)-(1.4) is to rescale

t as in (1.5) but retain x as the independent variable:

$$u_{TT} + \sin(u) = \epsilon^2 u_{xx}, \quad u(x,0) = F(x), \quad u_T(x,0) = G(x). \tag{1.7}$$

This scaling suggests neglecting $\epsilon^2 u_{xx}$ as a small perturbation, in which case the sine-Gordon PDE reduces to an independent ODE for each value of $x \in \mathbb{R}$. In undergraduate courses on differential equations one learns that the solution of the unperturbed problem (the simple pendulum) is of a different character depending on whether the total energy $E(x) := \frac{1}{2}u_T(x,T)^2 + (1 - \cos(u(x,T))) \geq 0$, which is independent of T for the unperturbed problem, is less than 2 (the *librational case*, where the pendulum swings back and forth) or greater than 2 (the *rotational case*, where the pendulum rotates around its pivot point). The borderline case $E(x) = 2$ characterizes the separatrix in the phase portrait and the corresponding motions are homoclinic orbits representing the nonlinear saturation of the linearized instability of the unstable vertical equilibrium configuration of the pendulum. It turns out that when $\epsilon > 0$ is small, the solutions of the sine-Gordon equation exhibit a similar dichotomy at least for a certain range of T, and interestingly the behavior can be different for different values of x because it is possible for smooth initial conditions $F(x)$ and $G(x)$ to give rise to librational motion for some x and rotational motion for other x.

In [12, 13], a family of solutions $u(x,t;\epsilon)$ closely related to the solution of the Cauchy problem for the sine-Gordon equation in the form (1.3)-(1.4) was studied under the assumption that the initial conditions of the system induced rotational motion for $|x| < L$ and librational motion for $|x| > L$. In [13] the family of solutions was shown to closely approximate the given initial conditions in the limit $\epsilon \to 0$, and in [12], the authors identified a certain type of universal wave pattern appearing for small time near the transition points $x = \pm L$.

This thesis concerns the less-energetic case, in which $E(x) < 2$ holds for all $x \in \mathbb{R}$. Thus the system is globally below threshold for rotation in the sense of the unperturbed simple pendulum problem. While this may seem at first to be less interesting, in fact we shall uncover a new universal wave pattern in this case that locally resolves a kind of focusing of pendulum energy near a certain point x at a positive time t.

Our approach is inspired by Bertola and Tovbis. Their approach uses a Riemann–Hilbert problem associated with the NLS equation. The sine-Gordon equation adds significant new challenges in the analysis, because the solution before catastrophe are described by theta-function of genus 1 Riemann surface, as opposed to genus 0 in NLS.

1.3 Universality

Dubrovin et al. conjectured in [25, 26] that for weakly dispersive Hamiltonian systems considered as perturbations of elliptic and hyperbolic first order systems, universal behaviours appear near the gradient catastrophe points of solutions of the unperturbed system in a weak-dispersion limit that is mathematically very similar to a semi-classical limit. By formally expanding the Hamiltonian perturbation, it is argued that for suitable initial conditions, the asymptotics of the solution near the catastrophe point are described by particular solutions to the Painlevé-I equation (elliptic case) or the second equation in the Painlevé-I hierarchy (hyperbolic case).

This conjecture for the hyperbolic case was first rigorously studied in the example of the weakly dispersive KdV equation

$$u_t - 6uu_x + \epsilon^2 u_{xxx} = 0 \tag{1.8}$$

by Claeys and Grava in [17], where they took advantage of the complete integrability of the KdV equation and successfully combined rigorous asymptotics for the direct scattering problem with steepest descent techniques for the Riemann-Hilbert problem of inverse scattering to rigorously prove the universality conjecture with respect to initial data. On the other hand, the conjecture for the elliptic case was first studied in [8] by Bertola and Tovbis for the focusing NLS equation. Again their work employed the integrability of the NLS equation, but since the direct scattering problem is less well-understood than in the KdV case, the authors had to settle for a rigorous analysis of a wide class of solutions that were not directly connected with given Cauchy data.

Some attempts to prove special cases of the conjecture without using complete integrability (near integrable cases) are made in [27]. However, the proof of the full conjecture, which asserts universality both with respect to initial data and (more strongly) with respect to the equation of motion, remains open.

Some numerical evidence of the universality phenomenon in this thesis for sine-Gordon with various initial conditions can be seen in figure 1.2. The numerical code to generate these pictures was generously provided by Christian Klein. The picture looks similar in all four cases pictured in the vicinity of the point where the waves appear to focus.

Since it is the case most relevant to this thesis, we give here some more details about the conjecture of Dubrovin et al. in the elliptic case [25], and its justification in the case of the focusing NLS equation by Bertola and Tovbis [4]. The semi-classical focusing NLS

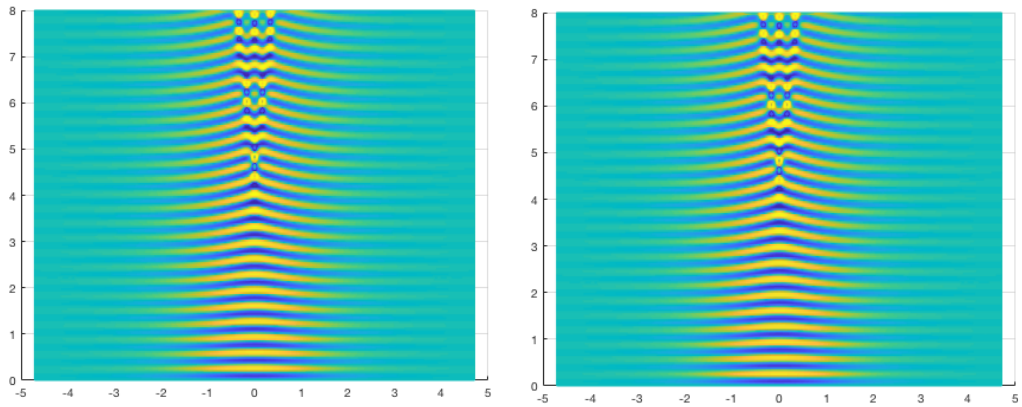

(a) $G(x) = -\exp(-x^2)$ (b) $G(x) = -\text{sech}(x)$

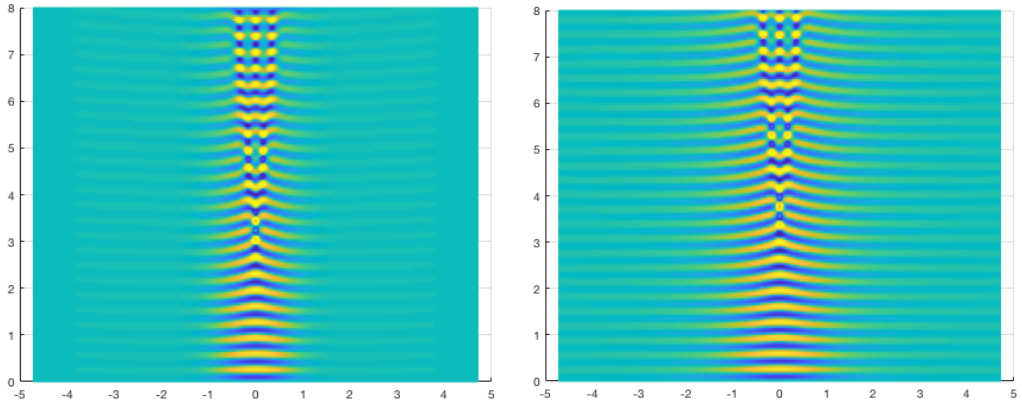

(c) $G(x) = -\exp(-x^2)\text{sech}(x)$ (d) $G(x) = -\frac{1}{1+x^2}$

Figure 1.2: Numerical demonstration of the universality behaviour for semi-classical sine-Gordon equation with various initial conditions, $\epsilon = 0.05$.

equation

$$i\epsilon\psi_t + \frac{1}{2}\epsilon^2\psi_{xx} + |\psi|^2\psi = 0 \tag{1.9}$$

can be easily recast as a weakly-dispersive perturbation of a first-order quasilinear system through the *Madelung transform* $\psi(x,t) = \sqrt{\rho(x,t)}e^{iS(x,t)/\epsilon}$, where $\rho > 0$ is the amplitude and $S \in \mathbb{R}$ is the phase. Letting $\mu := A^2 S_x$ denote the momentum density, the focusing NLS equation (1.9) can be written in terms of the real variables ρ and μ as a coupled system:

$$\rho_t + \mu_x = 0 \quad \text{and} \quad \mu_t + \left[\frac{\mu^2}{\rho} - \frac{1}{2}\rho^2\right]_x = \frac{1}{4}\epsilon^2\left[\rho(\log(\rho))_x\right]_x . \tag{1.10}$$

The terms proportional to ϵ^2 represent a weakly dispersive correction to a quasilinear system of conservation laws that is easily checked to be elliptic by a simple computation of the characteristic velocities. If the dispersive terms are neglected and the dispersionless

equation is solved with analytic initial data on ρ and μ, a certain typical singularity called an elliptic umbilic catastrophe (also gradient catastrophe) occurs generically in the solution at a certain point $x = x_{\text{gc}} \in \mathbb{R}$ at a certain breaking time $t = t_{\text{gc}} \in \mathbb{R}$, the subscript gc denotes gradient catastrophe. The conjecture of [26] asserts that in a neighborhood of an elliptic umbilic catastrophe point of the unperturbed system, the dispersive terms generate a subleading correction to the solution of the full problem that is written in terms of a special function $Y(\nu)$ solving the Painlevé-I equation

$$Y''(\nu) = -6Y(\nu)^2 + \nu \tag{1.11}$$

known as a *tritronquée* solution. This solution is distinguished by the property that it behaves like $Y(\nu) \sim \sqrt{\nu/6}$ as $\nu \to \infty$ in a maximally wide sector: $4\pi/5 < \arg(\nu) < 11\pi/5$. However within the complementary sector of opening angle $2\pi/5$, the solution has infinitely many double poles (and their confinement to the indicated sector is not just asymptotic near $\nu = \infty$ but exact according to recent work of Costin, Huang, and Tanveer [20]). In support of the conjecture of [26], Bertola and Tovbis proved the following result, in which H denotes the Hamiltonian of Y

$$H = -2Y(\nu)^3 - \frac{Y'(\nu)^2}{2} + Y(\nu)\nu. \tag{1.12}$$

In particular this theorem describes $\psi(x,t)$ in a shrinking neighbourhood of $(x_{\text{gc}}, t_{\text{gc}})$, with radius $\sim \epsilon^{\frac{4}{5}}$. Inside the neighbourhood (x,t) will also be bounded away from points corresponding to the poles of the tritronquée solution. The cut out disks also scale like $\epsilon^{\frac{4}{5}}$.

Theorem 1.3.1 (Bertola and Tovbis, [8])**.** *There exists a mapping $s : \mathbb{R}^2 \to \mathbb{C}$ taking $(x_{\text{gc}}, t_{\text{gc}})$ to 0, with $e^{-i\pi/5}s_x$ positive real and $e^{-i\pi/5}s_t$ purely imaginary at the catastrophe point, such that the following is true. Suppose that with $\nu := s(x,t)/\epsilon^{4/5}$, $|\nu| < M$ and $|Y(\nu)| < M$ for some $M > 0$ independent of ϵ, then*

$$\begin{aligned}\psi(x,t) =& b\left[1 - 2\epsilon^{\frac{2}{5}}\operatorname{Im}\left(\frac{Y(\nu)}{Cb}\right) + \mathcal{O}(\epsilon^{\frac{3}{5}})\right] \\ &\times \exp\frac{i}{\epsilon}\left[S(x_{\text{gc}}, t_{\text{gc}}) - 2(a\Delta x + (2a^2 - b^2)\Delta t) + 2\epsilon^{\frac{6}{5}}\operatorname{Re}\left(\sqrt{\frac{2i}{Cb}}H(\nu)\right)\right].\end{aligned} \tag{1.13}$$

Here $a := -\frac{1}{2}S_x(x_{\text{gc}}, t_{\text{gc}})$, $b := \sqrt{\rho(x_{\text{gc}}, t_{\text{gc}})}$, $C := \left(\frac{5C_1}{4}\right)^{\frac{2}{5}}$, C_1 is a well-defined coefficient in the fraction expansion of a phase function (details not important here), $Y(\nu)$ is the aforementioned tritronquée solution of Painlevé-I and H is its Hamiltonian.

This estimation fails when ν is near the poles of the Y, where "spikes" form in the fNLS equation. The "spikes" are discussed in detail in the next theorem. The condition $|Y(\nu)|< M$ makes sure the theorem to work 'away from spikes", i.e., ν remains uniformly bounded away from the poles of the tritronquée solution.

Due to the double pole singularities of $Y(\nu)$, the conjecture of [26] makes no statement about the accuracy of the approximation in the sector containing the poles. However, the reader will see that Theorem 1.3.1 also gives the accuracy of the same approximate formula for (x,t) in the image of the tritronquée pole sector, provided one also avoids small neighbourhoods of each of the poles. Zooming in on a neighbourhood of a typical pole of $Y(\nu)$, Bertola and Tovbis were also able to characterize the solution $\psi(x,t)$ of (1.9) near the image of the pole. They found that locally $|\psi(x,t)|$ has a peaked amplitude which resembles a "spike". They obtained the following result:

Theorem 1.3.2 (Bertola and Tovbis, [8])**.** *In the same domain near the gradient catastrophe but instead close to the poles of the tritronquée solution:*

- *The mapping $\nu = s(x_p,t_p)/\epsilon^{\frac{4}{5}} : \mathbb{R}^2 \to \mathbb{C}$ defines a one-to-one correspondence between the poles of the tritronquée solution ν_p and spikes of the NLS solution, centered at its preimages (x_p,t_p),*

- *The shape of each spike is universally described by*

$$\psi(x,t) = e^{\frac{i}{\epsilon}S(x_p,t_p)} Q_{\mathrm{br}}\left(\frac{x-x_p}{\epsilon}, \frac{t-t_p}{\epsilon}\right)(1+\mathcal{O}(\epsilon^{\frac{1}{5}})), \tag{1.14}$$

  for $|x-x_p|$ and $|t-t_p|$ both bounded by $\mathcal{O}(\epsilon)$. Here Q_{br} denotes the rational breather (Peregrine breather solution) of the NLS equation in the from $iQ_\eta + \frac{1}{2}Q_{\xi\xi} + |Q|^2Q = 0$,

$$Q_{\mathrm{br}}(\xi,\eta) = e^{-2i(a\xi+(2a^2-b^2)\eta)} b\left(1 - 4\frac{1+4ib^2\eta}{1+4b^2(\xi+4a\eta)^2+16b^4\eta^2}\right). \tag{1.15}$$

  Equation (1.15) *implies the each spike has 3 times the amplitude of the background.*

This is an important result because it describes the field $\psi(x,t)$ near points where the conjecture of [26] is not effective because the approximation blows up while the solution $\psi(x,t)$ itself remains bounded.

1.4 Whitham modulation system for sG

It is the Whitham modulation system for the sine-Gordon equation that acts as the unperturbed system which gives rise to the *elliptic umbilic catastrophe* point in the perturbation of the elliptic system case in accordance with the Dubrovin–Grava–Klein conjecture in [26].

Taking the averaging idea from [46], assume the solution to (1.3) forms a modulated periodic wavetrain of period 2π,

$$\begin{gathered} u(x,t) = U\left(\frac{\Phi(x,t)}{\epsilon}\right), \qquad \Phi(x,t) = kx - \omega t, \\ \text{and} \quad U(\zeta + 2\pi) = U(\zeta), \end{gathered} \tag{1.16}$$

where k is the wave number and ω is frequency of the wavetrain.

Integrate once to

$$\frac{1}{2}(\omega^2 - k^2)\left(\frac{\mathrm{d}U}{\mathrm{d}\zeta}\right)^2 - \cos(U) = \mathcal{E}. \tag{1.17}$$

Here $\mathcal{E}$ is the integration constant that has the physical meaning of energy. Another physical quantity of interest is the *phase velocity* v_p,

$$v_p = \frac{\omega}{k}. \tag{1.18}$$

The Lagrangian density of the semi-classical sine-Gordon equation is given by

$$L[u] := \frac{1}{2}\epsilon^2 u_t^2 - \left(\frac{1}{2}\epsilon^2 u_x^2 - \cos(u)\right), \tag{1.19}$$

and the sG equation is the result of the variational principle. Substitute $U\left(\dfrac{kx-\omega t}{\epsilon}\right)$ and then take average of L over one period, denoted by $\langle L\rangle$. View $\langle L\rangle$ as a functional of $\mathcal{E}$ and θ, with

$$k = \theta_x, \quad \text{and} \quad \omega = \theta_t. \tag{1.20}$$

One can then apply the *averaged variational principle* on $\langle L\rangle$, with respect to the functions $\mathcal{E}$ and θ. This will lead us to a linear system for $\mathcal{E}$ and $n_p = \frac{1}{v_p}$ (the reciprocal is just for eliminating a singularity of the modulation equation that does not fundamentally change the system otherwise) called the *Whitham modulation system*. The Whitham modulation

equation for the sine-Gordon equation takes the form

$$\frac{\partial}{\partial t}\begin{bmatrix} n_p \\ \mathcal{E} \end{bmatrix} + \mathcal{A}(n_p, \mathcal{E})\frac{\partial}{\partial x}\begin{bmatrix} n_p \\ \mathcal{E} \end{bmatrix} = \mathbf{0}, \tag{1.21}$$

where $\mathcal{A}(n_p, \mathcal{E})$ is a known 2×2 matrix whose elements are certain elliptic integrals. The system (1.21) is the correct dispersionless system corresponding to the sine-Gordon equation in the sense of the Dubrovin universality theory. One can show that the system (1.21) is elliptic for librational wave solutions, and hyperbolic for rotational wave solutions. As mentioned above, this thesis concerns the dynamics of the Cauchy problem (1.3)-(1.4) in the situation that the initial data gives $E(x) < 2$ for all x, so the problem is globally below the threshold for rotation, hence the dispersionless problem (1.21) is in the elliptic case. In accordance with Dubrovin et al.'s conjecture in [25] and [26], we have found that it is the tritronquée solution of the Painlevé-I transcendent and its modification at the poles that describe the asymptotics near the point of gradient catastrophe for (1.21) when $\epsilon > 0$ is small.

Our work provides a new example of universality near the elliptic umbilic catastrophe that has not been studied before. To our knowledge, after the work of Bertola-Tovbis for the focusing NLS [8], this is only the second rigorously studied example for the elliptic case of the aforementioned universality conjecture.

1.5 Results and outline of the thesis

Figure 1.3 is an illustration of how the poles of tritronquée solution is related to the solution of the sine-Gordon equation in our main results. Notice that the pole location picture is

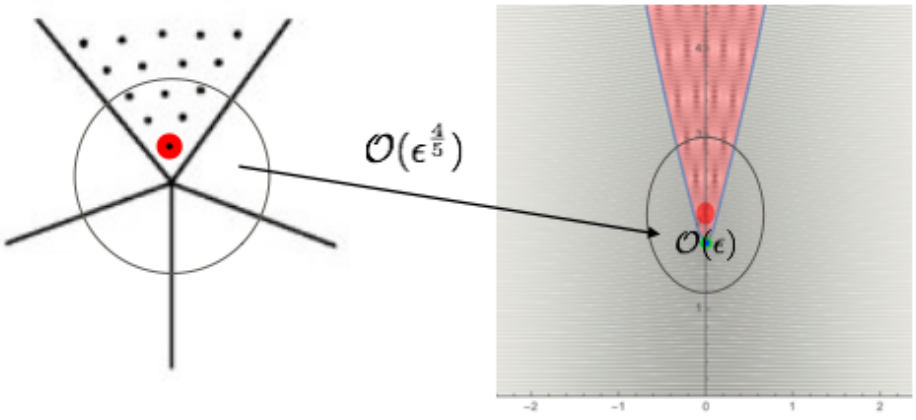

Figure 1.3: Left: poles of tritronquée from [31]

rotated to showcase the correspondence of poles and the local structures. In the left figure, the vertical line pointing downward is the x-axis. In fact, the picture of PI tritronquée solution from [31] is not quite what we used either. For their tritronquée solution, the pole-free sector is $-\frac{4\pi}{5} < \arg\nu < \frac{4\pi}{5}$. However, the two solutions are related by a simple transformation and the relative pole locations are exactly the same.

Theorem 1.5.1 (First correction near the gradient catastrophe away from poles of the Painlevé-I tritronquée solution)**.**

Let $u_N(x,t)$ be the fluxon condensate associated with suitable Cauchy data (1.4)*, for which the elliptic system* (1.21) *exhibits an elliptic umbilic catastrophe point at $(x,t) = (x_{\rm gc} = 0, t_{\rm gc})$. Then there exists a real-analytic univalent mapping $s : \mathbb{R}^2 \to \mathbb{C}$ defined on a neighbourhood of the catastrophe point, such that the following is true. Supposing that $\nu := s/\epsilon^{\frac{4}{5}}$, $|\nu| < M$ and $|Y(\nu)| < M$ for some constant $M > 0$ independent of ϵ, then the following asymptotic formulæ hold:*

$$\begin{aligned}\cos(\tfrac{1}{2}u_N(x,t)) =& \dot{C} + \epsilon^{\frac{1}{5}}\left(\mathcal{E}^{(1)}_{11}\dot{C} + \mathcal{E}^{(1)}_{12}\dot{S}\right) + \mathcal{O}(\epsilon^{\frac{2}{5}}),\\ \sin(\tfrac{1}{2}u_N(x,t)) =& \dot{S} + \epsilon^{\frac{1}{5}}\left(\mathcal{E}^{(1)}_{21}\dot{C} + \mathcal{E}^{(1)}_{22}\dot{S}\right) + \mathcal{O}(\epsilon^{\frac{2}{5}}).\end{aligned} \tag{1.22}$$

The exact expressions of $\dot{C}$ and $\dot{S}$ are given by (3.97) *and* (3.98)*, and the first correction matrix $\mathcal{E}^1$ is given by*

$$\begin{aligned}\mathcal{E}^1 =& \left(\frac{1}{-z_0^{\rm gc}} \frac{1}{2z_0^{\rm gc} W'(w_0^{\rm gc})} \mathbf{C}(w_0^{\rm gc}) \begin{bmatrix} 0 & H(\nu) \\ 0 & 0 \end{bmatrix} \mathbf{C}(w_0^{\rm gc})^{-1} \right.\\ &+ \frac{1}{-z_0^{\rm gc*}} \frac{1}{2z_0^{\rm gc*} W'(w_0^{\rm gc})^*} \sigma_2 \mathbf{C}(w_0^{\rm gc})^* \begin{bmatrix} 0 & H(\nu)^* \\ 0 & 0 \end{bmatrix} \mathbf{C}(w_0^{\rm gc})^{*-1} \sigma_2\\ &- \frac{1}{z_0^{\rm gc}} \frac{1}{2z_0^{\rm gc} W'(w_0^{\rm gc})} \sigma_2 \mathbf{C}(w_0^{\rm gc}) \begin{bmatrix} 0 & H(\nu) \\ 0 & 0 \end{bmatrix} \mathbf{C}(w_0^{\rm gc})^{-1} \sigma_2\\ &\left. - \frac{1}{z_0^{\rm gc*}} \frac{1}{2z_0^{\rm gc*} W'(w_0^{\rm gc})^*} \mathbf{C}(w_0^{\rm gc})^* \begin{bmatrix} 0 & H(\nu)^* \\ 0 & 0 \end{bmatrix} \mathbf{C}(w_0^{\rm gc})^{*-1} \right),\end{aligned} \tag{1.23}$$

where $w_0^{\rm gc}$ is w_0 first defined in section 3.1.4 evaluated at the gradient catastrophe point, $z_0^{\rm gc} = \sqrt{w_0^{\rm gc}}$ principal branch and $\mathbf{C}(w_0^{\rm gc})$ are constant matrices with definition given by (5.95)*, and $W'(w_0^{\rm gc})$ given by*(4.112)*.*

The importance is that $\mathcal{E}^1$ is only dependent on (x,t) and ϵ via H in the complex variable $\nu = s(x,t)/\epsilon^{\frac{4}{5}}$.

Theorem 1.5.2 (Rational solutions emerging at the poles of the tritronquée solution)**.** *Under the same assumptions as in theorem 1.5.1, suppose that ν_p is a pole of the tritronquée solution. There $\exists M$, when $|\nu|< M$ and $H(\nu)/(\nu-\nu_p) > M\epsilon^{-\frac{1}{5}}$, such that the corresponding (x,t) neighbourhood of (x_p,t_p), where $\nu_p = s(x_p,t_p)/\epsilon^{\frac{4}{5}}$ and $\nu = s(x,t)/\epsilon^{\frac{4}{5}}$, has a universal leading asymptotic behaviour (we call them local structures), described by a special soliton solution of sG, given by*

$$\begin{aligned} \sin(\tfrac{1}{2}u_N) &= \mathbf{G}_{11}^{\text{out}}\dot{C} + \mathbf{G}_{12}^{\text{out}}\dot{S} + \mathcal{O}(\epsilon^{\frac{1}{5}}), \\ \cos(\tfrac{1}{2}u_N) &= \mathbf{G}_{21}^{\text{out}}\dot{C} + \mathbf{G}_{22}^{\text{out}}\dot{S} + \mathcal{O}(\epsilon^{\frac{1}{5}}), \end{aligned} \tag{1.24}$$

$$\mathbf{G}^{\text{out}} = \mathbb{I} - \frac{\mathbf{G}_0}{\sqrt{w_0^{\text{gc}}}} - \frac{\sigma_2\mathbf{G}_0^*\sigma_2}{\sqrt{w_0^{\text{gc}*}}} - \frac{\sigma_2\mathbf{G}_0\sigma_2}{\sqrt{w_0^{\text{gc}}}} - \frac{\mathbf{G}_0^*}{\sqrt{w_0^{\text{gc}*}}}, \tag{1.25}$$

where

$$\mathbf{G}_0 = \begin{bmatrix} a \\ b \end{bmatrix} \begin{bmatrix} C_{0,21}^{\text{gc}} & -C_{0,11}^{\text{gc}} \end{bmatrix}. \tag{1.26}$$

and $C_{0,ij}^{\text{gc}}$ is the (i,j) element of the matrix $\mathbf{C}(w_0)$ evaluated at the gradient catastrophe point. The coefficients (a,b) solve a 4×4 linear system with $\epsilon^{-\frac{1}{5}}\frac{1}{H(\nu)}$ in the coefficients. The solution exists for every (x,t) in the area we consider.

The rest of this thesis is concerned with setting up the necessary background and giving the proofs of these two results. Specifically, in Chapter 2, we introduce some assumptions on the initial data (1.4), the most important of which is that the perturbed simple pendulum system (1.7) corresponding to (1.3) is below the energy threshold for rotation at each $x \in \mathbb{R}$, and we properly define the notion of the corresponding fluxon condensate and the Riemann-Hilbert problem by means of which it will be studied. Chapter 3 concerns the analysis of the fluxon condensate before the catastrophe occurs. This analysis uses aspects of the Deift-Zhou steepest descent method, which in turn relies on the construction of an ϵ-independent scalar exponent function known in the literature as a g-function. We observe that the g-function exhibits a certain type of singularity at the catastrophe point, which complicates any further local analysis in the neighbourhood of this point. Then, in Chapter 4, we show how the g-function can be modified to avoid the aforementioned singularity, and obtain as a by-product the mapping function $s(x,t) = \epsilon^{\frac{4}{5}}\nu(x,t)$ mentioned in the statement of Theorem 1.5.1. Another by-product is the existence of a conformal mapping that allows us to study the fluxon condensate $u_N(x,t)$ in the neighbourhood of the catastrophe point by the construction of a certain local parametrix in the complex plane of the spectral parameter. In Chapter 5 we construct this parametrix and show how it is connected with the Painlevé-I tritronquée function $Y(\nu)$. After that, the parametrix reduces the Riemann-

Hilbert problem characterizing $u_N(x,t)$ to a small-norm problem whose solution we describe also in Chapter 5, allowing us to complete the proof of Theorem 1.5.1. Then in Chapter 6, we explain how to modify the parametrix in order to zoom in on the neighbourhood of a particular pole of $Y(\nu)$, and hence we complete the proof of Theorem 1.5.2. In Chapter 7 we list some possible future work to expand the results in this thesis.

Chapter 2

Fluxon condensates for librational Cauchy data and Riemann-Hilbert problem

2.1 Lax pair and inverse scattering transform for the semi-classical sG Cauchy problem

The more well-known form of Lax pair equation for the sine-Gordon equation in characteristic coordinates comes from [35]. Kaup observed that the sG equation in the form (1.2) is the compatibility condition of the following *Lax pair* of linear equations

$$\begin{aligned} 4i\mathbf{v}_x &= \mathbf{U}(z;x,t,1)\mathbf{v} = \begin{bmatrix} 4E(z)+z^{-1}(1-\cos(u)) & -z^{-1}\sin(u)-i(u_x+u_t) \\ -z^{-1}\sin(u)+i(u_x+u_t) & -4E(z)-z^{-1}(1-\cos(u)) \end{bmatrix}\mathbf{v}, \\ 4i\mathbf{v}_t &= \mathbf{V}(z;x,t,1)\mathbf{v} = \begin{bmatrix} 4D(z)-z^{-1}(1-\cos(u)) & z^{-1}\sin(u)-i(u_x+u_t) \\ z^{-1}\sin(u)+i(u_x+u_t) & -4D(z)+z^{-1}(1-\cos(u)) \end{bmatrix}\mathbf{v}, \end{aligned} \tag{2.1}$$

where z is a complex *spectral parameter* while

$$E(z) := \frac{1}{4}\left(z-\frac{1}{z}\right) \quad \text{and} \quad D(z) := \frac{1}{4}\left(z+\frac{1}{z}\right). \tag{2.2}$$

More precisely, $\mathbf{v}$ is a vector function of the spectral variable $z \in \mathbb{C}$ and two real independent variables x and t. The Lax pair equations in (2.1) can admit simultaneous solution if and only if $u(x,t)$ is a solution of the sine-Gordon equation. In this thesis, we make two small changes. First of all, because we will be considering the semi-classical sG equation in the form (1.3), we simply scale ϵ into the parameters x,t in (2.1). Secondly, because of the symmetry in the Lax operators $\mathbf{U}$ and $\mathbf{V}$, the corresponding eigenfunctions

and the Riemann–Hilbert problem will also be symmetric with respect to the involution $z \mapsto -z$. We are going to reduce the symmetry by replacing z with w so that $z = i\sqrt{-w}$. Whenever we use a square root, we always mean the principal branch.

The choice of w rather than z as the spectral parameter in (2.1) is not essential for our purpose. In principle the analysis can be done in the z-plane in a fashion completely parallel to what is done in the w-plane in this thesis. We use w in place of z as the spectral parameter in (2.1) because this work is continued from [13], in which the authors chose to work with w. The reason they chose this variable is because, roughly speaking, the asymptotic approximation of the solution of sG is built from the theta function on a Riemann surface with cuts that preserves symmetries from the Riemann–Hilbert problem. The symmetry $z \mapsto -z$ means that the cuts in the z-plane always come in pairs. In general, this will result in more cuts, hence higher genus, in the Riemann surface, which could potentially make the theta function representation more complicated. Working in the w-plane reduces the number of cuts by a factor of 2 (and then adds an additional cut from the square root). Thus if the number of cuts is large, it is far more efficient to take advantage of the symmetry and work in the w-plane.

After the minor changes, $E(w)$ and $D(w)$ become

$$E(w) := \frac{i}{4}\left[\sqrt{-w} + \frac{1}{\sqrt{-w}}\right] \quad \text{and} \quad D(w) := \frac{i}{4}\left[\sqrt{-w} - \frac{1}{\sqrt{-w}}\right]. \tag{2.3}$$

We arrive at the Lax pair for the semi-classical sG equation in the form (1.3):

$$\begin{aligned} 4i\epsilon \mathbf{v}_x &= \mathbf{U}(z;x,t,\epsilon)\mathbf{v} = \begin{bmatrix} 4E(w) - \dfrac{i}{\sqrt{-w}}(1-\cos(u)) & \dfrac{i}{\sqrt{-w}}\sin(u) - i\epsilon(u_x+u_t) \\ \dfrac{i}{\sqrt{-w}}\sin(u) + i\epsilon(u_x+u_t) & -4E(w) + \dfrac{i}{\sqrt{-w}}(1-\cos(u)) \end{bmatrix}\mathbf{v}, \\ 4i\epsilon \mathbf{v}_t &= \mathbf{V}(z;x,t,\epsilon)\mathbf{v} = \begin{bmatrix} 4D(w) + \dfrac{i}{\sqrt{-w}}(1-\cos(u)) & -\dfrac{i}{\sqrt{-w}}\sin(u) - i\epsilon(u_x+u_t) \\ -\dfrac{i}{\sqrt{-w}}\sin(u) + i\epsilon(u_x+u_t) & -4D(w) - \dfrac{i}{\sqrt{-w}}(1-\cos(u)) \end{bmatrix}\mathbf{v}, \end{aligned} \tag{2.4}$$

The Cauchy initial-value problem (1.3)-(1.4) is generally studied by the inverse-scattering method as follows ([35, 29] and [10, Appendix A]).

- Firstly, one replaces u, u_x, and ϵu_t in the x-ODE in (2.4) with their initial conditions at $t = 0$, $F(x)$, $F'(x)$, and $G(x)$, respectively. One then studies how the solutions $\mathbf{v}$ of this linear ODE depend on the spectral parameter z and collects certain *scattering data*. This is the *direct spectral transform*.

- Secondly, one uses the scattering data to formulate a matrix-valued Riemann-Hilbert problem in which $(x, t) \in \mathbb{R}^2$ appear as parameters. From the solution of the Riemann-Hilbert problem one extracts certain coefficients depending on the parameters (x, t) giving the values of $\sin(\frac{1}{2}u(x,t))$, $\cos(\frac{1}{2}u(x,t))$, and $\epsilon u_t(x,t)$ solving the Cauchy problem.

Both of these steps involve the small parameter $\epsilon > 0$ in a singular way that requires substantial analysis to resolve.

2.2 Initial data and the corresponding fluxon condensate

We can significantly simplify the Lax pair at $t = 0$ by choosing the initial condition $u(x, 0; \epsilon) = F(x) \equiv 0$. All the u and u_x terms disappear. The spatial differential equation (in x) in (2.4) is called the *Faddeev–Takhtajan eigenvalue problem*. The Faddeev-Takhtajan eigenvalue problem is reduced to the well-known Zakharov-Shabat eigenvalue problem:

$$\epsilon \mathbf{v}_x = \begin{bmatrix} -i\lambda & \psi(x) \\ -\psi(x)^* & i\lambda \end{bmatrix} \mathbf{v}, \qquad \psi(x) := -\frac{1}{4}G(x), \quad \lambda := E(w) \tag{2.5}$$

Therefore we adopt

Assumption 2.2.1 (Pure impulse initial data)**.** *In the initial condition* (1.4)

$$F(x) \equiv 0. \tag{2.6}$$

When viewed as an eigenvalue problem $\mathcal{L}\mathbf{v} = \lambda\mathbf{v}$, several properties are known for real ψ. From the symmetric structure of the operator $\mathcal{L}$, the spectrum comes in quartets, i.e., if λ is in the spectrum, then $-\lambda$ and $\pm\lambda^*$ are also in the spectrum. Furthermore, Klaus and Shaw [36] showed that if $\psi \in L^1(\mathbb{R}) \cap C^1(\mathbb{R})$ is real, of one sign, and has single critical point ("bell-shaped"), then the discrete spectrum is purely imaginary and nondegenerate.

On $G(x)$ we assume

Assumption 2.2.2. *In the initial condition* (1.4) *for* ϵu_t*, the function* $G(x)$ *is a nonpositive function of Klaus-Shaw type, i.e.,* $G \in L^1(\mathbb{R}) \cap C^1(\mathbb{R})$ *and* G *has a unique local and global minimum.*

For Klaus-Shaw type nonpositive functions $G(x)$ in our pure impulse initial data, the purely imaginary eigenvalues λ can be approximated by a WKB method when $\epsilon \ll 1$ [36]. The initial condition $G(x)$ is associated with the WKB phase integral

$$\Psi(\lambda) := \frac{1}{4}\int_{x_-(\lambda)}^{x_+(\lambda)} \sqrt{G(s)^2 + 16\lambda^2}\mathrm{d}s, \qquad 0 < -i\lambda < \max(-\frac{1}{4}G), \tag{2.7}$$

where $x_-(\lambda) < x_+(\lambda)$ are the two roots of $G(s)^2 + 16\lambda^2$. Then by the Bohr-Sommerfeld quantization rule, the eigenvalues are approximated by

$$\Psi(\lambda_k) = \pi\epsilon\left(k + \frac{1}{2}\right), \quad k = 0, 1, 2, \ldots, N(\epsilon) - 1, \tag{2.8}$$

with

$$N(\epsilon) = \left\lfloor \frac{1}{2} + \frac{1}{4\pi\epsilon} \parallel G \parallel_1 \right\rfloor. \tag{2.9}$$

We refer the readers to [13] for details of the following assumptions we make on our initial data and choices of parameter. In this thesis, we will assume the following:

Assumption 2.2.3. *The small parameter* ϵ *is taken from the infinite sequence*

$$\epsilon = \epsilon_N := \frac{\parallel G \parallel_1}{4\pi N}, \quad N = 1, 2, 3, \ldots \tag{2.10}$$

Under this assumption,

$$\frac{\Psi(0)}{\epsilon} = \pi N, \quad N = 1, 2, 3, \ldots. \tag{2.11}$$

Also, it is implied that the reflection coefficient is *uniformly* small for $\lambda \in \mathbb{R}$, making the reflection coefficient negligible in a neighborhood of $\lambda = 0$), or equivalently $w = 1$. This assumption is needed later to control the jump on the real line, and thus justifies our neglecting an additional jump on the real line for the Riemann–Hilbert problem that generally is not negligible. See its use in [13, Prop. 3.3].

Assumption 2.2.4. $G(x)$ *is an even function. Thus* $\min G$ *is taken at* $x = 0$.

Therefore G is completely defined by its inverse G^{-1} on the positive x-axis.

Assumption 2.2.5. *The function G is strictly increasing for $x > 0$, real-analytic, and the positive real-analytic function*

$$\mathcal{G}(m) := \frac{\sqrt{m}\sqrt{G(0)^2 - m}}{2G'(G^{-1}(-\sqrt{-m}))}, \quad 0 < m < G(0)^2 \tag{2.12}$$

can be analytically continued to neighborhoods of $m = 0$ and $m = G(0)^2$, with $\mathcal{G}(0) > 0$, and $\mathcal{G}(G(0)^2) > 0$.

An important consequence of this assumption is that the WKB integral $\Psi(\lambda)$ is holomorphic in a simply connected strip neighbourhood containing the segment where the discrete spectrum accumulate (on the imaginary axis $0 \leq -i\lambda \leq -G(0)/4$. This strip corresponds to a neighbourhood of an arc of the unit circle.

Assumption 2.2.6. *The initial data is below the threshold of rotation, i.e.*

$$|G(0)| < 2. \tag{2.13}$$

The reader may notice in [13] for a similar set up of the Riemann–Hilbert problem for sG, there is an assumption that $\frac{\Psi(\frac{i}{2})}{\| G \|_1}$ is irrational. We would not need this assumption here because the purpose of the assumption is to avoid a double pole occuring at $w = -1$. However, in our case, because our initial data is below threshold, the spectrum will end up away from -1.

So far nobody has succeeded in obtaining enough control on the errors in the WKB analysis to be able to carry these errors forward into the inverse-scattering step and therefore solve the Cauchy problem. Therefore we follow another approach, which has been used with some success in several other situations.

Examples in the past include, Lax–Levermore for KdV [37], Kamvissis–McLaughlin–Miller for focusing NLS [33], Miller-Xu for Benjamin-Ono [39, 40], Buckingham–Miller for sG [13], and Buckingham-Jenkins-Miller for the 3-wave interaction system [11]. Namely, we replace the true scattering data by its formal small-ϵ approximation, neglecting the reflection coefficient and retaining only the eigenvalues which are replaced by their Bohr-Sommerfeld approximations. Putting this approximate data into the inverse scattering problem yields a family of exact solutions of sG parametrized by ϵ_N that we call the fluxon condensate corresponding to the true Cauchy data. In general, the fluxon condensate does not match the given Cauchy data for any $\epsilon_N > 0$ (but it does for all ϵ_N in the Satsuma-Yajima case [42] where G is proportional to $\mathrm{sech}(x)$).

Definition 2.2.1 (Fluxon condensate)**.** The fluxon condensate $u_N(x,t)$ is the exact solution to the inverse scattering problem for $\epsilon = \epsilon_N$, with the continuum spectrum of the scattering data neglected, the eigenvalues and auxiliary discrete spectrum get replaced with their WKB approximations in the second step in the inverse scattering transform in section 2.1. An alternative, yet more precise definition of the fluxon condensate, is the exact solution $u_N(x,t)$ of the semi-classical sine-Gordon equation for $\epsilon = \epsilon_N$ recovered from A_N in the Riemann–Hilbert problem 1, given by (2.23).

One can view the fluxon condensate as a quantised (as the name fluxon suggests), exactly solvable approximation of the original Cauchy problem. However, the approximation needs justification. Theorem 2.2.7 tells us that the initial condition is well approximated by the fluxon condensate. However, as we explained, the connection between the fluxon condensate and the Cauchy problem is generally a hard problem.

It is shown in [13] that the fluxon condensate for some $0 < t < T(x)$ is approximated by an elliptic function with uniformly $\mathcal{O}(\epsilon)$ sized error. In fact what was proved is that this is true inside any compact subset of the librational region and any compact subset of the rotational region. A very similar argument will work for us. Therefore we woud not give the detailed proof here. Interested readers can find it in [13, Theorem 1.1, Theorem 1.2]. In this thesis, however, we are dealing with the below threshold initial data. Therefore the librational region is the whole real axis.

At $t = 0$, the leading term approximation of $u_N(x,0)$ and $\epsilon_N u_{N,t}(x,0)$ calculated from the elliptic function are 0 and $G(x)$ respectively. In that sense, the fluxon condensate $\{u_N(x,t)\}$ for the Cauchy problem (1.3) with $\epsilon = \epsilon_N$ and with pure-impluse initial data of the Klaus–Shaw type is close to the Cauchy problem. More precisely,

Theorem 2.2.7. *When $t = 0$, the fluxon condensate $\{u_N(x,t)\}$ associated with the pure-impulse initial condition of impulse profile $G(x)$ satisfies*

$$\begin{aligned} u_N(x,0) =& \mathcal{O}(\epsilon_N) \\ \epsilon_N \frac{\partial u_N}{\partial t}(x,0) =& G(x) + \mathcal{O}(\epsilon_N). \end{aligned} \tag{2.14}$$

where the error is valid for $x \neq 0$ and uniform on any compact subsets on the real line.

Terminology

Definition 2.2.2. Throughout this thesis paper we will use the standard **Pauli matrices**:

$$\sigma_1 := \begin{bmatrix} 0 & 1 \\ 1 & 0 \end{bmatrix}, \quad \sigma_2 := \begin{bmatrix} 0 & -i \\ i & 0 \end{bmatrix}, \quad \sigma_3 := \begin{bmatrix} 1 & 0 \\ 0 & -1 \end{bmatrix}. \tag{2.15}$$

2.3 The Riemann-Hilbert problem for librational fluxon condensates

The fluxon condensate, by definition, is reflectionless. This implies that the Riemann–Hilbert problem will only have isolated singularities and a trivial jump from taking the square root $\sqrt{-w}$ on $\mathbb{R}_+$. The set up here is very similar to [13].

Define $Q(w)$ as

$$Q(w) = Q(w; x, t) := E(w)x + D(w)t, \quad \text{for } |\arg(-w)| < \pi. \tag{2.16}$$

Define the Blaschke product

$$\prod_N(w) := \prod_{k=0}^{N-1} \frac{E(w) + \lambda_{N,k}^0}{E(w) - \lambda_{N,k}^0} = \prod_{y \in P_N} \frac{\sqrt{-w} + \sqrt{-y}}{\sqrt{-w} - \sqrt{-y}}, \tag{2.17}$$

where $\lambda_{N,k}^0$ are the approximated spectrum from (2.8) and P_N are the location of the poles of $\prod_N$ where $E(y) = \lambda_{N,k}^0$ for some k. According to assumption 2.11, $\prod_N$ has $2N$ simple poles.

The discrete spectrum stays constant. Inserting the correct time dependence, we arrive at the Riemann–Hilbert problem

Riemann-Hilbert Problem 1
To Find: 2×2 matrix function $\mathbf{H}(w) = \mathbf{H}_N(w; x, t)$
Analyticity: $\mathbf{H}(w)$ is analytic for $w \in \mathbb{C} \backslash (P_N \bigcup \mathbb{R}_+)$
Jump Condition: $\mathbf{H}_+(\xi) = \sigma_2 \mathbf{H}_-(\xi)\sigma_2$. $\xi \in \mathbb{R}_+$.
Singularities: Each of the points of P_N is a simple pole of $\mathbf{H}(w)$,

$$\operatorname*{Res}_{w=y} \mathbf{H}(\omega) = \lim_{w \to y} \mathbf{H}(w) \begin{bmatrix} 0 & 0 \\ (-1)^{k+1} \operatorname*{Res}_{w=y} e^{2iQ(w;x,t)/\epsilon_N} \prod_N(w) & 0 \end{bmatrix} \tag{2.18}$$

Normalization:

$$\lim_{w\to\infty} \mathbf{H}(w) = \mathbb{I}$$

Note that this is not the only way to formulate the Riemann–Hilbert problem (RHP). In fact, in [13], the authors found that another formulation of the Riemann–Hilbert problem is essential for the analysis of the Riemann–Hilbert problem when t is very small. The idea behind this RHP is the following: dividing the set of eigenvalues in two sets, ∇ and Δ. The spectral data from ∇ are viewed as scattering from the left, while Δ are scattering from the right. Since our case is not concerned with very small time, our formulation of Riemann–Hilbert problem for $\mathbf{H}$ is equivalent to $\Delta = \emptyset$ in [13], the simplest case that suffices for our purposes.

Using a Liouville argument on $\det(\mathbf{H})$, one can show that the solution to Riemann–Hilbert problem 1 has to be unique. In addition, the Riemann–Hilbert problem itself is Schwarz symmetric, therefore, the solution also has symmetry

$$\mathbf{H}(w^*) = \mathbf{H}(w)^*. \tag{2.19}$$

If we formulate the Riemann–Hilbert problem 1 in variable z for $w = z^2$, see section 5.3.2, then the standard Riemann–Hilbert theory tells us that, supposing the solution to the Riemann–Hilbert problem exists, then it will admit a power series expansion. Equivalently, $\mathbf{H}(w)$ has convergent series expansions of the following forms

$$\mathbf{H}(w) = \sum_{k=0}^{\infty} \mathbf{H}_N^{0,k}(x,t)(\sqrt{-w})^k, \quad |w| < r \tag{2.20}$$

and

$$\mathbf{H}(w) = \mathbb{I} + \sum_{k=1}^{\infty} \mathbf{H}_N^{\infty,k}(x,t)(\sqrt{-w})^{-k}, \quad |w| > R. \tag{2.21}$$

The radius r and R are independent of N.

Define

$$\begin{gathered} \mathbf{A}_N(x,t) := \mathbf{H}_N^{0,0}(x,t), \quad \mathbf{B}_N^0(x,t) := \mathbf{H}_N^{0,0}(x,t)^{-1}\mathbf{H}_N^{0,1}(x,t), \\ \mathbf{B}_N^{\infty}(x,t) := \mathbf{H}_N^{\infty,1}(x,t), \qquad N > N_0. \end{gathered} \tag{2.22}$$

Proposition 2.3.1. *Let*

$$\cos\left(\frac{1}{2}u_N(x,t)\right) = A_{n,11}(x,t) \quad \textit{and} \quad \sin\left(\frac{1}{2}u_N(x,t)\right) = A_{N,21}(x,t). \tag{2.23}$$

Also assume that $\Omega \subset \mathbb{R}^2$ is open and for a given integer N_0 the Riemann–Hilbert problem 1

has a solution whenever $(x,t) \in \Omega$ *and* $N \geq N_0$*. Then for each* $N > N_0$*,* $u = u_N(x,t)$ *is an exact real-valued solution on* Ω *of the sine-Gordon equation* (1.2) *with* $\epsilon = \epsilon_N$*. Moreover,*

$$\epsilon_N \frac{\partial u_N}{\partial t}(x,t) = B^0_{N,12}(x,t) + B^\infty_{N,12}(x,t). \tag{2.24}$$

The reader can find the proof in [13]. In Chapter 3, we will sketch a proof that this solution at $t = 0$ is close to the initial condition in the Cauchy problem (1.3)-(1.4).

The result of this proposition is that now we can use the solution of the Riemann–Hilbert problem 1 to study the asymptotics of the Cauchy problem of the sine-Gordon equation.

2.4 Removing Poles of $\mathbf{H}$

The original Riemann–Hilbert problem 1 contains $2N$ poles, where $N \propto \frac{1}{\epsilon}$. Technically we can solve a linear algebra problem associated with this Riemann–Hilbert problem. However we are interested in the semi-classical limit when ϵ goes to zero, therefore the number of poles will become very large. The matrix in the linear algebra problem is very ill-conditioned for large N, and in this set-up it is difficult to do analysis.

In this section we are going to do an explicit invertible transformation of Riemann–Hilbert problem 1 in order to convert it to a form that is better suited for analysis. For convenience, we will use the notation

$$\theta_0(w) := \Psi(E(w)) \tag{2.25}$$

for the WKB phase integral determined by the initial conditions.

As a consequence of the Bohr-Sommerfeld quantization (2.8), whenever we are at an eigenvalue: $y \in P_N$ such that $E(y) = \lambda^0_{N,k}$, we have

$$\mp i e^{\pm i\theta_0(y)/\epsilon_N} = (-1)^k, \quad k = 0, \ldots, N-1. \tag{2.26}$$

Introduce regions Ω_+ and Ω_- that enclose the discrete poles P_N. Denote $\Sigma_\pm$ as the boundary of $\Omega_\pm$. See figure 2.1.

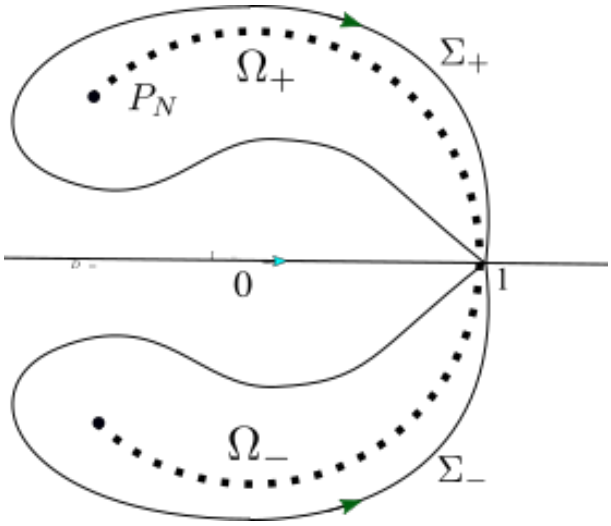

Figure 2.1: Introducing regions Ω_+, Ω_- and contours Σ_+, Σ_-

Let

$$\mathbf{M}(w) := \begin{cases} \mathbf{H}(w) \begin{bmatrix} 1 & 0 \\ \pm i \prod_N(w) e^{(2iQ(w;x,t) \mp i\theta_0(w))/\epsilon_N} & 1 \end{bmatrix}, & w \in \Omega_\pm, \\ \mathbf{H}(w), & w \in \mathcal{C} \backslash (\overline{\Omega} \cup \mathbb{R}_+). \end{cases} \tag{2.27}$$

$\mathbf{M}$ inherits the Schwarz symmetry from $\mathbf{H}$, i.e. $\mathbf{M}(w^*) = \mathbf{M}(w)^*$.

From the residue condition (2.18) in the original Riemann–Hilbert problem, we can verify that $\mathbf{M}(w)$ only has removable singularities inside $\Omega = \Omega_+ \cup \Omega_-$. Thus $\mathbf{M}(w)$ may be considered an analytic function in different regions and continuous on the boundary, but it has jump discontinuities across the boundary of the regions. Here in order to use this transform to eliminate the poles from the original Riemann–Hilbert problem, the key of choosing Ω is that $\Sigma = \Sigma_+ \cup \Sigma_- = \partial\Omega$ must be closed and enclose all the poles. Also, the region should be chosen in a symmetrical way that preserves the Schwarz symmetry of $\mathbf{H}$, so that $\mathbf{M}$ inherits the Schwarz symmetry of $\mathbf{H}$.

2.5 The equivalent Riemann-Hilbert Problem for $\mathbf{M}$

Choose the orientation of Σ_+ as clockwise on the upper half plane, and let the lower half plane mirror the upper half plane. Thus Σ_- is counterclockwise in the lower half plane.

From (2.27), it is clear the the jump for $\mathbf{M}(w)$ is

$$\mathbf{M}_+ = \mathbf{M}_- \begin{bmatrix} 1 & 0 \\ -i\prod_N(w)e^{(2iQ(w;x,t)\mp i\theta_0(w))/\epsilon_N} & 1 \end{bmatrix} \tag{2.28}$$

The function $\prod_N$ still has multiple poles. For our analysis, we only use the value of the function near the boundary Σ. To simplify the analysis, we will approximate the product $\prod_N(w)$ near the region of consideration.

The goal here is to express the product as an exponential. Introduce the logarithm-type function, for $y \notin \mathbb{R}_+$, let

$$l(w,y) := \log\left(\frac{\sqrt{-w}+\sqrt{-y}}{\sqrt{-w}-\sqrt{-y}}\right). \tag{2.29}$$

Here both the log and the square root are denoting the principal branch. The branch cut of l therefore is on $\mathbb{R}_+$ and a line segment from $w = y$ to $w = 0$, see figure 2.2. Moreover,

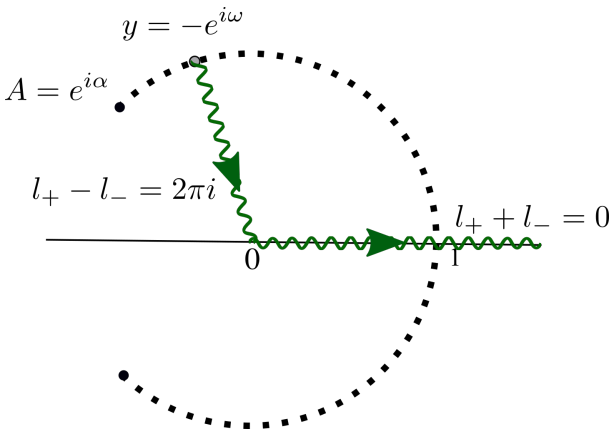

Figure 2.2: Jump for l

on $\mathbb{R}_+$, $l_+(w)+l_-(w) = 0$; on y to 0, the jump is $l_+(w)-l_-(w) = 2\pi i$. We move the branch cut to the unit circle. When y varies along the circle, the branch cut of $m(w;y)$ will always be a subset of the same union of curves. Suppose $y = -e^{i\omega}$ with $-\pi < \omega < \pi$. Define

$$m(w;y) = l(w;y) + \begin{cases} -2i\pi, & \text{when } 0 < \omega < \pi |w| < 1 \text{ and } 0 < \arg(w) < \omega, \\ 2i\pi, & \text{when } -\pi < \omega < 0,\ |w| < 1 \text{ and } \omega < \arg(w) < 0, \\ 0, & |w| > 1 \text{ or } |\omega| < |\arg(w)| \leq 2\pi i. \end{cases} \tag{2.30}$$

See figure 2.3.

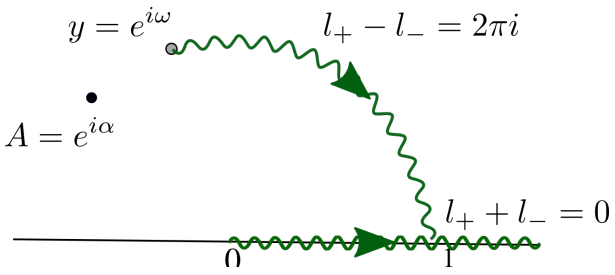

Figure 2.3: Jump for m

Next, set

$$L_N^0(w) := \sum_{y \in P_N} m(w; y)\epsilon_N. \tag{2.31}$$

This function is analytic for where each summand is analytic, while there is a jump discontinuity on the arc of the unit circle starting from the last eigenvalue y_N, as well as on $\mathbb{R}_+$. The jump contour is illustrated in figure 2.4. It also has Schwarz symmetry. Both properties are inherited from m term-wise.

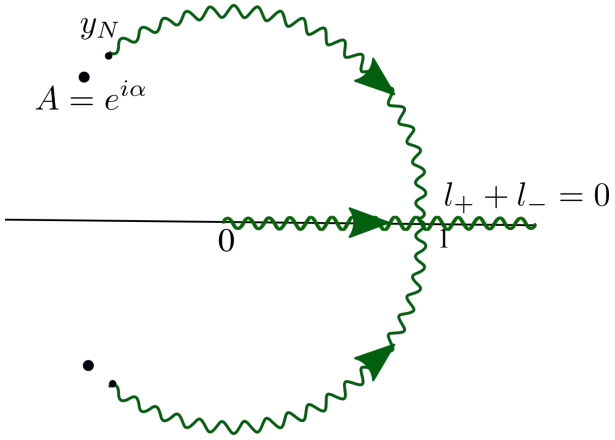

Figure 2.4: Jump contour for L_N^0

We also have the identity

$$\prod_N(w) = e^{L_N^0(w)/\epsilon_N}, \quad w \in \mathbb{C}\backslash(P_\infty \cup \mathbb{R}_+). \tag{2.32}$$

P_∞ is the arc of the unit circle where P_N accumulate as $N \to \infty$. Notice that the $\pm 2i\pi$ will cancel in the end because P_N come in pairs.

By Bohr-Sommerfeld quantization rule (2.8),

$$\theta_0(y_{n+1}) - \theta_0(y_{n-1}) = 2\pi\epsilon_N. \tag{2.33}$$

(In accordance with the orientation of y_n the orientation of P_∞ is from endpoints to $w = 1$.) Expanding the left hand side around y_n,

$$\Delta y_n := \frac{y_{n+1} - y_{n-1}}{2} = \frac{\pi \epsilon_N}{\theta_0'(y_n)} + \mathcal{O}(\epsilon_N^3). \tag{2.34}$$

As $\epsilon_N \to 0$, (2.31) can be approximated by a Riemann integral. To be precise, for each $w \in \mathbb{C}\backslash(P_\infty \cup \mathbb{R}_+)$,

$$\sum_{y \in P_N} m(w;y)\epsilon_N = \frac{1}{\pi} \sum_{y \in P_N} \theta_0'(y) m(w;y) \Delta y = \frac{1}{\pi} \int_{P_\infty} \theta_0'(y) m(w;y) \mathrm{d}y + \mathcal{O}(\epsilon_N^2). \tag{2.35}$$

So if we define the integral part as $L^0(w)$,

$$L^0(w) = \frac{1}{\pi} \int_{P_\infty} \theta_0'(y) m(w;y) \mathrm{d}y, \tag{2.36}$$

then the jump contour of L^0 is illustrated along with curves $\Sigma_\pm$ in figure 2.5. L_N^0 is approximated by

$$L_N^0(w) = L^0(w) + \mathcal{O}(\epsilon_N^2) \quad \text{and} \quad \prod_N (w) e^{-L^0(w)/\epsilon_N} = 1 + \mathcal{O}(\epsilon_N),\ N \to \infty. \tag{2.37}$$

when w is bounded away from P_N. Since $\mathbf{H}$ and $\mathbf{M}$ agree in neighborhoods of $w = 0$ and $w = \infty$, the same formulæ apply to extract the fluxon condensate from each.

Next we integrate L^0 in (2.36) by parts. At the two endpoints, $E(y) = -iG(0)/4$, thus $\theta_0(y)$ vanishes. At $w = 1$, $m(w;1+) + m(w;1-) = 0$. Therefore,

$$L^0(w) = \frac{\sqrt{-w}}{\pi} \int_{P_\infty} \frac{\theta_0(y)}{\sqrt{-y}} \frac{\mathrm{d}y}{y - w}. \tag{2.38}$$

By the Plemelj formula [41], the function L^0 has a jump of difference $-2i\theta_0$ on P_∞.

Define

$$Y(w) := \prod_N (w) e^{-L^0(w)/\epsilon_N}. \tag{2.39}$$

Proposition 2.5.1. *(Baik et al. [3]) The function $Y(w)$ is analytic for $w \in \mathbb{C}\backslash(\Sigma \cup P_\infty \cup \mathbb{R}_+)$. On compact sets in the domain of analyticity disjoint from P_∞, $Y(w)$ admits the approximation*

$$Y(w) = 1 + \mathcal{O}(\epsilon_N). \tag{2.40}$$

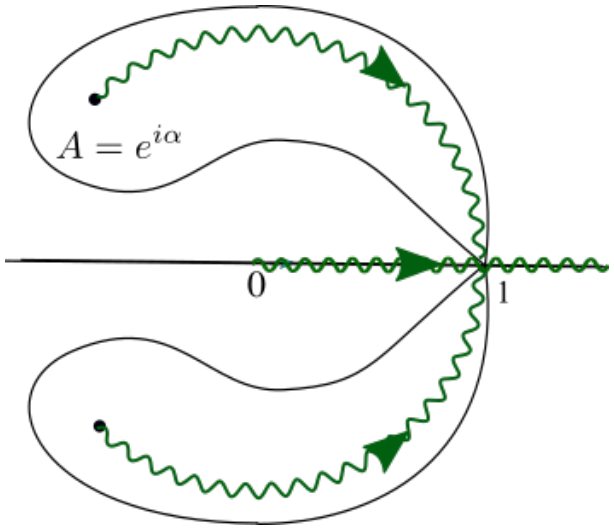

Figure 2.5: L^0 jump contour along with the contours $\Sigma_\pm$

Modified contours near $w = 1$

We want to control Y on the boundary of the whole region. However, the proposition 2.5.1 only guaranteed Y is near 1 away from the accumulation of the spectrum P_∞. The region $\Omega_\pm$ of our choice closes at 1 which is a point on P_∞. To deal with this problem, we follow the idea from [38], by adding small regions Ω_+ and Ω_- near the point 1. We fix a point B on the original Σ_+, then draw a contour to the right of 1 on the real line. Then continue back to 1 along $\mathbb{R}$ to close the contour. On the other side, we simply deform the contour a little to land on the real line away from 1 before connecting to 1 along the real line, as shown in figure 2.6:

We require that the jump from $\Omega_\pm$ to the exterior region remain the same as (2.28) on Σ_+ and Σ_-. Note that the definition of Σ_+ and Σ_- has changed since the region $\Omega_\pm$ has changed. A new arc denoted by $\Sigma_\mp$ has been introduced between Ω_+ and Ω_-. Calculating the jump matrix on $\Sigma_\mp$:

$$\mathbf{M}_+(\xi) = \mathbf{M}_-(\xi) \begin{bmatrix} 1 & 0 \\ -2i \prod_N(\xi) \cos(\frac{\theta_0}{\epsilon_N}) e^{\frac{2iQ(\xi;x,t)}{\epsilon_N}} & 1 \end{bmatrix}, \quad \xi \in \Sigma_\mp. \tag{2.41}$$

If we let T be

$$T(w) := 2 \prod_N(\xi) \cos\left(\frac{\theta_0}{\epsilon_N}\right) e^{-\frac{L^0(w)}{\epsilon_N}} \times \begin{cases} e^{i\theta_0/\epsilon_N}, & \mathrm{Im}(w) > 0 \text{ and } |w| > 1, \\ e^{-i\theta_0/\epsilon_N}, & \mathrm{Im}(w) < 0 \text{ and } |w| > 1, \end{cases} \tag{2.42}$$

then we can eliminate the Blaschke product $\prod_N(\xi)$ from the jump on the new contour $\Sigma_\mp$

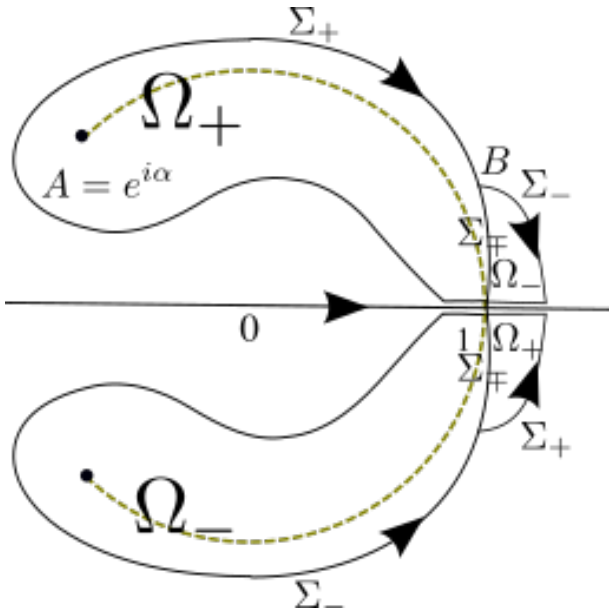

Figure 2.6: Avoiding 1. Introducing additional regions and moving the contour to approach 1 from $\mathbb{R}$.

in favor of $T(\xi)$.

For convenience, denote the upper half plane as $\mathbb{C}_+ := \{w : \mathrm{Im}(w) > 0\}$ and the lower half plane as $\mathbb{C}_- := \{w : \mathrm{Im}(w) < 0\}$.

According to Bohr-Sommerfeld quantization, the poles will vanish for T. Thus, T stays bounded near P_∞. Comparing the definition of T and Y, they have relation

$$T(w) = Y(w)(1 + e^{\pm 2i\theta_0(w)/\epsilon_N}), \quad \text{for } w \in \mathbb{C}_\pm \tag{2.43}$$

For w away from P_∞ and $|w|> 1$. In particular, the neighbourhood of the arc where T will be used, $\mathrm{Re}(i\theta_0)$ has the correct sign and $e^{\pm 2i\theta_0/\epsilon_N}$ decays exponentially, thus $T \approx 1$. When w approaches P_∞, more attention is needed. However, one can consult [3] for the proof that

$$T(w) = 1 + \mathcal{O}(\epsilon_N), \quad w \notin \mathbb{R}_+. \tag{2.44}$$

Now the boundary of the whole region is bounded away from P_∞ except on the real line. To calculate the jump on the two segments on $\mathbb{R}_+$ near 1, we collapse the three copies and reorganise the orientation. Let the two segments be Σ_{1_-} and Σ_{1_+}, as shown in figure 2.7. Using the definition in (2.27), we can replace RHP 1 by the following Riemann–Hilbert problem:

Riemann-Hilbert Problem 2

Find a 2×2 matrix function $\mathbf{M}(w)$ that satisfies the following conditions:
Analyticity: $\mathbf{M}(w)$ is analytic for $w \in \mathbb{C} \backslash (\Sigma_+ \bigcup \Sigma_- \bigcup \Sigma_\mp \bigcup \mathbb{R}_+)$
Jump Condition: On jump contour in figure 2.6:

$$\mathbf{M}_+(\xi) = \sigma_2 \mathbf{M}_-(\xi) \sigma_2 \text{ for } \xi \in \mathbb{R}_+, \tag{2.45}$$

$$\mathbf{M}_+(\xi) = \mathbf{M}_-(\xi) \begin{bmatrix} 1 & 0 \\ -iY(\xi) e^{[2iQ(w)+L^0(\xi)-i\theta_0(w)]/\epsilon_N} & 1 \end{bmatrix} \text{ for } \xi \in \Sigma_+ \cup \mathrm{Im}(w) > 0, \tag{2.46}$$

$$\mathbf{M}_+(\xi) = \mathbf{M}_-(\xi) \begin{bmatrix} 1 & 0 \\ -iY(\xi) e^{[2iQ(w)+L^0(\xi)+i\theta_0(w)]/\epsilon_N} & 1 \end{bmatrix} \text{ for } \xi \in \Sigma_- \cup \mathrm{Im}(w) < 0, \tag{2.47}$$

$$\mathbf{M}_+(\xi) = \mathbf{M}_-(\xi) \begin{bmatrix} 1 & 0 \\ iY(\xi) e^{[2iQ(w)+L^0(\xi)-i\theta_0(w)]/\epsilon_N} & 1 \end{bmatrix} \text{ for } \xi \in \Sigma_+ \cup \mathrm{Im}(w) < 0, \tag{2.48}$$

$$\mathbf{M}_+(\xi) = \mathbf{M}_-(\xi) \begin{bmatrix} 1 & 0 \\ iY(\xi) e^{[2iQ(w)+L^0(\xi)+i\theta_0(w)]/\epsilon_N} & 1 \end{bmatrix} \text{ for } \xi \in \Sigma_- \cup \mathrm{Im}(w) > 0, \tag{2.49}$$

$$\mathbf{M}_+(\xi) = \mathbf{M}_-(\xi) \begin{bmatrix} 1 & 0 \\ -iT e^{[2iQ(w)+L^0(\xi)-i\theta^0]/\epsilon_N} & 1 \end{bmatrix} \text{ for } \xi \in \Sigma_\mp \cup \mathrm{Im}(w) > 0. \tag{2.50}$$

$$\mathbf{M}_+(\xi) = \mathbf{M}_-(\xi) \begin{bmatrix} 1 & 0 \\ -iT e^{[2iQ(w)+L^0(\xi)+i\theta^0]/\epsilon_N} & 1 \end{bmatrix} \text{ for } \xi \in \Sigma_\mp \cup \mathrm{Im}(w) < 0. \tag{2.51}$$

$$\mathbf{M}_+(\xi) = \sigma_2 \mathbf{M}_-(\xi) \sigma_2 \begin{bmatrix} 1 + e^{(i\theta_{0\pm} - i\theta_{0\mp})/\epsilon_N} & \mp iY_-(\xi) e^{(2iQ_-(\xi)+L_{0-}(\xi)\mp i\theta_{0-}(\xi))/\epsilon_N} \\ \mp iY_+(\xi) e^{(2iQ_+(\xi)+L_{0+}(\xi)\pm i\theta_{0+}(\xi))/\epsilon_N} & 1 \end{bmatrix} \text{ for } \xi \in \Sigma_{1_\pm}. \tag{2.52}$$

Normalization:

$$\lim_{w \to \infty} \mathbf{M}(w) = \mathbb{I} \tag{2.53}$$

We will study this Riemann–Hilbert problem for the purpose of analysing the asymptotics of the sine-Gordon equation.

2.6 Notes on small time

In the next chapter, we will see that at $t = 0$, the β curve coincides with part of P_∞. Thus $Y(\xi)$ is not small on the entire β curve. In this case we have to set up the Ω_+ and Ω_- regions in a different way. Indeed when t is small, the former single loop set-up does not

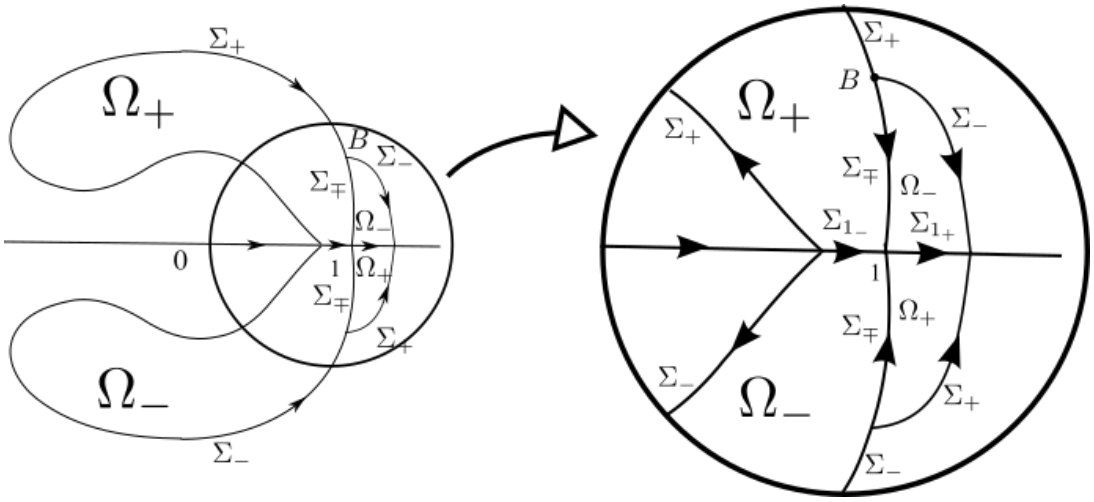

Figure 2.7: Zoom in the jump contours near 1, introducing $\Sigma_{1_\pm}$

work. The correct way to set up the Riemann–Hilbert problem is to use two regions on each side of β. The small region added to handle the singularity near 1 will instead end at A, so we can use T, the quantity without poles along $\Sigma_\mp$, for the entire β and its extension to A (at $t = 0$ this curve happens to be P_∞). The details are described in [13].

In fact, we started off setting the Riemann–Hilbert problem that way. Later we discovered that the g-function first fails to control the exponential for two regions set-up. However, when we analytically continue the g-function by collapsing the inside loop and only use the outside loop, the g-function can again control the exponential. So the failure in the original set-up is not related to the breaking, but rather a technical failure. Instead, we switched to Riemann–Hilbert problem 2. In the next few chapters, we will describe how the failure of RHP 2 actually captures the mechanism of the sG solution breaking curve.

Chapter 3

Asymptotic behavior of fluxon condensates before the gradient catastrophe

The Deift–Zhou steepest descent method was first developed to analyse the Riemann–Hilbert problem for the mKdV equation in 1993 [22], in which they implemented the contour deformation and well-known steepest descent method. Followed by the contour deformation attempt, they introduced a so-called g function to study problems where the Riemann–Hilbert problem is qualitatively different and involves Riemann surfaces of genus 1 in [23]. This method since then has become the well-established tool to study Riemann–Hilbert problem. We try to control the exponentials and study the asymptotics of the Riemann–Hilbert problem by introducing an auxiliary scalar function g with suitable jumps. This breaks down the Riemann–Hilbert problem into several steps which are better suited for study. The idea is similar to the steepest descent method, where the asymptotics of an exponential type integral is expressed by information at certain points on the contour, and there is negligible exponential decay elsewhere on the contour. The Deift–Zhou steepest descent method is a well-known technique in the field, yet in this Chapter we still try to motivate the construction of the g-function. The reasons for this are twofold: 1) this is central to the analysis and while the technique is well-known, it took some time to learn and we wish to document the details for future reference; and 2) motivating the old g-function also helps to explain how to change the new $\mathfrak{g}$ near the gradient catastrophe point.

3.1 The g-function and the Deift-Zhou steepest descent method

Let's take a look at how we can proceed to analyse the Riemann–Hilbert problem 2. The jump condition (2.46) contains the essential piece of information that is going to give us

the asymptotics of $\mathbf{M}$. Due to the presence of the coefficients of ϵ_N^{-1} in the exponents, the exponential factor is going to make significant contributions to the asymptotics.

Recall the idea of steepest descent. In an oversimplified summary: suppose we are doing an exponential type of integral, where we can deform the contour to a path that passes through the saddle point and following the direction of steepest descent, then the leading contribution will be from the saddle point alone.

Similarly, the Deift–Zhou steepest descent method seeks to simplify the exponential factors in the jump condition by identifying the the significant contributions and neglecting the exponentially small terms. In the case of matrix functions however, the significant contributions will not always come from isolated points. Indeed, in some cases there are whole arcs of the jump contour on which the jump matrix is not negligible but rather converges to constant but non-identity values. As it turns out, neglecting all but these arcwise-constant jumps leads to a model Riemann-Hilbert problem that can be solved exactly.

Convention

When we set up the Riemann–Hilbert problem or discuss the jumps on the boundary, we use variable ξ instead of w. ξ is still the complex spectral variable,. However, where it is used, we are emphasizing that we are evaluating a function on a contour, i.e. a 1-dimensional manifold instead of an open set in the complex plane.

3.1.1 Introducing the g-function

The way we simplify the jump in order to control the exponentials is to introduce an auxiliary scalar g-function in our matrix function. Let

$$\mathbf{N}(w) := \mathbf{M}(w)e^{-g(w)\sigma_3/\epsilon_N}. \tag{3.1}$$

We do not want g to disturb the structure of our jump contours. The matrix function $\mathbf{N}$ should have the same regions of analyticity, same jump on the positive real axis, the Schwarz symmetry and same normalisation at infinity. These will translate into conditions we place on g as:

$$g(w) \text{ is analytic in } \mathbb{C}\backslash(\mathbb{R}_+ \cup \Sigma_\pm),$$

$$g_+(\xi) + g_-(\xi) = 0, \quad \xi \in \mathbb{R}_+, \tag{3.2}$$

$$g(w) = g(w^*)^*, \tag{3.3}$$

$$\lim_{w\to\infty} g(w) = 0. \tag{3.4}$$

To see (3.2), we give a simple proof.

Proof. Recall the jump of $\mathbf{M}$ on the real line is

$$\mathbf{M}_+(\xi) = \sigma_2 \mathbf{M}_-(\xi)\sigma_2, \quad \xi \in \vec{\mathbb{R}}_+. \tag{3.5}$$

Combining with the definition of $\mathbf{N}$ in (3.1), the jump for $\mathbf{N}$ in $\mathbb{R}_+$ is:

$$\mathbf{N}_+(\xi) = \sigma_2 \mathbf{N}_-(\xi) e^{g_-\sigma_3/\epsilon_N} \sigma_2 e^{-g_+\sigma_3/\epsilon_N} \sigma_2^2. \tag{3.6}$$

In order for $\mathbf{N}$ to have the same jump as $\mathbf{M}$ on $\mathbb{R}_+$, on the right hand side of the jump condition (3.6) sandwiched between $\mathbf{N}_-$ and the last σ_2 must be identity:

$$\begin{bmatrix} e^{g_-/\epsilon_N} & 0 \\ 0 & e^{-g_-/\epsilon_N} \end{bmatrix} \begin{bmatrix} & -i \\ i & \end{bmatrix} \begin{bmatrix} e^{-g_+/\epsilon_N} & 0 \\ 0 & e^{g_+/\epsilon_N} \end{bmatrix} \begin{bmatrix} & -i \\ i & \end{bmatrix} = \begin{bmatrix} e^{(g_+ + g_-)/\epsilon_N} & 0 \\ 0 & e^{-(g_+ + g_-)/\epsilon_N} \end{bmatrix}. \tag{3.7}$$

In order for this matrix to be the identity, we require $g_+(\xi) + g_-(\xi) = 0$ on $\mathbb{R}_+$. □

This also implies $g'_+(\xi) + g'_-(\xi) = 0$ on $\mathbb{R}_+$.

We will investigate the jump of g on $\Sigma = \Sigma_+ \cup \Sigma_- \cup \Sigma_\mp$ soon. Essentially, we will be solving a Riemann–Hilbert problem for a scalar function. The benefit is that while we have fewer tools for a general matrix Riemann–Hilbert problem, for scalar analytic functions, we have the Cauchy integral theory at our disposal to help us construct g explicitly. A general reference for the theory of Cauchy integrals, singular integral equations, boundary-value problems for complex functions, and the Plemelj formula is [41]. Notice here that up to now Σ is just the boundary of a region that encloses all the poles in Riemann–Hilbert problem 1, the location of the boundary, like the integration contours in standard steepest descent methods, is somewhat arbitrary and will be chosen later. We are going to position the contours to help us best to identify the asymptotic behaviours.

On certain part of the boundaries of $\Omega_\pm$ either $T(w)$ or $Y(w)$ occur as ingredients in the approximation of the Blaschke product $\prod_N$. The point is that they are both $1+\mathcal{O}(\epsilon_N)$ and will not affect the asymptotics more significantly than $\mathcal{O}(\epsilon_N)$. From (3.1), it follows that $\mathbf{N}$ has the following jump along Σ:

$$\mathbf{N}_+(\xi) = \mathbf{N}_-(\xi) \begin{bmatrix} e^{-(g_+(\xi)-g_-(\xi))/\epsilon_N} & 0 \\ -ie^{[L(\xi)+2iQ(\xi)\mp i\theta_0(\xi)-(g_+(\xi)+g_-(\xi))]/\epsilon_N} + \mathcal{O}(\epsilon_N) & e^{(g_+(\xi)-g_-(\xi))/\epsilon_N} \end{bmatrix}, \quad \xi \in \Sigma, \tag{3.8}$$

Define the phases as

$$\theta(\xi) := i(g_+(\xi) - g_-(\xi)), \tag{3.9}$$

$$\phi(\xi) := 2iQ(\xi) + L^0(\xi) \pm i\theta_0(\xi) - (g_+(\xi) + g_-(\xi)) \quad \xi \in \mathbb{C}_\pm. \tag{3.10}$$

Therefore the jump matrix we wish to control can be rewritten as

$$\begin{bmatrix} e^{i\theta/\epsilon_N} & 0 \\ -ie^{\phi/\epsilon_N} & e^{-i\theta/\epsilon_N} \end{bmatrix} = \begin{bmatrix} e^{i\theta/\epsilon_N} & 0 \\ -ie^{\phi/\epsilon_N} & e^{-i\theta/\epsilon_N} \end{bmatrix}, \tag{3.11}$$

which also admits the following factorisation:

$$= \begin{bmatrix} 1 & ie^{(i\theta-\phi)/\epsilon_N} \\ 0 & 1 \end{bmatrix} \begin{bmatrix} 0 & -ie^{-\phi/\epsilon_N} \\ -ie^{\phi/\epsilon_N} & 0 \end{bmatrix} \begin{bmatrix} 1 & ie^{(-i\theta-\phi)/\epsilon_N} \\ 0 & 1 \end{bmatrix}. \tag{3.12}$$

Because

$$\begin{aligned} i\theta - \phi =& -2iQ - L^0 \pm i\theta_0 + g_+ + g_- - g_+ + g_- = -2iQ - L^0 \pm i\theta_0 + 2g_-, \\ -i\theta - \phi =& g_+ - g_- - 2iQ - L^0 \pm i\theta_0 + g_+ + g_- = -2iQ - L^0 \pm i\theta_0 + 2g_+. \end{aligned} \tag{3.13}$$

The second factorised jump matrix can be written as

$$\begin{bmatrix} 1 & ie^{(-2iQ-L^0\pm i\theta_0+2g_-)/\epsilon_N} \\ 0 & 1 \end{bmatrix} \begin{bmatrix} 0 & -ie^{-\phi/\epsilon_N} \\ -ie^{\phi/\epsilon_N} & o \end{bmatrix} \begin{bmatrix} 1 & ie^{(-2iQ-L^0\pm i\theta_0+2g_+)/\epsilon_N} \\ 0 & 1 \end{bmatrix}. \tag{3.14}$$

In the next subsection, we consider what properties θ and ϕ need to have for the steepest descent analysis.

3.1.2 Desired properties of g

From the jump conditions (3.11) and (3.12), the jump matrix on Σ that produces the leading asymptotics is

$$\begin{bmatrix} e^{i\theta/\epsilon_N} & 0 \\ -ie^{\phi/\epsilon_N} & e^{-i\theta/\epsilon_N} \end{bmatrix} = \begin{bmatrix} 1 & ie^{(i\theta-\phi)/\epsilon_N} \\ 0 & 1 \end{bmatrix} \begin{bmatrix} 0 & -ie^{-\phi/\epsilon_N} \\ -ie^{\phi/\epsilon_N} & 0 \end{bmatrix} \begin{bmatrix} 1 & ie^{(-i\theta-\phi)/\epsilon_N} \\ 0 & 1 \end{bmatrix}. \tag{3.15}$$

Suppose that $\theta = 0$ and $\mathrm{Re}(\phi) < 0$, then the jump matrix ion the left hand side tends to identity matrix exponentially fast as $\epsilon_N \to 0$. Thus this part of the contour will not contribute to the asymptotics. However, this will not be true for the whole jump contour. One reason is because the behaviour of the solution suggests the elliptic function in the

background, which in turn suggests that the solution to the Riemann–Hilbert problem is produced by genus-1 Riemann theta functions. This relates to the g-function having a significant jump on Σ.

The right hand side factorised the matrix into three matrices. To use the other form of the jump matrix, we connect two ends of an arc with two additional curves, and then build the jump matrices by these three matrices. The original arc has the middle matrix as its jump matrix. We choose the arc in such a way that ϕ will be a constant. See figure 3.1. On the two additional arcs, we make sure the real part of the exponentials has the right sign to decay exponentially fast. Thus they will not contribute to the asymptotics. This procedure is standard in the Deift–Zhou steepest descent method, and is called *opening a lens* [23].

We have discussed that for t small, another configuration to set up the Riemann–Hilbert problem is needed. Since the two setups result in the identical g function for t not so small, we can continue the current setup from the other when t starts evolving. Therefore, we can use the known results near $t = 0$ from [13]. Later on, we demonstrate that at $t = 0$, $\phi \leq 0$ on γ.

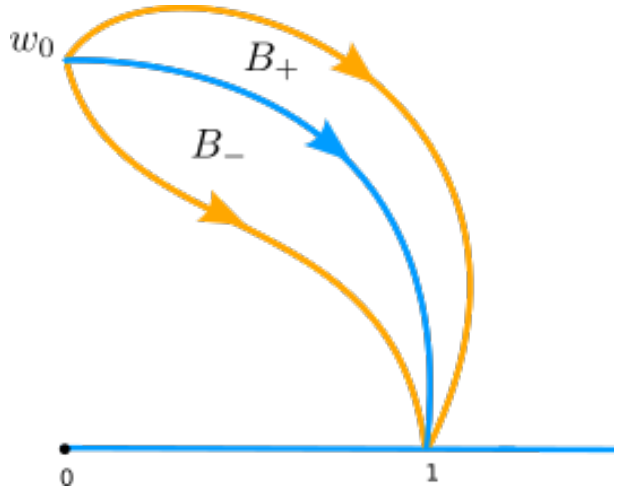

Figure 3.1: Opening a lens

Modify the matrix value inside the two lenses in the following way:

$$\mathbf{O}(w) = \begin{cases} \mathbf{N} \begin{bmatrix} 1 & -ie^{(-i\theta-\phi)/\epsilon_N} \\ 0 & 1 \end{bmatrix}, & w \in B_+, \\ \mathbf{N} \begin{bmatrix} 1 & ie^{(i\theta-\phi)/\epsilon_N} \\ 0 & 1 \end{bmatrix}, & w \in B_-, \\ \mathbf{N}, & \text{otherwise.} \end{cases} \tag{3.16}$$

Let's name the contour where we use the factorized version of the jump matrix in (right hand side of (3.15)) as the **bands**. On the bands, we require the phase ϕ to be imaginary constants, while $i\theta$ has positive real part in B_+ and negative real part in B_+.

How can we make sure the real part of $i\theta$ has the right sign in the specified regions? Observe in figure 3.2. Choose unit vectors $\hat{n}$ orthogonal to β and $\hat{s}$ tangent to β. Suppose

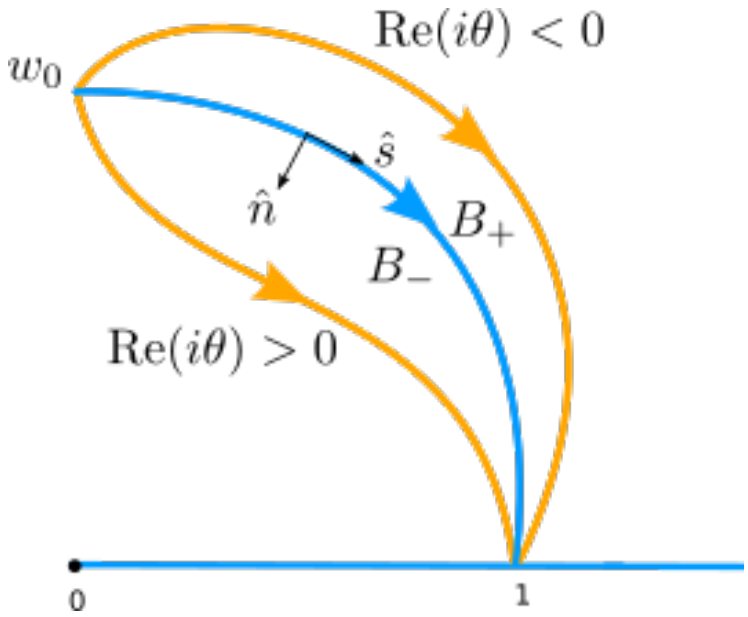

Figure 3.2: $\mathrm{Re}(i\theta)$ sign

on the band $i\theta$ is purely imaginary, while θ has positive directional derivative $\frac{\mathrm{d}}{\mathrm{d}s}\theta$ along the band (thus increasing), then following the Cauchy–Riemann condition, the derivative of $\mathrm{Re}(i\theta)$ along the orthogonal direction $\hat{n}$ is positive real. Thus, if the lens is close enough the the band, $\mathrm{Re}(i\theta)$ will have the desired sign.

Next, let's call the other part of the contour the **gaps**. On the gaps we will use the original jump (left hand side of (3.15)). We would like for the jump to go to the identity matrix exponentially fast. Therefore, on the gaps we demand $\theta \equiv 0$ and $\mathrm{Re}(\phi) < 0$.

We will call the bands β_i and the gaps γ_i. We formulate the requirement on the bands and gaps. We want the exponentials to have the following properties:

Bands:
$\phi(w) =$ imaginary constant,
$\theta(w) =$ real increasing function,

Gaps:

$\mathrm{Re}(\phi(w)) < 0$,
$\theta(w) \equiv 0$.

3.1.3 The scalar RH problem for $g(w)$

Next we will formalize the requirements we have made on g. Firstly, since some conditions we asked for g and the phase θ and ϕ are unknown constants, it is easier for us to formulate the jump conditions in terms of their derivatives, in which case, all constants will become zero.

Riemann–Hilbert Problem 3.1.1 (Scalar Riemann–Hilbert problem)**.** Seek a function $g'(w)$ satisfying the following conditions:

(1.) $\xi \in$ bands,

$$g'_+(\xi) + g'_-(\xi) = 2iQ'(\xi) + L^{0\prime}(\xi) \mp i\theta^{0\prime}(\xi), \quad \xi \in \beta_\pm, \tag{3.17}$$

(2.) $\xi \in$ gaps

$$g'_+(\xi) - g'_-(\xi) = 0, \tag{3.18}$$

(3.)

$$g'(w) = g'(w^*)^*, \tag{3.19}$$

(4.)

$$g'(w) = O(w^{-2}), \qquad w \to \infty \tag{3.20}$$

(5.)

$$g'_+(\xi) + g'_-(\xi) = 0, \qquad w \in \vec{\mathbb{R}}_+ \tag{3.21}$$

3.1.4 Constructing the g-function

Right now we have not determined where the bands or the gaps are. In particular, their endpoints. The simplest case is to put one band and one gap in each half plane. Indeed, roughly speaking, for sine-Gordon equations, on each band the constant phase ϕ in the jump gives rise to one highly oscillatory phase in the leading asymptotics. Before the first qualitative change which we call the first breaking, the solution looks like the single phase oscillation. Thus the behaviour of the solution confirms our use of one band and one gap.

Because of Schwarz symmetry, we can, without loss of generality, consider the problem in the upper half plane. Sometimes for simplicity I will only give description for the upper half plane.

Define the derivative of the g-function as $f(w)$. Suppose the band starts at 1 and ends at w_0 and $w_1 = w_0^*$. $w_0 = p + i\sqrt{-q}$ and $w_1 = p - i\sqrt{-q}$, where p and q are positive real numbers. In order to build $f = g'$ that has a branch cut on the band, we use a standard trick. We define a function $R(w)$ that has branch cut and opposite values on two sides of the band, i.e.

$$R^2(w) := (w - w_0)(w - w_1), \qquad R \to w \text{ when } w \to \infty. \tag{3.22}$$

Take the branch cut of R along β (the bands). Equivalently

$$R(w; p, q)^2 = (w - p)^2 - q, \qquad R \to w \text{ when } w \to \infty. \tag{3.23}$$

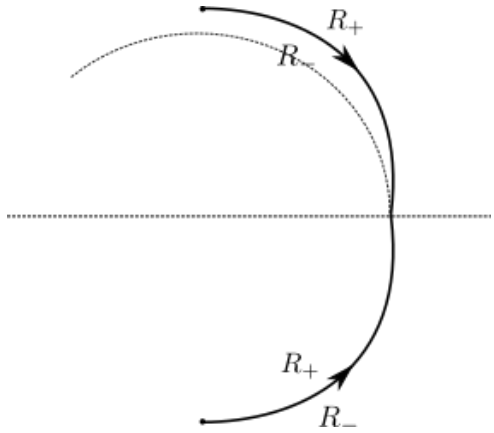

Figure 3.3: R and β

From the Riemann–Hilbert problem 3.1.3, f has cut along the bands β and $\mathbb{R}_+$. Set

$$f(w) = \frac{R(w)h(w)}{\sqrt{-w}} \qquad \Longrightarrow \qquad h(w) = \frac{f(w)\sqrt{-w}}{R(w)}, \tag{3.24}$$

where $\sqrt{-w}$ denotes the principal branch, with cut on $\mathbb{R}_+$.

Using the conditions in Riemann–Hilbert problem 3.1.3, h needs to satisfy

1.) $\xi \in \beta$

$$h_+(\xi)R_+(\xi)\frac{1}{\sqrt{-\xi}} - h_-(\xi)R_+(\xi)\frac{1}{\sqrt{-\xi}} = 2iQ'(\xi) + L^{0\prime}(\xi) \mp i\theta_0{}'(\xi), \quad \xi \in \beta_\pm, \tag{3.25}$$

which is equivalent to

$$h_+(\xi) - h_-(\xi) = \frac{(2iQ'(\xi) + L^{0\prime}(\xi) \mp i\theta_0'(\xi))\sqrt{-\xi}}{R_+(\xi)}, \quad \xi \in \beta_\mp \tag{3.26}$$

2.) h preserves the Schwarz symmetry

$$h(w) = h(w^*)^* \tag{3.27}$$

3.)

$$g' = O(w^{-2}), \quad w \to \infty \qquad \Longrightarrow \qquad h = \frac{g'\sqrt{-w}}{R(w)} = O(w^{-\frac{5}{2}}), \quad w \to \infty. \tag{3.28}$$

Therefore, by the Plemelj formula,

$$\begin{aligned} h(w) =& \frac{1}{2\pi i} \int_{\beta_\pm} \frac{(2iQ'(s) + L^{0\prime}(s) \mp i\theta_0'(s))\sqrt{-s}}{R_+(s)(s-w)} \mathrm{d}s \\ f(w) =& \frac{R(w)}{2\pi i\sqrt{-w}} \int_{\beta_\pm} \frac{(2iQ'(s) + L^{0\prime}(s) \mp i\theta^{0\prime}(s))\sqrt{-s}}{R_+(s)(s-w)} \mathrm{d}s. \end{aligned} \tag{3.29}$$

3.1.5 Rewriting the formula for f

Using the fact that R has opposite signs across β, we can rewrite f as the average of the integral along $\vec{\beta}$ plus side and $-\vec{\beta}$ minus side. Then using the integrability of h at the end point w_0 and w_1, we blow up both sides of the contour β, and name it C_1 as shown in figure 3.4. Thus we have a closed contour.

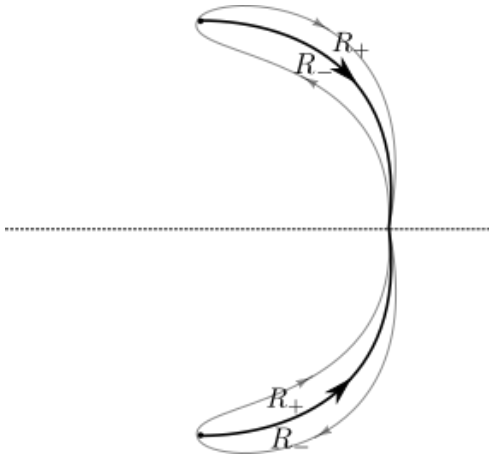

Figure 3.4: C_β

The integral evaluates the same,

$$f(w) = \frac{R(w)}{4\pi i\sqrt{-w}} \int_{C_\beta} \frac{(2iQ'(s) + L^{0\prime}(s) \mp i{\theta_0}'(s))\sqrt{-s}}{R(s)(s-w)} \mathrm{d}s. \tag{3.30}$$

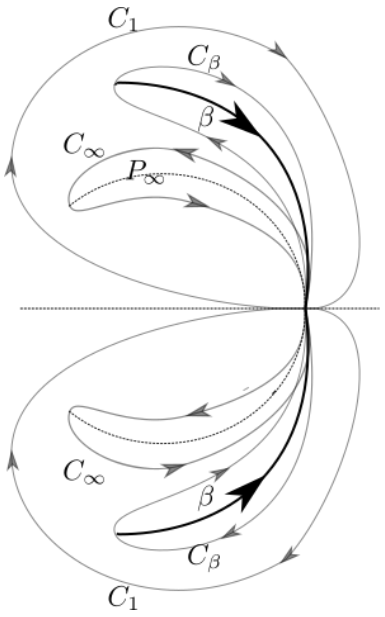

Figure 3.5: The three curves C_1, C_β and C_∞

To complete the steepest descent analysis procedures, we want the γ curve to go around back to 1. However, recall L^0 in the integrand in equation (3.30) has a jump discontinuity along P_∞. It is inconvenient for γ to cross P_∞ for the following construction of g-function. Therefore we introduce two more contours, C_1 and C_∞, as shown in figure 3.5. Like C_β enclosing β, C_∞ encloses P_∞. Next we are going to rewrite the formula of $f(w)$. The $2iQ'\sqrt{-s}/(R(s)(s-w))$ term in the integrand h has simple poles at 0 and w. We can use residue theory to extract the value of the integral contributed by the residue. Furthermore, we can also deform the contour so it does not depend on the now still undetermined band β curve. Note here that the end point of β, w_0 and w_1, will still depend on the space and time parameters (x,t) that are independent variables in the sine-Gordon equation.

First, deform the lobe C_β so w is inside. The residue at w is:

$$\frac{R(w)}{4\pi i\sqrt{-w}}\int_{B_{(w,\epsilon)}}\frac{(2iQ'(s)+L^{0\prime}(s)\mp i\theta_0'(s))\sqrt{-s}}{R(s)(s-w)}\mathrm{d}s = iQ'(w;x,t)+\frac{1}{2}\frac{\mathrm{d}}{\mathrm{d}w}L^0(w)\mp i\frac{1}{2}\frac{\mathrm{d}}{\mathrm{d}w}\theta_0(w). \tag{3.31}$$

After picking up the residue at w,

$$\begin{aligned} f(w) :=& iQ'(w;x,t) + \frac{1}{2}\frac{\mathrm{d}}{\mathrm{d}w}L^0(w) + \frac{R(w;p,q)}{4\pi\sqrt{-w}}\int_{C_{\beta_\pm}} \frac{(2iQ'(s) + L^{0\prime}(s) \mp i{\theta_0}'(s))\sqrt{-s}\mathrm{d}s}{R(s;p,q)(s-w)} \\ &+ \begin{cases} -i\frac{1}{2}\frac{\mathrm{d}}{\mathrm{d}w}\theta_0(w) & w \in \mathbb{C}_+, \\ i\frac{1}{2}\frac{\mathrm{d}}{\mathrm{d}w}\theta_0(w) & w \in \mathbb{C}_-. \end{cases} \end{aligned} \tag{3.32}$$

Deforming C_β to C_∞ and C_1 (because L^0 has a jump along P_∞), we obtain a new expression for f

$$\begin{aligned} f(w) :=& i\frac{\mathrm{d}Q}{\mathrm{d}w}(w;x,t) + \frac{1}{2}\frac{\mathrm{d}}{\mathrm{d}w}L^0(w) \mp i\frac{1}{2}\frac{\mathrm{d}}{\mathrm{d}w}\theta_0(w) + \frac{R(w;p,q)}{4\pi i\sqrt{-w}}\int_{C_\infty} \frac{L^{0\prime}(s)\sqrt{-s}}{R(s;p,q)(s-w)}\mathrm{d}s \\ &+ \frac{R(w;p,q)}{2\pi i\sqrt{-w}}\int_{C_1} \frac{(2iQ'(s) + L^{0\prime}(s) \mp i{\theta_0}'(s))\sqrt{-s}\mathrm{d}s}{R(s;p,q)(s-w)}. \end{aligned} \tag{3.33}$$

The integral along C_1 can be further simplified by calculating the residue at 0, which comes from the simple pole in the $Q'(s)\sqrt{-s}$ term. Notice that although in general the integrand in h has a branch cut on $\mathbb{R}_+$, for $Q(s)\sqrt{-s}$ they cancel out.

$$\begin{aligned} Q'(s) =& \frac{\mathrm{d}}{\mathrm{d}s}\left(\frac{i}{4}\left(E(s)x + D(s)t\right)\right) = \frac{i}{4}\frac{\mathrm{d}}{\mathrm{d}s}\left[\left(\sqrt{-s} + \frac{1}{\sqrt{-s}}\right)x + \left(\sqrt{-s} - \frac{1}{\sqrt{-s}}\right)t\right] \\ =& -\frac{i}{4}\cdot\left(\frac{1}{-s}\right)^{-\frac{3}{2}}\cdot\left(-\frac{1}{2}\right)(x-t) + \text{other terms}. \end{aligned} \tag{3.34}$$

The s^{-1} power in $Q'(s)\sqrt{-s}$ is $\frac{i}{8}\frac{1}{2s}(x-t)$. Therefore,

$$\begin{aligned} \frac{R(w)}{4\pi i\sqrt{-w}}\int_{B_{(0,\epsilon)}} \frac{2iQ'(s)\sqrt{-s}}{R(s)(s-w)}\mathrm{d}s =& \frac{R(w)}{4\pi i\sqrt{-w}}\int_{B_{(0,\epsilon)}} -2\left(\frac{x-t}{8}\frac{1}{2s}\right)\frac{1}{R(s)(s-w)}\mathrm{d}s \\ =& -\frac{R(w)}{\sqrt{-w}}\cdot\left(\frac{x-t}{8}\right)\frac{1}{R(0)(-w)} = \frac{x-t}{8}\frac{R(w)}{w(-w)^{\frac{1}{2}}\sqrt{p^2-q}}. \end{aligned} \tag{3.35}$$

Collapsing C_∞ along P_∞,

$$\begin{aligned}\frac{R(w;p,q)}{4\pi i\sqrt{-w}}\int_{C_\infty}\frac{L^{0\prime}\sqrt{-s}}{R(s;p,q)(s-w)}\mathrm{d}s &= -\frac{R(w;p,q)}{4\pi i\sqrt{-w}}\int_{P_\infty}\frac{(L_+^{0\,\prime}(s)-L_-^{0\,\prime}(s))\sqrt{-s}}{R(s;p,q)(s-w)}\mathrm{d}s\\ &= -\frac{R(w;p,q)}{2\pi i\sqrt{-w}}\int_{P_\infty}\frac{i\theta_0'(s)\sqrt{-s}}{R(s;p,q)(s-w)}\mathrm{d}s.\end{aligned} \tag{3.36}$$

We combine (3.35) and (3.36). Observe that one can collapse C_1 to $P_{\infty-}\cup\beta_+$ and a straight line connecting A and w_0, while in the lower half plane, from w_1 to A^*. The direction is reversed in the lower half plane (so the integral has a Schwarz-symmetric form). This pair of lines is denoted by γ_0, see figure 3.6. The integral with the $i\theta_0'$ term cancels on P_∞ and β. It follows that

$$\begin{aligned}f(w) :=& \frac{x-t}{8}\frac{R(w;p,q)}{w(-w)^{\frac{1}{2}}\sqrt{p^2-q}}+i\frac{\mathrm{d}Q}{\mathrm{d}w}(w;x,t)+\frac{1}{2}\frac{\mathrm{d}}{\mathrm{d}w}L^0(w)\\ &\mp i\frac{1}{2}\frac{\mathrm{d}}{\mathrm{d}w}\theta_0(w)-\frac{R(w;p,q)}{2\pi\sqrt{-w}}\int_{\gamma_0}\frac{\theta_0{}'(s)\sqrt{-s}}{R(s;p,q)(s-w)}\mathrm{d}s.\end{aligned} \tag{3.37}$$

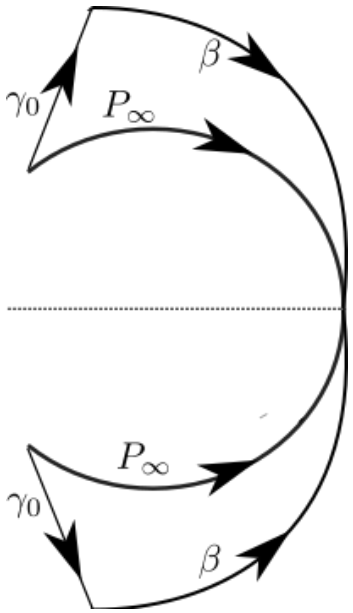

Figure 3.6: γ_0

Assuming the integrand has proper decay at infinity, and the WKB integral associated with the initial condition (2.7) is an entire function (generally not true, we only assume θ_0 is analytic in a neighbourhood of P_∞), then one can also deform C_1 to infinity and along the real line. Notice, the integral cancels on the positive real axis. In this deformation, f

has the form

$$\begin{aligned} f(w) :=& \frac{x-t}{8}\frac{R(w;p,q)}{w(-w)^{\frac{1}{2}}\sqrt{p^2-q}} + i\frac{\mathrm{d}Q}{\mathrm{d}w}(w;x,t) + \frac{1}{2}\frac{\mathrm{d}}{\mathrm{d}w}L^0(w) \mp i\frac{1}{2}\frac{\mathrm{d}}{\mathrm{d}w}\theta_0(w) \\ &- \frac{R(w;p,q)}{2\pi\sqrt{-w}}\int_{P_\infty}\frac{{\theta_0}'(s)\sqrt{-s}}{R(s;p,q)(s-w)}\mathrm{d}s - \frac{R(w;p,q)}{2\pi\sqrt{-w}}\int_{-\infty}^{0}\frac{{\theta_0}'(s)\sqrt{-s}}{R(s;p,q)(s-w)}\mathrm{d}s. \end{aligned} \tag{3.38}$$

This formulation is particularly useful when we are proving certain quantities are real valued, or in numerical simulation. It utilises the Schwarz symmetry, and avoids the branch cuts that shows up in the numerical computation.

Another deformation useful for the analysis is to use the fact that R has opposite signs along β to make two copies of $\gamma_0 \cup \beta$ and make two lobes that contain both β and P_∞. Name this contour C (see figure 3.7). Under this construction, f has the form

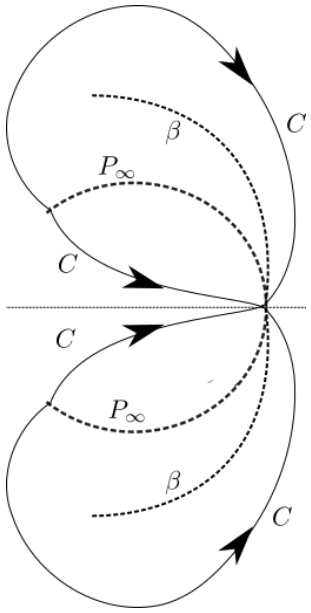

Figure 3.7: Contour C

$$\begin{aligned} f(w) :=& \frac{x-t}{8}\frac{R(w;p,q)}{w(-w)^{\frac{1}{2}}\sqrt{p^2-q}} + i\frac{\mathrm{d}Q}{\mathrm{d}w}(w;x,t) + \frac{1}{2}\frac{\mathrm{d}}{\mathrm{d}w}L^0(w) \\ &\mp i\frac{1}{2}\frac{\mathrm{d}}{\mathrm{d}w}\theta_0(w) - \frac{R(w;p,q)}{4\pi\sqrt{-w}}\int_{C}\frac{{\theta_0}'(s)\sqrt{-s}}{R(s;p,q)(s-w)}\mathrm{d}s. \end{aligned} \tag{3.39}$$

3.1.6 Constructing the desired properties of g, introducing M, H and I

Define:

$$g(w) := \int_0^w f(s)\mathrm{d}s. \tag{3.40}$$

Let's see how many of the desired properties of g are already satisfied and what else we need from equation (3.25) to (3.28). The jump condition on β (3.25) and on is automatically built in from the construction using the Cauchy integral along β. The jump on $\mathbb{R}_+$ is ensured by the $\sqrt{-w}$ factor. Note g automatically has Schwarz symmetry from construction. Recall that θ is the jump of g. Since g is analytic on γ, $\theta \equiv 0$ on γ as well. So we still need the following:

1.)

$$\lim_{w\to\infty} g(w) = 0, \quad w \to \infty, \tag{3.41}$$

2.)

$$\phi(\xi) \equiv \pm i\Phi, \quad w \in \beta_\pm \text{ for some real } \Phi, \tag{3.42}$$

3.)

$$\theta \text{ is real and monotone on } \beta, \tag{3.43}$$

4.)

$$\mathrm{Re}(\phi) < 0 \text{ on } \gamma. \tag{3.44}$$

We consider each condition in turn.

For (3.41), recall h is $\dfrac{g'\sqrt{-w}}{R(w)}$. Since h is defined by the Cauchy integral of a piecewise analytic function in a finite contour, h admits a Laurent expansion. Thus, $g \to 0$ at infinity implies the $\frac{1}{w}$ term in h's expansion at infinity has to be 0. Or equivalently, the $w^{-1/2}$ is 0 for the expansion of f at infinity.

Expanding f in (3.30), the coefficient of $\frac{1}{\sqrt{-w}}$ is

$$\frac{1}{8}\left(x + t + \frac{x-t}{\sqrt{p^2-q}} - \frac{4}{\pi}\int_{\gamma_0} \frac{\theta_0'(s)\sqrt{-s}}{R(s;p,q)(s-w)}\mathrm{d}s.\right) \tag{3.45}$$

Define the quantity we want to be identically 0 as

$$M(w;x,t,p,q) = x + t + \frac{x-t}{\sqrt{p^2-q}} - \frac{4}{\pi}\int_{\gamma_0} \frac{\theta_0'(s)\sqrt{-s}}{R(s;p,q)(s-w)}\mathrm{d}s \equiv 0. \tag{3.46}$$

The equation (3.46) only implies the g' is decaying fast enough. There is still the integration constant

$$g(\infty) = \int_0^\infty f(s)\mathrm{d}s \tag{3.47}$$

that we need to confirm is zero.

We integrate along $\mathbb{R}_-$ to $-\infty$. Since f is jump free on the negative real axis, we can split it into two parts and deform it to the positive axis but circumventing $\beta_\pm$. Since $f_+ + f_- = 0$, the two parts cancel out along $\mathbb{R}_+$. So what remains is the integral along β, (see figure below) i.e.

$$\int_{\vec{\beta}} f_+ - f_-(s)\mathrm{d}s \tag{3.48}$$

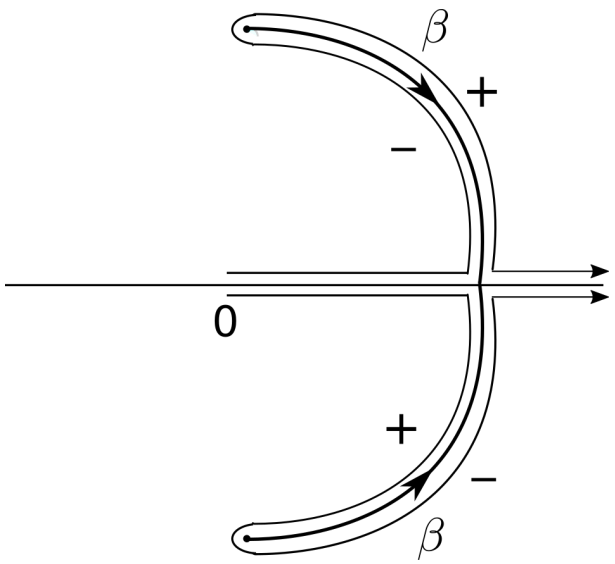

Figure 3.8: $g(\infty)$ contour of integration

Computing $f_+(\xi) - f_-(\xi)$, we find that

$$\begin{aligned} f_+(\xi) - f_-(\xi) =& R_+(\xi;p,q)\left(\frac{x-t}{4\xi\sqrt{p^2-q}\sqrt{-\xi}} + \frac{1}{2\pi\sqrt{-\xi}}\int_C \frac{\theta_0'(s)\sqrt{-s}\mathrm{d}s}{R(s;p,q)(s-\xi)}\right) \\ =& -R_+(\xi)H(\xi;p,q,x,t), \quad \xi\in\beta. \end{aligned} \tag{3.49}$$

Here we define H as

$$H(w;p,q,x,t) := -\frac{1}{4\sqrt{-w}}\left(\frac{x-t}{w\sqrt{p^2-q}} - \frac{2}{\pi}\int_{C_1}\frac{\theta_0'(s)\sqrt{-s}\mathrm{d}s}{R(s;p,q)(s-w)}\right). \tag{3.50}$$

Then (3.48) is equivalent to

$$\begin{aligned} I(x,t,p,q) :=& \mathrm{Re}\left\{\int_{\beta_+} R_+(\xi)H(\xi)\mathrm{d}\xi\right\} \\ =& \frac{1}{2}\left\{\int_{\beta_+} R_+(\xi)H(\xi)\mathrm{d}\xi + \frac{1}{2}\int_{\beta_-} R_-(\xi)H(\xi)\mathrm{d}\xi\right\} \equiv 0. \end{aligned} \tag{3.51}$$

Next, for (3.42), by the formula for f in (3.30), it can be simply verified that

$$f_+(\xi) + f_-(\xi) = 2i\frac{\mathrm{d}Q}{\mathrm{d}\xi}(\xi; x, t) + \frac{\mathrm{d}L^0}{\mathrm{d}\xi}(\xi) \mp i\theta_0(\xi), \quad \xi \in \beta_\pm. \tag{3.52}$$

Thus, by definition of ϕ , it has to be a constant along the β curve.

Furthermore, it is handy for us to have a formula for $\dfrac{\mathrm{d}\theta}{\mathrm{d}\xi}$ and $\dfrac{\mathrm{d}\phi}{\mathrm{d}\xi}$ on β and γ respectively, in order to evaluate ϕ or θ later. A direct consequence of (3.49) gives

$$\frac{\mathrm{d}\theta}{\mathrm{d}\xi}(\xi) = iR_+(\xi; p, q)H(\xi), \quad \xi \in \beta. \tag{3.53}$$

On the other hand, on γ, we directly compute $f_+ + f_-$ from (3.30), and find

$$2i\frac{\mathrm{d}Q}{\mathrm{d}\xi}(\xi; x, t) + \frac{\mathrm{d}L}{\mathrm{d}\xi}(\xi) - f_+(\xi) - f_-(\xi) = R(\xi)H(\xi), \quad \xi \in \gamma. \tag{3.54}$$

Comparing to definition of ϕ (3.10), we obtain

$$\frac{\mathrm{d}\phi}{\mathrm{d}\xi}(\xi) = R(\xi; p, q)H(\xi), \quad \xi \in \gamma. \tag{3.55}$$

Among the desired properties, θ monotone is going to come after we have defined β in proposition 3.1.6. See [13] for details.

So far, in this section we found that in order for g to satisfy the properties we need, we have to impose two more conditions: $M \equiv 0$ and $I \equiv 0$. Once these conditions are all satisfied, we still need to have $\mathrm{Re}(\phi) < 0$. Indeed, the behaviour of $\mathrm{Re}(\phi)$ will characterise the first breaking of the qualitative behaviour of the solution, which we will study next. Also, we proved some useful properties of θ, ϕ and the g-function.

To summarise, in this section we proved

Proposition 3.1.1. *Suppose $M(x, t, p, q) \equiv 0$ and $I(x, t, p, q) \equiv 0$, then*

$$g(w^*) = g(w)^*, \tag{3.56}$$

$$\lim_{w\to\infty} g(w) = 0, \tag{3.57}$$

$$\phi(\xi) \equiv \pm i\Phi \text{ on } \beta_\pm, \ \Phi \text{ real}, \tag{3.58}$$

$$\theta(\xi) \text{ is real and monotone on } \beta, \tag{3.59}$$

$$\frac{\mathrm{d}\phi}{\mathrm{d}\xi}\phi = R(\xi; p, q)H(\xi) \text{ on } \gamma, \tag{3.60}$$

$$\frac{\mathrm{d}\theta}{\mathrm{d}\xi}\theta = -iR_+(\xi;p,q)H(\xi) \text{ on } \beta. \tag{3.61}$$

Note we have not discussed the sign of $\mathrm{Re}(\phi)$ yet. In fact this condition turns out to be crucial in analyzing the behaviour of the solution to the sine-Gordon equation.

3.1.7 Other properties of g

Here are some other known properties about g that can be found in [13, Chapter 4], where interested readers can find more details. We will quote without proof.

Proposition 3.1.2. *At $t = 0$, the equations $M \equiv 0$ and $I \equiv 0$ are satisfied identically if*

$$p = p(x) = 1 - \frac{1}{2}G(x)^2, \quad x \in \mathbb{R} \tag{3.62}$$

and $q = q(x) = p(x)^2 - 1$.

In fact, this proposition is also a special case of the M and H symmetry in the next section, which we will prove in details.

Proposition 3.1.3. *At $t = 0$, β coincides with the arc of the unit circle, and*

- $\Phi = 0$,
- $\phi < 0$ *on γ except for in a neighbourhood of the endpoints.*
- θ *is real, monotone nondecreasing on β,*
- $H(\xi)$ *is bounded away from 0 on γ.*

Proposition 3.1.4. *Recall $w_{0,1}$ are the two roots of R as well as the two ends of β. For $k = 0, 1$,*

$$\frac{\partial M}{\partial w_k} = 2\sqrt{-w_k}H(w_k) \tag{3.63}$$

$$\frac{\partial I}{\partial w_k} = -\frac{1}{4}H(w_k)\left(\int_{\beta_+}\frac{R_+(s)\mathrm{d}s}{\sqrt{-s}(s-w_k)} + \int_{\beta_-}\frac{R_-(s)\mathrm{d}s}{\sqrt{-s}(s-w_k)}\right), \tag{3.64}$$

where in each case the partial derivatives w.r.t. w_k is calculated holding the other root fixed. By the chain rule, p and q are expressed in terms of the two roots.

As a consequence,

Proposition 3.1.5. *The Jacobian*

$$\mathcal{J}(w_0, w_1) := \det \begin{bmatrix} \frac{\partial M}{\partial w_0} & \frac{\partial M}{\partial w_1} \\ \frac{\partial I}{\partial w_0} & \frac{\partial I}{\partial w_1} \end{bmatrix} \tag{3.65}$$

is equal to

$$\mathcal{J}(w_0, w_1) = -\mathcal{D}\sqrt{-w_0}\sqrt{-w_1}H(w_0)H(w_1)(w_1 - w_0). \tag{3.66}$$

Here

$$\mathcal{D} = \frac{K(m)}{(p^2 - q)^{\frac{1}{4}}}, \quad m := \frac{1}{2}\left(1 - \frac{p}{\sqrt{p^2 - q}}\right) \in (0, 1). \tag{3.67}$$

And K denotes the the complete elliptic integral of the first kind

$$K(m) := \int_0^1 \frac{\mathrm{d}s}{\sqrt{(1 - s^2)(1 - ms^2)}}, \quad 0 < m < 1. \tag{3.68}$$

3.1.8 Determining $w_0(x, t)$ and $w_1(x, t)$

M and I are both functions of (x, t, w_0, w_1). The proposition 3.1.5 implies that as long as $H(w_k)$ is nonzero, and by assumption w_k will lie inside the upper/lower half plane, then the Jacobian will be nonzero. Then we can use the implicit function theorem to determine locally the dependence of (w_0, w_1) on (x, t). In fact, using w_0 and w_1 in proposition 3.1.2 at initial value $w_k(x, 0)$, we can determine as functions $w_0(x, t)$ and $w_1(x, t)$, or, equivalently, the dependence $p(x, t)$ and $q(x, t)$.

This scheme will fail when $H = 0$ which is what happens at the gradient catastrophe.

Proposition 3.1.6. *Suppose the β curve is parametrised by $\xi(\tau)$, where ξ is determined by a well-posed autonomous initial value problem*

$$\frac{\mathrm{d}\xi^*}{\mathrm{d}\tau} = -iR_+(\xi; p(x, t), q(x, t))H(\xi; p(x, t), q(x, t), x, t), \quad \tau > 0, \quad \xi(0) = 1. \tag{3.69}$$

Then

$$\frac{\mathrm{d}\theta(\xi(\tau))}{\mathrm{d}\tau} = \frac{\mathrm{d}\theta}{\mathrm{d}\xi} \cdot \frac{\mathrm{d}\xi}{\mathrm{d}\tau} = [iR_+(\xi)H(\xi)][-iR_+(\xi)H(\xi)]^* = -|iR_+(\xi)H(\xi)|^2 \leq 0. \tag{3.70}$$

Thus θ is monotone on β.

Indeed, proposition 3.1.6 gives us a scheme to find β. The only missing piece in g function for analysing the Riemann–Hilbert problem for N is the sign of $\mathrm{Re}(\phi)$. And since

we have determined β, we can compute the value of ϕ by integrating $\frac{\mathrm{d}\phi}{\mathrm{d}\xi} = RH$ and continue analytically when necessary.

3.1.9 Qualitative behaviour of ϕ and the solution to sine-Gordon equation, numerical examples

Let's consider a numerical example of the g-function, i.e. the sign chart of $\mathrm{Re}(\phi)$.

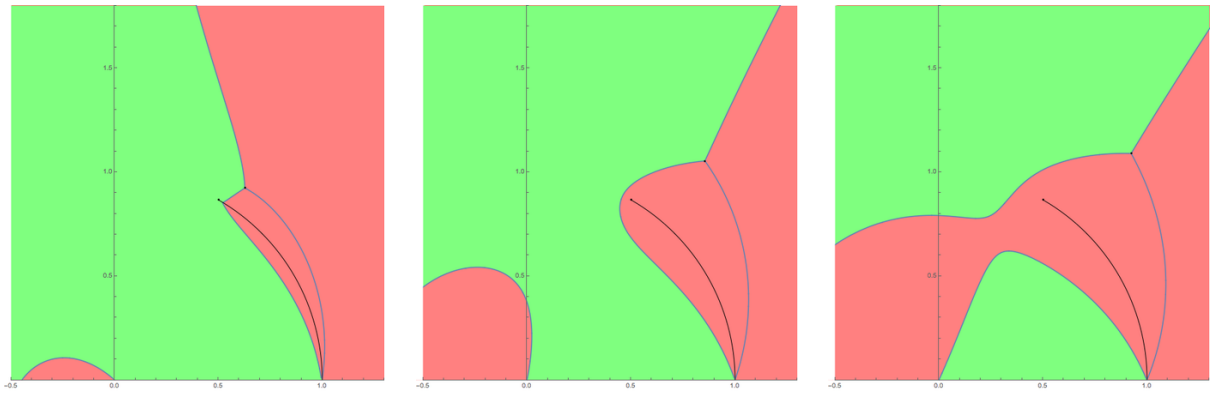

(a) $t = 0.60$ (b) $t = 1.80$ (c) $t = 2.16$

Figure 3.9: $x = 0.2$, $G(x) = -\mathrm{sech}(x)$. The green region denotes $\mathrm{Re}(\phi) < 0$, while red is where $\mathrm{Re}(\phi) > 0$.

In order to place the γ curve where $\mathrm{Re}(\phi) < 0$, we want the green region to connect w_0 and $w = 1$. As we can see from the previous figure, for the initial conditions we used, at $t = 0.2$ and $t = 0.6$, the green region does connect the two end points. However, at $t = 0.72$, the red region blocks the green. Somewhere in between, when a saddle point occurs, and after this the original g function built from one band and one gap is not sufficient for our analysis any more. This suggests that we need to introduce more bands and gaps, corresponding to the multiphase qualitative behaviour of the sine-Gordon solution. The phase transition is matched with the phase transition of the solution of the sine-Gordon equation.

Indeed, we can overlay the region on the (x, t) plane where the g-function transition occurs with a picture of the sine-Gordon solution in the same frame. We find the g-function transition convincingly describes the qualitative change in the solution we study.

The end point w_0 is where $\mathrm{Re}(\phi) = 0$. Unlike in the example for $x = 0.2$ or for any generic breaking point except for the gradient catastrophe point, $\mathrm{Re}(\phi)$ near the endpoint behaves like $(w - w_0)^{\frac{3}{2}}$. However, for $x = 0$, at the gradient catastrophe point, the saddle point and the end point w_0 will coincide. Thus the local behaviour of $(\phi - \phi(w_0))$ becomes

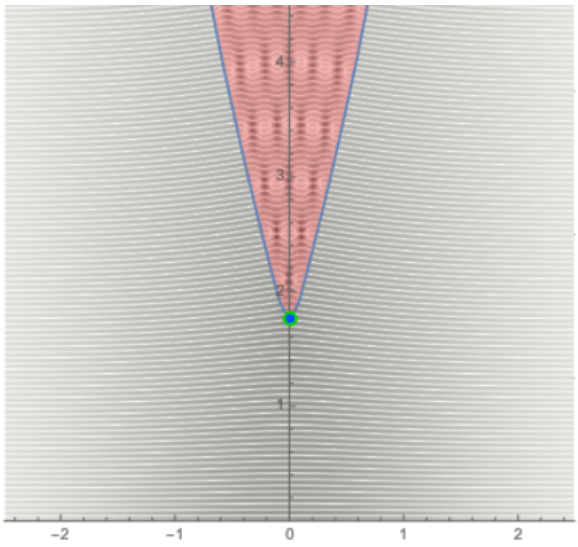

Figure 3.10: g breaking curve

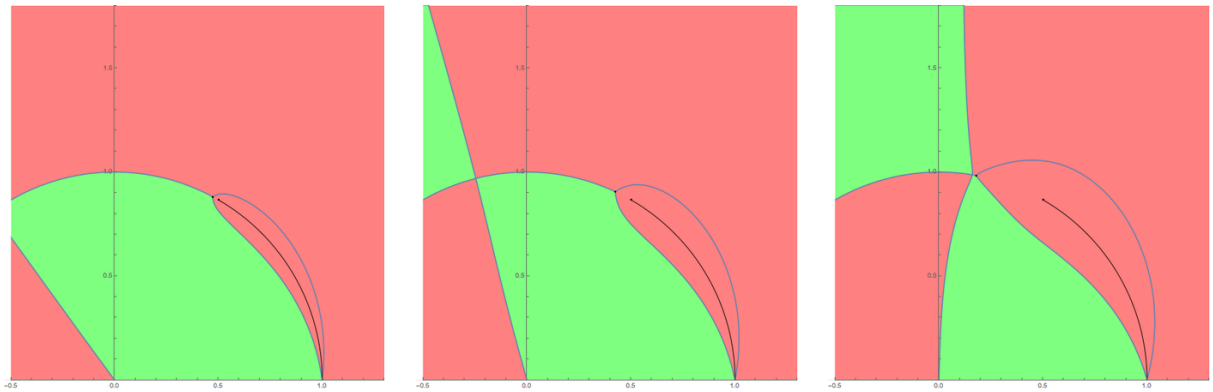

(a) $t = 0.80$ (b) $t = 1.20$ (c) $t = 1.62$

Figure 3.11: $x = 0$, $G(x) = -\text{sech}(x)$

$(w - w_0)^{\frac{5}{2}}$. This will turn out to require additional strategy to analyse.

We give some numerical examples:

One interesting phenomenon we found after the numerical experiment is that it looks like the endpoints, as well as the level curve of $\text{Re}(\phi) = 0$ seems to always lie on the unit circle for our example. We wondered if it would be true in general. In fact, for the focusing Nonlinear Schrödinger equation, there is a corresponding symmetry on the imaginary axis. This correspondence can be found in [33]. In the next section 3.2, we are going to prove the symmetry result.

3.2 Symmetries at $x = 0$ before the gradient catastrophe

In this section, we are going to show that when $x = 0$, the Riemann-Hilbert Problem will have extra symmetrical properties. Using the symmetry information, we can easily find the angles of the local coordinates near the endpoint w_0 of the jump contour. We can even explicitly express a condition when the gradient catastrophe happens, i.e. $(0, t_{\text{gc}})$. (From the way we chose initial data (even, with minimum at $x = 0$), we can deduce that the gradient catastrophe point also lies on $x = 0$).

Essentially, we will show that for $x = 0$ and t small,

1. The endpoints will always lie on the unit circle, moving to the left when t increases
2. One branch of the phase function ϕ will be purely imaginary on an arc of the unit circle. Note that because ϕ locally behaves like $(w-w_0)^{\frac{3}{2}}$, there are three such curves, with angle $\frac{2\pi}{3}$ apart.

3.2.1 θ^0 symmetry

Recall at $t = 0$, β coincides with the arc of the unit circle P_∞. Denote the end point as $a_0 = e^{i\alpha}$.

Theorem 3.2.1. *When $x = 0$ and t is small, if we continue the g-function from the right ($x \geq 0$) side,*

$$\theta^0(w) \in i\mathbb{R}, \qquad w = e^{i\tau}, \quad \alpha \leq \tau < \pi \tag{3.71}$$

Proof. Recall from the definition of θ^0 (2.25).

Step One: The analytic continuation to the left of A on the unit circle

$$\Psi(\lambda) := \frac{1}{4}\int_{x_-(\lambda)}^{x_+(\lambda)} \sqrt{G(s)^2 + 16\lambda^2}\mathrm{d}s. \qquad 0 < -i\lambda < \max(-\frac{1}{4}G) \tag{3.72}$$

with $\lambda(w) = \dfrac{i}{4}\left(\sqrt{-w} + \dfrac{1}{\sqrt{-w}}\right)$. Let $\mathrm{A}_0 = -\frac{1}{4}G(0)$, and A in upper unit circle such that $\mathrm{A}_0 = \lambda(A)$.

Define function $B(s;\lambda)$ in such a way that $B(s)^2 = G(s)^2 + 16\lambda^2$ and $B(s)$ has the cut from $x_-(\lambda)$ to $x_+(\lambda)$. Along the cut on the upper half plane, $B_+(s)$ is positive real valued. Across the cut in the lower half plane, $B_-(s) = -B_+(s)$. So we can rewrite the integral as

$$\Psi(\lambda) := \frac{1}{8}\oint_L B(s;\lambda)\mathrm{d}s. \tag{3.73}$$

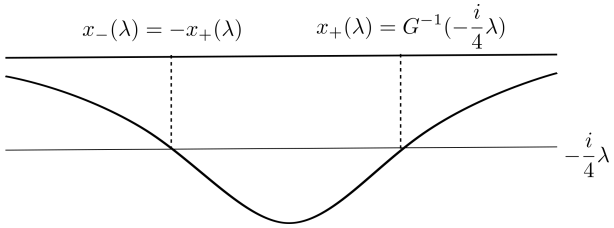

Figure 3.12: Initial condition $G(x)$ and $x_+(\lambda)$, $x_-(\lambda)$

where L is a clockwise contour enclosing the cut. Using this definition, we can choose L to be independent of λ.

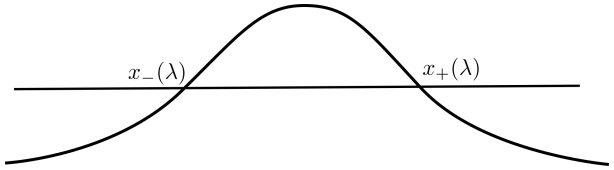

Figure 3.13: Picture of function $G^2(s)+16\lambda^2 = B^2(s;\lambda)$, which has two zeros at $x_+(\lambda)$ and $x_-(\lambda)$.

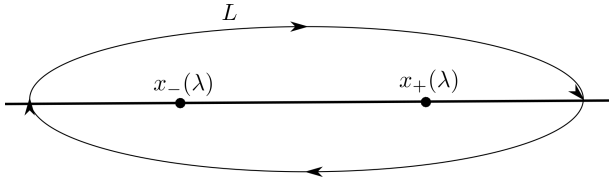

Figure 3.14: Loop L clockwise enclosing $x_+(\lambda)$ and $x_-(\lambda)$

Assume that $G''(0) > 0$, then the two roots $x_\pm(\lambda)$ will coalesce at 0 when $\lambda = i\mathrm{A}_0$ ($w = \mathrm{a}_0$), and split into two purely imaginary complex conjugates if λ goes above $i\mathrm{A}_0$ (w in the extension to the left of the arc from 1 to a_0). This way we showed that $\Psi(\lambda(w))$ can be analytically continued to the left of A on the unit circle, and in proximity of the original arc where it is defined, with the exception of point 1 corresponding to $\lambda = 0$ or $x_\pm(\lambda) = \infty$.

$$M = 0 \text{ when } x = 0$$

So suppose that for all $x > 0$ small time $t > 0$, the point $w_0 = p + i\sqrt{-q}$, the origin of the β curve, and the β curve is located at the outside of the unit circle. Take $x = 0$, then we deform the contour C to enclose β in L_+ region. M is defined as

$$M(x,t,p,q) := \frac{x-t}{\sqrt{p^2-q}} + x + t - \frac{2}{\pi}\int_C \frac{\theta_0'(\xi)\sqrt{-\xi}\mathrm{d}\xi}{R(\xi;p,q)} \tag{3.74}$$

If we take $x = 0$ and w_0 on the unit circle, i.e. $p^2 - q = 1$, then M becomes

$$M := -\frac{2}{\pi} \int_C \frac{\theta_0'(\xi)\sqrt{-\xi}\mathrm{d}\xi}{R(\xi; p, q)} \tag{3.75}$$

Now since we continue $w_0(x, t)$ from outside the unit circle before hitting it, we can deform the contour C so that the upper region L_+ encloses w_0 and the β curve. That means enlarging the outer/upper region L_+ to include a part of the unit disk. The lower half plane reflects the upper half plane so M has Schwarz symmetry.

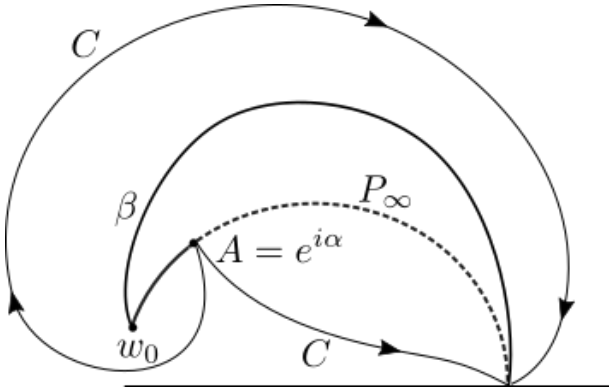

Figure 3.15: Contour C when $x = 0$

Deform C to start from A to w_0 along the unit circle, then from w_0 along β to 1. We will have two copies from both sides.

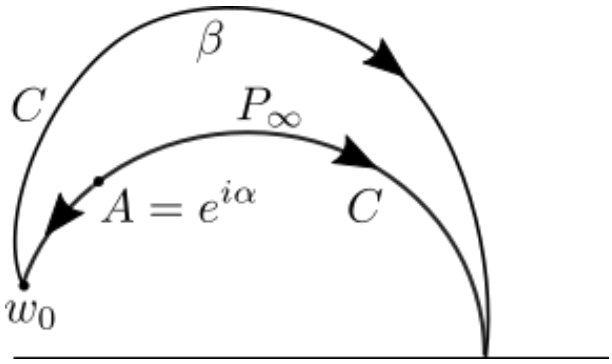

Figure 3.16: Symmetry: deformation of C overlapping β and the arc of the unit circle

Because R has a cut along β, where $R_+ = R_-$, the integral cancels along β. What is left for the integral are two copies of the contour from a_0 to w_0. We can choose it to be along the unit circle.

One can show that along the unit circle, to the left of a_0, $\frac{\sqrt{-\xi}}{R(\xi;p,q)}$ is real valued.

In the same part of the unit circle,

$$\theta_0(\xi) = \Psi(\lambda(\xi)) = \frac{1}{8}\oint_L B(s;\lambda)\mathrm{d}s. \tag{3.76}$$

$B(s;\lambda)$ has two purely imaginary conjugate roots, namely $x_-(\lambda) = -ib_0$, $x_+(\lambda) = ib_0$. We interpret B with a vertical cut along the two roots. On the left of the cut, B_- is negative imaginary valued, and $B_+(s) = -B_-(s)$. Now we can collapse the contour L along the vertical cut and write θ_0 as

$$\theta_0(\xi) = \frac{1}{4}\int_{-ib_0}^{ib_0} B_-(s;\lambda(\xi))\mathrm{d}s. \tag{3.77}$$

Clearly $\theta_0(\xi)$ is purely imaginary. By Schwarz symmetry, the upper half plane cancels with the lower half plane. Hence, we have proved the following:

Theorem 3.2.2. *$M = 0$ for w_0 on the unit circle to the left of a_0, when $x = 0$ and t is small.*

□

3.2.2 H symmetry

Using a similar argument, we can show:

Theorem 3.2.3. *For some $T > 0$ when $t < T$, $\mathrm{Re}(\phi)$ is 0 on the arc of the unit circle to the left of w_0 and w_1.*

One implication of this theorem is it shows the mechanism of the occurrence of the gradient catastrophe point. Indeed, theorem 3.2.2 tells us that w_0 will lie on the unit circle. Theorem 3.2.3 says the unit circle to the left of w_0 is a level curve of $\mathrm{Re}(H) = 0$. Suppose that H has a zero on the level curve and as t grows, the zero is moving towards the right while w_0 is moving to the left. If they are moving closer to each other at nonzero speed then eventually they collide. This is exactly where the gradient catastrophe happens.

3.3 Parametrix construction before breaking

3.3.1 Global parametrix

In the standard Riemann–Hilbert theory, the jump condition is a Hölder continuous function and the solution we are seeking is also Hölder continuous. The matrix function $\dot{\mathbf{O}}^{\mathrm{out}}$

has the same jump matrices as in the RHP for $\mathbf{O}$ on β. As it turns out, this is the main constant jump that gives the leading asymptotics of the solution. However, $\dot{\mathbf{O}}^{\text{out}}$ blows up in powers of $\mathcal{O}((w-w_{0,1})^{-\frac{1}{4}})$ near the two endpoints.

To overcome this difficulty, we put two disks U_0 and U_1 around w_0 and w_1. The disks are of size $\mathcal{O}(1)$ (independent of ϵ). Then $\dot{\mathbf{O}}^{\text{out}}$ is uniformly bounded outside of the disks. Inside the disks, we will use another parametrix, we call it $\dot{\mathbf{O}}^{\text{in}}$, to approximate $\mathbf{O}$. $\dot{\mathbf{O}}^{\text{in}}$ will solve a Riemann–Hilbert problem with the same jump as $\mathbf{O}$ inside the disks.

Then we patch together $\dot{\mathbf{O}}^{\text{in}}$ and $\dot{\mathbf{O}}^{\text{out}}$, and call it the global parametrix $\dot{\mathbf{O}}$,

$$\dot{\mathbf{O}}(w) = \begin{cases} \dot{\mathbf{O}}^{\text{in}}(w) & w \in U_0 \cup U_1 \\ \dot{\mathbf{O}}^{\text{out}}(w) & w \in \mathbb{C}\backslash(U_0 \cup U_1) \end{cases} \tag{3.78}$$

Assembling the jump conditions for the inner and outer parametrices, the jump for the global parametrix is shown in figure 3.17.

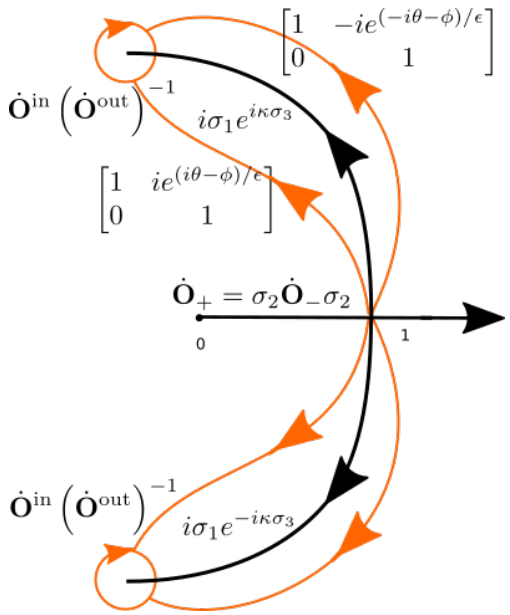

Figure 3.17: Riemann–Hilbert problem for the global parmetrix

Of course $\dot{\mathbf{O}}^{\text{in}}$ and $\dot{\mathbf{O}}^{\text{out}}$ will be two different matrix functions and they do not match exactly on the boundary of the regions of definition. However, we have some more freedom with $\dot{\mathbf{O}}^{\text{in}}$. We can left multiply it by a holomorphic function and still have it satisfy the same jump condition. We will try to find a holomorphic function such that on the boundary of the disks $\partial U_{0,1}$, the mismatch is as small as possible. We will characterise this mismatch by a jump condition, and use the small-norm theory to prove that this global parametrix is a good approximation of $\mathbf{O}$, and characterize the corrections.

As a preview of the later chapters, after we approached the gradient catastrophe, a different inner parametrix will be called for. In particular, the error term is going to be more significant than in this chapter. Moreover, the new model for the inner parametrix has poles. When close to the poles, no matter how we choose $\dot{\mathbf{O}}^{\text{in}}$, the change alone would not match $\dot{\mathbf{O}}^{\text{out}}$ closely enough. We will then need to modify $\dot{\mathbf{O}}^{\text{out}}$. For now we lay out a strategy to achieve the asymptotics of the solution before the first breaking, where the solution to the fluxon condensate is given by elliptic functions, corrections described by the Airy functions. This is not the focus of the thesis, by all means it is explained in literature, among them [13]. However, it motivates what we need to modify near the gradient catastrophe point in the later chapters.

3.3.2 The outer parametrix

Suppose we try to solve the Riemann–Hilbert problem with the constant jump.

Introduce

$$\kappa = \frac{\Phi}{\epsilon}. \tag{3.79}$$

Riemann–Hilbert Problem 3.3.1 (Outer Parametrix)**.** Find a matrix $\dot{\mathbf{O}}^{\text{out}}$ that satisfies the following conditions

Analyticity: $\dot{\mathbf{O}}^{\text{out}}$ is analytic for $w \in (\mathbb{C}\backslash\beta_+ \cup \beta_- \cup \mathbb{R}_+)$ and Hölder-α continuous for any $\alpha \leq 0$ except for an arbitrarily small neighbourhood of w_0 and w_1. In the neighbourhood U_k of w_k, the elements of $\dot{\mathbf{O}}^{\text{out}}(w)$ are bounded by $|w - w_k|^{-\frac{1}{4}}$.

Jump condition:

$$\dot{\mathbf{O}}^{\text{out}}_+(\xi) = \dot{\mathbf{O}}^{\text{out}}_-(\xi) i\sigma_1 e^{\pm i\kappa\sigma_3}, \quad \xi \in \beta_\pm, \tag{3.80}$$

$$\dot{\mathbf{O}}^{\text{out}}_+(\xi) = \sigma_2 \dot{\mathbf{O}}^{\text{out}}_-(\xi)\sigma_2, \quad \xi \in \mathbb{R}_+. \tag{3.81}$$

Normalisation:

$$\lim_{w\to\infty} \dot{\mathbf{O}}^{\text{out}}(w) = \mathbb{I}. \tag{3.82}$$

Even though the constant jump in Riemann–Hilbert problem 3.3.1 is the most significant part, the solution $\dot{\mathbf{O}}^{\text{out}}$ is not Hölder continuous everywhere, hence we cannot yet conclude this will give us the approximation of the solution to the sine-Gordon equation.

Instead we fix U_k independent of ϵ, and only use the outer parametrix outside of the disks. Inside the disks we will build a new parametrix we call the inner parametrix, such that the inner and outer parametrices matches well enough on the boundary of U_k.

This Riemann–Hilbert problem for the outer parametrix has a unique solution that can be built from the Riemann theta function associated with the Riemann surface with

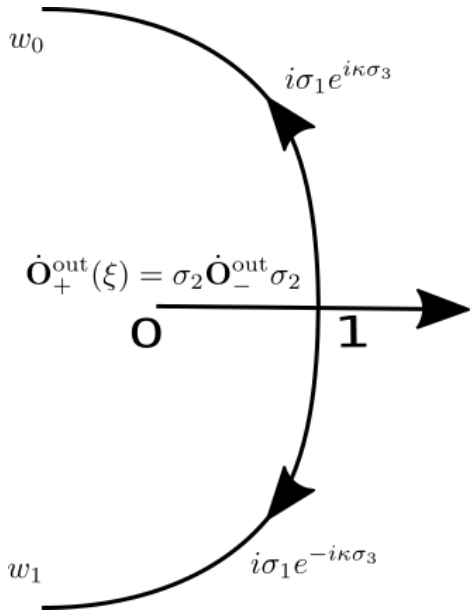

Figure 3.18: Jump for the outer parametrix

2 cuts (genus 1). The discontinuity of the function $\dot{\mathbf{O}}^{\text{out}}$ can be viewed as connecting two sheets of the surface. The approach is to build the Baker–Akheizer function with the Abel map. A general reference for Baker–Akheizer function and its application in solving nonlinear equations is in [28]. In the current setting, we will follow the careful explanation in [13]. Riemann theta functions of genus 1 are closely related to the classical Jacobi elliptic functions see [24, Chapter22]. However, the connection is not always clear. In [13, Appendix B] the authors also related the Jacobi elliptic function to $\dot{\mathbf{O}}^{\text{out}}$.

Here I list both expressions. The elliptic functions help us better understand the oscillatory waves, while the Riemann theta function expression will come in handy later when we need to evaluate near the endpoints w_0 and w_1 of the band.

Riemann theta function

Let X be the Riemann surface of the equation

$$y^2 = S(w)^2 := w(w - w_0)(w - w_0^*), \tag{3.83}$$

compactified at $y = w = \infty$. View X as two copies of w-plane glued along the cut of $S(w)$. $S(w)$ is analytic in the complement of the jump contours, and $S(w) = w^{3/2}(1 + \mathcal{O}(w^{-1}))$ as $w \to \infty$.

Let $w(P)$ denote the sheet projection function. Let $P_k(w)$ denote the preimage of w under $w(P)$ on sheet k of X.

For $\mathrm{Im}(w) > 0$,

$$\dot{\mathbf{O}}^{\mathrm{out}}(w) = \frac{q}{2}\begin{bmatrix} t_1(P_1)e^{-i\varphi_1 h} + t_2(P_1)e^{-i\varphi_2 h} & -i(t_1(P_2)e^{i\varphi_1 h} - t_2(P_2)e^{i\varphi_2 h}) \\ -i(t_2(P_1)e^{-i\varphi_2 h} - t_1(P_1)e^{-i\varphi_1 h}) & t_1(P_2)e^{i\varphi_1 h} + t_2(P_2)e^{i\varphi_2 h} \end{bmatrix}. \tag{3.84}$$

For $\mathrm{Im}(w) < 0$,

$$\dot{\mathbf{O}}^{\mathrm{out}}(w) = \frac{q}{2}\begin{bmatrix} t_1(P_2)e^{i\varphi_1 h} + t_2(P_2)e^{i\varphi_2 h} & -i(t_1(P_1)e^{-i\varphi_1 h} - t_2(P_1)e^{-i\varphi_2 h}) \\ -i(t_2(P_2)e^{i\varphi_2 h} - t_1(P_2)e^{i\varphi_1 h}) & t_1(P_1)e^{-i\varphi_1 h} + t_2(P_1)e^{-i\varphi_2 h} \end{bmatrix}. \tag{3.85}$$

In this expression φ_i and q are defined as the following,

$$\varphi_1 := \kappa - \frac{\pi}{2} \quad \text{and} \quad \varphi_2 := \kappa + \frac{\pi}{2}. \tag{3.86}$$

$$q(w)^4 = \frac{w - w_0}{w - w_0^*}, \tag{3.87}$$

with cut along β and $q(w) = 1 + \mathcal{O}(w^{-1})$ as $w \to \infty$.

The function t_j are built from the Baker-Akheizer function and the Abel map. These pieces in the elements of $\dot{\mathbf{O}}^{\mathrm{out}}$ turn out to be

$$t_j(P_1(w))e^{-i\varphi_j h(w)} = \frac{\Theta(i\pi;\mathcal{H})\Theta(A(P_1(w)) + \mathcal{K} - i\varphi_j;\mathcal{H})}{\Theta(i\pi - i\varphi_j;\mathcal{H})\Theta(A(P_1(w)) + \mathcal{K};\mathcal{H})}, \tag{3.88}$$

whereas

$$t_j(P_2(w))e^{-i\varphi_j h(w)} = \frac{\Theta(i\pi;\mathcal{H})\Theta(A(P_1(w)) + \mathcal{K} + i\varphi_j;\mathcal{H})}{\Theta(i\pi + i\varphi_j;\mathcal{H})\Theta(A(P_1(w)) + \mathcal{K};\mathcal{H})}. \tag{3.89}$$

Here, $\Theta(z;\mathcal{H})$ denotes the Riemann-theta function [28]

$$\Theta(z;\mathcal{H}) := \sum_{n=-\infty}^{\infty} e^{\frac{1}{2}\mathcal{H}n^2} e^{nz}. \tag{3.90}$$

$\mathcal{H}$, $\mathcal{K}$ and the Abel map $A(P_1(w))$ are defined as follows. Let $\widetilde{S}(P)$ denote the lift to X of $S(w)$

$$\tilde{S}(P) := \begin{cases} S(w(P)), & P \in \text{sheet 1}, \\ S(w(P)), & P \in \text{sheet 2}. \end{cases} \tag{3.91}$$

The holomorphic differential

$$\omega(P) = c\frac{\mathrm{d}w(P)}{\widetilde{S}(P)}. \tag{3.92}$$

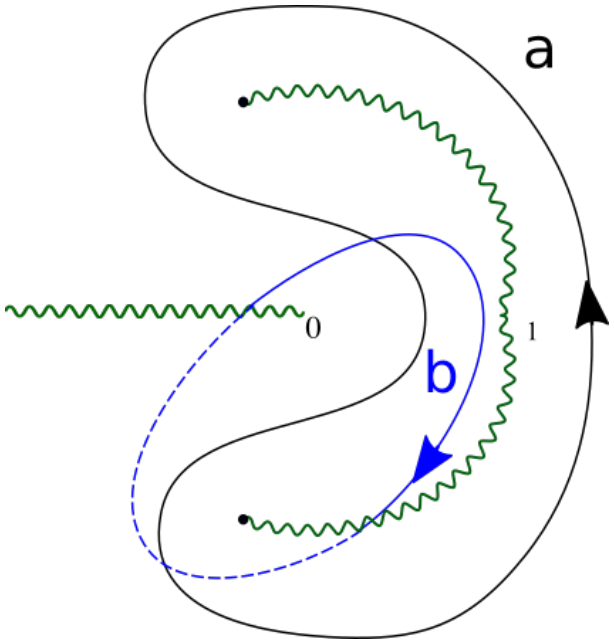

Figure 3.19: The homology basis on X, loop a and b

The constant c is chosen such that

$$\oint_a \omega(P) = 2\pi i. \tag{3.93}$$

And $\mathcal{H}$ is the other loop integral

$$\mathcal{H} := \oint_b \omega(P). \tag{3.94}$$

$$\mathcal{K} := i\pi + \frac{1}{2}\mathcal{H} \tag{3.95}$$

$$A(P) := \int_{P_0}^{P} \omega(P') \qquad (\text{mod } 2\pi i m + \mathcal{H} n), \quad m, n \in \mathbb{Z}. \tag{3.96}$$

The reader can find more details about using the Θ-function in nonlinear waves and the motivations for this particular construction in [28]. Because in our case, the genus is 1, equation 3.90 can be written in terms of the Jacobi θ-function. For more details and properties of the Jacobi θ-function the reader can refer to [24, Chapter20]. Note that the Riemann theta function we use is almost identical to Jacobi theta function θ_3.

Elliptic Function Expression

The expression in terms of the elliptic functions on the other hand are listed in this section. Recall the elements to express $\sin(\frac{1}{2}u)$, $\cos(\frac{1}{2}u)$ and $\frac{\mathrm{d}u}{\mathrm{d}t}$ are certain elements in the coefficient

matrices of $\dot{\mathbf{O}}$ expansions: $\dot{\mathbf{O}}^{0,0}$, $\dot{\mathbf{O}}^{0,1}$ and $\dot{\mathbf{O}}^{\infty,1}$,

$$\dot{C} := \dot{O}_{11}^{0,0}, \tag{3.97}$$

$$\dot{S} := \dot{O}_{21}^{0,0}, \tag{3.98}$$

and

$$\begin{aligned} \dot{G} :=& \dot{O}_{12}^{\infty,1} + \left[(\dot{\mathbf{O}}^{0,0})^{-1}\dot{\mathbf{O}}^{0,1}\right]_{12} \\ =& \dot{O}_{12}^{\infty,1} + \dot{O}_{22}^{0,0}\dot{O}_{12}^{0,1} - \dot{O}_{12}^{0,0}\dot{O}_{22}^{0,1}. \end{aligned} \tag{3.99}$$

While $\dot{C}$, $\dot{S}$ and $\dot{G}$ are given by

$$\dot{C} = \mathrm{dn}\left(\frac{2\Phi K(m)}{\pi\epsilon}; m\right), \tag{3.100}$$

$$\dot{S} = -\sqrt{m}\,\mathrm{sn}\left(\frac{2\Phi K(m)}{\pi\epsilon}; m\right), \tag{3.101}$$

$$\dot{G} = -\frac{4K(m)}{\pi}\frac{\partial\Phi}{\partial t}\sqrt{m}\,\mathrm{cn}\left(\frac{2\Phi K(m)}{\pi\epsilon}; m\right). \tag{3.102}$$

The elliptic parameters are given by

$$m := \sin\left(\frac{1}{2}\arg(w_0)\right)^2, \quad 0 < \frac{1}{2}\arg(w_0) < \frac{\pi}{2}, \tag{3.103}$$

while $K(\cdot)$ denotes the complete elliptic integral of the first kind:

$$K(m) := \int_0^1 \frac{\mathrm{d}s}{\sqrt{(1-s^2)(1-ms^2)}}, \quad 0 < m < 1. \tag{3.104}$$

3.3.3 Inner parametrix

Locally the phases $\phi(w) - \phi(w_0)$ and $i\theta$ is has asymptotic behaviours like $(w - w_0)^{\frac{3}{2}}$. In fact one can map $(\phi(w) - \phi(w_0))^{\frac{2}{3}}$ to a new variable ζ. Both ϕ and $i\theta$ in the original jump matrix U_0 are mapped to the jump of the standard Airy parametrix (see figure 3.20).

Moreover, using the expansion of the Airy paremetrix at infinity, we are able to show that on the boundary of the inner and outer solutions, the mismatch of the two parametrices are given by

$$\dot{\mathbf{O}}_k^{\mathrm{in}}(\xi)\dot{\mathbf{O}}^{\mathrm{out}}(\xi)^{-1} = \mathbb{I} + \mathcal{O}(\epsilon), \quad \xi \in \partial U_k, \quad k = 0, 1. \tag{3.105}$$

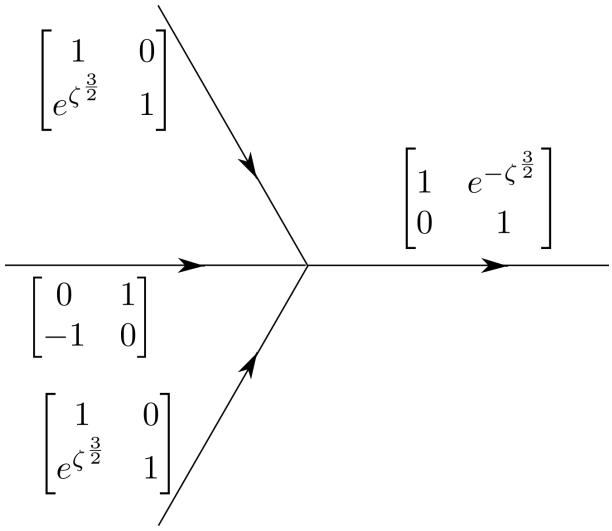

Figure 3.20: Airy parametrix

3.3.4 Error

We aim to illustrate in this section that the global parametrix (3.78) gives the leading term in the asymptotics of $\mathbf{O}(w)$.

The way we measure how good the global parametrix $\dot{\mathbf{O}}$ is an approximation of the matrix $\mathbf{O}$ is by looking at an error matrix defined as the following:

$$\mathcal{E}(w) = \mathbf{O}(w)\dot{\mathbf{O}}^{-1}(w). \tag{3.106}$$

By construction of the global parametrix, the constant jumps on β and $\mathbb{R}$ are already taken care of exactly. In essence they will cancel when we multiply $\mathbf{O}$ by the inverse of $\dot{\mathbf{O}}$ and therefore will not show up in the error matrix $\mathcal{E}$. What is left now for the jump of $\mathcal{E}$ should be the lens opened and the circles that separate the inner and outer parametrix, as shown in the figure 3.21.

This is not exactly true, as the jump on $\mathbb{R}_+$ is not in the standard form by right multiplication. This jump is created by using $\sqrt{-w}$ as spectral variable. It is not essential for the Riemann–Hilbert problem we are trying to solve. The way to handle this problem is by returning to z variable. We will discuss the technical details in Chapter 5.

As it turns out, the Riemann–Hilbert problem for $\mathcal{E}$ is a so-called small-norm problem [5], a summary can be found in [14, Appendix B]. We can write out the asymptotic expansion in powers of ϵ by analysing the jump for $\mathcal{E}$. We are going to demonstrate it in detail when we calculate the first correction term near the gradient catastrophe point. For now, we will refer to [13] for the following facts:

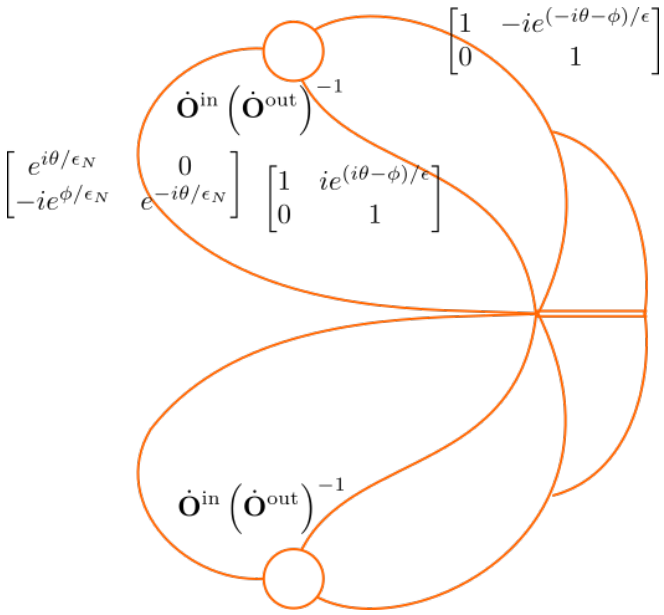

Figure 3.21: Jumps for $\mathcal{E}$

- The inner parametrix built from the Airy parametrix has $\mathcal{O}(\epsilon)$ mismatch with the outer parametrix on the boundary of disks U_k;
- All the other jumps are decaying exponentially;
- As a result, $\dot{\mathbf{O}}^{\text{out}}$ is the leading term of $\mathbf{O}$, with error of size $\mathcal{O}(\epsilon)$.

Chapter 4

Modifying the g-function near the gradient catastrophe

At the gradient catastrophe point $(x_{\text{gc}} = 0, t_{\text{gc}})$, a saddle point of the phase function ϕ and the endpoints w_0, w_1 of the band β coalesce together. Thus the local behaviours change. This can be seen in a zoomed-in picture at a generic end point like in figure 3.9 and one at the gradient catastrophe as in figure 3.11 (c), as shown in 4.1 At a generic point, the phase

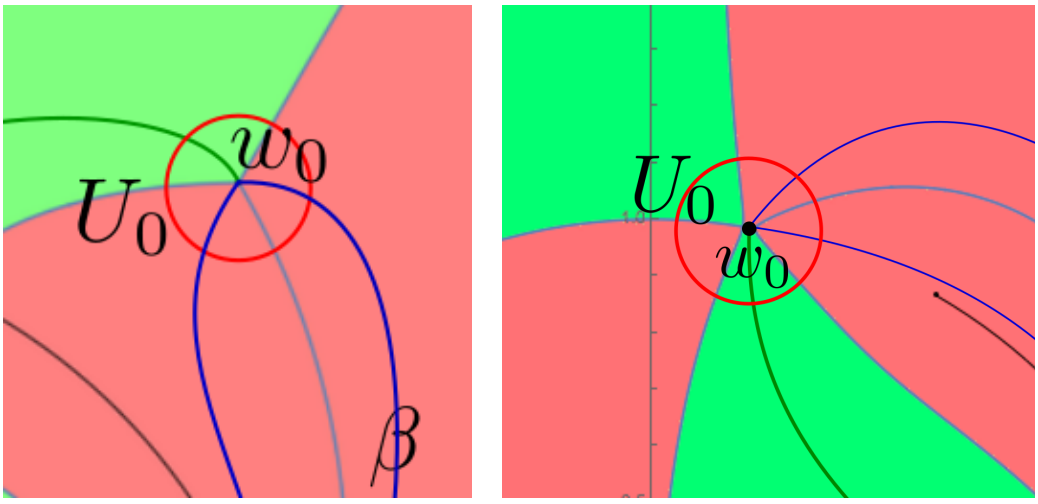

(a) Generic point (b) Gradient catastrophe point

Figure 4.1: Comparing zoomed-in pictures near w_0 at a generic point and at the gradient catastrophe point

$\phi - i\Phi$ locally behaves like $(w - w_0)^{\frac{3}{2}}$ and can be conformally mapped to the new coordinate $\zeta^{\frac{3}{2}}$ that shows up in the Airy parametrix. This is no longer true at the gradient catastrophe point. In addition, when we get closer to the gradient catastrophe point, even if the Airy

parametrix still can be used, the coefficient for the dominant power $(w-w_0)^{\frac{3}{2}}$ becomes smaller. Thus as we approach the gradient catastrophe point, the approximation becomes less accurate and as the gradient catastrophe point is approached, the approximation fails completely. Another failure of our old approach caused by the higher degeneracy of the gradient catastrophe point is that, since $H(w; x_{\rm gc}, t_{\rm gc})$ vanishes at $w_0(x_{\rm gc}, t_{\rm gc})$, the Jacobian defined in (3.1.5) is 0, and we can no longer use the implicit function theorem to determine the location of the endpoints w_0 and w_1.

We will need to introduce a new inner parametrix to replace the Airy parametrix. The $\frac{5}{2}$ power behaviour near the endpoint w_0, as well as the previous example of NLS [8] suggest that we should use the Painlevé-I parametrix.

The phase exponent suggested by the Painlevé-I parametrix (see section 5.2) is

$$\phi(w) - \phi(w_k) = 2\left(\frac{4}{5}W^{\frac{5}{2}} - sW^{\frac{1}{2}}\right). \tag{4.1}$$

On the other hand the phase exponent $\phi(w; x, t)$ produced by the g function in (3.10), assuming M and $I \equiv 0$ are satisfied, has the expansion

$$\phi(w;x,t)-\phi(w_0(x,t);x,t) = C_3(x,t)(w-w_0)^{\frac{3}{2}}+C_5(x,t)(w-w_0)^{\frac{5}{2}}+\mathcal{O}\left((w-w_0)^{\frac{7}{2}}\right), \tag{4.2}$$

where $C_3(x_{\rm gc}, t_{\rm gc})$ vanishes, while $C_5(x_{\rm gc}, t_{\rm gc}) \neq 0$. An analogous expansion holds at $w_0^*(x_{\rm gc}, t_{\rm gc})$ following the Schwarz symmetry in the exponent ϕ. This expansion does not have the more dominant $\frac{1}{2}$ power terms like the Painlevé-I exponent. While it is possible to map the local phase (4.2) to (4.1), we find it requires less effort to identify branches of multivalued functions if we are able to match the dominant power.

Our strategy is to introduce a new $\mathfrak{g}$-function to replace the old one; it will be well-defined in a neighbourhood of the gradient catastrophe point, before or after breaking. The corresponding local phase has the expansion

$$\phi-\phi_0 = C_1(x,t)(w-w_0)^{\frac{1}{2}}+C_3(x,t)(w-w_0)^{\frac{3}{2}}+C_5(x,t)(w-w_0)^{\frac{5}{2}}+\mathcal{O}\left((w-w_0)^{\frac{7}{2}}\right) \tag{4.3}$$

in a neighbourhood of the gradient catastrophe point. It is also exactly the same as the old g-function at the gradient catastrophe point. This means

$$\phi - \phi_0^{\rm gc} = C_5(x_{\rm gc}, t_{\rm gc})(w - w_0^{\rm gc})^{\frac{5}{2}} + \mathcal{O}\left((w-w_0)^{\frac{7}{2}}\right). \tag{4.4}$$

In other words, the coefficients C_1 and C_3 vanish at the gradient catastrophe point. In the Painlevé exponent 4.1, $s(x,t)$ depends on and varies continuously with respect to (x,t).

In fact we will prove later that s is a real analytic function of (x,t). At the gradient catastrophe point, $s(x_{\rm gc},t_{\rm gc})$ vanishes. In order to use this construction in the parametrices for the Riemann–Hilbert analysis for our sine-Gordon Riemann–Hilbert problem we are going to prove theorem 4.3.1 in this chapter:

A conformal mapping from the local coordinate $(w-w_0)$ to a normal form coordinate W exists for each (x,t) near the gradient catastrophe point $(x_{\rm gc},t_{\rm gc})$, and depends smoothly on (x,t). Under this conformal mapping, the new phase function ϕ is exactly in the normal form: $\frac{1}{2}\phi(w)-\frac{1}{2}\phi(w_0)=\frac{4}{5}W(w)^{\frac{4}{5}}-sW(w)^{\frac{1}{2}}$, and at the gradient catastrophe point $s(x_{\rm gc},t_{\rm gc})=0$. The same holds true in the lower half plane near w_1. The most precise statement and proof of theorem 4.3.1 will follow after we have properly introduced the new $\mathfrak{g}$-function.

Notation

In this chapter, we are going to emphasize that although similar in form, the $\mathfrak{g}$-function and all variables and functions whose definition are dependent on $\mathfrak{g}$ implicitly, are not the same as the generic g before breaking in Chapter 3.

For example, we will still use $\mathfrak{R}^2=(w-\mathfrak{w}_0)(w-\mathfrak{w}_1)$ to produce a jump on $\widetilde{\beta}$. However, we should keep in mind that the endpoints $\mathfrak{w}_0$ and $\mathfrak{w}_1$ are implicitly solved from equations defined by the $\mathfrak{g}$-function. The fact that $\mathfrak{g}$ is changed implies that the endpoints are also not the same as w_0 and w_1 even if the definition of the old g still makes sense at the given (x,t) location. In particular, since the endpoints are no longer the same, the band β will also change into $\widetilde{\beta}$, the original line connecting A and w_0, γ_0 into $\widetilde{\gamma}_0$, and even the phase exponents ϕ and θ into φ and ϑ. Alas, thankfully Greek letters happen to have two different writings for these two letters. In addition, those new quantities also include: $\mathfrak{g}$, $\mathfrak{w}_0$, $\mathfrak{w}_1$, $\mathfrak{M}$, $\mathfrak{H}$, $\mathfrak{I}$ and $\mathfrak{R}$. Another useful sub/superscript is gc, denoting the gradient catastrophe point.

4.1 Modifying g

As discussed earlier, the dominant term in the Painlevé-I exponent has an $\frac{1}{2}$ power term. In the original ϕ, the expansion starts in $\frac{3}{2}$ power. The first step is to simply add a term with behaviour $(w-w_0)^{\frac{1}{2}}$ and another similar term at w_1. Instead of harnessing the Schwarz symmetry and only studying in detail the upper half plane, as we did in the previous chapters, in this chapter we will define two copies of the quantities: one for the upper half plane, and one for the lower half plane. The reason behind will be clear in the proof of

our main theorem 4.3.1. Basically we want to be able to treat the dependence on (x,t) like complex variables and avoid conjugating, because conjugation is not a linear operator. The fact that (x,t) and the solution of sine-Gordon are still real will be a result from a uniqueness argument.

Recall that g is more conveniently constructed from its derivative f. Our new $\mathfrak{g}$ will be built in similar steps. In its derivative, the two added terms should be $m(w-\mathfrak{w}_0)^{-\frac{1}{2}}$ and $n(w-\mathfrak{w}_1)^{-\frac{1}{2}}$, where m and n are coefficients to be determined. The initial steps are motivated by the same reasoning as in Chapter 3.

4.1.1 Defining $\mathfrak{f}$

Define $\mathfrak{f}$, the new version of f, as the following:

$$\begin{aligned}\mathfrak{f}(w;x,t,\mathfrak{w}_0,\mathfrak{w}_1,m,n) \ :=& i\frac{\mathrm{d}Q}{\mathrm{d}w}+\frac{x-t}{8\sqrt{\mathfrak{w}_0\mathfrak{w}_1}}\frac{\mathfrak{R}(w)}{w\sqrt{-w}}-\frac{\mathfrak{R}(w)}{2\pi\sqrt{-w}}\int_{\tilde{\gamma}}\frac{\theta_0'(\xi)}{\mathfrak{R}(\xi)}\frac{\sqrt{-\xi}}{\xi-w}\mathrm{d}\xi\\ &+\frac{1}{2}\frac{\mathrm{d}}{\mathrm{d}w}L^0(w)\mp i\frac{1}{2}\frac{\mathrm{d}}{\mathrm{d}w}\theta_0(w)+\frac{m}{\sqrt{-w}}\frac{\mathfrak{R}(w)}{w-\mathfrak{w}_0}+\frac{n}{\sqrt{-w}}\frac{\mathfrak{R}(w)}{w-\mathfrak{w}_1}.\end{aligned} \tag{4.5}$$

Analogous to equation (3.49), the difference of $\mathfrak{f}$ along the new $\widetilde{\beta}$ curve is given by:

$$\begin{aligned}\mathfrak{f}_+(\xi)-\mathfrak{f}_-(\xi) \ =\mathfrak{R}_+(\xi)\Bigg(&\frac{x-t}{4\sqrt{\mathfrak{w}_0\mathfrak{w}_1}\xi\sqrt{-\xi}}-\frac{1}{2\pi\sqrt{-\xi}}\int_C\frac{\theta_0'(s)\sqrt{-s}}{\mathfrak{R}(s)(s-\xi)}\mathrm{d}s\\ &+\frac{2m}{\sqrt{-\xi}(\xi-\mathfrak{w}_0)}+\frac{2n}{\sqrt{-\xi}(\xi-\mathfrak{w}_1)}\Bigg)\end{aligned} \tag{4.6}$$

The analogue of H in (3.50), the new $\mathfrak{H}$ is given by

$$\mathfrak{H}(w)=-\frac{1}{4\sqrt{-w}}\left(\frac{x-t}{\sqrt{\mathfrak{w}_0\mathfrak{w}_1}w}-\frac{2}{\pi}\int_C\frac{\theta_0'(s)\sqrt{-s}}{\mathfrak{R}(s)(s-w)}\mathrm{d}s+\frac{8m}{w-\mathfrak{w}_0}+\frac{8n}{w-\mathfrak{w}_1}\right). \tag{4.7}$$

Recall that

$$\begin{aligned}&\vartheta=-i(\mathfrak{g}_+-\mathfrak{g}_-) \ \text{ on } \ \tilde{\beta},\\ &\vartheta'=-i(\mathfrak{f}_+-\mathfrak{f}_-) \ \text{ on } \ \tilde{\beta},\\ &\varphi=2i\theta_0+L^0\mp i\theta_0-\mathfrak{g}_+-\mathfrak{g}_- \ \text{ on } \ \tilde{\gamma},\\ &\varphi'=\mathfrak{R}\mathfrak{H} \text{ on } \widetilde{\gamma},\\ &\vartheta'=i\mathfrak{R}_+\mathfrak{H} \ \text{ on } \ \widetilde{\beta}.\end{aligned} \tag{4.8}$$

4.1.2 Analogues of $M \equiv 0$ and $I \equiv 0$, $\mathfrak{M} \equiv 0$ and $\mathfrak{I} \equiv 0$

Recall in Chapter 3, the condition $M = 0$ is used to make sure f has proper decay at infinity (so g is well defined and go to 0 at infinity), while the condition $I = 0$ is used to make sure ϕ is a constant on the band. Both of these properties are still needed for the new $\mathfrak{g}$-function. By the same reasoning as in Chapter 3, this condition has to be that the new $\mathfrak{M}$ and $\mathfrak{I}$ are equal to 0, where $\mathfrak{M}$ and $\mathfrak{I}$ are defined as follows

$$\begin{aligned}\mathfrak{M} :=& \frac{x-t}{\sqrt{w_0 w_1}} + x + t - \frac{2}{\pi}\int_C \frac{\theta_0'(\xi)\sqrt{-\xi}}{\mathfrak{R}(\xi; w_0, w_1)}\mathrm{d}\xi + 8m + 8n \\ =:& M + 8m + 8n\end{aligned} \tag{4.9}$$

Notice M has almost the same expression as in Chapter 3.

$$\begin{aligned}\mathfrak{I} :=& \int_{\widetilde{\beta}_+} \mathfrak{R}_+\mathfrak{H} + \int_{\widetilde{\beta}_-} \mathfrak{R}_-\mathfrak{H} \\ =& \int_{\widetilde{\beta}_+} \mathfrak{R}_+ \left[-\frac{1}{4\sqrt{-\xi}}\left(\frac{x-t}{\sqrt{\mathfrak{w}_0\mathfrak{w}_1}\xi} - \frac{2}{\pi}\int_C \frac{\theta_0'(s)\sqrt{-s}}{\mathfrak{R}(s)(s-\xi)}\mathrm{d}s + \frac{8m}{\xi-\mathfrak{w}_0} + \frac{8n}{\xi-\mathfrak{w}_1}\right)\right]\mathrm{d}\xi \\ &+ \int_{\widetilde{\beta}_-} \mathfrak{R}_- \left[-\frac{1}{4\sqrt{-\xi}}\left(\frac{x-t}{\sqrt{\mathfrak{w}_0\mathfrak{w}_1}\xi} - \frac{2}{\pi}\int_C \frac{\theta_0'(s)\sqrt{-s}}{\mathfrak{R}(s)(s-\xi)}\mathrm{d}s + \frac{8m}{\xi-\mathfrak{w}_0} + \frac{8n}{\xi-\mathfrak{w}_1}\right)\right]\mathrm{d}\xi \\ =& \int_{\widetilde{\beta}_+} \mathfrak{R}_+ \left[-\frac{1}{4\sqrt{-\xi}}\left(\frac{x-t}{\sqrt{\mathfrak{w}_0\mathfrak{w}_1}\xi} - \frac{2}{\pi}\int_C \frac{\theta_0'(s)\sqrt{-s}}{\mathfrak{R}(s)(s-\xi)}\mathrm{d}s\right)\right]\mathrm{d}\xi \\ &+ \int_{\widetilde{\beta}_-} \mathfrak{R}_- \left[-\frac{1}{4\sqrt{-\xi}}\left(\frac{x-t}{\sqrt{\mathfrak{w}_0\mathfrak{w}_1}\xi} - \frac{2}{\pi}\int_C \frac{\theta_0'(s)\sqrt{-s}}{\mathfrak{R}(s)(s-\xi)}\mathrm{d}s\right)\right]\mathrm{d}\xi \\ &+ \int_{\widetilde{\beta}_+} -\frac{\mathfrak{R}_+}{4\sqrt{-\xi}}\left(\frac{8m}{\xi-\mathfrak{w}_0} + \frac{8n}{\xi-\mathfrak{w}_1}\right)\mathrm{d}\xi + \int_{\widetilde{\beta}_-} -\frac{\mathfrak{R}_-}{4\sqrt{-\xi}}\left(\frac{8m}{\xi-\mathfrak{w}_0} + \frac{8n}{\xi-\mathfrak{w}_1}\right)\mathrm{d}\xi \\ =:& I + 8m\left\{\int_{\widetilde{\beta}_+} -\frac{\mathfrak{R}_+(\xi)}{4\sqrt{-\xi}}\frac{1}{\xi-\mathfrak{w}_0}\mathrm{d}\xi + \int_{\widetilde{\beta}_-} -\frac{\mathfrak{R}_-(\xi)}{4\sqrt{-\xi}}\frac{1}{\xi-\mathfrak{w}_0}\mathrm{d}\xi\right\} \\ &+ 8n\left\{\int_{\widetilde{\beta}_+} -\frac{\mathfrak{R}_+(\xi)}{4\sqrt{-\xi}}\frac{1}{\xi-\mathfrak{w}_1}\mathrm{d}\xi + \int_{\widetilde{\beta}_-} -\frac{\mathfrak{R}_-(\xi)}{4\sqrt{-\xi}}\frac{1}{\xi-\mathfrak{w}_1}\mathrm{d}\xi\right\}\end{aligned} \tag{4.10}$$

For convenience, define

$$\begin{aligned}c_m &= \left\{\int_{\widetilde{\beta}_+} -\frac{\mathfrak{R}_+(\xi)}{4\sqrt{-\xi}}\frac{1}{\xi-\mathfrak{w}_0}\mathrm{d}\xi + \int_{\widetilde{\beta}_-} -\frac{\mathfrak{R}_-(\xi)}{4\sqrt{-\xi}}\frac{1}{\xi-\mathfrak{w}_0}\mathrm{d}\xi\right\}, \\ c_n &= \left\{\int_{\widetilde{\beta}_+} -\frac{\mathfrak{R}_+(\xi)}{4\sqrt{-\xi}}\frac{1}{\xi-\mathfrak{w}_1}\mathrm{d}\xi + \int_{\widetilde{\beta}_-} -\frac{\mathfrak{R}_-(\xi)}{4\sqrt{-\xi}}\frac{1}{\xi-\mathfrak{w}_1}\mathrm{d}\xi\right\}.\end{aligned} \tag{4.11}$$

We may compare $\mathfrak{M}$ and $\mathfrak{I}$ with the form of the original M and I.

$$\mathfrak{M} = M + 8m + 8n, \tag{4.12}$$

$$\mathfrak{I} = I + 8mc_m + 8nc_n. \tag{4.13}$$

Here we are abusing notation in the sense that, in equation (4.9) and (4.10), M and I actually mean $M(x,t,\mathfrak{w}_0,\mathfrak{w}_1)$ and $I(x,t,\mathfrak{w}_0,\mathfrak{w}_1)$, where among other things, the contour of integration is the changed to the new $\widetilde{\beta}$. Nevertheless, at the gradient catastrophe point, m and n are both 0, in which case $\mathfrak{M} = M$, and $\mathfrak{I} = I$.

4.1.3 Eliminating the parameters m and n

In chapter 3 the conditions $M \equiv 0$ and $I \equiv 0$ are used to solve for the endpoints w_0 and w_1 as implicit functions of (x,t), i.e. $w_0(x,t)$ and $w_1(x,t)$. Here the new $\mathfrak{M} \equiv 0$ and $\mathfrak{I} \equiv 0$ are used for a different purpose. We are going to use them to eliminate m and n. In order to express m and n explicitly, we only need $c_m - c_n \neq 0$.

Lemma 4.1.1. *If $\mathfrak{w}_0 \neq \mathfrak{w}_1$, then $c_m - c_n \neq 0$.*

Proof.

$$\begin{aligned}
c_m - c_n =& \int_{\beta_+} -\frac{\mathfrak{R}_+(\xi)}{4\sqrt{-\xi}}\left(\frac{1}{\xi-\mathfrak{w}_0} - \frac{1}{\xi-\mathfrak{w}_1}\right)\mathrm{d}\xi + \int_{\beta_-} -\frac{\mathfrak{R}_-(\xi)}{4\sqrt{-\xi}}\left(\frac{1}{\xi-\mathfrak{w}_0} - \frac{1}{\xi-\mathfrak{w}_1}\right)\mathrm{d}\xi \\
=& \int_{\beta_+} -\frac{\mathfrak{R}_+}{4\sqrt{-\xi}}\frac{\mathfrak{w}_0-\mathfrak{w}_1}{(\xi-\mathfrak{w}_0)(\xi-\mathfrak{w}_1)}\mathrm{d}\xi + \int_{\beta_-} -\frac{\mathfrak{R}_-}{4\sqrt{-\xi}}\frac{\mathfrak{w}_0-\mathfrak{w}_1}{(\xi-\mathfrak{w}_0)(\xi-\mathfrak{w}_1)}\mathrm{d}\xi \\
=& -\frac{\mathfrak{w}_0-\mathfrak{w}_1}{4}\left[\int_{\beta_+}\frac{1}{\sqrt{-\xi}}\frac{1}{\mathfrak{R}_+}\mathrm{d}\xi + \int_{\beta_-}\frac{1}{\sqrt{-\xi}}\frac{1}{\mathfrak{R}_-}\mathrm{d}\xi\right] \\
=& -\frac{\mathfrak{w}_0-\mathfrak{w}_1}{4}\times 2\int_0^{-\infty}\frac{1}{\sqrt{-x}}\frac{1}{\mathfrak{R}}\mathrm{d}\xi \neq 0,
\end{aligned} \tag{4.14}$$

□

Observe $w_0^{\mathrm{gc}} \neq w_1^{\mathrm{gc}}$. Later we will show that the $\mathfrak{w}_j$, $j = 0, 1$ are continuous function of (x,t), and $\mathfrak{w}_j^{\mathrm{gc}} = w_j^{\mathrm{gc}}$. Therefore we may assume that $c_m - c_n \neq 0$.

Thus, we arrive at the expressions for m and n,

$$\begin{aligned}
8m(x,t,\mathfrak{w}_0,\mathfrak{w}_1) =& \frac{-c_nM + I}{c_n - c_m}, \\
8n(x,t,\mathfrak{w}_0,\mathfrak{w}_1) =& \frac{c_mM - I}{c_n - c_m},
\end{aligned} \tag{4.15}$$

where

$$\begin{aligned} M =& \frac{x-t}{\sqrt{w_0 w_1}} + x + t - \frac{2}{\pi}\int_C \frac{\theta_0'(\xi)\sqrt{-\xi}}{\mathfrak{R}(\xi; w_0, w_1)}\mathrm{d}\xi, \\ I =& \int_{\beta_+} \mathfrak{R}_+ \left[-\frac{1}{4\sqrt{-\xi}} \left(\frac{x-t}{\sqrt{\mathfrak{w}_0\mathfrak{w}_1}\xi} - \frac{2}{\pi}\int_C \frac{\theta_0'(s)\sqrt{-s}}{\mathfrak{R}(s)(s-\xi)}\mathrm{d}s \right) \right] \mathrm{d}\xi \\ &+ \int_{\beta_-} \mathfrak{R}_- \left[-\frac{1}{4\sqrt{-\xi}} \left(\frac{x-t}{\sqrt{\mathfrak{w}_0\mathfrak{w}_1}\xi} - \frac{2}{\pi}\int_C \frac{\theta_0'(s)\sqrt{-s}}{\mathfrak{R}(s)(s-\xi)}\mathrm{d}s \right) \right] \mathrm{d}\xi \end{aligned} \tag{4.16}$$

Henceforth we will assume m and n have already been eliminated, and all related quantities are determined by (x, t, w_0, w_1) instead.

It remains to determine the dependence of $\mathfrak{w}_0(x,t)$ and $\mathfrak{w}_1(x,t)$. Since $\mathfrak{M} = 0$ and $\mathfrak{I} = 0$ are already used for other purposes, we will need a different approach in the next section.

4.2 φ expansion

The main goal of this chapter is to map the phase near the endpoints $\mathfrak{w}_{0,1}$ to the Painlevé-I exponent. For convenience, we avoid carrying fractional powers in the expansion by introducing local substitutions:

$$\begin{aligned} w - \mathfrak{w}_0 &= {q_0}^2, \quad w = q_0^2 + \mathfrak{w}_0, \\ w - \mathfrak{w}_1 &= {q_1}^2, \quad w = q_1^2 + \mathfrak{w}_1, \end{aligned} \tag{4.17}$$

(therefore $\sqrt{w - \mathfrak{w}_0} = q_0$, and similar for q_1, where the branches are chosen later, see figure 4.2). Suppose ϕ has expansion, similar in form to 4.3,

$$\begin{aligned} \varphi - \varphi(\mathfrak{w}_0) &= C_1^0 q_0 + C_3^0 q_0^3 + C_5^0 q_0^5 + C_7^0 q_0^7 + \mathcal{O}(q_0^9) \\ \varphi - \varphi(\mathfrak{w}_1) &= C_1^1 q_1 + C_3^1 q_1^3 + C_5^1 q_1^5 + C_7^1 q_1^7 + \mathcal{O}(q_1^9). \end{aligned} \tag{4.18}$$

Here we have written out two expansions and two local substitutions near the endpoints $\mathfrak{w}_0$ and $\mathfrak{w}_1$ for the aforementioned reason: we are going to treat (x,t) as complex variables and forget for now about the conjugation symmetries. The knowledge of the expansion coefficients is sometimes convenient and in some other cases essential. The fact that the conformal mapping we seek has smooth dependence relies on C_1 and C_3 being 0 at the gradient catastrophe point (which we will prove at the end of this section).

Near $\mathfrak{w}_0$, we want to compute the expansion of

$$\varphi(w)-\varphi(\mathfrak{w}_0)=\int_{\mathfrak{w}_0}^{w}-\frac{\mathfrak{R}(\xi)}{4\sqrt{-\xi}}\left(\frac{x-t}{\sqrt{\mathfrak{w}_0\mathfrak{w}_1}\xi}-\frac{2}{\pi}\int_C\frac{\theta_0'(s)\sqrt{-s}}{\mathfrak{R}(s)(s-\xi)}\mathrm{d}s+\frac{8m}{\xi-\mathfrak{w}_0}+\frac{8n}{\xi-\mathfrak{w}_1}\right)\mathrm{d}\xi, \tag{4.19}$$

or after substituting w for q,

$$\begin{aligned}\varphi=\int_0^{q}-\frac{\mathfrak{R}(\xi(q))}{4\sqrt{-\mathfrak{w}_0-q'^2}}\Bigg(\frac{x-t}{\sqrt{\mathfrak{w}_0\mathfrak{w}_1}(\mathfrak{w}_0+q'^2)}-\frac{2}{\pi}\int_C\frac{\theta_0'(s)\sqrt{-s}}{\mathfrak{R}(s)(s-\mathfrak{w}_0-q'^2)}\mathrm{d}s+\frac{8m}{q'^2}\\ +\frac{8n}{q'^2+\mathfrak{w}_0-\mathfrak{w}_1}\Bigg)2q'\mathrm{d}q'.\end{aligned} \tag{4.20}$$

A similar computation can be done near $\mathfrak{w}_1$.

4.2.1 Picking branches for the square roots

The more convenient way to specify the branch of the multivalued square root functions here is not to use the principal branches. The branch cuts for $\sqrt{w-\mathfrak{w}_0}$ and $\sqrt{w-\mathfrak{w}_1}$ are chosen to be congruent with the branch cut of $\mathfrak{R}(w)$, where $\mathfrak{R}$ is given by

$$\mathfrak{R}^2(w)=(w-\mathfrak{w}_0)(w-\mathfrak{w}_1),\qquad \mathfrak{R}\sim w,\ w\to\infty. \tag{4.21}$$

See figure 4.2. After branch cuts are chosen, we specify the branch through its behaviour at $+\infty$. Suppose:

$S_0=(w-\mathfrak{w}_0)^{\frac{1}{2}}$ with branch cut on $\beta_+\cup(-\infty,1)$,

$S_1=(w-\mathfrak{w}_1)^{\frac{1}{2}}$ with branch cut on $\beta_-\cup(-\infty,1)$,

$S_0,\ S_1\sim\sqrt{w}$ at $+\infty$.

Let $q=S_0$, then

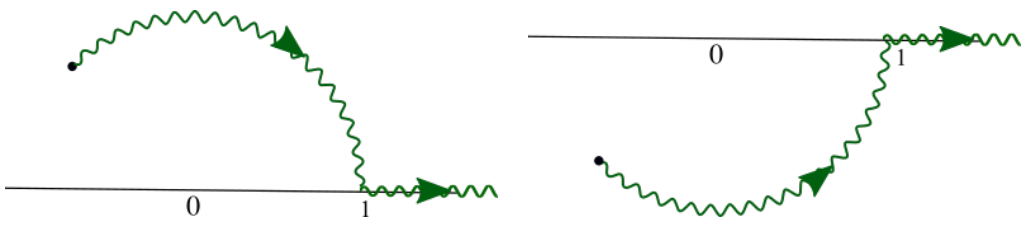

(a) S_0 branch cut (b) $S1$ branch cut

Figure 4.2: Branch cuts for S_0 and S_1

$$\begin{aligned}\Delta_0\varphi :=&\varphi(w)-\varphi(\mathfrak{w}_0)=\int_0^q\Bigg[-\frac{x-t}{4\sqrt{\mathfrak{w}_0\mathfrak{w}_1}}\frac{q'S_1(q'^2+\mathfrak{w}_1)}{(-\mathfrak{w}_0-q'^2)^{\frac{3}{2}}\cdot(-1)}\\&+\frac{q'S_1(q'^2+\mathfrak{w}_0)}{2\pi(-\mathfrak{w}_0-q'^2)^{\frac{1}{2}}}\int_C\frac{\theta_0's\sqrt{-s}}{\mathfrak{R}(s)}\frac{1}{s-\mathfrak{w}_0-q'^2}\mathrm{d}s-\frac{S_1(q'^2+\mathfrak{w}_0)}{(-\mathfrak{w}_0-q'^2)^{\frac{1}{2}}q'}2m\\&-\frac{q'}{S_1(q'^2+\mathfrak{w}_0)(-\mathfrak{w}_0-q'^2)^{\frac{1}{2}}}2n\Bigg]2q'\mathrm{d}q'.\end{aligned}\tag{4.22}$$

We xxpand for small q', and note that $S_1(q'^2+\mathfrak{w}_0)=\sqrt{\mathfrak{w}_0-\mathfrak{w}_1}\left(1+\frac{q'^2}{\mathfrak{w}_0-\mathfrak{w}_1}\right)^{\frac{1}{2}}$, $(-\mathfrak{w}_0-q')^{\frac{3}{2}}=(-\mathfrak{w}_0)^{\frac{3}{2}})\left(1+\frac{q'^2}{\mathfrak{w}_0}\right)^{\frac{3}{2}}$, here square root $\sqrt{\mathfrak{w}_0-\mathfrak{w}_1}$ means the principal branch.

$$\begin{aligned}\Delta_0\varphi_0=&\int_0^q\Bigg[-\frac{x-t}{4\sqrt{\mathfrak{w}_0\mathfrak{w}_1}}\frac{q'\sqrt{\mathfrak{w}_0-\mathfrak{w}_1}\left(1+\frac{q'^2}{\mathfrak{w}_0-\mathfrak{w}_1}\right)^{\frac{1}{2}}}{(-\mathfrak{w}_0)^{\frac{3}{2}}\left(1+\frac{q'^2}{\mathfrak{w}_0}\right)^{\frac{3}{2}}\cdot(-1)}\\&+\frac{q'\sqrt{\mathfrak{w}_0-\mathfrak{w}_1}\left(1+\frac{q'^2}{\mathfrak{w}_0-\mathfrak{w}_1}\right)^{\frac{1}{2}}}{2\pi\sqrt{-\mathfrak{w}_0}\left(1+\frac{q'^2}{\mathfrak{w}_0}\right)^{\frac{1}{2}}}\int_C\frac{\theta_0's\sqrt{-s}}{\mathfrak{R}(s)}\frac{1}{s-\mathfrak{w}_0}\frac{1}{1-\frac{q'^2}{s-\mathfrak{w}_0}}\mathrm{d}s-\frac{\sqrt{\mathfrak{w}_0-\mathfrak{w}_1}\left(1+\frac{q'^2}{\mathfrak{w}_0-\mathfrak{w}_1}\right)^{\frac{1}{2}}}{\sqrt{-\mathfrak{w}_0}\left(1+\frac{q'^2}{\mathfrak{w}_0}\right)^{\frac{1}{2}}q'}2m\\&-\frac{q'}{\sqrt{\mathfrak{w}_0-\mathfrak{w}_1}\sqrt{-\mathfrak{w}_0}\left(1+\frac{q'^2}{\mathfrak{w}_0-\mathfrak{w}_1}\right)^{\frac{1}{2}}\left(1+\frac{q'^2}{\mathfrak{w}_0}\right)^{\frac{1}{2}}}2n\Bigg]2q'\mathrm{d}q'.\end{aligned}\tag{4.23}$$

4.2.2 Computing the expansion coefficients of φ

From (4.23), we can easily determine the coefficients in the expansion

$$C_1 = \frac{4m(\mathfrak{w}_0 - \mathfrak{w}_1)}{\sqrt{-\mathfrak{w}_0}\sqrt{\mathfrak{w}_0 - \mathfrak{w}_1}}, \tag{4.24}$$

$$\begin{aligned} C_3 =& \frac{1}{6\pi(-\mathfrak{w}_0)^{\frac{3}{2}}\sqrt{\mathfrak{w}_0 - \mathfrak{w}_1}\sqrt{\mathfrak{w}_0\mathfrak{w}_1}} \left[8m\pi\mathfrak{w}_0\sqrt{\mathfrak{w}_0\mathfrak{w}_1} + 16n\pi\mathfrak{w}_0\sqrt{\mathfrak{w}_0\mathfrak{w}_1}\right. \\ & - \left(-\frac{3}{2\mathfrak{w}_0} - \frac{1}{2(\mathfrak{w}_0 - \mathfrak{w}_1)}\right)\left(-8m\pi\mathfrak{w}_0^2\sqrt{\mathfrak{w}_0\mathfrak{w}_1} + 8m\pi\mathfrak{w}_0\mathfrak{w}_1\sqrt{\mathfrak{w}_0\mathfrak{w}_1}\right) \\ & \left. -\pi(\mathfrak{w}_0 - \mathfrak{w}_1)(t-x) - 2\mathfrak{w}_0(\mathfrak{w}_0 - \mathfrak{w}_1)\sqrt{\mathfrak{w}_0\mathfrak{w}_1}\int_C \frac{\sqrt{-s}\theta_0'(s)}{(s-\mathfrak{w}_0)\mathfrak{R}(s)}\mathrm{d}s\right], \end{aligned} \tag{4.25}$$

$$\begin{aligned} C_5 =& \frac{1}{2\pi(-\mathfrak{w}_0)(3/2)\sqrt{\mathfrak{w}_0 - \mathfrak{w}_1}\sqrt{\mathfrak{w}_0\mathfrak{w}_1}} \left[8n\pi\sqrt{\mathfrak{w}_0\mathfrak{w}_1} - \frac{3}{2}\pi(t-x)\right. \\ & - \left(\frac{15}{8\mathfrak{w}_0^2} + \frac{3}{8(\mathfrak{w}_0 - \mathfrak{w}_1)^2} + \frac{3}{4\mathfrak{w}_0(\mathfrak{w}_0 - \mathfrak{w}_1)}\right)\left(-8m\pi\mathfrak{w}_0^2\sqrt{\mathfrak{w}_0\mathfrak{w}_1} + 8m\pi\mathfrak{w}_0\mathfrak{w}_1\sqrt{\mathfrak{w}_0\mathfrak{w}_1}\right) \\ & - 2\sqrt{\mathfrak{w}_0\mathfrak{w}_1}\left(\mathfrak{w}_0(\mathfrak{w}_0 - \mathfrak{w}_1)\int_C \frac{\sqrt{-s}\theta_0'(s)}{(s-\mathfrak{w}_0)^2\mathfrak{R}(s)}\mathrm{d}s + (2\mathfrak{w}_0 - \mathfrak{w}_1)\int_C \frac{\sqrt{-s}\theta_0'(s)}{(s-\mathfrak{w}_0)\mathfrak{R}(s)}\mathrm{d}s\right) \\ & - \left(-\frac{3}{2\mathfrak{w}_0} - \frac{1}{2(\mathfrak{w}_0 - \mathfrak{w}_1)}\right)\left(\pi(t-x)(\mathfrak{w}_0 - \mathfrak{w}_1) - 8\pi\mathfrak{w}_0\sqrt{\mathfrak{w}_0\mathfrak{w}_1}(m+2n)\right. \\ & \left.\left. + 2\mathfrak{w}_0(\mathfrak{w}_0 - \mathfrak{w}_1)\sqrt{\mathfrak{w}_0\mathfrak{w}_1}\int_C \frac{\sqrt{-s}\theta_0'(s)}{(s-\mathfrak{w}_0)\mathfrak{R}(s)}\mathrm{d}s\right)\right]. \end{aligned} \tag{4.26}$$

4.2.3 At the gradient catastrophe point, $C_1 = C_3 = 0$ snd $C_5 \neq 0$

The universality in our result relies on the gradient catastrophe being the lowest degeneracy. It happens when a simple zero merges with the end point of the band. To be precise, we assume:

Assumption 4.2.1. *At the gradient catastrophe, H vanishes. We would assume that the vanishing is generic with first derivative nonzero, i.e. supposing H has expansion near w_0 (and similarly w_1)*

$$H(w; x, t, w_0, w_1) = H_0(x, t, w_0, w_1) + H_1(x, t, w_0, w_1)(w - w_0) + \mathcal{O}((w - w_0)^2), \quad w \to w_0, \tag{4.27}$$

then at the gradient catastrophe, $H_0^{\mathrm{gc}} = 0$, while

$$H_1^{\mathrm{gc}} \neq 0. \tag{4.28}$$

A direct consequence following this assumption and the expansion of ϕ is that

Proposition 4.2.2. *At the gradient catastrophe C_1, C_3 are zero, while C_5 is bounded away*

from 0, i.e.

$$C_5^{0/1,\mathrm{gc}} \neq 0; \quad C_3^{0/1,\mathrm{gc}} = C_1^{0/1,\mathrm{gc}} = 0. \tag{4.29}$$

Proof. We will do the upper half plane in detail. The lower half plane follows from an analogous argument.

For convenience, denote the expansion of $\mathfrak{R}$ near $\mathfrak{w}_0$ as follows:

$$\mathfrak{R}(q_0) = \sqrt{\mathfrak{w}_0 - \mathfrak{w}_1} q_0 \left(1 + \frac{q_0^2}{\mathfrak{w}_0 - \mathfrak{w}_1}\right)^{\frac{1}{2}} =: \mathfrak{R}_1^0 q_0 + \mathfrak{R}_3^0 q_0^3 + \mathcal{O}(q_0^5). \tag{4.30}$$

where

$$\mathfrak{R}_1^0 = \sqrt{\mathfrak{w}_0 - \mathfrak{w}_1}, \quad \mathfrak{R}_3^0 = \frac{1}{2\sqrt{\mathfrak{w}_0 - \mathfrak{w}_1}}. \tag{4.31}$$

Similarly the expansion of H near $\mathfrak{w}_0$ is

$$H^0 = H_0^0 + H_2^0 q_0^2 + \mathcal{O}(q_0^4), \tag{4.32}$$

and

$$\begin{aligned}\Delta_0\varphi = \int_0^q \left(\mathfrak{R}_1^0 q_0' + \mathfrak{R}_3^0 {q_0'}^3 + \mathcal{O}({q_0'}^5)\right) \Bigg[&\frac{2m}{\sqrt{-\mathfrak{w}_0}} {q_0'}^{-2} - H_0^0 - \frac{m}{\mathfrak{w}_0\sqrt{-\mathfrak{w}_0}} + \frac{2n}{\sqrt{-\mathfrak{w}_0}(\mathfrak{w}_0 - \mathfrak{w}_1)} \\ &\left(-H_2^0 + \frac{3}{2}\frac{m}{\mathfrak{w}_0^2\sqrt{-\mathfrak{w}_0}} - \frac{n}{\mathfrak{w}_0\sqrt{-\mathfrak{w}_0}(\mathfrak{w}_0 - \mathfrak{w}_1)} - \frac{2n}{\sqrt{-\mathfrak{w}_0}(\mathfrak{w}_0 - \mathfrak{w}_1)^2}\right) {q_0'}^2 \\ &+\mathcal{O}({q_0'}^4)\Bigg] 2q_0' \mathrm{d}q_0'\end{aligned} \tag{4.33}$$

When only evaluating at the gradient catastrophe point, one can assume m and n to be 0, thus the expression simplifies to

$$\Delta_0\varphi = \int_0^{q_0} \left(\mathfrak{R}_1^0 q_0' + \mathfrak{R}_3^0 {q_0'}^3 + \mathcal{O}({q_0'}^5)\right) \left(-H_0^0 - H_2^0 {q_0'}^2 + \mathcal{O}({q_0'}^4)\right) 2q_0' \mathrm{d}q_0' \tag{4.34}$$

We see immediately

$$C_1^{0,\mathrm{gc}} = 0, \quad C_3^{0,\mathrm{gc}} = 0, \quad C_5^{0,\mathrm{gc}} = -\frac{2}{5}(\mathfrak{R}_3^0 H_0^0 + \mathfrak{R}_1^0 H_2^0). \tag{4.35}$$

By assumption, at the gradient catastrophe the two endpoints lie inside either side of the complex half plane. Thus they are not identical. $\sqrt{\mathfrak{w}_0 - \mathfrak{w}_1} \neq 0$, and H_2^0 is nonzero, but H_0^0 is zero, thus

$$C_5^{0,\mathrm{gc}} = -\frac{2}{5}\sqrt{\mathfrak{w}_0 - \mathfrak{w}_1} H_2^0 \neq 0, \tag{4.36}$$

which completes the proof. □

4.3 Theorem 0: conformal coordinates near $\mathfrak{w}_0$ and $\mathfrak{w}_1$

In this section we try to find conformal coordinates such that the jump matrices, in particular the exponential terms $\exp[\pm(\varphi - \varphi(\mathfrak{w}_0))/\epsilon_N]$ and $\exp[(\varphi - \varphi(\mathfrak{w}_0))/\epsilon_N]$, near the end points locally map exactly to the Painlevé-I jump matrices with exponential $\exp \pm 2(\frac{4}{5}\zeta^{\frac{5}{2}} - \nu\zeta^{\frac{1}{2}})$.

We are viewing (x,t) as parameters in the phase function as well as the conformal mapping. In other words we are going to choose $\mathfrak{w}_0(x,t)$ and $\mathfrak{w}_1(x,t)$, $\nu(x,t)$ depending on (x,t), so that we are able to map $\frac{1}{2}(\varphi - \varphi(\mathfrak{w}_k))$ to a *normal form* $\frac{4}{5}W_k(w)^{\frac{5}{2}} - s_k(x,t)W_k(w)^{\frac{1}{2}}$ for each chosen (x,t), $k = 0, 1$ corresponding to the upper or lower half planes, i.e.

$$\begin{aligned} W_k(x,t) : U_k &\to \mathbb{C}, \\ w &\mapsto W_k(w;x,t), \end{aligned} \tag{4.37}$$

where for each (x,t) the mapping W_k is conformal, while for each value of w, the $W_k(w;x,t)$ are continuously dependent on (x,t) in a neighbourhood of the gradient catastrophe point $(x_{\text{gc}}, t_{\text{gc}})$. Inside the neighbourhood of $(x_{\text{gc}}, t_{\text{gc}})$, the phase is exactly

$$\frac{1}{2}\Delta_k\varphi(w) = \frac{4}{5}W_k(w)^{\frac{5}{2}} - s_k(x,t)W_k(w)^{\frac{1}{2}}. \tag{4.38}$$

Recall that we do not assume Schwarz symmetry of the modified $\mathfrak{g}$ functions, hence the need to define two mappings both near $\mathfrak{w}_0$ and $\mathfrak{w}_1$.

The first example of a local normal form in the setting of coalescing saddle points in a steepest descent expansion was worked out in [16]. We use a different approach inspired by [15], by building the mapping from differentiating the operators with respect to x and t.

Behind both approaches, the fundamental idea is that the normal form on the right hand side can be viewed as polynomial (for half powers) of fixed power. Thus, a fixed number of roots appear. A smooth mapping will only be possible when the zeros of the function on the left hand side are mapped exactly to the roots on the right hand side, and varies with respect to the parameters in a smooth fashion.

Statement of the theorem for conformal coordinates near $\mathfrak{w}_0$ and $\mathfrak{w}_1$

Theorem 4.3.1 (Conformal mapping near the endpoint of the band)**.** *There exist real analytic functions $\mathfrak{w}_0(x,t)$, $\mathfrak{w}_1(x,t)$, $s(x,t)$, well defined in a neighbourhood of the gradient catastrophe point $(x^{\rm gc},t^{\rm gc})$. At the gradient catastrophe point, $s^{\rm gc}:=s(x^{\rm gc},t^{\rm gc})=0$, $\mathfrak{w}_0^{\rm gc}:=\mathfrak{w}_0(x^{\rm gc},t^{\rm gc})=w_0^{\rm gc}$, $\mathfrak{w}_1^{\rm gc}=w_1^{\rm gc}=\overline{w_0^{\rm gc}}$. For $(x-x^{\rm gc})$ and $(t-t^{\rm gc})$ small, there is a conformal mapping W_k that takes the disk U_k to the complex plane, such that the phase is exactly*

$$\frac{1}{2}\Delta_k\varphi(w)=\frac{4}{5}W_k(w;x,t)^{\frac{5}{2}}-s_k(x,t)W_k(w;x,t)^{\frac{1}{2}}. \tag{4.39}$$

In particular, the center of the disks $\mathfrak{w}_k$, $k=0,1$, are mapped to the origin of the W plane.

At the gradient catastrophe, derivatives of s_k and $\mathfrak{w}_k$ with respect to x and t are:

$$s_x^{\rm gc}=-\frac{C_{1,x}^{\rm gc}}{\left(\frac{5}{8}\right)^{\frac{1}{5}}\rho_0^{\rm gc}},\ s_t^{\rm gc}=-\frac{C_{1,t}^{\rm gc}}{\left(\frac{5}{8}\right)^{\frac{1}{5}}\rho_1^{\rm gc}}, \tag{4.40}$$

where

$$\rho_k^{\rm gc5}=C_5^{k,\rm gc},\quad \textit{and}\quad \arg(\rho_k)=(-1)^k\left(\frac{7\pi}{20}+\frac{1}{2}\arg(w_0^{\rm gc})\right)\ (\mathrm{mod}\ 2\pi), \tag{4.41}$$

and ρ is ${C_5}^{\frac{1}{5}}$ with the branch determined such that β is mapped into $\mathbb{R}_-$.

Notation

For convenience we use ∂_x in place of $\frac{\partial}{\partial x}$, as well as $\partial_t:=\frac{\partial}{\partial x}$, $\partial_0:=\frac{\partial}{\partial_{\mathfrak{w}_0}}$ and $\partial_1:=\frac{\partial}{\partial_{\mathfrak{w}_1}}$. Also, recall for simplicity, we have introduced notation $\Delta_0\varphi_0:=\varphi-\varphi_0$, and similarly $\Delta_1\varphi_1$.

Proof. We continue to use q_0 and q_1 defined in (4.17) with branches and branch cuts specified in S_0 and S_1. See figure 4.2. Along the same line of reasoning, i.e. to use integer instead of half integer powers, we define

$$\begin{aligned} Q_0=&W_0^{\frac{1}{2}},\\ Q_1=&W_1^{\frac{1}{2}}, \end{aligned} \tag{4.42}$$

where $W_k^{\frac{1}{2}}$ denotes the principal branch. Equation (4.39) implies that we want to find

conformal mappings $Q_k(q_k; x, t)$ such that

$$\begin{aligned}\frac{1}{2}\Delta_0\varphi(q_0) =& \frac{4}{5}Q_0^5 - s_0 Q_0,\\ \frac{1}{2}\Delta_1\varphi(q_1) =& \frac{4}{5}Q_1^5 - s_1 Q_1,\end{aligned} \tag{4.43}$$

where $Q_j(q; x, t)$ is a univalent function near $q_j = 0$. We will determine the dependence of $s_0(x,t)$, $s_1(x,t)$, $\mathfrak{w}_0(x,t)$ and $\mathfrak{w}_1(x,t)$. Since both sides of (4.43) are odd functions of q_k and Q_k, Q_k should also be an odd function of q_k.

At the gradient catastrophe point $(x^{\mathrm{gc}}, t^{\mathrm{gc}})$, $s^{\mathrm{gc}} = 0$. Thus the right hand side of (4.43) has only one root of multiplicity 5. Equation (4.29) also suggests the same for the left hand side:

$$\frac{1}{2}\Delta_k\varphi = \frac{1}{2}C_5^{k,\mathrm{gc}}q_0^5 + \frac{1}{2}C_7^{k,\mathrm{gc}}q_0^7 + \cdots = \frac{1}{2}C_5^{k,\mathrm{gc}}q_0^5\left(1 + \frac{1}{5}\frac{C_7^{k,\mathrm{gc}}}{C_5^{k,\mathrm{gc}}}q_0^2 + \mathcal{O}(q_0^4)\right). \tag{4.44}$$

Therefore we can take fifth root and write

$$Q_k^{\mathrm{gc}}(q_0) = \left(\frac{5}{8}\right)^{\frac{1}{5}}\rho_k^{\mathrm{gc}}q_0\left(1 + \frac{1}{5}\frac{C_7^{k,\mathrm{gc}}}{C_5^{k,\mathrm{gc}}}q^2 + O(q^4)\right), \tag{4.45}$$

where $\rho_k^5 = C_5^{k,\mathrm{gc}}$. The branch we choose should be congruent with the local picture of the $\mathfrak{g}$-function. Note by definition, for every (x,t),

$$Q_k(0) = 0. \tag{4.46}$$

4.3.1 Branch of ρ_k^{gc}

In section 3.2 we have shown that the left arc of the unit circle is a level curve of $\mathrm{Re}(\phi)$. By definition of ϕ, $\mathrm{Re}(\phi(w))|_\beta$ is also 0. At the gradient catastrophe point the local behaviour of ϕ is like $(w-w_0)^{\frac{5}{2}}$, therefore five level curves of $\mathrm{Re}(\phi)$ emanate from w_0. Between β and the two adjacent level curves, as well as the region between the two curves not adjacent to β, $\mathrm{Re}(\phi)$ is positive; the rest of the two sectors have $\mathrm{Re}(\phi) < 0$, (see figure 4.3). The curve γ is placed in one of the regions where $\mathrm{Re}(\phi) < 0$, such that γ can go back to 1.

At the gradient catastrophe, $\Delta_0\phi^{\mathrm{gc}}(w) = C_5^{0,\mathrm{gc}}(w-w_0)^{\frac{5}{2}}(1+\mathcal{O}(w-w_0))$. Suppose

$$0 < \lambda = \arg(w_0) < \pi, \tag{4.47}$$

because w_0 is on the unit circle, the level curve overlapping with the unit circle necessarily

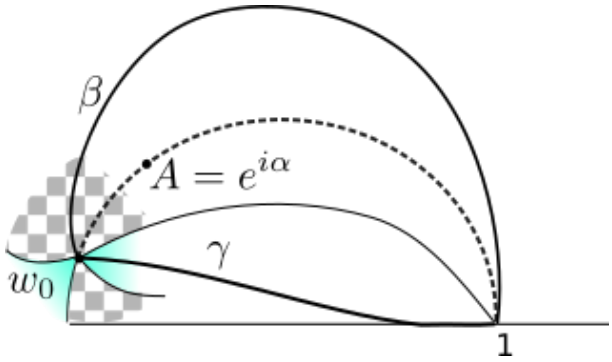

Figure 4.3: The local picture of β, the unit circle, and local sign chart of $\mathrm{Re}(\phi)$. The checkerboard region denotes positive $\mathrm{Re}(\phi)$; the green region denotes negative $\mathrm{Re}(\phi)$.

has argument $\lambda + \frac{\pi}{2}$.

Thus, the angle of β at w_0 is $\lambda - \frac{3\pi}{10}$. Therefore $\arg(q_0) = \frac{1}{2}\lambda - \frac{3\pi}{20}$, and

$$\arg(q_0^5) = \frac{5}{2}\lambda - \frac{3\pi}{4} \ (\mathrm{mod}\ 2\pi). \tag{4.48}$$

On the other hand

$$\phi = 2 \times \left(\frac{4}{5} Q_0^5\right) = C_5^0 q_0^5 (1 + \mathcal{O}(q^2)). \tag{4.49}$$

The β curve is mapped to $W_0(w) < 0$, thus we choose the corresponding $Q_0(q) = W_0(w)^{\frac{1}{2}}$ to be $i\mathbb{R}_+$, i.e. $\arg(C_5^0) + \arg(q^5) = \frac{5\pi}{2}$. Hence $\arg(C_5^0) = \frac{5\pi}{2} + \frac{5}{2}\lambda - \frac{3\pi}{4}$.

Choose ρ_0 such that

$$\arg(\rho_0) = \frac{7\pi}{20} + \frac{1}{2}\lambda \ (\mathrm{mod}\ 2\pi). \tag{4.50}$$

Because here the ρ_k are evaluated at the gradient catastrophe point where the old g coincides with the new $\mathfrak{g}$, it is convenient for us to keep the Schwartz symmetry. Therefore, we choose $\rho_1^{\mathrm{gc}} = \rho_0^{\mathrm{gc},*}$. In particular

$$\arg(\rho_1) = -\frac{7\pi}{20} - \frac{1}{2}\lambda \ (\mathrm{mod}\ 2\pi). \tag{4.51}$$

4.3.2 Differentiating with respect to x and t

Now, let (x, t) move away from the catastrophe point. Hold q fixed and let $Q(q; x, t)$ and $\varphi(q; x, t, \mathfrak{w}_0, \mathfrak{w}_1)$ evolve. Assuming differentiability in x and t, we take x derivative of (4.43) and obtain

$$\partial_x \varphi_0 + \partial_0 \varphi \, \partial_x \mathfrak{w}_0 + \partial_1 \varphi \, \partial_x \mathfrak{w}_1 = 8 Q_0^4 \, \partial_x Q_0 - 2 \partial_x s_0 \, Q_0 - 2 s_0 \, \partial_x Q_0 \tag{4.52}$$

Therefore

$$\partial_x Q_0 = \frac{\partial_x \varphi + \partial_0 \varphi \, \partial_x \mathfrak{w}_0 + \partial_1 \varphi \, \partial_x \mathfrak{w}_1 + \partial_x s_0 Q_0}{2(4Q_0^4 - s_0)} \tag{4.53}$$

The denominator has 4 roots

$$Q_0(q) = \pm \left(\frac{s_0}{4}\right)^{\frac{1}{4}}, \pm i \left(\frac{s_0}{4}\right)^{\frac{1}{4}}, \qquad \Upsilon_0 := \left(\frac{s_0}{4}\right)^{\frac{1}{4}} \tag{4.54}$$

In order for the right hand side of (4.53) to be an analytic function for small q, we require that the numerator vanishes at the four corresponding values of q.

$$\begin{aligned} \partial_x \varphi \left(Q_0^{-1}(\Upsilon_0)\right)_x + \partial_0 \varphi_0 \left(Q_0^{-1}(\Upsilon_0)\right) \partial_x \mathfrak{w}_0 + \partial_1 \varphi_0 \left(Q_0^{-1}(\Upsilon_0)\right) \partial_x \mathfrak{w}_1 + 2\partial_x s_0 \cdot \Upsilon_0 = 0 \\ \partial_x \varphi \left(Q_0^{-1}(i\Upsilon_0)\right)_x + \partial_0 \varphi_0 \left(Q_0^{-1}(i\Upsilon_0)\right) \partial_x \mathfrak{w}_0 + \partial_1 \varphi_0 \left(Q_0^{-1}(i\Upsilon_0)\right) \partial_x \mathfrak{w}_1 + 2\partial_x s_0 \cdot i\Upsilon_0 = 0 \end{aligned} \tag{4.55}$$

Similarly, in the lower half plane, near $\mathfrak{w}_1$. Notice the use of a different φ function φ_1.

$$\begin{aligned} \partial_x \varphi_1 \left(Q_1^{-1}(\Upsilon_1)\right)_x + \partial_0 \varphi_1 \left(Q_1^{-1}(\Upsilon_1)\right) \partial_x \mathfrak{w}_0 + \partial_1 \varphi_1 \left(Q_1^{-1}(\Upsilon_1)\right) \partial_x \mathfrak{w}_1 + 2\partial_x s_1 \cdot \Upsilon_1 = 0 \\ \partial_x \varphi_1 \left(Q_1^{-1}(i\Upsilon_1)\right)_x + \partial_0 \varphi_1 \left(Q_1^{-1}(i\Upsilon_1)\right) \partial_x \mathfrak{w}_0 + \partial_1 \varphi_1 \left(Q_1^{-1}(i\Upsilon_1)\right) \partial_x \mathfrak{w}_1 + 2\partial_x s_1 \cdot i\Upsilon_1 = 0 \end{aligned} \tag{4.56}$$

If we view $\partial_x s_0$, $\partial_x s_1$, $\mathfrak{w}_{0,x}$ and $\mathfrak{w}_{1,x}$ as unknowns in (4.55) and (4.56) to be solved, we have a linear system of equations. Written in matrix form, this linear system is

$$\begin{bmatrix} 2\Upsilon_0 & 0 & \partial_0 \varphi_0 \left(Q_0^{-1}(\Upsilon_0)\right) & \partial_1 \varphi_0 \left(Q_0^{-1}(\Upsilon_0)\right) \\ 2i\Upsilon_0 & 0 & \partial_0 \varphi_0 \left(Q_0^{-1}(i\Upsilon_0)\right) & \partial_1 \varphi_0 \left(Q_0^{-1}(i\Upsilon_0)\right) \\ 0 & 2\Upsilon_1 & \partial_0 \varphi_1 \left(Q_1^{-1}(\Upsilon_1)\right) & \partial_1 \varphi_1 \left(Q_1^{-1}(\Upsilon_1)\right) \\ 0 & 2i\Upsilon_1 & \partial_0 \varphi_1 \left(Q_1^{-1}(i\Upsilon_1)\right) & \partial_1 \varphi_1 \left(Q_1^{-1}(i\Upsilon_1)\right) \end{bmatrix} \begin{bmatrix} \partial_x s_0 \\ \partial_x s_1 \\ \partial_x \mathfrak{w}_0 \\ \partial_x \mathfrak{w}_1 \end{bmatrix} = \begin{bmatrix} -\partial_x \varphi_0 \left(Q_0^{-1}(\Upsilon_0)\right) \\ -\partial_x \varphi_0 \left(Q_0^{-1}(i\Upsilon_0)\right) \\ -\partial_x \varphi_1 \left(Q_1^{-1}(\Upsilon_1)\right) \\ -\partial_x \varphi_1 \left(Q_1^{-1}(i\Upsilon_1)\right) \end{bmatrix}. \tag{4.57}$$

Name the coefficent matrix $\mathfrak{G}$, then the system can be written as

$$\mathfrak{G} \begin{bmatrix} \partial_x s_0 \\ \partial_x s_1 \\ \partial_x \mathfrak{w}_0 \\ \partial_x \mathfrak{w}_1 \end{bmatrix} = \begin{bmatrix} -\partial_x \varphi_0 \left(Q_0^{-1}(\Upsilon_0)\right) \\ -\partial_x \varphi_0 \left(Q_0^{-1}(i\Upsilon_0)\right) \\ -\partial_x \varphi_1 \left(Q_1^{-1}(\Upsilon_1)\right) \\ -\partial_x \varphi_1 \left(Q_1^{-1}(i\Upsilon_1)\right) \end{bmatrix} \tag{4.58}$$

Repeat the same procedure to t derivatives, we obtain a linear system for $\partial_t s_k(x,t)$,

$\partial_t \mathfrak{w}_k(x,t)$ and $\partial_t Q_k(q;x,t)$,

$$\mathfrak{G}\begin{bmatrix}\partial_t s_0\\ \partial_t s_1\\ \partial_t \mathfrak{w}_0\\ \partial_t \mathfrak{w}_1\end{bmatrix} = \begin{bmatrix}-\partial_t\varphi_0\left(Q_0^{-1}(\Upsilon_0)\right)\\ -\partial_t\varphi_0\left(Q_0^{-1}(i\Upsilon_0)\right)\\ -\partial_t\varphi_1\left(Q_1^{-1}(\Upsilon_1)\right)\\ -\partial_t\varphi_1\left(Q_1^{-1}(i\Upsilon_1)\right)\end{bmatrix} \tag{4.59}$$

The essence of the proof is to view $s_k(x;t)$, $\mathfrak{w}_k(q;x,t)$, $Q_k(q;x,t)$ as solutions to the partial differential equation system. At the gradient catastrophe s_k should be 0. Furthermore, the old g-function and the new modified $\mathfrak{g}$-function are the same. Consequently $\mathfrak{w}_k = w_k$. Lastly, for each q the initial $Q_k^{\mathrm{gc}}(q;x_{\mathrm{gc}},t_{\mathrm{gc}})$ is given by (4.45). Thus the initial condition is

$$(s_0(x,t), s_1(x,t), \mathfrak{w}_0(x,t), \mathfrak{w}_(x,t), Q_0(\cdot;x,t), Q_1^(\cdot;x,t)) = (0,0,w_0^{\mathrm{gc}}, w_1^{\mathrm{gc}}, Q_0^{\mathrm{gc}}(\cdot), Q_1^{\mathrm{gc}}(\cdot)) \tag{4.60}$$

for $(x,t) = (x_{\mathrm{gc}}, t_{\mathrm{gc}})$. We will show that in an ϵ-dependent neighbourhood of $(x_{\mathrm{gc}}, t_{\mathrm{gc}})$, when q is in a neighbourhood of the origin (independent of x, t and ϵ), the system of partial differential equations has a unique continuous solution. Thus the conformal mapping $Q_k(q;x,t)$ is smoothly dependent on the parameters x and t.

4.3.3 Simplifying the integrals

To solve the linear system 4.57, in particular to eliminate the inverse functions $Q_k^{-1}(\cdot)$, we use the Lagrange-Bürmann formula to rewrite the following quantities

$$\begin{aligned}&\partial_0\varphi_0\left(Q_0^{-1}(i\Upsilon_0)\right) - i\partial_0\varphi_0\left(Q_0^{-1}(\Upsilon_0)\right)\\ =&\frac{1}{2\pi i}\oint_{|q|=\rho}\frac{\partial_0\varphi_0(q')Q_0'(q')}{Q_0(q')-i\Upsilon_0}\mathrm{d}q' - \frac{1}{2\pi i}\oint_{|q|=\rho}\frac{i\partial_0\varphi_0(q')Q_0'(q')}{Q_0(q')-\Upsilon_0}\mathrm{d}q'\\ =&-\frac{4\Upsilon_0^3}{\pi}\oint_{|q|=\rho}\frac{\partial_0\varphi_0(q')Q_0{}'(q')}{4Q_0^4(q')-s}\mathrm{d}q'\end{aligned} \tag{4.61}$$

The second identity comes from making substitution $q' \mapsto -q'$. The circle of radius ρ is taken to enclose all four roots of $4Q_0^4(q') - s_0$, orientated counterclockwise. Using the oddness of the functions Q_0 and $\partial_0\varphi$, we replace the original two integrals by the average of the originals and the new ones. Then we use the identity $4\Upsilon_0^4 - s = 0$ to simplify the expression.

Definition 4.3.1. Introducing the notations:

$$W^k_{i\mathfrak{w}_j} := \oint_{|q|=\rho} \frac{\partial_j \varphi i(q') Q_i^k(q') Q_i'(q')}{4Q_i^4(q') - s} \mathrm{d}q', \tag{4.62}$$

where $i, j \in \{0, 1\}$ denote the upper or lower half plane, and $k = 0, 2$ is the power in the integral expression. Similarly, to evaluate the x, t derivatives of $\varphi(Q^{-1}(\cdot))$, we can apply the Lagrange-Bürmann formula to x or t derivatives to versions of formula (4.61). We define the following quantities:

$$X_j^k := \oint_{|q|=\rho} \frac{\varphi_{j,x}(q') Q_j^k Q_j'(q')}{4Q_j^4(q') - s} \mathrm{d}q' \tag{4.63}$$

$$T_j^k := \oint_{|q|=\rho} \frac{\varphi_{j,t}(q') Q_j^k Q_j'(q')}{4Q_j^4(q') - s} \mathrm{d}q' \tag{4.64}$$

$j \in 0, 1$ and $k = 0, 2$.

Using definition 4.3.1, equation (4.61) is equivalent to

$$\partial_0 \varphi_0 \left(Q_0^{-1}(i\Upsilon_0)\right) - i\partial_0 \varphi_0 \left(Q_0^{-1}(\Upsilon_0)\right) = -\frac{4\Upsilon_0^3}{\pi} W^0_{0\mathfrak{w}_0}. \tag{4.65}$$

Applying the same trick, we can compute the sum

$$\partial_0 \varphi_0 \left(Q_0^{-1}(i\Upsilon_0)\right) + i\partial_0 \varphi_0 \left(Q_0^{-1}(\Upsilon_0)\right) = \frac{4\Upsilon_0}{\pi} W^2_{0\mathfrak{w}_0}. \tag{4.66}$$

Therefore, we can write the evaluation of φ at the inverse image of the critical points

of the right hand side of (4.43) as follows:

$$\begin{aligned}
\partial_0\varphi_0\left(Q_0^{-1}(i\Upsilon_0)\right) =& \frac{2\Upsilon_0}{\pi}\left(-\Upsilon_0^2 W^0_{0\mathfrak{w}_0} + W^2_{0\mathfrak{w}_0}\right),\\
\partial_0\varphi_0\left(Q_0^{-1}(\Upsilon_0)\right) =& -\frac{2i\Upsilon_0}{\pi}\left(W^2_{0\mathfrak{w}_0} + \Upsilon_0^2 W^0_{0\mathfrak{w}_0}\right),\\
\partial_1\varphi_0\left(Q_0^{-1}(i\Upsilon_0)\right) =& \frac{2\Upsilon_0}{\pi}\left(-\Upsilon_0^2 W^0_{0\mathfrak{w}_1} + W^2_{0\mathfrak{w}_1}\right),\\
\partial_1\varphi_0\left(Q_0^{-1}(\Upsilon_0)\right) =& -\frac{2i\Upsilon_0}{\pi}\left(W^2_{0\mathfrak{w}_1} + \Upsilon_0^2 W^0_{0\mathfrak{w}_1}\right),\\
\partial_0\varphi_1\left(Q_1^{-1}(i\Upsilon_1)\right) =& \frac{2\Upsilon_1}{\pi}\left(-\Upsilon_1^2 W^0_{1\mathfrak{w}_0} + W^2_{1\mathfrak{w}_0}\right),\\
\partial_0\varphi_1\left(Q_1^{-1}(\Upsilon_1)\right) =& -\frac{2i\Upsilon_1}{\pi}\left(W^2_{1\mathfrak{w}_0} + \Upsilon_1^2 W^0_{1\mathfrak{w}_0}\right),\\
\partial_1\varphi_1\left(Q_1^{-1}(i\Upsilon_1)\right) =& \frac{2\Upsilon_1}{\pi}\left(-\Upsilon_1^2 W^0_{1\mathfrak{w}_1} + W^2_{1\mathfrak{w}_1}\right),\\
\partial_1\varphi_1\left(Q_1^{-1}(\Upsilon_1)\right) =& -\frac{2i\Upsilon_1}{\pi}\left(W^2_{1\mathfrak{w}_1} + \Upsilon_1^2 W^0_{1\mathfrak{w}_1}\right).
\end{aligned} \tag{4.67}$$

Similarly, the parallel results for the x and t derivatives are

$$\begin{aligned}
\partial_x\varphi_0\left(Q_0^{-1}(i\Upsilon_0)\right) =& \frac{2\Upsilon_0}{\pi}\left(-\Upsilon_0^2 X_0^0 + X_0^2\right),\\
\partial_x\varphi_0\left(Q_0^{-1}(\Upsilon_0)\right) =& -\frac{2i\Upsilon_0}{\pi}\left(X_0^2 + \Upsilon_0^2 X_0^0\right),\\
\partial_x\varphi_1\left(Q_1^{-1}(i\Upsilon_1)\right) =& \frac{2\Upsilon_1}{\pi}\left(-\Upsilon_1^2 X_1^0 + X_1^2\right),\\
\partial_x\varphi_1\left(Q_1^{-1}(\Upsilon_1)\right) =& -\frac{2i\Upsilon_1}{\pi}\left(X_1^2 + \Upsilon_1^2 X_1^0\right).
\end{aligned} \tag{4.68}$$

$$\begin{aligned}
\varphi_{0,t}\left(Q_0^{-1}(i\Upsilon_0)\right) =& \frac{2\Upsilon_0}{\pi}\left(-\Upsilon_0^2 T_0^0 + T_0^2\right)\\
\varphi_{0,t}\left(Q_0^{-1}(\Upsilon_0)\right) =& -\frac{2i\Upsilon_0}{\pi}\left(T_0^2 + \Upsilon_0^2 T_0^0\right)\\
\varphi_{1,t}\left(Q_1^{-1}(i\Upsilon_1)\right) =& \frac{2\Upsilon_1}{\pi}\left(-\Upsilon_1^2 T_1^0 + T_1^2\right)\\
\varphi_{1,t}\left(Q_1^{-1}(\Upsilon_1)\right) =& -\frac{2i\Upsilon_1}{\pi}\left(T_1^2 + \Upsilon_1^2 T_1^0\right).
\end{aligned} \tag{4.69}$$

4.3.4 Evaluating $\det(\mathfrak{G})$

To prove the system is solvable, it is sufficient to have $\det(\mathfrak{G}) \neq 0$ at the gradient catastrophe. Unfortunately this is not quite true. Observe on the right hand side of (4.57), each element has the quantity Υ_k. At the gradient catastrophe, Υ_k are the multiple roots of $Q_k^4 = 0$, thus they are all equal to 0. What is going to happen is, instead, that these

quantities which go to 0 when the system approaches the gradient catastrophe point, can be factored out from both sides of equation (4.57), and the rest of the system is invertible. Thus what happens at the gradient catastrophe point is well-defined viewed from the limit.

In order to solve for the system (4.57) at the gradient catastrophe, we first evaluate $\det(\mathfrak{G})$.

$$\begin{aligned}\frac{1}{4}\det(\mathfrak{G}) = &\Upsilon_0\Upsilon_1\partial_0\varphi_0\left(Q_0^{-1}(\Upsilon_0)\right)\partial_1\varphi_1\left(Q_1^{-1}(\Upsilon_1)\right) + i\Upsilon_0\Upsilon_1\partial_0\varphi_0\left(Q_0^{-1}(i\Upsilon_0)\right)\partial_1\varphi_1\left(Q_1^{-1}(\Upsilon_1)\right)\\ &+ i\Upsilon_0\Upsilon_1\partial_0\varphi_0\left(Q_0^{-1}(\Upsilon_0)\right)\partial_1\varphi_1\left(Q_1^{-1}(i\Upsilon_1)\right)\\ &- \Upsilon_0\Upsilon_1\partial_0\varphi_0\left(Q_0^{-1}(i\Upsilon_0)\right)\partial_1\varphi_1\left(Q_1^{-1}(i\Upsilon_1)\right)\\ &- \Upsilon_0\Upsilon_1\partial_1\varphi_0\left(Q_0^{-1}(\Upsilon_0)\right)\partial_0\varphi_1\left(Q_1^{-1}(\Upsilon_1)\right)\\ &- i\Upsilon_0\Upsilon_1\partial_1\varphi_0\left(Q_0^{-1}(i\Upsilon_0)\right)\partial_0\varphi_1\left(Q_1^{-1}(\Upsilon_1)\right)\\ &- i\Upsilon_0\Upsilon_1\partial_1\varphi_0\left(Q_0^{-1}(\Upsilon_0)\right)\partial_0\varphi_1\left(Q_1^{-1}(i\Upsilon_1)\right)\\ &+ \Upsilon_0\Upsilon_1\partial_1\varphi_0\left(Q_0^{-1}(i\Upsilon_0)\right)\partial_0\varphi_1\left(Q_1^{-1}(i\Upsilon_1)\right).\end{aligned} \tag{4.70}$$

Substituting (4.67) into $\det(\mathfrak{G})$ and simplifying, we arrive at

$$\begin{aligned}\frac{1}{4}\det(\mathfrak{G}) =&\frac{16\Upsilon_0^4\Upsilon_1^4(W^0_{0\mathfrak{w}_1}W^0_{1\mathfrak{w}_0} - W^0_{0\mathfrak{w}_0}W^0_{1\mathfrak{w}_1})}{\pi^2}\\ =&\frac{16\Upsilon_0^4\Upsilon_1^4}{\pi^2}\left(\oint_{|q'|=\rho}\frac{\partial_1\varphi_0(q')Q_0'(q')}{4Q_0^4(q')-s}\mathrm{d}q'\oint_{|q'|=\rho}\frac{\partial_0\varphi_1(q')Q_1'(q')}{4Q_1^4(q')-s}\mathrm{d}q'\right.\\ &\left.-\oint_{|q'|=\rho}\frac{\partial_0\varphi_0(q')Q_0'(q')}{4Q_0^4(q')-s}\mathrm{d}q'\oint_{|q'|=\rho}\frac{\partial_1\varphi_1(q')Q_1'(q')}{4Q_1^4(q')-s}\mathrm{d}q'\right)\end{aligned} \tag{4.71}$$

We will see later that the $\Upsilon_0^4\Upsilon_1^4$ will be cancelled in solutions to (4.57) and the system having continuous solution near the gradient catastrophe point will be equivalent to the condition

$$\det\begin{bmatrix}\oint_{|q'|=\rho}\frac{\partial_0\varphi_0(q')Q_0'(q')}{4Q_0^4(q')-s}\mathrm{d}q' & \oint_{|q'|=\rho}\frac{\partial_1\varphi_0(q')Q_0'(q')}{4Q_0^4(q')-s}\mathrm{d}q'\\ \oint_{|q'|=\rho}\frac{\partial_0\varphi_1(q')Q_1'(q')}{4Q_1^4(q')-s}\mathrm{d}q' & \oint_{|q'|=\rho}\frac{\partial_1\varphi_1(q')Q_1'(q')}{4Q_1^4(q')-s}\mathrm{d}q'\end{bmatrix} = \det\begin{bmatrix}W^0_{0\mathfrak{w}_0} & W^0_{0\mathfrak{w}_1}\\ W^0_{1\mathfrak{w}_0} & W^0_{1\mathfrak{w}_1}\end{bmatrix} \neq 0. \tag{4.72}$$

4.3.5 Evaluating $W^0_{i\mathfrak{w}_j}$

In general, the integrals $W^0_{i\mathfrak{w}_j}$ are difficult to evaluate. However, at the gradient catastrophe point the integrand has poles only at 0. The coefficients too can usually more easily evaluated at the gradient catastrophe point. We can apply the residue theorem to the expansion at 0. Recall that, from (4.29), the $C_1^{k,\mathrm{gc}}$ and $C_3^{k,\mathrm{gc}}$ are zero while $C_5^{k,\mathrm{gc}}$ is nonzero

$$\varphi_k^{\mathrm{gc}}(q) = C_5^{k,\mathrm{gc}}q_k^5 + C_7^{k,\mathrm{gc}}q_k^7 + \cdots, \tag{4.73}$$

$$\frac{4}{5}Q_k^{\rm gc}(q)^5=\frac{1}{2}C_5^{k,{\rm gc}}q_k^5+\frac{1}{2}C_7^{k,{\rm gc}}q_k^7+\cdots. \tag{4.74}$$

Expand term by term, we find

$$Q_k^{\rm gc}(q_k)=\left(\frac{5}{8}\right)^{\frac{1}{5}}\rho_k q_k\left(1+\frac{1}{5}\frac{C_7^{k,{\rm gc}}}{C_5^{k,{\rm gc}}}q_k^2+\cdots\right), \tag{4.75}$$

$$Q_k^{\rm gc}(q_k)^{-4}=\frac{1}{\left(\frac{5}{8}\right)^{\frac{4}{5}}\rho_k^4 q_k^4}\left(1-\frac{4}{5}\frac{C_7^{k,{\rm gc}}}{C_5^{k,{\rm gc}}}q_k^2+\cdots\right), \tag{4.76}$$

$$\partial_j\varphi_k(q_k)=\partial_j C_1^{k,{\rm gc}}q_k+\partial_j C_1^{k,{\rm gc}}q_k^3+\cdots, \tag{4.77}$$

$$Q_k^{\rm gc\prime}(q_k)=\left(\frac{5}{8}\right)^{\frac{1}{5}}\rho_k+3\left(\frac{5}{8}\right)^{\frac{1}{5}}\rho_k\cdot\frac{1}{5}\frac{C_7^{k,{\rm gc}}}{C_5^{k,{\rm gc}}}q_k^2+\cdots. \tag{4.78}$$

Substituting in the integrand of $lW_{i\mathfrak{w}_j}^0$ the terms on the left hand side of (4.75)–(4.78) by the expansions on the right hand side, then use a residue calculation, we obtain

$$\begin{aligned}W_{0\mathfrak{w}_0}^0=&\oint_{|q'|=\rho}\frac{\partial_0\varphi_0(q')Q_0'(q')}{4Q_0^4(q')-s_0}{\rm d}q'=\frac{\partial_0 C_1^{0,{\rm gc}}\left(\frac{5}{8}\right)^{\frac{1}{5}}\rho_0}{4\left(\frac{5}{8}\right)^{\frac{4}{5}}\rho_0^4}\times\\&\times\oint_{|q|=\rho}\left(1+\frac{\partial_0 C_3^{0,{\rm gc}}}{\partial_0 C_1^{0,{\rm gc}}}q^2+\cdots\right)\left(1+\frac{3}{5}\frac{C_7^{0,{\rm gc}}}{C_5^{0,{\rm gc}}}q^2+\cdots\right)\left(1-\frac{4}{5}\frac{C_7^{0,{\rm gc}}}{C_5^{0,{\rm gc}}}q^2+\cdots\right)\frac{1}{q^3}{\rm d}q\\=&\frac{2\pi i\partial_0 C_1^{0{\rm gc}}\left(\frac{5}{8}\right)^{\frac{1}{5}}\rho_0}{4\left(\frac{5}{8}\right)^{\frac{4}{5}}\rho_0^4}\left(\frac{\partial_0 C_3^{0{\rm gc}}}{C_{0,\mathfrak{w}_0}^{0{\rm gc}}}-\frac{1}{5}\frac{\partial_0 C_7^{0{\rm gc}}}{\partial_0 C_5^{0{\rm gc}}}\right)=\frac{2\pi i}{4\left(\frac{5}{8}\right)^{\frac{3}{5}}\rho_0^3}\left(\partial_0 C_3^{0,{\rm gc}}-\frac{1}{5}\frac{\partial_0 C_1^{0,{\rm gc}}\partial_0 C_7^{0,{\rm gc}}}{\partial_0 C_5^{0,{\rm gc}}}\right).\end{aligned} \tag{4.79}$$

Similarly, one can show

$$\begin{aligned}W_{0\mathfrak{w}_1}^0=&\frac{2\pi i}{4\left(\frac{5}{8}\right)^{\frac{3}{5}}\rho_0^3}\left(\partial_1 C_3^{0,{\rm gc}}-\frac{1}{5}\frac{\partial_1 C_1^{0,{\rm gc}}\partial_1 C_7^{0,{\rm gc}}}{\partial_1 C_5^{0,{\rm gc}}}\right),\\W_{1\mathfrak{w}_0}^0=&\frac{2\pi i}{4\left(\frac{5}{8}\right)^{\frac{3}{5}}\rho_1^3}\left(\partial_0 C_3^{1,{\rm gc}}-\frac{1}{5}\frac{\partial_0 C_1^{1,{\rm gc}}\partial_0 C_7^{1,{\rm gc}}}{\partial_0 C_5^{1,{\rm gc}}}\right),\\W_{1\mathfrak{w}_1}^0=&\frac{2\pi i}{4\left(\frac{5}{8}\right)^{\frac{3}{5}}\rho_1^3}\left(\partial_1 C_3^{1,{\rm gc}}-\frac{1}{5}\frac{\partial_1 C_1^{1,{\rm gc}}\partial_1 C_7^{1,{\rm gc}}}{\partial_1 C_5^{1,{\rm gc}}}\right).\end{aligned} \tag{4.80}$$

4.3.6 $\det W^0_{i\mathfrak{w}_j} \neq 0$

Using expansion of φ, in particular,

$$C_3^{0,\mathrm{gc}} = \frac{2}{3}(\mathfrak{H}_0^0\mathfrak{R}_1^0 + \mathfrak{R}_3^0\mathfrak{H}_{-2}^0), \tag{4.81}$$

as well as, at gradient catastrophe,

$$\partial_k C_1^{j,\mathrm{gc}} = 0, \qquad \mathfrak{H}_{-2}^{0,\mathrm{gc}} = \mathfrak{H}_{-2,\mathfrak{w}_k}^{0,\mathrm{gc}} = 0 \tag{4.82}$$

where $j,k \in \{0,1\}$, the expression of $\det(\mathfrak{G})$ at the gradient catastrophe becomes

$$\det(\mathfrak{G}^{\mathrm{gc}}) = 4\frac{\Upsilon_0^4\Upsilon_1^4}{\pi^2}(2\pi i)^2\frac{1}{\left(\frac{5}{8}\right)^{\frac{6}{5}}\rho_0^3\rho_1^3}(\partial_0 C_3^0\partial_1 C_3^1 - \partial_1 C_3^0\partial_0 C_3^1). \tag{4.83}$$

Recall that the gradient catastrophe point bridges the original g and the modified $\mathfrak{g}$-function. So we have $R^{\mathrm{gc}} = \mathfrak{R}^{\mathrm{gc}}$, $H^{\mathrm{gc}} = \mathfrak{H}^{\mathrm{gc}}$, $w_0^{\mathrm{gc}} = \mathfrak{w}_0^{\mathrm{gc}}$, $w_1^{\mathrm{gc}} = \mathfrak{w}_1^{\mathrm{gc}}$ and so on. Thus

$$\begin{aligned}\partial_k C_1^{0,\mathrm{gc}} =& \frac{2}{3}R_3^0 H_{0,\mathfrak{w}_k}^{0,\mathrm{gc}} = \frac{2}{3}\sqrt{\mathfrak{w}_0-\mathfrak{w}_1}H_{0,\mathfrak{w}_k}^{0,\mathrm{gc}} = \frac{2}{3}\sqrt{\mathfrak{w}_0-\mathfrak{w}_1}\frac{\partial}{\partial\mathfrak{w}_k}\left(H_0^0(\mathfrak{w}_0)\right)\\ =& \frac{2}{3}\sqrt{\mathfrak{w}_0-\mathfrak{w}_1}\frac{\partial}{\partial\mathfrak{w}_k}\left(-\frac{1}{4\sqrt{-\mathfrak{w}_0}}\left(\frac{x-t}{\sqrt{\mathfrak{w}_0\mathfrak{w}_1}\mathfrak{w}_0} - \frac{2}{\pi}\int_C \frac{\theta_0'(\xi)\sqrt{-\xi}}{\mathfrak{R}(\xi)(\xi-\mathfrak{w}_0)}\mathrm{d}\xi\right)\right).\end{aligned} \tag{4.84}$$

Similarly,

$$\partial_k C_1^{1,gc} = \frac{2}{3}\sqrt{\mathfrak{w}_1-\mathfrak{w}_0}H_{0,\mathfrak{w}_k}^{1,\mathrm{gc}}. \tag{4.85}$$

Therefore

$$\begin{vmatrix} \partial_0 C_3^{0,\mathrm{gc}} & \partial_1 C_3^{0,\mathrm{gc}} \\ \partial_0 C_3^{1,\mathrm{gc}} & \partial_1 C_3^{1,\mathrm{gc}} \end{vmatrix} = \frac{4}{9}(\mathfrak{w}_0-\mathfrak{w}_1)(\mathfrak{w}_1-\mathfrak{w}_0)\begin{vmatrix} \partial_0 H_0^{0,\mathrm{gc}} & \partial_1 H_0^{0,\mathrm{gc}} \\ \partial_0 H_0^{1,\mathrm{gc}} & \partial_1 H_0^{1,\mathrm{gc}} \end{vmatrix} \tag{4.86}$$

It remains to show $\frac{\partial(H_0^0,H_0^1)}{\partial(\mathfrak{w}_0,\mathfrak{w}_1)}$ is nonzero.

Note that at the gradient catastrophe point we are interchanging the old g and new $\mathfrak{g}$-functions. They have the same value. Because the derivatives of the added terms m, n are also 0, the $\mathfrak{w}_k$ derivatives of $\mathfrak{H}$ is the same as H_{w_k}. We compute $\frac{\partial(H_0^0,H_0^1)}{\partial(w_0,w_1)}$ here instead for simplicity. As a reminder, $\mathfrak{w}_0 = w_0$, $\mathfrak{w}_1 = w_1$, $H^0 = H^0 = \mathfrak{H}^0$, $H^1 = H^1 = \mathfrak{H}^1$ when we are only considering the gradient catastrophe.

By assumption (4.28), $H_0^{0,\mathrm{gc}} = H_0^{1,gc} = 0$, $H_2^{0,\mathrm{gc}} \neq 0$, $H_2^{1,\mathrm{gc}} \neq 0$. Taylor expanding

$H^0(w)$ near $\mathfrak{w}_0$ gives

$$H^{0,\mathrm{gc}}(w) = H_0^{0,\mathrm{gc}} + H_2^{0,\mathrm{gc}}(w - \mathfrak{w}_0) + \cdots. \tag{4.87}$$

Differentiate with respect to $\mathfrak{w}_0$ and $\mathfrak{w}_1$

$$\frac{\partial}{\partial \mathfrak{w}_0}\left(H^{0,\mathrm{gc}}(w)\right)\Big|_{w=\mathfrak{w}_0} = \partial_0 H_0^{0,\mathrm{gc}} - H_2^{0,\mathrm{gc}}, \tag{4.88}$$

$$\frac{\partial}{\partial \mathfrak{w}_1}\left(H^{1,\mathrm{gc}}(w)\right)\Big|_{w=\mathfrak{w}_1} = \partial_1 H_0^{0,\mathrm{gc}}, \tag{4.89}$$

and using equations (4.82) and (4.83) in [13], we find that

$$\begin{aligned}
\frac{\partial}{\partial w_k} R(\xi)H(\xi) =& -\frac{1}{2}\frac{\sqrt{-w_k}}{\sqrt{-\xi}}\frac{R(\xi)}{\xi - w_k}H(w_k) \\
=& -\frac{1}{2}\frac{R(\xi)}{\xi - w_k}H(\xi) + R(\xi)\frac{\partial}{\partial w_k}H(\xi), \\
\Longrightarrow \frac{\partial}{\partial w_k}H(\xi) =& \frac{1}{2}\frac{1}{\sqrt{-\xi}}\frac{\sqrt{-\xi}H(\xi) - \sqrt{-w_k}H(w_k)}{\xi - w_k}.
\end{aligned} \tag{4.90}$$

Expanding $H^0(\xi)$ near $\mathfrak{w}_0$, we can deduce $\dfrac{\partial}{\partial \mathfrak{w}_0}\left(H^{0,\mathrm{gc}}(w)\right)\Big|_{w=\mathfrak{w}_0} = \dfrac{1}{2}H_2^{0,\mathrm{gc}}$. Then we see

$$\partial_0 H_0^{0,\mathrm{gc}} = \frac{\partial}{\partial \mathfrak{w}_0}\left(H^{0,\mathrm{gc}}(w)\right)\Big|_{w=\mathfrak{w}_0} + H_2^{0,\mathrm{gc}} = \frac{3}{2}H_2^{0,\mathrm{gc}}. \tag{4.91}$$

Notice for $\mathfrak{w}_1 = w_1$ the derivatives of $H^0 = H^0$ and the coefficients in the expansion, we do need the assumption that H^0 and H^1 are conjugates of each other. This is true at the gradient catastrophe point. Assume they remain conjuating each other,

$$\partial_1 H_0^{0,\mathrm{gc}} = \frac{1}{2}H_2^{0,\mathrm{gc}^*} = \frac{1}{2}H_2^{1,\mathrm{gc}}. \tag{4.92}$$

Repeating the exact same computation for H^1, we can conclude

$$\begin{vmatrix} \partial_0 H_0^{0,\mathrm{gc}} & \partial_1 H_0^{0,\mathrm{gc}} \\ \partial_0 H_0^{1,\mathrm{gc}} & \partial_1 H_0^{1,\mathrm{gc}} \end{vmatrix} = \begin{vmatrix} \frac{3}{2}H_2^{0,\mathrm{gc}} & \frac{1}{2}H_2^{1,\mathrm{gc}} \\ \frac{1}{2}H_2^{1,\mathrm{gc}} & \frac{3}{2}H_2^{0,\mathrm{gc}} \end{vmatrix} = 2H_2^{0,\mathrm{gc}}H_2^{1,\mathrm{gc}} \neq 0. \tag{4.93}$$

Hence we have shown $\det W^0_{i\mathfrak{w}_j} \neq 0$, and

$$\det(\mathfrak{G}^{\mathrm{gc}}) = 4\frac{\Upsilon_0^4\Upsilon_1^4}{\pi^2}(2\pi i)^2\frac{1}{\left(\frac{5}{8}\right)^{\frac{6}{5}}\rho_0^3\rho_1^3}\frac{4}{9}(\mathfrak{w}_0-\mathfrak{w}_1)(\mathfrak{w}_1-\mathfrak{w}_0)2H_2^{0,\mathrm{gc}}H_2^{1,\mathrm{gc}}. \tag{4.94}$$

4.3.7 Computing $\partial_x s_0$, $\partial_x s_1$, $\partial_x \mathfrak{w}_0$, $\partial_x \mathfrak{w}_1$

Recalling the formula (4.57), we note that the solution to the linear system is

$$\begin{bmatrix}\partial_x s_0\\ \partial_x s_1\\ \mathfrak{w}_{0,x}\\ \mathfrak{w}_{1,x}\end{bmatrix} = \begin{bmatrix} 2\Upsilon_0 & 0 & \partial_0\varphi_0\left(Q_0^{-1}(\Upsilon_0)\right) & \partial_1\varphi_0\left(Q_0^{-1}(\Upsilon_0)\right)\\ 2i\Upsilon_0 & 0 & \partial_0\varphi_0\left(Q_0^{-1}(i\Upsilon_0)\right) & \partial_1\varphi_0\left(Q_0^{-1}(i\Upsilon_0)\right)\\ 0 & 2\Upsilon_1 & \partial_0\varphi_1\left(Q_1^{-1}(\Upsilon_1)\right) & \partial_1\varphi_1\left(Q_1^{-1}(\Upsilon_1)\right)\\ 0 & 2i\Upsilon_1 & \partial_0\varphi_1\left(Q_1^{-1}(i\Upsilon_1)\right) & \partial_1\varphi_1\left(Q_1^{-1}(i\Upsilon_1)\right)\end{bmatrix}^{-1}\begin{bmatrix}-\partial_x\varphi\left(Q_0^{-1}(\Upsilon_0)\right)\\ -\partial_x\varphi\left(Q_0^{-1}(i\Upsilon_0)\right)\\ -\partial_x\varphi_1\left(Q_1^{-1}(\Upsilon_1)\right)\\ -\partial_x\varphi_1\left(Q_1^{-1}(i\Upsilon_1)\right)\end{bmatrix} \tag{4.95}$$

Recall section (4.3.3), using the integral representation by Lagrange-Bürmann formula, the solution to this linear system can be written as

$$\begin{aligned}\begin{bmatrix}\partial_x s_0\\ \partial_x s_1\\ \mathfrak{w}_{0,x}\\ \mathfrak{w}_{1,x}\end{bmatrix} &= -\frac{1}{\det(\mathfrak{G})}\begin{bmatrix}\left(\frac{64i\Upsilon_0^4\Upsilon_1^4W^2_{0\mathfrak{w}_1}W^0_{1\mathfrak{w}_0}X^0_0}{\pi^3} - \frac{64i\Upsilon_0^4\Upsilon_1^4W^2_{0\mathfrak{w}_0}W^0_{1\mathfrak{w}_1}X^0_0} - \frac{64i\Upsilon_0^4\Upsilon_1^4W^0_{0\mathfrak{w}_1}W^0_{1\mathfrak{w}_0}X^2_0}{\pi^3}\right.\\ \left.+\frac{64i\Upsilon_0^4\Upsilon_1^4W^0_{0\mathfrak{w}_0}W^0_{1\mathfrak{w}_1}X^2_0}{\pi^3} + \frac{64i\Upsilon_0^4\Upsilon_1^4W^2_{0\mathfrak{w}_0}W^0_{1\mathfrak{w}_0}X^1_0}{\pi^3} - \frac{64i\Upsilon_0^4\Upsilon_1^4W^0_{0\mathfrak{w}_0}W^2_{0\mathfrak{w}_1}X^1_0}{\pi^3}\right)\\ \left(-\frac{64i\Upsilon_0^4\Upsilon_1^4W^2_{1\mathfrak{w}_0}W^0_{1\mathfrak{w}_1}X^0_0}{\pi^3} + \frac{64i\Upsilon_0^4\Upsilon_1^4W^0_{1\mathfrak{w}_0}W^2_{1\mathfrak{w}_1}X^0_0}{\pi^3} - \frac{64i\Upsilon_0^4\Upsilon_1^4W^0_{0\mathfrak{w}_1}W^2_{1\mathfrak{w}_0}X^1_0}{\pi^3}\right.\\ \left.-\frac{64i\Upsilon_0^4\Upsilon_1^4W^0_{0\mathfrak{w}_0}W^2_{1\mathfrak{w}_1}X^1_0}{\pi^3} - \frac{64i\Upsilon_0^4\Upsilon_1^4W^0_{0\mathfrak{w}_1}W^0_{1\mathfrak{w}_0}X^2_1}{\pi^3} - \frac{64i\Upsilon_0^4\Upsilon_1^4W^0_{0\mathfrak{w}_0}W^0_{1\mathfrak{w}_1}X^2_1}{\pi^3}\right)\\ -\frac{32\Upsilon_0^4\Upsilon_1^4W^0_{1\mathfrak{w}_1}X^0_0}{\pi^2} + \frac{32\Upsilon_0^4\Upsilon_1^4W^0_{0\mathfrak{w}_1}X^0_1}{\pi^2}\\ \frac{32\Upsilon_0^4\Upsilon_1^4W^0_{1\mathfrak{w}_0}X^0_0}{\pi^2} - \frac{32\Upsilon_0^4\Upsilon_1^4W^0_{0\mathfrak{w}_0}X^0_1}{\pi^2}\end{bmatrix}\\ &= -\left(\frac{1}{\pi^2}(2\pi i)^2\frac{1}{\left(\frac{5}{8}\right)^{\frac{6}{5}}\rho_0^3\rho_1^3}\frac{4}{9}(\mathfrak{w}_0-\mathfrak{w}_1)(\mathfrak{w}_1-\mathfrak{w}_0)2H_2^{0,\mathrm{gc}}H_2^{1,\mathrm{gc}}\right)^{-1}\\ &\quad\begin{bmatrix}\left(\frac{16iW^2_{0\mathfrak{w}_1}W^0_{1\mathfrak{w}_0}X^0_0}{\pi^3} - \frac{16iW^2_{0\mathfrak{w}_0}W^0_{1\mathfrak{w}_1}X^0_0}{\pi^3} - \frac{16iW^0_{0\mathfrak{w}_1}W^0_{1\mathfrak{w}_0}X^2_0}{\pi^3} + \frac{16iW^0_{0\mathfrak{w}_0}W^0_{1\mathfrak{w}_1}X^2_0}{\pi^3}\right.\\ \left.+\frac{16iW^2_{0\mathfrak{w}_0}W^0_{1\mathfrak{w}_0}X^1_0}{\pi^3} - \frac{16iW^0_{0\mathfrak{w}_0}W^2_{0\mathfrak{w}_1}X^1_0}{\pi^3}\right)\\ \left(-\frac{16iW^2_{1\mathfrak{w}_0}W^0_{1\mathfrak{w}_1}X^0_0}{\pi^3} + \frac{16iW^0_{1\mathfrak{w}_0}W^2_{1\mathfrak{w}_1}X^0_0}{\pi^3} - \frac{16iW^0_{0\mathfrak{w}_1}W^2_{1\mathfrak{w}_0}X^1_0}{\pi^3} - \frac{16iW^0_{0\mathfrak{w}_0}W^2_{1\mathfrak{w}_1}X^1_0}{\pi^3}\right.\\ \left.-\frac{16iW^0_{0\mathfrak{w}_1}W^0_{1\mathfrak{w}_0}X^2_1}{\pi^3} - \frac{16iW^0_{0\mathfrak{w}_0}W^0_{1\mathfrak{w}_1}X^2_1}{\pi^3}\right)\\ -\frac{8W^0_{1\mathfrak{w}_1}X^0_0}{\pi^2} + \frac{8W^0_{0\mathfrak{w}_1}X^1_0}{\pi^2}\\ \frac{8W^0_{1\mathfrak{w}_0}X^0_0}{\pi^2} - \frac{8W^0_{0\mathfrak{w}_0}X^1_0}{\pi^2}\end{bmatrix}\end{aligned} \tag{4.96}$$

Thus we have shown the solution $(\partial_x s_0, \partial_x s_1, \mathfrak{w}_{0,x}, \mathfrak{w}_{1,x})$ can be solved from a nonsingular differential equation system with respect to x.

4.3.8 The interchangeability of x, t derivatives

Up till now we have shown that with fixed t, the conformal mapping exists for each x near the gradient catastrophe point, and it evolves smoothly with respect to the parameter t. We can proceed in the same way and show the same results for t dependence when x is fixed. However, the system dependence for both parameters are not necessarily smooth. We still need to show the differential system is $x-t$ interchangeable. We rewrite system (4.57) for solving $\partial_x s_k$ and $\partial_x \mathfrak{w}_k$ as follows:

$$\vec{u} := (s_0, s_1, \mathfrak{w}_0, \mathfrak{w}_1)^T \tag{4.97}$$

and

$$\vec{F}(\vec{u}(x,t),x,t) := \begin{bmatrix} \varphi_0 - \frac{4}{5}\Upsilon_0^5 - s_0\Upsilon_0 \\ \varphi_0 - \frac{4}{5}i\Upsilon_0^5 - s_0 i\Upsilon_0 \\ \varphi_1 - \frac{4}{5}\Upsilon_1^5 - s_1\Upsilon_1 \\ \varphi_0 - \frac{4}{5}i\Upsilon_1^5 - s_1 i\Upsilon_1 \end{bmatrix} = 0. \tag{4.98}$$

Then the original system is equivalent to

$$\frac{\partial}{\partial x}\vec{F} = 0. \tag{4.99}$$

Similarly, $s_{i,t}$ and $\mathfrak{w}_{i,t}$ can be derived from $\dfrac{\partial}{\partial t}\vec{F} = 0$. Since $\varphi_{i,xt} = \varphi_{i,tx}$, and Υ_j are directly determined by s_j, we conclude that the x and t-derivatives of s_k and $\mathfrak{w}_k$ are also interchangeable.

Now if we let q be in a neighbourhood of 0, so the conformal mapping is well-defined. Fix q and define G as follows

$$G(Q_0(q), s_0, x, t, \mathfrak{w}_0, \mathfrak{w}_1) := \varphi_0(x,t,\mathfrak{w}_0,\mathfrak{w}_1;q) - \frac{4}{5}Q_0^5 - s_0 Q_0 = 0 \tag{4.100}$$

$$\begin{aligned} G_x =& \partial_x\varphi_0 + \partial_0\varphi_0\partial_x\mathfrak{w}_0 + \partial_1\varphi_0\partial_x\mathfrak{w}_1 - 4Q_0^4\partial_x Q_0 - \partial_x s_0 Q_0 - s_0\partial_x Q_0 \\ G_{xt} =& \partial_{xt}\varphi_0 + \partial_{x0}\varphi_0\partial_t\mathfrak{w}_0 + \partial_x\varphi_0\partial_t\mathfrak{w}_1 + \partial_{0t}\varphi_0\partial_x\mathfrak{w}_0 + \partial_0\varphi_0\partial_{xt}\mathfrak{w}_0 + \partial_{1t}\varphi_0\partial_x\mathfrak{w}_1 + \partial_1\varphi_0\partial_{xt}\mathfrak{w}_1 \\ &+ \partial_{10}\varphi_0\partial_x\mathfrak{w}_1\partial_t\mathfrak{w}_0 + \partial_{11}\varphi_0\partial_x\mathfrak{w}_1\partial_t\mathfrak{w}_1 + \partial_{00}\varphi_0\partial_x\mathfrak{w}_0\partial_t\mathfrak{w}_0 + \partial_{01}\varphi_0\partial_x\mathfrak{w}_0\partial_t\mathfrak{w}_1 \\ &- 4Q_0^4\partial_{xt}Q_0 - 16Q_0^3\partial_t Q_0\partial_x Q_0 - \partial_{xt}s_0 Q_0 - \partial_x s_0\partial_t Q_0 - \partial_t s_0\partial_x Q_0 - s_0\partial_{xt}Q_0. \end{aligned} \tag{4.101}$$

We have show $\partial_{xt}s_k = \partial_{tx}s_k$ and $\partial_{xt}\mathfrak{w}_k = \partial_{tx}\mathfrak{w}_k$. By definition, $G_{tx} = G_{xt}$. For function φ, x and t derivatives appear symmetrically and will be canceled. This implies $\partial_{xt}Q_0 = \partial_{tx}Q_0$. The same arguments hold true in the lower half plane. Thus we have

shown that the system of differential equations: (4.53), (4.57) and the corresponding t-version, does give us conformal mappings $Q_k(q_k; x, t)$ that are smoothly dependent on the parameters (x, t).

4.3.9 Schwarz symmetry

Since the initial condition is Schwarz symmetric because they came from the old g function, and the system of differential equations also has symmetric form, one can prove through a uniqueness argument that the solution to the system also preserves the Schwarz symmetry. Thus from now on we can again assume the $\mathfrak{g}$-function is Schwarz symmetric.

4.3.10 Solution at the gradient catastrophe

Having proved the differential equations define the conformal mapping for us, now we are going to evaluate the x and t derivatives of s_k and $\mathfrak{w}_k$ at the gradient catastrophe.

Repeating what we have done in (4.79), we evaluate all the integrals in the solution system at the gradient catastrophe by calculating the residues

$$Q_0^{\mathrm{gc}}(q)^{-2} = \frac{1}{\left(\frac{5}{8}\right)^{\frac{2}{5}} \rho_0^2 q^2} \left(1 - \frac{2}{5}\frac{C_7^{0,\mathrm{gc}}}{C_5^{0,\mathrm{gc}}} q^2 + \cdots\right) \tag{4.102}$$

$$\partial_0 \varphi_0(q) = \partial_0 C_1^{0,\mathrm{gc}} q + \partial_0 C_3^{0,\mathrm{gc}} q^3 + \cdots \tag{4.103}$$

$$Q_0^{\mathrm{gc}\prime}(q) = \left(\frac{5}{8}\right)^{\frac{1}{5}} \rho_0 + 3\left(\frac{5}{8}\right)^{\frac{1}{5}} \rho_0 \cdot \frac{1}{5}\frac{C_7^{0,\mathrm{gc}}}{C_5^{0,\mathrm{gc}}} q^2 + \cdots \tag{4.104}$$

$$\begin{aligned} W_{0\mathfrak{w}_0}^2 = &\oint_{|q'|=\rho} \frac{\partial_0\varphi_0(q') Q_0^2(q') Q_0'(q')}{4Q_0^4(q') - s_0} \mathrm{d}q' = \frac{\partial_0 C_1^{0,\mathrm{gc}} \left(\frac{5}{4}\right)^{\frac{1}{5}} \rho_0}{4\left(\frac{5}{8}\right)^{\frac{2}{5}} \rho_0^2} \times \\ &\times \oint_{|q|=\rho} \left(1 + \frac{\partial_0 C_3^{0,\mathrm{gc}}}{\partial_0 C_1^{0,\mathrm{gc}}} q^2 + \cdots\right) \left(1 + \frac{3}{5}\frac{C_7^{0,\mathrm{gc}}}{C_5^{0,\mathrm{gc}}} q^2 + \cdots\right) \left(1 - \frac{2}{5}\frac{C_7^{0,\mathrm{gc}}}{C_5^{0,\mathrm{gc}}} q^2 + \cdots\right) \frac{1}{q} \mathrm{d}q \\ = &\frac{2\pi i \partial_0 C_1^{0,\mathrm{gc}}}{4\left(\frac{5}{8}\right)^{\frac{1}{5}} \rho_0} = 0 \end{aligned} \tag{4.105}$$

The last equality follows because we have shown $\partial_0 C_1^{0,\mathrm{gc}} = 0$. Similarly, all $W_{i\mathfrak{w}_j}^2$ are

equal to zero, and X_j^k's are

$$\begin{aligned}
X_0^0 =& \frac{2\pi i}{4\left(\frac{5}{8}\right)^{\frac{3}{5}}\rho_0^3}\left(\partial_x C_3^{0,\mathrm{gc}} - \frac{1}{5}\frac{\partial_x C_1^{0,\mathrm{gc}}\partial_x C_7^{0,\mathrm{gc}}}{\partial_x C_5^{0,\mathrm{gc}}}\right),\\
X_0^2 =& \frac{2\pi i \partial_x C_1^{0,\mathrm{gc}}}{4\left(\frac{5}{8}\right)^{\frac{1}{5}}\rho_0},\\
X_1^0 =& \frac{2\pi i}{4\left(\frac{5}{8}\right)^{\frac{3}{5}}\rho_1^3}\left(\partial_x C_3^{1,\mathrm{gc}} - \frac{1}{5}\frac{\partial_x C_1^{1,\mathrm{gc}}\partial_x C_7^{1,\mathrm{gc}}}{\partial_x C_5^{1,\mathrm{gc}}}\right),\\
X_1^2 =& \frac{2\pi i \partial_x C_1^{1,\mathrm{gc}}}{4\left(\frac{5}{8}\right)^{\frac{1}{5}}\rho_1}.
\end{aligned} \tag{4.106}$$

Finally, by simplifying the fractions, we arrive at

$$\begin{aligned}
\partial_x s_0^{\mathrm{gc}} =& -\frac{\partial_x C_1^{0,\mathrm{gc}}}{\left(\frac{5}{4}\right)^{\frac{1}{5}}\rho_0^{\mathrm{gc}}}\\
\partial_x s_1^{\mathrm{gc}} =& -\frac{\partial_x C_1^{1,\mathrm{gc}}}{\left(\frac{5}{4}\right)^{\frac{1}{5}}\rho_1^{\mathrm{gc}}}.
\end{aligned} \tag{4.107}$$

4.3.11 Formal expansion

Once we have proved the existence of such a conformal mapping, we can also compute the derivatives by formally expanding the expression to obtain the coefficients in Theorem 4.3.1. We will describe the upper half plane endpoint $\mathfrak{w}^0$ carefully but the lower half plane follows automatically with the Schwarz symmetry.

Suppose the conformal mapping $W^0(w)$ has an expansion near $\mathfrak{w}^0$. We drop the subscript and superscript 0 for convenience. Then

$$W(w) = p_0(w-w_0)\left(1 + p_1(w-w_0) + p_2(w-w_)^2 + \mathcal{O}\left((w-w_0)^3\right)\right) \tag{4.108}$$

Substituting in the right hand side of (4.1), we have

$$\begin{aligned}
&\frac{4}{5}W(w)^{\frac{5}{2}} - sW(w)^{\frac{1}{2}}\\
=&\frac{4}{5}\left[p_0(w-w_0)\left(1 + p_1(w-w_0) + p_2(w-w_0)^2 + \mathcal{O}\left((w-w_0)^3\right)\right)\right]^{\frac{5}{2}}\\
&- s\left[p_0(w-w_0)\left(1 + p_1(w-w_0) + p_2(w-w_)^2 + \mathcal{O}\left((w-w_0)^3\right)\right)\right]^{\frac{1}{2}}.
\end{aligned} \tag{4.109}$$

Comparing the coefficients, we conclude

$$s_0 = -\frac{C_1^0}{{p_0^{\mathrm{gc}}}^{\frac{1}{2}}}, \tag{4.110}$$

where

$$(p_0^{\mathrm{gc}})^{\frac{1}{2}} = \rho_0^{\mathrm{gc}} = \left(\frac{8}{5}C_5^{\mathrm{gc}}\right)^{\frac{1}{5}}, \tag{4.111}$$

with branch chosen the same as in (4.50). □

Recall in the statement of theorem 1.5.1, $W'(w_0^{\mathrm{gc}})$ was yet to defined. Here we can see

$$W'(w_0)^{\mathrm{gc}} = p_0^{0,\mathrm{gc}}. \tag{4.112}$$

Chapter 5

Theorem 1: away from the poles

5.1 Statement of theorem 1

In this Chapter we prove the first main theorem 1.5.1

Theorem 1.5.1 (First correction near the gradient catastrophe away from poles of the Painlevé-I tritronquée solution) *Let $u_N(x,t)$ be the fluxon condensate associated with suitable Cauchy data* (1.4)*, for which the elliptic system* (1.21) *exhibits an elliptic umbilic catastrophe point at $(x,t) = (x_{\rm gc} = 0, t_{\rm gc})$. Then there exists a real-analytic univalent mapping $s : \mathbb{R}^2 \to \mathbb{C}$ defined on a neighbourhood of the catastrophe point, such that the following is true. Supposing that $\nu := s/\epsilon^{\frac{4}{5}}$, $|\nu| < M$ and $|Y(\nu)| < M$ for some constant $M > 0$ independent of ϵ, then the following asymptotic formulæ hold:*

$$\begin{aligned} \cos(\tfrac{1}{2}u_N(x,t)) =& \dot{C} + \epsilon^{\frac{1}{5}}\left(\mathcal{E}_{11}^{(1)}\dot{C} + \mathcal{E}_{12}^{(1)}\dot{S}\right) + \mathcal{O}(\epsilon^{\frac{2}{5}}), \\ \sin(\tfrac{1}{2}u_N(x,t)) =& \dot{S} + \epsilon^{\frac{1}{5}}\left(\mathcal{E}_{21}^{(1)}\dot{C} + \mathcal{E}_{22}^{(1)}\dot{S}\right) + \mathcal{O}(\epsilon^{\frac{2}{5}}). \end{aligned} \tag{5.1}$$

The exact expressions of $\dot{C}$ and $\dot{S}$ are given by (3.97) *and* (3.98)*, and the first correction*

matrix $\mathcal{E}^1$ *is given by*

$$\begin{aligned}\mathcal{E}^1 = \Bigg(& \frac{1}{-z_0^{\mathrm{gc}}} \frac{1}{2z_0^{\mathrm{gc}} W'(w_0^{\mathrm{gc}})} \mathbf{C}(w_0^{\mathrm{gc}}) \begin{bmatrix} 0 & H(\nu) \\ 0 & 0 \end{bmatrix} \mathbf{C}(w_0^{\mathrm{gc}})^{-1} \\ & + \frac{1}{-z_0^{\mathrm{gc}*}} \frac{1}{2z_0^{\mathrm{gc}*} W'(w_0^{\mathrm{gc}})^*} \sigma_2 \mathbf{C}(w_0^{\mathrm{gc}})^* \begin{bmatrix} 0 & H(\nu)^* \\ 0 & 0 \end{bmatrix} \mathbf{C}(w_0^{\mathrm{gc}})^{*-1} \sigma_2 \\ & - \frac{1}{z_0^{\mathrm{gc}}} \frac{1}{2z_0^{\mathrm{gc}} W'(w_0^{\mathrm{gc}})} \sigma_2 \mathbf{C}(w_0^{\mathrm{gc}}) \begin{bmatrix} 0 & H(\nu) \\ 0 & 0 \end{bmatrix} \mathbf{C}(w_0^{\mathrm{gc}})^{-1} \sigma_2 \\ & - \frac{1}{z_0^{\mathrm{gc}*}} \frac{1}{2z_0^{\mathrm{gc}*} W'(w_0^{\mathrm{gc}})^*} \mathbf{C}(w_0^{\mathrm{gc}})^* \begin{bmatrix} 0 & H(\nu)^* \\ 0 & 0 \end{bmatrix} \mathbf{C}(w_0^{\mathrm{gc}})^{*-1} \Bigg), \end{aligned} \tag{5.2}$$

where w_0^{gc} *is* w_0 *first defined in section 3.1.4 evaluated at the gradient catastrophe point,* $z_0^{\mathrm{gc}} = \sqrt{w_0^{\mathrm{gc}}}$ *principal branch and* $\mathbf{C}(w_0^{\mathrm{gc}})$ *are constant matrices with definition given by* (5.95)*, and* $W'(w_0^{\mathrm{gc}})$ *given by*(4.112)*.*

5.2 Tritronquée Parametrix

5.2.1 Standard Painlevé I Riemann–Hilbert problem

Following [30], the Painlevé-I equation shows up in the asymptotics to the Painlevé-I (P_I) parametrix, where a matrix satisfies the jump condition in figure 5.1. Here, the Painlevé-I

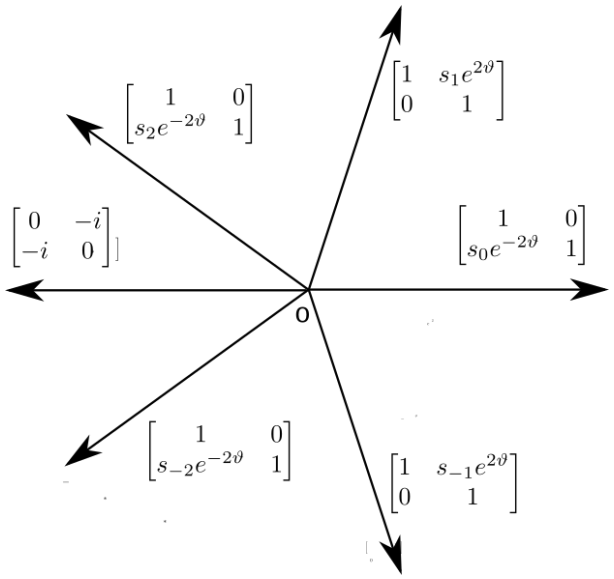

Figure 5.1: The Painlevé-I parametrix

exponent ϑ is given by

$$\vartheta := \frac{4}{5}\zeta^{\frac{5}{2}} - \nu\zeta^{\frac{1}{2}}. \tag{5.3}$$

The jump matrices $\mathbf{V}_{\text{jump}}$ are shown in figure 5.1. We seek a solution to the Riemann–Hilbert problem (see Riemann–Hilbert problem 5.2.1), where

$$\mathbf{T}_+ = \mathbf{T}_-\mathbf{V}_{\text{jump}}, \tag{5.4}$$

$\mathbf{T}$ is analytic except on the rays and satisfies some normalisation condition at infinity. As it turns out, such a solution only exists when

$$s_{k+5} = s_k, \quad 1 + s_k s_{k+1} = -is_{k+3}, \quad k \in \mathbb{Z}. \tag{5.5}$$

Generically, two of the Stokes multipliers s_k determines all others. In particular, for our purpose, a special solution to P_I, known as the tritronquée solution, is what describes the inner parametrix near the gradient catastrophe point for sG.

In [34], Kapaev studied the asymptotics of the P_I equation and in particular the tritronquée solution in detail.

5.2.2 Painlevé-I Riemann–Hilbert problem

To briefly recapitulate the idea of using a tritronquée parametrix:

In order to estimate the inner parametrix, we seek a local coordinate such that the jump conditions inside the disks U_0 and U_1 are mapped to a standard parametrix. The standard parametrix satisfies a Riemann–Hilbert problem that we either already know the asymptotic solution, or have a strategy to solve it. In the Riemann–Hilbert problem for $\mathbf{O}$, at a generic x-t point before the first breaking, the disks are mapped to the Airy parametrix. The Airy function comes up in Airy parametrix and that is why it will come up in the correction terms for $\mathbf{O}$ expansion. For the same reason, Painlevé-I equation shows up in the approximation of the Riemann–Hilbert problem for the global parametrix $\mathbf{O}$ near the gradient catastrophe point. Because the phase function ϕ has a very different behaviour near this elliptic umbilic catastrophe point. Painlevé-I parametrix, instead of the Airy parametrix, is the candidate to capture the solution for the inner parametrix inside the disks.

Riemann–Hilbert Problem 5.2.1. (Tritronquée Parametrix)

Jump Conditions:

$$\mathbf{T}_+(\zeta;\nu) = \mathbf{T}_- \begin{bmatrix} 0 & -i \\ -i & 0 \end{bmatrix}, \qquad \arg(\zeta) = \pi. \tag{5.6}$$

$$\mathbf{T}_+ = \mathbf{T}_- \begin{bmatrix} 1 & 0 \\ ie^{-2\vartheta(\zeta;\nu)} & 1 \end{bmatrix}, \qquad \arg(\zeta) = \pm\frac{4}{5}\pi. \tag{5.7}$$

$$\mathbf{T}_+ = \mathbf{T}_- \begin{bmatrix} 1 & ie^{2\vartheta(\zeta;\nu)} \\ 0 & 1 \end{bmatrix}, \qquad \arg(\zeta) = \frac{2}{5}\pi. \tag{5.8}$$

where $\vartheta(\zeta;\nu) := \frac{4}{5}\zeta^{\frac{5}{2}} - \nu\zeta^{\frac{1}{2}}$.

Normalization:

$$\lim_{\zeta\to\infty} \mathbf{T}\mathbf{M}\zeta^{\frac{\sigma_3}{4}} = \mathbb{I} \tag{5.9}$$

with $\mathbf{M}$ defined as

$$\mathbf{M} = \frac{1}{\sqrt{2}} \begin{bmatrix} 1 & 1 \\ -1 & 1 \end{bmatrix} \tag{5.10}$$

For the rest of the chapter, recall the outer parametrix has a constant jump $-i\sigma_3 e^{\pm i\kappa\sigma_3}$ on β. We have already solved the outer parametrix in Chapter 3. As for the inner parametrix, peeling off $e^{\pm i\kappa\sigma_3}$, it shares the constant jump i $sigma_3$ with the tritronqueée parametrix. Furthermore, in Chapter 4 we laid out that the phase $\Delta\varphi$ can be mapped to the normal form 2ϑ in the Painlevé-I parametrix. Thus we can map the inner parametrix exactly to one of the painlevé-I parametrix. In fact we are going to use a very special PI parametrix, the tritronquée parametrix, to build asymptotic solution for the inner parametrix. Furthermore, we want the inner parametrix and outer parametrix to match close enough on the boundary of the disks. When the difference is small enough, we will be able to use Fredholm theory to write an expansion for a *small norm problem* [5]. The matching boundary is ensured by the normalization condition at infinity in the tritronquée parametrix. We will later see why, but basically it boils down to the outer parametrix blows up in the same power as the behaviour of the standard PI tritronquée parametrix power at infinity.

5.2.3 Diagonalizing the jump

Now we try to find asymptotic expansion at infinity for the Painlevé-I parametrix. First, in (5.9), $\mathbf{M}$ can be seen as a diagonalization matrix. Notice that except for $\mathbb{R}_-$, all of the off diagonal terms in the jump matrices on the five rays are decaying exponentially at infinity. Near infinity, the constant jump on $\mathbb{R}_-$ is the only significant one. We first find

a holormorphic matrix function that has the same constant jump on $\mathbb{R}_-$, then we try to characterize the relation between this matrix function and the solution to 5.2.1. We begin by diagonalizing the jump on $\mathbb{R}_-$,

$$\left(\frac{1}{\sqrt{2}}\begin{bmatrix}1 & -1\\ 1 & 1\end{bmatrix}\right)\begin{bmatrix}0 & -i\\ -i & 0\end{bmatrix}\left(\frac{1}{\sqrt{2}}\begin{bmatrix}1 & 1\\ -1 & 1\end{bmatrix}\right)=\begin{bmatrix}i & 0\\ 0 & -i\end{bmatrix} \tag{5.11}$$

If we choose

$$\mathbf{M}=\frac{1}{\sqrt{2}}\begin{bmatrix}1 & 1\\ -1 & 1\end{bmatrix},\qquad \mathbf{M}^{-1}=\frac{1}{\sqrt{2}}\begin{bmatrix}1 & -1\\ 1 & 1\end{bmatrix}, \tag{5.12}$$

then on the negative real axis, $\mathbf{TM}$ has jump

$$\mathbf{T}_+\mathbf{M}=\mathbf{T}_-\mathbf{M}\begin{bmatrix}i & 0\\ 0 & -i\end{bmatrix} \tag{5.13}$$

Let us define $\tilde{\mathbf{T}}=\mathbf{TM}$.

The simplest choice of a function with the same jump matrix $\begin{bmatrix}i & 0\\ 0 & -i\end{bmatrix}$ on $\mathbb{R}_-$ would be $\zeta^{-\frac{\sigma_3}{4}}$. If we multiply $\widetilde{\mathbf{T}}$ by the inverse of $\zeta^{-\frac{\sigma_3}{4}}$, the jump on $\mathbb{R}_-$ disappears, and the jumps for $\widetilde{\mathbf{T}}\zeta^{\frac{\sigma_3}{4}}$ all decay exponentially at infinity. We require the matrix $\widetilde{\mathbf{T}}\zeta^{\frac{\sigma_3}{4}}$ to normalize to identity at infinity, then we have the Riemann–Hilbert problem 5.2.1.

5.2.4 Power series expansion

At infinity, the matrix $\widetilde{\mathbf{T}}\zeta^{\frac{\sigma_3}{4}}$ has near identity jumps, and the matrix also goes to the identity matrix. Fredholm theory tells us that $\widetilde{\mathbf{T}}\zeta^{\frac{\sigma_3}{4}}$ itself can be expanded in a sequence near infinity, i.e. there exists a sequence $\{\mathbf{T}_p(\nu)\}_{p=1}^{\infty}$, such that $\forall P\geq 0$,

$$\mathbf{T}_{\mathrm{s}}:=\mathbf{T}(\zeta;\nu)\mathbf{M}\zeta^{\frac{\sigma_3}{4}}=\mathbb{I}+\sum_{p=1}^{P}\mathbf{T}_p(\nu)\zeta^{-p}+O(\zeta^{-P-1}),\qquad \zeta\to\infty. \tag{5.14}$$

where $\mathbf{T}_p(\nu)$ are meromorphic matrix functions in parameter ν. The poles which do not accumulate anywhere in the complex plane are the only singularity allowed (analytic Fredholm theory discussed in details in [30]).

It can be shown that $\det\mathbf{T}(\zeta;\nu)=1$. This implies $\operatorname{tr}\mathbf{T}_1(\nu)=0$, a constraint we will use soon to find out the exact expression of the first few terms in the expansion.

5.2.5 Ridding of the phase: constant jump Riemann-Hilbert problem

Using $\vartheta_+(\zeta) + \vartheta_-(\zeta) = 0$ on $\mathbb{R}_-$, define

$$\mathbf{L}(\zeta;\nu) = \mathbf{T}e^{\vartheta(\zeta;\nu)\sigma_3}. \tag{5.15}$$

Then

$$\mathbf{L}_+ = \mathbf{L}_- e^{-\vartheta_-\sigma_3}\mathbf{V_T}e^{\vartheta_+\sigma_3}, \tag{5.16}$$

where $\mathbf{V_T}$ stands for the jump matrices in Riemann–Hilbert problem 5.2.1. This step gets rid of the $e^{\pm 2\vartheta}$ in the off diagonal elements of the jumps. $\mathbf{L}$ solves the following constant jump Riemann-Hilbert problem illustrated in the picture:

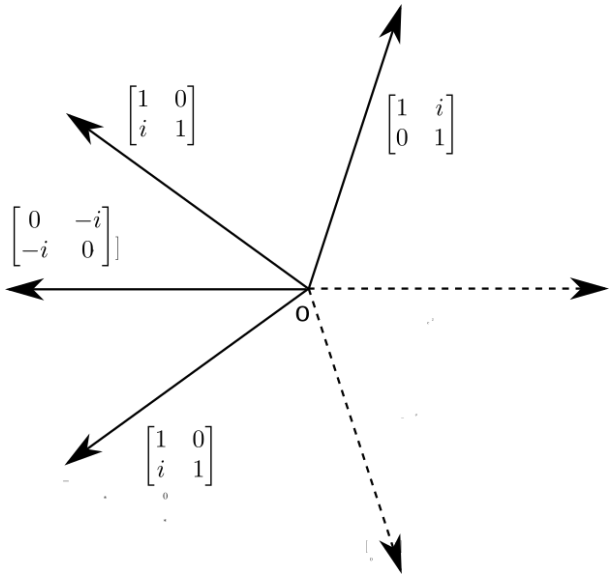

Figure 5.2: $\mathbf{L}$ jump contour

Riemann–Hilbert Problem 5.2.2.
Jump Conditions:

$$\begin{aligned}
\mathbf{L}_+(\zeta;\nu) &= \mathbf{L}_- \begin{bmatrix} 0 & -i \\ -i & 0 \end{bmatrix}, \qquad \arg(\zeta) = \pi. \\
\mathbf{L}_+ &= \mathbf{L}_- \begin{bmatrix} 1 & 0 \\ i & 1 \end{bmatrix}, \qquad \arg(\zeta) = \pm\frac{4}{5}\pi. \\
\mathbf{L}_+ &= \mathbf{L}_- \begin{bmatrix} 1 & i \\ 0 & 1 \end{bmatrix}, \qquad \arg(\zeta) = \frac{2}{5}\pi.
\end{aligned} \tag{5.17}$$

Normalization:

$$\lim_{\zeta\to\infty} \mathbf{L} e^{-\vartheta(\zeta;\nu)\sigma_3} \mathbf{M} \zeta^{\frac{\sigma_3}{4}} = \mathbb{I} \tag{5.18}$$

5.2.6 Solving $\mathbf{L}$

$$\mathbf{A}(\zeta;\nu) := \frac{\partial \mathbf{L}}{\partial \zeta}(\zeta;\nu)\mathbf{L}(\zeta;\nu)^{-1} \tag{5.19}$$

$$\mathbf{U}(\zeta;\nu) := \frac{\partial \mathbf{L}}{\partial \nu}(\zeta;\nu)\mathbf{L}(\zeta;\nu)^{-1} \tag{5.20}$$

Because the jump matrices for $\mathbf{L}$ are all constant matrices, $\dfrac{\partial \mathbf{L}}{\partial \zeta}$, $\dfrac{\partial \mathbf{L}}{\partial \nu}$ and $\mathbf{L}$ have the same jumps. Therefore, both functions $\mathbf{A}$ and $\mathbf{U}$ defined as above have no jumps or poles. Therefore, they are entire function in variable ζ. We are going expand $\mathbf{A}$ and $\mathbf{U}$, then using the fact that the terms with negative powers must be exactly zero, we derive information from $\mathbf{T}_p(\nu)$, which is a crucial step to understand the solution to the standard Painlevé-I parametrix.

5.2.7 $\mathbf{A}$ and $\mathbf{U}$ Expansions

To express the expansions of $\mathbf{A}$ and $\mathbf{U}$ in terms of $\mathbf{T}_p$, recall

$$\mathbf{L} = \mathbf{T} e^{\vartheta\sigma_3} = \mathbf{T}_{\mathrm{s}} \zeta^{-\frac{\sigma_3}{4}} \mathbf{M}^{-1} e^{\vartheta\sigma_3}. \tag{5.21}$$

Firstly, differentiate $\mathbf{L}$ termwise except for the expansion in $\mathbf{T}_{\mathrm{s}}$

$$\begin{aligned}
\frac{\partial \mathbf{L}}{\partial \zeta} =& \frac{\partial}{\partial \zeta}\left(\mathbf{T}_{\mathrm{s}} \zeta^{-\frac{\sigma_3}{4}} \mathbf{M}^{-1} e^{\vartheta\sigma_3}\right) \\
=& \frac{\partial \mathbf{T}_{\mathrm{s}}}{\partial \zeta} \zeta^{-\frac{\sigma_3}{4}} \mathbf{M}^{-1} e^{\vartheta\sigma_3} + \mathbf{T}_{\mathrm{s}} \begin{bmatrix} -\frac{1}{4}\zeta^{-\frac{5}{4}} & \\ & \frac{1}{4}\zeta^{-\frac{3}{4}} \end{bmatrix} \mathbf{M}^{-1} e^{\vartheta\sigma_3} \\
&+ \mathbf{T}_{\mathrm{s}} \zeta^{-\frac{\sigma_3}{4}} \mathbf{M}^{-1} \frac{\partial \vartheta}{\partial \zeta} \sigma_3 e^{\vartheta\sigma_3},
\end{aligned} \tag{5.22}$$

and

$$\begin{aligned}
\frac{\partial \mathbf{L}}{\partial \nu} =& \frac{\partial}{\partial \nu}\left(\mathbf{T}_{\mathrm{s}} \zeta^{-\frac{\sigma_3}{4}} \mathbf{M}^{-1} e^{\vartheta\sigma_3}\right) \\
=& \frac{\partial \mathbf{T}_{\mathrm{s}}}{\partial \nu} \zeta^{-\frac{\sigma_3}{4}} \mathbf{M}^{-1} e^{\vartheta\sigma_3} + \mathbf{T}_{\mathrm{s}} \zeta^{-\frac{\sigma_3}{4}} \mathbf{M}^{-1} \frac{\partial \vartheta}{\partial \nu} \sigma_3 e^{\vartheta\sigma_3}.
\end{aligned} \tag{5.23}$$

Next, take derivatives of ϑ,

$$\vartheta(\zeta;\nu) = \frac{4}{5}\zeta^{\frac{5}{2}} - \nu\zeta^{\frac{1}{2}} \tag{5.24}$$

$$\frac{\partial\vartheta(\zeta;\nu)}{\partial\zeta} = 2\zeta^{\frac{3}{2}} - \frac{1}{2}\nu\zeta^{-\frac{1}{2}}, \tag{5.25}$$

$$\frac{\partial\vartheta(\zeta;\nu)}{\partial\nu} = -\zeta^{\frac{1}{2}}. \tag{5.26}$$

Substituting them in $\dfrac{\partial\mathbf{L}}{\partial\zeta}$ and $\dfrac{\partial\mathbf{L}}{\partial\nu}$, we can simplify $\mathbf{A}$ and $\mathbf{U}$ to

$$\begin{aligned}\mathbf{A} =& \frac{\partial\mathbf{L}}{\partial\zeta}\mathbf{L}^{-1}\\ =& \frac{\partial\mathbf{T}_{\mathrm{s}}}{\partial\zeta}\mathbf{T}_{\mathrm{s}}^{-1} + \mathbf{T}_{\mathrm{s}}\begin{bmatrix}-\frac{1}{4\zeta} & \\ & \frac{1}{4\zeta}\end{bmatrix}\mathbf{T}_{\mathrm{s}}^{-1} + \mathbf{T}_{\mathrm{s}}\zeta^{-\frac{\sigma_3}{4}}\mathbf{M}^{-1}(\vartheta_\zeta)\sigma_3\mathbf{M}\zeta^{\frac{\sigma_3}{4}}\mathbf{T}_{\mathrm{s}}^{-1}\\ =& \frac{\partial\mathbf{T}_{\mathrm{s}}}{\partial\zeta}\mathbf{T}_{\mathrm{s}}^{-1} + \frac{1}{4\zeta}\mathbf{T}_{\mathrm{s}}\begin{bmatrix}-1 & \\ & 1\end{bmatrix}\mathbf{T}_{\mathrm{s}}^{-1} + \mathbf{T}_{\mathrm{s}}\begin{bmatrix}0 & -\frac{\nu}{2\zeta}+2\zeta\\ -\frac{\nu}{2}+2\zeta^2 & 0\end{bmatrix}\mathbf{T}_{\mathrm{s}}^{-1},\end{aligned} \tag{5.27}$$

and

$$\begin{aligned}\mathbf{U} =& \frac{\partial\mathbf{L}}{\partial\nu}\mathbf{L}^{-1}\\ =& \frac{\partial\mathbf{T}_{\mathrm{s}}}{\partial\nu}\mathbf{T}_{\mathrm{s}}^{-1} + \mathbf{T}_{\mathrm{s}}\zeta^{-\frac{\sigma_3}{4}}\mathbf{M}^{-1}(-\zeta^{\frac{1}{2}})\sigma_3\mathbf{M}\zeta^{\frac{\sigma_3}{4}}\mathbf{T}_{\mathrm{s}}^{-1}\\ =& \frac{\partial\mathbf{T}_{\mathrm{s}}}{\partial\nu}\mathbf{T}_{\mathrm{s}}^{-1} + \mathbf{T}_{\mathrm{s}}\begin{bmatrix}0 & -1\\ -\zeta & 0\end{bmatrix}\mathbf{T}_{\mathrm{s}}^{-1}.\end{aligned} \tag{5.28}$$

Observing the highest power of ζ in the expressions for $\mathbf{A}$ and $\mathbf{U}$, we know that the expansions should be

$$\mathbf{A} = \mathbf{A}_2\zeta^2 + \mathbf{A}_1\zeta + \mathbf{A}_0 + \mathcal{O}(1/\zeta), \tag{5.29}$$

$$\mathbf{U} = \mathbf{U}_1\zeta + \mathbf{U}_0 + \mathcal{O}(1/\zeta). \tag{5.30}$$

However, as explained before, because $\mathbf{A}$ and $\mathbf{U}$ are entire, the $\mathcal{O}(1/\zeta)$ terms become zero, therefore, the expansions must be of the following form.

$$\mathbf{A} = \mathbf{A}_2\zeta^2 + \mathbf{A}_1\zeta + \mathbf{A}_0 \tag{5.31}$$

$$\mathbf{U} = \mathbf{U}_1\zeta + \mathbf{U}_0. \tag{5.32}$$

Using the expansion of $\mathbf{T}_\mathrm{s}$,

$$\mathbf{T}_\mathrm{s} = \mathbb{I} + \frac{\mathbf{T}_1}{\zeta} + \frac{\mathbf{T}_2}{\zeta^2} + \frac{\mathbf{T}_3}{\zeta^3} + \mathcal{O}(\zeta^{-4}), \tag{5.33}$$

to obtain the expansions of $\mathbf{A}$ and $\mathbf{U}$. Define

$$\sigma_+ = \begin{bmatrix} 0 & 1 \\ 0 & 0 \end{bmatrix}, \qquad \sigma_- = \begin{bmatrix} 0 & 0 \\ 1 & 0 \end{bmatrix} \tag{5.34}$$

$$\mathbf{A}_2 = 2\sigma_- \tag{5.35}$$

$$\mathbf{A}_1 = (2\sigma_+ + 2[\mathbf{T}_1(\nu), \sigma_-]) \tag{5.36}$$

$$\mathbf{A}_0 = -\frac{1}{2}\nu\sigma_- + 2[\mathbf{T}_1, \sigma_+] + 2[\mathbf{T}_2, \sigma_-] + 2\sigma_-\mathbf{T}_1^2 \tag{5.37}$$

$$\mathbf{U}_0 = -\sigma_+ + [\sigma_-, \mathbf{T}_1] \tag{5.38}$$

$$\mathbf{U}_1 = -\sigma_- \tag{5.39}$$

The elements of the coefficent matrices are

$$\mathbf{A}_2 = 2\begin{bmatrix} 0 & 0 \\ 1 & 0 \end{bmatrix} \tag{5.40}$$

$$\mathbf{A}_1 = -2\mathbf{U}_0 \tag{5.41}$$

$$\mathbf{A}_0 = 2\begin{bmatrix} -(\mathbf{T}_{1,11}\mathbf{T}_{1,12} + \mathbf{T}_{1,21} - \mathbf{T}_{2,12}) & (\mathbf{T}_{1,11} - \mathbf{T}_{1,22}) - \mathbf{T}_{1,12}^2 \\ \mathbf{T}_{1,11}^2 - \mathbf{T}_{1,11}\mathbf{T}_{1,22} + \mathbf{T}_{1,12}\mathbf{T}_{1,21} - \mathbf{T}_{2,11} + \mathbf{T}_{2,22} - \frac{\nu}{4} & \mathbf{T}_{1,11}\mathbf{T}_{1,12} + \mathbf{T}_{1,21} - \mathbf{T}_{2,12} \end{bmatrix} \tag{5.42}$$

$$\mathbf{U}_0 = \begin{bmatrix} -\mathbf{T}_{1,12} & -1 \\ \mathbf{T}_{1,11} - \mathbf{T}_{1,22} & \mathbf{T}_{1,12} \end{bmatrix} \tag{5.43}$$

$$\mathbf{U}_1 = -\begin{bmatrix} 0 & 0 \\ 1 & 0 \end{bmatrix} \tag{5.44}$$

5.2.8 Compatibility Condition

It is worth a reminder here that what we are after is the asymptotic expansion for the tritronquée parametrix, which is a solution to Riemann–Hilbert problem 5.2.1. So we want to figure out what exactly are the elements in the $\mathbf{A}$ and $\mathbf{U}$ expansions we just obtained.

In fact, $\mathbf{A}$ and $\mathbf{U}$ are not completely independent. By definitions (5.19) and (5.20),

$$\frac{\partial \mathbf{L}}{\partial \zeta} = \mathbf{A}\mathbf{L}, \tag{5.45}$$

$$\frac{\partial \mathbf{L}}{\partial \nu} = \mathbf{U}\mathbf{L}, \tag{5.46}$$

where $\mathbf{L}$ is an existing function. It is holomorphic expect for jump discontinuities on some rays. Therefore, generically its ζ and ν derivatives must be interchangeable, i.e. the system of equaions (5.45) needs to be compatible.We differentiate the first equation with respect to $\partial\nu$, and the second equation with respect to ζ. The above two expressions are necessarily identical, in other words

$$\begin{aligned} &\frac{\partial \mathbf{A}}{\partial \nu}\mathbf{L} + \mathbf{A}\frac{\partial \mathbf{L}}{\partial \nu} = \frac{\partial \mathbf{U}}{\partial \zeta}\mathbf{L} + \mathbf{U}\frac{\partial \mathbf{L}}{\partial \zeta} \\ \iff &\frac{\partial \mathbf{U}}{\partial \zeta} - \frac{\partial \mathbf{A}}{\partial \nu} + [\mathbf{U}, \mathbf{A}] = 0. \end{aligned} \tag{5.47}$$

5.2.9 Differential Equations

Next we expand the compatibility condition (5.47) in powers of ζ. First calculate the commutator,

$$\begin{aligned} [\mathbf{U}, \mathbf{A}] &= [\mathbf{U}_0 + \mathbf{U}_1\zeta, \mathbf{A}_0 + \mathbf{A}_1\zeta + \mathbf{A}_2\zeta^2] \\ &= [\mathbf{U}_0, \mathbf{A}_0] + ([\mathbf{U}_0, \mathbf{A}_1] + [\mathbf{U}_1, \mathbf{A}_0])\zeta + ([\mathbf{U}_1, \mathbf{A}_1] + [\mathbf{U}_0, \mathbf{A}_2])\zeta^2 + [\mathbf{U}_1, \mathbf{A}_2]\zeta^3, \end{aligned} \tag{5.48}$$

and set every order term in (5.47) to be equal to 0.

$$\begin{aligned} &\zeta^3 \text{ term} && [\mathbf{U}_1, \mathbf{A}_2] = 0 \\ &\zeta^2 \text{ term} && ([\mathbf{U}_1, \mathbf{A}_1] + [\mathbf{U}_0, \mathbf{A}_2]) + \frac{\mathrm{d}\mathbf{A}_2}{\mathrm{d}\nu} = 0 \\ &\zeta^1 \text{ term} && \frac{\mathrm{d}\mathbf{A}_1}{\mathrm{d}\nu} + [\mathbf{U}_1, \mathbf{A}_0] - \mathbf{U}_1 = 0 \\ &\zeta^0 \text{ term} && \frac{\mathrm{d}\mathbf{A}_0}{\mathrm{d}\nu} + [\mathbf{U}_0, \mathbf{A}_0] = 0 \end{aligned}$$

Using $\mathbf{A}_1 = -2\mathbf{U}_0$, it is easy to verify that the ζ^2 and ζ^3 coefficients are 0. Therefore, the compatibility condition boils down to the following two nontrivial differential equations

$$\frac{\mathrm{d}\mathbf{A}_1}{\mathrm{d}\nu} = [\mathbf{A}_0, \mathbf{U}_1] + \mathbf{U}_1 \tag{5.49}$$

$$\frac{\mathrm{d}\mathbf{A}_0}{\mathrm{d}\nu} = [\mathbf{A}_0, \mathbf{U}_0] \tag{5.50}$$

Define

$$H = \mathbf{T}_{1,12} \tag{5.51}$$

$$Y = \mathbf{T}_{1,11} - \mathbf{T}_{1,22} - \mathbf{T}_{1,12}^2 \tag{5.52}$$

$$Z = 4\mathbf{T}_{1,11}\mathbf{T}_{1,12} - 2\mathbf{T}_{1,12}^3 - 2\mathbf{T}_{1,12}\mathbf{T}_{1,22} + 2\mathbf{T}_{1,21} - 2\mathbf{T}_{2,12}. \tag{5.53}$$

Theorem 5.2.1. *H, Y, Z satisfy a system of ordinary differential equations*

$$\begin{cases} \dfrac{\mathrm{d}H}{\mathrm{d}\nu} = -Y, \\ \dfrac{\mathrm{d}Y}{\mathrm{d}\nu} = Z, \\ \dfrac{\mathrm{d}Z}{\mathrm{d}\nu} = -6Y^2 + \nu. \end{cases} \tag{5.54}$$

Before we prove the theorem, we remark here that if we take the second derivative of Y, we arrive at the Painlevé I equation:

$$\frac{\mathrm{d}^2 Y}{\mathrm{d}\nu^2} + 6Y^2 - \nu = 0 \tag{5.55}$$

Proof.

$$Z = H^3 + 3YH + 2(\mathbf{T}_{1,21} - \mathbf{T}_{2,12}) \tag{5.56}$$

If we write equation (5.49) in elements

$$\begin{aligned} -2\frac{\mathrm{d}}{\mathrm{d}\nu}\begin{bmatrix} -\mathbf{T}_{1,12} & -1 \\ \mathbf{T}_{1,11} - \mathbf{T}_{1,22} & \mathbf{T}_{1,12} \end{bmatrix} = -2\begin{bmatrix} \mathbf{T}_{1,11} - \mathbf{T}_{1,12}^2 - \mathbf{T}_{1,22} & 0 \\ 2\mathbf{T}_{1,11}\mathbf{T}_{1,12} + 2\mathbf{T}_{1,21} - 2\mathbf{T}_{2,12} & -\mathbf{T}_{1,11} + \mathbf{T}_{1,12}^2 + \mathbf{T}_{1,22} \end{bmatrix} \\ - \begin{bmatrix} 0 & 0 \\ 1 & 0 \end{bmatrix}. \end{aligned} \tag{5.57}$$

The $(1,1)$ element of (5.49) is equivalent to

$$\frac{\mathrm{d}H}{\mathrm{d}\nu} = -Y. \tag{5.58}$$

While equation (5.50) is more complicated, we only need the second row,

$$\begin{aligned}
&2\frac{\mathrm{d}}{\mathrm{d}\nu}\begin{bmatrix}(\mathbf{T}_{1,11}-\mathbf{T}_{1,22})-\mathbf{T}_{1,12}^2\\ \mathbf{T}_{1,11}\mathbf{T}_{1,12}+\mathbf{T}_{1,21}-\mathbf{T}_{2,12}\end{bmatrix}\\
&=2\begin{bmatrix}4\mathbf{T}_{1,11}\mathbf{T}_{1,12}-2\mathbf{T}_{1,12}^3+2\mathbf{T}_{1,21}-2\mathbf{T}_{1,12}\mathbf{T}_{1,22}-2\mathbf{T}_{2,12}\\ \frac{\nu}{4}-2\mathbf{T}_{1,11}^2+\mathbf{T}_{1,11}\mathbf{T}_{1,12}^2-\mathbf{T}_{1,12}+3\mathbf{T}_{1,11}\mathbf{T}_{1,22}-\mathbf{T}_{1,12}^2\mathbf{T}_{1,22}-\mathbf{T}_{1,22}^2+\mathbf{T}_{2,11}-\mathbf{T}_{2,22}\end{bmatrix}
\end{aligned} \tag{5.59}$$

Therefore, the $(1,2)$ element of (5.50) is

$$\frac{\mathrm{d}Y}{\mathrm{d}\nu}=Z, \tag{5.60}$$

and the $(2,2)$ element of (5.50) is

$$\begin{aligned}
&\frac{\mathrm{d}(Z-2YH)}{\mathrm{d}\nu}+6\mathbf{T}_{1,11}^2-2\mathbf{T}_{1,11}\mathbf{T}_{1,12}^2+2\mathbf{T}_{1,12}\mathbf{T}_{1,21}-4\mathbf{T}_{1,11}\mathbf{T}_{1,22}\\
&\quad+2\mathbf{T}_{1,12}^2\mathbf{T}_{1,22}+2\mathbf{T}_{1,22}^2-2\mathbf{T}_{2,11}+2\mathbf{T}_{2,22}-\frac{\nu}{2}=0.
\end{aligned} \tag{5.61}$$

Rearranging the terms, we get

$$\frac{\mathrm{d}Z}{\mathrm{d}\nu}=2ZH-H^4-4H^2Y-5Y^2+\frac{\nu}{2}-2H\mathbf{T}_{1,21}+2\mathbf{T}_{2,11}-2\mathbf{T}_{2,22}. \tag{5.62}$$

A few elements of the $\mathbf{T}_\mathrm{s}$ expansion coefficients are still unknown in $\frac{\mathrm{d}Z}{\mathrm{d}\nu}$. However, one of the standard procedures is that we can expand $\mathbf{A}$ in its negative powers at infinity. Since we have established all of the negative powers must disappear, every such term must be zero. These relations will help us eliminate certain terms. It turns out that H, Y and Z can be determined by a system of ODE's. Equations (5.64) to (5.65) are the steps of the calculation. Notice $\operatorname{tr}\mathbf{T}_1=0$, so

$$\mathbf{T}_{1,22}=-\mathbf{T}_{1,11}. \tag{5.63}$$

For simplicity, we can eliminate all $\mathbf{T}_{1,22}$ terms.

First, $\mathbf{A}_{-1,12}=0$, therefore

$$\begin{aligned}
0&=\mathbf{A}_{-1,12}\\
&=4\mathbf{T}_{1,11}^2+2\mathbf{T}_{1,12}\mathbf{T}_{1,21}+2\mathbf{T}_{2,11}-4\mathbf{T}_{1,12}\mathbf{T}_{2,12}-2\mathbf{T}_{2,22}-\frac{\nu}{2}.
\end{aligned} \tag{5.64}$$

Using definition of H and Y,

$$H^4+4H(\mathbf{T}_{1,21}-\mathbf{T}_{2,12})-2H\mathbf{T}_{1,21}+2\mathbf{T}_{2,11}-2\mathbf{T}_{2,22}+2H^2Y+Y^2-\frac{\nu}{2}=0$$

$$\begin{aligned}\iff -2H\mathbf{T}_{1,21} + 2\mathbf{T}_{2,11} - 2\mathbf{T}_{2,22} =& \frac{\nu}{2} - 2H^2Y - Y^2 - H^4 - 4H(\mathbf{T}_{1,21} - \mathbf{T}_{2,12}) \\ =& \frac{\nu}{2} - 2H^2Y - Y^2 - H^4 - 2H(Z - H^3 - 3YH)\end{aligned}$$

Using the expression for $\frac{\mathrm{d}Z}{\mathrm{d}\nu}$ in (5.62), we conclude,

$$\frac{\mathrm{d}Z}{\mathrm{d}\nu} = -6Y^2 + \nu. \tag{5.65}$$

□

5.2.10 Hamiltonian

In addition, another quantity that is going to be useful to us is the Hamiltonian associated with the system of ODE's (5.54). The Hamiltonian H is given by,

$$H = -2Y^3 - \frac{Z^2}{2} + Y\nu. \tag{5.66}$$

Indeed, if we use this as definition of a Hamiltonian, and Y, Z as the canonical variables, then the system (5.54) is indeed equivalent to

$$\begin{cases} \dfrac{\mathrm{d}Y}{\mathrm{d}\nu} = -\dfrac{\partial H}{\partial Z}, \\ \dfrac{\mathrm{d}Z}{\mathrm{d}\nu} = \dfrac{\partial H}{\partial Y}. \end{cases} \tag{5.67}$$

To verify relation (5.66), we do so by computing a few more elements in $\mathbf{A}_{-1}$ and $\mathbf{A}_{-2}$. The following proof is all about computing the terms needed to eliminate the variables.

Proof.

$$\begin{aligned}\mathbf{A}_{-1,11} =& -\frac{1}{4} + 2\mathbf{T}_{1,11}^2\mathbf{T}_{1,12} - 2\mathbf{T}_{1,11}\mathbf{T}_{1,21} + 2\mathbf{T}_{1,12}^2\mathbf{T}_{1,21} \\ & - 2\mathbf{T}_{1,12}\mathbf{T}_{2,11} - 2\mathbf{T}_{1,11}\mathbf{T}_{2,12} - 2\mathbf{T}_{2,21} + 2\mathbf{T}_{3,12} - \mathbf{T}_{1,12}\frac{\nu}{2} \\ =& \, 0\end{aligned} \tag{5.68}$$

$$\begin{aligned}\implies \mathbf{T}_{3,12} =& -\frac{1}{2}\left(-\frac{1}{4} + 2\mathbf{T}_{1,11}^2\mathbf{T}_{1,12} - 2\mathbf{T}_{1,11}\mathbf{T}_{1,21} + 2\mathbf{T}_{1,12}^2\mathbf{T}_{1,21}\right. \\ & \left. -2\mathbf{T}_{1,12}\mathbf{T}_{2,11} - 2\mathbf{T}_{1,11}\mathbf{T}_{2,12} - 2\mathbf{T}_{2,21} - \mathbf{T}_{1,12}\frac{\nu}{2}\right).\end{aligned} \tag{5.69}$$

$$\begin{aligned}\mathbf{A}_{-1,21} = &-4\mathbf{T}_{1,11}^3 - 4\mathbf{T}_{1,11}\mathbf{T}_{1,12}\mathbf{T}_{1,21} - 2\mathbf{T}_{1,21}^2 + 6\mathbf{T}_{1,11}\mathbf{T}_{2,11} + 2\mathbf{T}_{1,21}\mathbf{T}_{2,12} \\ &+ 2\mathbf{T}_{1,12}\mathbf{T}_{2,21} - 2\mathbf{T}_{1,11}\mathbf{T}_{2,22} - 2\mathbf{T}_{3,11} + 2\mathbf{T}_{3,22} + \mathbf{T}_{1,11}\nu \\ = &\ 0\end{aligned} \tag{5.70}$$

$$\begin{aligned}\Longrightarrow \mathbf{T}_{3,11} - \mathbf{T}_{3,22} = &\frac{1}{2}\left(-4\mathbf{T}_{1,11}^3 - 4\mathbf{T}_{1,11}\mathbf{T}_{1,12}\mathbf{T}_{1,21} - 2\mathbf{T}_{1,21}^2 + 6\mathbf{T}_{1,11}\mathbf{T}_{2,11}\right. \\ &\left. +2\mathbf{T}_{1,21}\mathbf{T}_{2,12} + 2\mathbf{T}_{1,12}\mathbf{T}_{2,21} - 2\mathbf{T}_{1,11}\mathbf{T}_{2,22} + \mathbf{T}_{1,11}\right).\end{aligned} \tag{5.71}$$

$$\begin{aligned}\mathbf{A}_{-2,21} = &-\frac{\mathbf{T}_{1,12}}{2} - 2\mathbf{T}_{1,11}^2\mathbf{T}_{1,12}^2 - 2\mathbf{T}_{1,12}^3\mathbf{T}_{1,21} - 2\mathbf{T}_{1,11}\mathbf{T}_{1,12}^2\mathbf{T}_{1,22} - 4\mathbf{T}_{1,12}\mathbf{T}_{1,21}\mathbf{T}_{1,22} \\ &+ 2\mathbf{T}_{1,11}\mathbf{T}_{1,22}^2 - 2\mathbf{T}_{1,12}^2\mathbf{T}_{1,22}^2 - 2\mathbf{T}_{1,22}^3 + 2\mathbf{T}_{1,12}^2\mathbf{T}_{2,11} - 2\mathbf{T}_{1,22}\mathbf{T}_{2,11} + 4\mathbf{T}_{1,11}\mathbf{T}_{1,12}\mathbf{T}_{2,12} \\ &+ 2\mathbf{T}_{1,21}\mathbf{T}_{2,12} + 4\mathbf{T}_{1,12}\mathbf{T}_{1,22}\mathbf{T}_{2,12} - 2\mathbf{T}_{2,12}^2 + 2\mathbf{T}_{1,12}\mathbf{T}_{2,21} - 2\mathbf{T}_{1,11}\mathbf{T}_{2,22} + 2\mathbf{T}_{1,12}^2\mathbf{T}_{2,22} \\ &+ 4\mathbf{T}_{1,22}\mathbf{T}_{2,22} + 2\mathbf{T}_{3,11} - 4\mathbf{T}_{1,12}\mathbf{T}_{3,12} - 2\mathbf{T}_{3,22} - \mathbf{T}_{1,11}\frac{\nu}{2} + \mathbf{T}_{1,12}^2\frac{\nu}{2} + \mathbf{T}_{1,22}\frac{\nu}{2} \\ = &\ 0.\end{aligned} \tag{5.72}$$

Using (5.64), (5.69), (5.71) and $\operatorname{tr}\mathbf{T}_1 = 0$, we get

$$\begin{aligned}&-\mathbf{T}_{1,12} + 2\mathbf{T}_{1,11}^2\mathbf{T}_{1,12}^2 - 4\mathbf{T}_{1,11}\mathbf{T}_{1,12}\mathbf{T}_{1,21} + 2\mathbf{T}_{1,12}^3\mathbf{T}_{1,21} \\ &- 2\mathbf{T}_{1,21}^2 - 4\mathbf{T}_{1,11}\mathbf{T}_{1,12}\mathbf{T}_{2,12} + 4\mathbf{T}_{1,21}\mathbf{T}_{2,12} - 2\mathbf{T}_{2,12}^2 \\ &+ (4\mathbf{T}_{1,11} - \mathbf{T}_{1,12}^2)(-4\mathbf{T}_{1,11}^2 - 2\mathbf{T}_{1,12}\mathbf{T}_{1,21} + 4\mathbf{T}_{1,12}\mathbf{T}_{2,12} + \frac{\nu}{2}) - \mathbf{T}_{1,12}^2\frac{\nu}{2} = 0.\end{aligned} \tag{5.73}$$

Then using the definition of H, Y, Z, $\mathbf{A}_{-2,21} = 0$ is equivalent to the identity

$$H = -2Y^3 - \frac{Z^2}{2} + Y\nu. \tag{5.74}$$

□

In particular, H is the Hamiltonian function associated with the solution Y of the well-known Painlevé-I equation.

5.2.11 Expansion of $\mathbf{T}$

According to (5.14),

$$\mathbf{T}(\zeta;\nu) = \left(\mathbb{I} + \sum_{p=1}^{P}\mathbf{T}_p(\nu)\zeta^{-p} + O(\zeta^{-P-1})\right)\zeta^{-\frac{\sigma_3}{4}}\mathbf{M}^{-1}, \qquad \zeta\to\infty. \tag{5.75}$$

From the previous sections, we were able to express some elements in $\mathbf{T}_n(\nu)$. In particular, by definition (5.51),

$$\mathbf{T}_{1,12} = H, \qquad \mathbf{T}_{1,11} = -\mathbf{T}_{1,22} = \frac{Y + H^2}{2}. \tag{5.76}$$

Therefore, the expansion for $\mathbf{T}$ can be written as the solution to the Painlevé-I equation,

$$\mathbf{T} = \left(\mathbb{I} + \frac{1}{\zeta} \begin{bmatrix} \frac{Y+H^2}{2} & H \\ * & -\frac{Y+H^2}{2} \end{bmatrix} + O(\zeta^{-2}) \right) \zeta^{-\frac{\sigma_3}{4}} \mathbf{M}^{-1}, \qquad \zeta \to \infty. \tag{5.77}$$

5.3 First correction at the gradient catastrophe

5.3.1 Small norm problem

Our goal is to characterise the solution to sG in the semiclassical limit, i.e. ϵ. We would like to 1) capture the leading asymptotic behaviour, 2) determine the size of the error, 3) and perhaps say something about the subleading terms as well. This chapter is more about 2) and 3). To achieve that, we will utilise the small norm theory [5]. To briefly summarise the strategy, suppose that a Riemann–Hilbert problem has "small" jump (in operator norm), then the solution should also be close to identity. The theory tells us that this solution not only admits the Laurent expansion $\mathbb{I} + \frac{\mathbf{E}_1}{z} + \frac{\mathbf{E}_2}{z^2} + \cdots$, but also the expansion can be computed by the iteration formula (5.108).

We begin by proving we have a small norm problem.

5.3.2 z-plane and symmetry

Unfolding to z-plane

Our Riemann–Hilbert Problem has a jump on $\mathbb{R}_+$ that has come from using the auxiliary complex variable w in the Lax-pair equation (2.4). More precisely, the variable appears in the equation as $\sqrt{-w}$. The natural jump of the square root function introduces the jump on the real line in our RHP. By working with $\sqrt{-w}$ instead of its square, we have avoided repeated symmetries. However, for certain parts of the analysis, particularly when we try to have a small-norm problem for the error matrix, the jump condition on $\mathbb{R}_+$ is hard to work with. It is not in the standard form where the jump matrix is a right multiplication. Therefore sometimes it is more convenient for us to use the symmetries to get rid of this

jump by considering the variable z, defined as

$$z^2 = w. \tag{5.78}$$

For all the RHPs we considered so far, the jump condition on the positive real axis has been $\mathbf{O}_+(w) = \sigma_2 \mathbf{O}_-(w)\sigma_2$. If we define

$$\mathbf{P}(z) = \begin{cases} \mathbf{O}(z^2) & \mathcal{I}(z) > 0, \\ \sigma_2 \mathbf{O}(z^2)\sigma_2 & \mathcal{I}(z) < 0, \end{cases} \tag{5.79}$$

then we can check that the matrix $\mathbf{P}$ has no jump on the real line. Indeed the jump contour $\beta_+ \in \mathcal{I}(w) > 0$ is mapped to two cuts on the first and third quadrants in the z-plane, and the $\beta_- \in \mathcal{I}(w) < 0$ is mapped to the second and fourth quadrant. Rearranging orientations of the new cuts mapped from β, we can see that they connect on the two points 1 and -1 on the real line, and the jump matrices are the same in both the upper half plane and the lower half plane. Instead of four separate cuts, what we actually have are two cuts, as shown in figure 5.3.

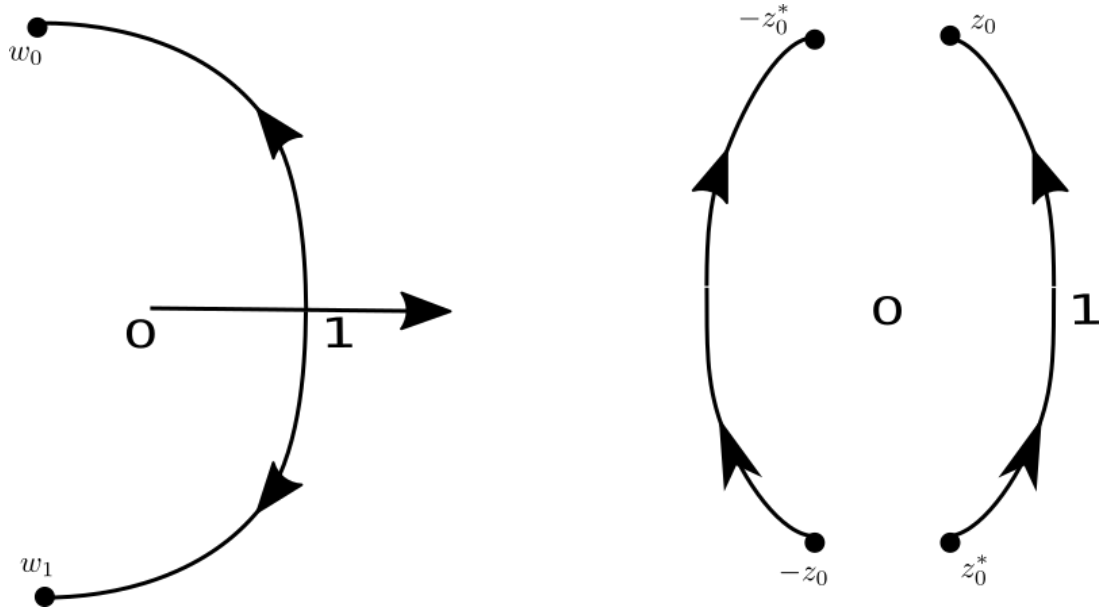

Figure 5.3: The jump contours for the outer parametrix on β and $\mathbb{R}_+$ are mapped to $\tilde{\beta}$

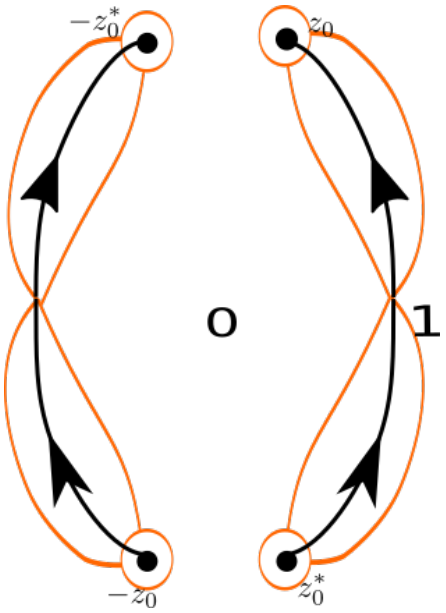

Figure 5.4: **P** jump contour

Symmetry

Now let's explore the symmetry of **P**. We know the $\mathbf{O}(w)$ has Schwarz symmetry, $\mathbf{O}(w) = \mathbf{O}(w^*)^*$. Using definition (5.79), we have

$$\mathbf{P}(z^*) = \sigma_2\mathbf{O}(z^{*2})\sigma_2 = \sigma_2\mathbf{O}(z^2)^*\sigma_2 = \left(\sigma_2\mathbf{O}(z^2)\sigma_2\right)^* = \left(\mathbf{P}(-z)\right)^*,$$

or equivalently,

$$\left(\mathbf{P}(-z^*)\right)^* = \mathbf{P}(z). \tag{5.80}$$

In addition to conjugation, we also have

$$\mathbf{P}(-z) = \sigma_2\mathbf{P}(z)\sigma_2. \tag{5.81}$$

Essentially the matrix **P** is completely determined by the information in one of the quadrants. Expressed in elements, the two symmetry conditions imply that

$$\mathbf{P}(z) = \begin{bmatrix} p(z) & q(z) \\ -q(-z) & p(-z) \end{bmatrix}, \quad \text{and} \quad \left(p(-z^*)\right)^* = p(z),\ \left(q(-z^*)\right)^* = q(z). \tag{5.82}$$

$\mathbf{P}_1$ rational function with simple poles

A rational function $\mathbf{P}_1(z)$ with simple poles that has the same symmetry as $\mathbf{P}$ will play an important role later. For future reference, we will give here the general form of the rational function $\mathbf{P}_1(z)$ with only one simple pole in each quadrant, which goes to $\mathbb{I}$ as $z \to \infty$. Suppose the pole in the first quadrant is at z_0, then by symmetry the other three poles are $-z_0$ and $\pm z_0^*$. Then $\mathbf{P}_1(z)$ can be written as:

$$\mathbf{P}_1(z) = \mathbb{I} + \frac{\mathbf{A}}{z - z_0} + \frac{\mathbf{B}}{z - z_0^*} + \frac{\mathbf{C}}{z + z_0} + \frac{\mathbf{D}}{z + z_0^*}. \tag{5.83}$$

Applying the first symmetry condition (5.80),

$$\mathbf{P}_1(-z^*)^* = \mathbb{I} + \frac{-\mathbf{D}^*}{z - z_0} + \frac{-\mathbf{C}^*}{z - z_0^*} + \frac{-\mathbf{B}^*}{z + z_0} + \frac{-\mathbf{A}^*}{z + z_0^*} = \mathbf{P}_1(z), \tag{5.84}$$

we find the relations between the constant matrices are

$$\mathbf{A} = -\mathbf{D}^*, \quad \mathbf{B} = -\mathbf{C}^*. \tag{5.85}$$

Similarly, using the second symmetry (5.81),

$$\begin{aligned} \sigma_2 \mathbf{P}(-z)\sigma_2 &= \sigma_2 \left(\mathbb{I} + \frac{\mathbf{B}^*}{z - z_0} + \frac{\mathbf{A}^*}{z - z_0^*} + \frac{-\mathbf{A}}{z + z_0} + \frac{-\mathbf{B}}{z + z_0^*} \right) \sigma_2 \\ &= \mathbb{I} + \frac{\sigma_2 \mathbf{B}^* \sigma_2}{z - z_0} + \frac{\sigma_2 \mathbf{A}^* \sigma_2}{z - z_0^*} - \frac{\sigma_2 \mathbf{A} \sigma_2}{z + z_0} - \frac{\sigma_2 \mathbf{B} \sigma_2}{z + z_0^*}, \end{aligned} \tag{5.86}$$

we conclude that

$$\mathbf{B} = \sigma_2 \mathbf{A}^* \sigma_2. \tag{5.87}$$

So to determine $\mathbf{P}_1$, we only need to determine one constant matrix $\mathbf{A}$, and it follows

$$\mathbf{P}_1(z) = \mathbb{I} + \frac{\mathbf{A}}{z - z_0} + \frac{\sigma_2 \mathbf{A}^* \sigma_2}{z - z_0^*} - \frac{\sigma_2 \mathbf{A} \sigma_2}{z + z_0} - \frac{\mathbf{A}^*}{z + z_0^*}. \tag{5.88}$$

5.3.3 Inner parametrix and the tritronquée parametrix

If we set,

$$\frac{1}{2}\frac{\phi}{\epsilon} = \frac{4}{5}\zeta^{\frac{5}{2}} - s\zeta^{\frac{1}{2}}, \tag{5.89}$$

then

$$\frac{1}{\epsilon}\left(\frac{4}{5} W(w)^{\frac{5}{2}} - s W(w)^{\frac{1}{2}} \right) = \frac{4}{5}\zeta^{\frac{5}{2}} - s\zeta^{\frac{1}{2}}, \tag{5.90}$$

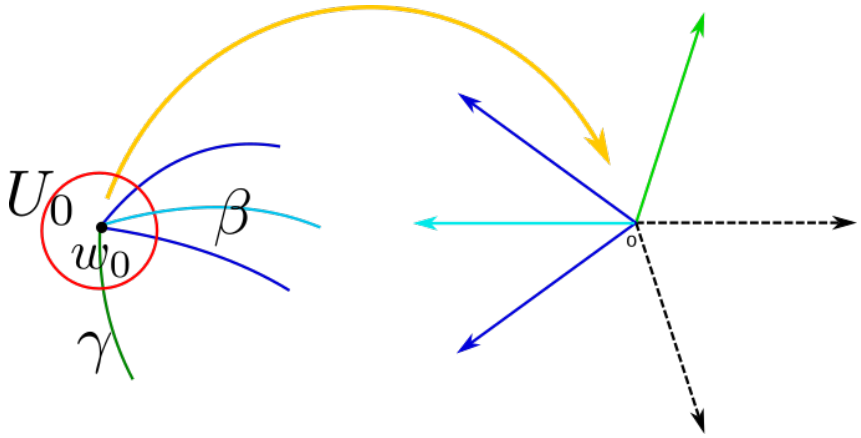

Figure 5.5: Inner parametrix mapped to the Painlevé variable

i.e.

$$\zeta = \frac{W(w)}{\epsilon^{\frac{2}{5}}}, \qquad \nu = \frac{s}{\epsilon^{\frac{4}{5}}} \tag{5.91}$$

Then the Riemann–Hilbert problem for the inner parametrix is exactly matched to the Riemann–Hilbert problem for the Painlevé-I parametrix in the variable ζ, in area $\zeta(U_0)$. In this area, the jump condition for $\dot{\mathbf{O}}^{\text{in}}(w)e^{-i\frac{\kappa}{2}\sigma_3}$ is identical to $\mathbf{T}(\zeta(w))$

Because of the scaling factor $\epsilon^{-\frac{2}{5}}$ in (5.91), when we are studying the equation in the semi-classical regime, which means ϵ is a very small real number, U_0 is mapped to a large area (of size $\mathcal{O}\left(\epsilon^{-\frac{2}{5}}\right)$) in the ζ plane. Therefore, we can use the asymptotic expansion of solutions to the tritronquée parametrix Riemann–Hilbert problem 5.2.1 for large ζ, to approximate the asymptotics of the inner parametrix on the boundary of disks $U_{0,1}$.

$$\begin{aligned}
\dot{\mathbf{O}}^{\text{in}}(w)e^{-i\frac{\kappa}{2}\sigma_3} =& \mathbf{H}(w)\mathbf{T}(\zeta(w)) + \mathcal{O}(\zeta^{-\infty}) \\
=& \mathbf{H}(w)\left(\mathbb{I} + \frac{1}{\zeta}\begin{bmatrix} \frac{Y+H^2}{2} & H \\ * & -\frac{Y+H^2}{2} \end{bmatrix} + O(\zeta^{-2})\right)\zeta^{-\frac{\sigma_3}{4}}\mathbf{M}^{-1}, \qquad \zeta \to \infty \\
=& \mathbf{H}(w)\left(\mathbb{I} + \frac{\epsilon^{\frac{2}{5}}}{W(w)}\begin{bmatrix} \frac{Y+H^2}{2} & H \\ * & -\frac{Y+H^2}{2} \end{bmatrix} + O(\epsilon^{\frac{4}{5}})\right)\epsilon^{\frac{1}{10}\sigma_3}W(w)^{-\frac{\sigma_3}{4}}\mathbf{M}^{-1}, \\
& \epsilon \to 0_+.
\end{aligned} \tag{5.92}$$

5.3.4 The local behaviour of $\dot{\mathbf{O}}^{\text{out}}$

The jump for $\mathbf{O}^{\text{out}}$ on the β curve, as shown in figure 3.18 is

$$\mathbf{O}^{\text{out}}_+ = \mathbf{O}^{\text{out}}_- i\sigma_1 e^{i\kappa\sigma_3}, \tag{5.93}$$

with jump matrix $= \begin{bmatrix} 0 & ie^{-i\kappa} \\ ie^{i\kappa} & 0 \end{bmatrix}$.

The jump for $\dot{\mathbf{O}}^{\text{out}}$ would be the same on the β curve. Furthermore,

$$\dot{\mathbf{O}}_+^{\text{out}} e^{-i\frac{\kappa}{2}\sigma_3}\mathbf{M} = \dot{\mathbf{O}}_-^{\text{out}} e^{-i\frac{\kappa}{2}\sigma_3}\mathbf{M}\, i\sigma_3. \tag{5.94}$$

Locally, $\dot{\mathbf{O}}_+^{\text{out}} e^{-i\frac{\kappa}{2}\sigma_3}\mathbf{M}$ has the same jump as $W(w)^{-\frac{\sigma_3}{4}}$ inside the disk U_0. In fact, by construction, we have chosen the outer parametrix to blow up like $(w-w_0)^{-\frac{1}{4}}$. We can either directly derive from construction, or use a uniqueness argument to show that,

$$\mathbf{C}(w) := \dot{\mathbf{O}}_+^{\text{out}} e^{-i\frac{\kappa}{2}\sigma_3}\mathbf{M} W(w)^{\frac{\sigma_3}{4}} \tag{5.95}$$

is a holomorphic function inside the disk. In particular, notice that $\det(\mathbf{C}) \equiv 1$.

5.3.5 Error Parametrix

As explained in section 5.3.2, when we are seeking for a small-norm problem, it is best to consider the z variable instead of w, so we do not have to deal with a constant jump on $\mathbb{R}_+$.

So assume $\mathbf{P}$ is the unfolded versions of $\mathbf{O}$, as well as $\dot{\mathbf{P}}$, $\dot{\mathbf{P}}^{\text{out}}$, $\dot{\mathbf{P}}^{\text{in}}$ for $\dot{\mathbf{O}}$, $\dot{\mathbf{O}}^{\text{out}}$ and $\dot{\mathbf{O}}^{\text{in}}$ respectively. The original error matrix we are considering is

$$\mathbf{E} = \mathbf{O}\dot{\mathbf{O}}^{-1}, \tag{5.96}$$

which has a jump across $\mathbb{R}$. Instead we consider

$$\mathcal{E} = \mathbf{P}\dot{\mathbf{P}}^{-1} = \begin{cases} \mathbf{E}(z^2) & \text{Im}(z) > 0 \\ \sigma_2\mathbf{E}(z^2)\sigma_2 & \text{Im}(z) < 0 \end{cases}, \tag{5.97}$$

which has no jump on the real axis.

Jump for $\mathbf{F}$

As explained in section 5.3.2, w_0 and w_1, the endpoints of β, are now mapped to four symmetrical points in four quadrants. The endpoint $z_0 = \sqrt{w_0}$ is in the first quadrant. Suppose $\dot{\mathbf{P}}^{\text{in}}$ is defined in four symmetrical $\mathcal{O}(1)$ disks around $\pm z_0$ and $\pm z_0^*$. Label the four disks by the quadrants they are in, namely U_I, U_{II}, U_{III} and U_{IV}. The global parametrix

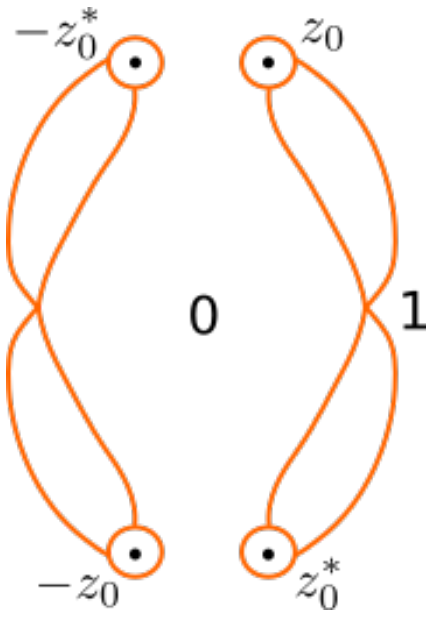

Figure 5.6: Jump for $\mathbf{F}$

is defined as

$$\dot{\mathbf{P}} = \begin{cases} \dot{\mathbf{P}}^{\text{in}} & z \in U_{I,II,III,IV}, \\ \dot{\mathbf{P}}^{\text{out}} & \text{otherwise} \end{cases}. \tag{5.98}$$

Like we have seen for $\mathcal{E}$ matrix in the original global parametrix, $\mathbf{F}$ has exponentially small jumps except on the boundaries of the disks.

Due to the symmetries, we only need to study one quadrant. Let's focus on the first quadrant, i.e. z_0 and U_I. Assuming a clockwise orientation, the relationship between $\mathbf{F}$ outside of the disk and inside the disk is given by

$$\mathbf{F}_+ = \mathbf{P}\left(\dot{\mathbf{P}}^{\text{out}}\right)^{-1} = \mathbf{P}\left(\dot{\mathbf{P}}^{\text{in}}\right)^{-1}\dot{\mathbf{P}}^{\text{in}}\left(\dot{\mathbf{P}}^{\text{out}}\right)^{-1} = \mathbf{F}_-\dot{\mathbf{P}}^{\text{in}}\left(\dot{\mathbf{P}}^{\text{out}}\right)^{-1}. \tag{5.99}$$

Therefore, the jump matrix along the circles are

$$\mathbf{V}_U = \dot{\mathbf{P}}^{\text{in}}\left(\dot{\mathbf{P}}^{\text{out}}\right)^{-1}. \tag{5.100}$$

By assumption, The center z_0 of disk U_I lies in the first quadrant, so U_1 is completely in the upper half plane. $\dot{\mathbf{P}}^{\text{in}}$ is the same as $\dot{\mathbf{O}}^{\text{in}}(z^2)$. Therefore, the jump on the boundary

of disk U_I is

$$\begin{aligned}\mathbf{V}_{U_I} =&\mathbf{H}(w)\left(\mathbb{I}+\frac{\epsilon^{\frac{2}{5}}}{W(w)}\begin{bmatrix}\frac{Y+H^2}{2} & H\\ * & -\frac{Y+H^2}{2}\end{bmatrix}+O(\epsilon^{\frac{4}{5}})\right)\epsilon^{\frac{1}{10}\sigma_3}W(w)^{-\frac{\sigma_3}{4}}\mathbf{M}^{-1}e^{i\frac{\kappa}{2}\sigma_3}\left(\dot{\mathbf{O}}^{\text{out}}\right)^{-1}\\ =&\mathbf{H}(w)\left(\mathbb{I}+\frac{\epsilon^{\frac{2}{5}}}{W(w)}\begin{bmatrix}\frac{Y+H^2}{2} & H\\ * & -\frac{Y+H^2}{2}\end{bmatrix}+O(\epsilon^{\frac{4}{5}})\right)\epsilon^{\frac{1}{10}\sigma_3}\mathbf{C}^{-1}, \qquad \epsilon\to 0_+.\end{aligned} \tag{5.101}$$

We want the jump to be close to the identity, in which case we will be able to expand the solution in powers of ϵ. Recall that we have not chosen the holomorphic function $\mathbf{H}$. However, we can see the formula for $\mathbf{V}$ is identity plus small powers in ϵ, sandwiched between $\mathbf{H}$ and $\epsilon^{\frac{1}{10}\sigma_3}\mathbf{C}^{-1}$. Suppose we choose

$$\mathbf{H}=\mathbf{C}\epsilon^{-\frac{1}{10}\sigma_3}, \tag{5.102}$$

then the matrix becomes

$$\begin{aligned}\mathbf{V}_{U_I} =&\mathbf{C}\left(\mathbb{I}+\frac{\epsilon^{\frac{1}{5}}}{W(w)}\begin{bmatrix}0 & H\\ 0 & 0\end{bmatrix}+\frac{\epsilon^{\frac{2}{5}}}{W(w)}\begin{bmatrix}\frac{Y+H^2}{2} & 0\\ 0 & -\frac{Y+H^2}{2}\end{bmatrix}+\mathcal{O}(\epsilon^{\frac{3}{5}})\right)\mathbf{C}^{-1}\\ =&\mathbb{I}+\frac{\epsilon^{\frac{1}{5}}}{W(w)}\mathbf{C}\begin{bmatrix}0 & H\\ 0 & 0\end{bmatrix}\mathbf{C}^{-1}+\frac{\epsilon^{\frac{2}{5}}}{W(w)}\mathbf{C}\begin{bmatrix}\frac{Y+H^2}{2} & 0\\ 0 & -\frac{Y+H^2}{2}\end{bmatrix}\mathbf{C}^{-1}+\mathcal{O}(\epsilon^{\frac{3}{5}}) \qquad \epsilon\to 0_+.\end{aligned} \tag{5.103}$$

Indeed the error parametrix $\mathbf{F}$ is the solution to a small norm Riemann–Hilbert problem. Thus next we need a systematic way to compute the solution as an expansion.

Inner Parametrix

$$\dot{\mathbf{O}}^{\text{in}}=\mathbf{C}\left(\mathbb{I}+\frac{\epsilon^{\frac{1}{5}}}{W(w)}\begin{bmatrix}0 & H\\ 0 & 0\end{bmatrix}+\frac{\epsilon^{\frac{2}{5}}}{W(w)}\begin{bmatrix}\frac{Y+H^2}{2} & 0\\ 0 & -\frac{Y+H^2}{2}\end{bmatrix}+O(\epsilon^{\frac{3}{5}})\right)W(w)^{-\frac{1}{4}\sigma_3}\mathbf{M}^{-1}e^{i\frac{\kappa}{2}\sigma_3}. \tag{5.104}$$

5.3.6 Error Estimate

Inner-Outer Mismatch

Define the inner-outer mismatch on the boundary of the disk ∂D_0 and ∂D_1 as

$$\mathbf{V}:=\dot{\mathbf{O}}^{\text{in}}\left(\dot{\mathbf{O}}^{\text{out}}\right)^{-1} \tag{5.105}$$

The upper and lower plane has symmetry, so we can restrict our attention to the upper plane for now. At the boundary of the disk,

$$\begin{aligned}\mathbf{V}_{U_I} &= \mathbb{I} + \frac{\epsilon^{\frac{1}{5}}}{W(w)}\mathbf{C}\begin{bmatrix}0 & H\\ 0 & 0\end{bmatrix}\mathbf{C}^{-1} + \frac{\epsilon^{\frac{2}{5}}}{W(w)}\mathbf{C}\begin{bmatrix}\frac{Y+H^2}{2} & 0\\ 0 & -\frac{Y+H^2}{2}\end{bmatrix}\mathbf{C}^{-1} + \mathcal{O}(\epsilon^{\frac{3}{5}}) \\ &= \mathbb{I} + \Delta\mathbf{V}^0\end{aligned} \tag{5.106}$$

This implies that the Riemann–Hilbert problem for $\mathbf{F}$ is a small norm problem. Small norm theory implies the solution has expansion

$$\mathcal{E}(z) = \mathbb{I} + \frac{\mathbf{E}_1}{z} + \frac{\mathbf{E}_2}{z^2} + \cdots. \tag{5.107}$$

Iteration

The solution of the small norm can be obtained by iteration. The iteration formula is given by

$$\begin{aligned}\mathcal{E}^{(0)} =& \mathbb{I}, \\ \mathcal{E}^{(j+1)}(z) =& \mathbb{I} + \frac{1}{2\pi i}\oint_{\partial U_I}\frac{\mathcal{E}^{(j)}(s)\Delta\mathbf{V}_{U_I}(s)}{s-z}\mathrm{d}s + \frac{1}{2\pi i}\oint_{\partial U_{II}}\frac{\mathcal{E}^{(j)}(s)\Delta\mathbf{V}_{U_{II}}(s)}{s-z}\mathrm{d}s \\ &+ \frac{1}{2\pi i}\oint_{\partial U_{III}}\frac{\mathcal{E}^{(j)}(s)\Delta\mathbf{V}_{U_{III}}(s)}{s-z}\mathrm{d}s + \frac{1}{2\pi i}\oint_{\partial U_{IV}}\frac{\mathcal{E}^{(j)}(s)\Delta\mathbf{V}_{U_{IV}}(s)}{s-z}\mathrm{d}s.\end{aligned} \tag{5.108}$$

Notice that the contour orientation is clockwise. The number of iteration will depend on the how many terms one is expanding for the asymptotic formula. We are going to look for the leading correction.

First Iteration

$\epsilon^{\frac{1}{5}}$ Correction:

We are interested in $z = 0$ and $z \to \infty$. So z is taken to be outside of all four disks. Here we only need to compute the integral in the first quadrant. We can obtain the rest by symmetry.

$$\begin{aligned}\frac{1}{2\pi i}\oint_{\partial U_I}\frac{\mathbb{I}\Delta\mathbf{V}_{U_I}(s)}{s-z}\mathrm{d}s &= \epsilon^{\frac{1}{5}}\frac{1}{2\pi i}\oint_{\partial U_I}\frac{1}{s-z}C(s)\begin{bmatrix}0 & H\\ 0 & 0\end{bmatrix}C(s)^{-1}\mathrm{d}s \\ &= \frac{1}{z-z_0}\frac{1}{2z_0W'(w_0)}C(w_0)\begin{bmatrix}0 & H\\ 0 & 0\end{bmatrix}C(w_0)^{-1}.\end{aligned} \tag{5.109}$$

Therefore,

$$\begin{aligned}\mathcal{E}^{(1)}(z) =&\mathbb{I}+\epsilon^{\frac{1}{5}}\frac{1}{2\pi i}\oint_{\partial U}\frac{\mathbb{I}\Delta\mathbf{V}_U(s)}{s-z}\mathrm{d}s+O(\epsilon^{\frac{2}{5}})\\ =&\mathbb{I}+\epsilon^{\frac{1}{5}}\left(\frac{1}{z-z_0}\frac{1}{2z_0W'(w_0)}C(w_0)\begin{bmatrix}0&H\\0&0\end{bmatrix}C(w_0)^{-1}\right.\\ &+\frac{1}{z-z_0^*}\frac{1}{2z_0^*W'(w_0)^*}\sigma_2\overline{C(w_0)}\begin{bmatrix}0&H^*\\0&0\end{bmatrix}\overline{C(w_0)}^{-1}\sigma_2\\ &-\frac{1}{z+z_0}\frac{1}{2z_0W'(w_0)}\sigma_2C(w_0)\begin{bmatrix}0&H\\0&0\end{bmatrix}C(w_0)^{-1}\sigma_2\\ &\left.-\frac{1}{z+z_0^*}\frac{1}{2z_0^*W'(w_0)^*}C(w_0)^*\begin{bmatrix}0&H^*\\0&0\end{bmatrix}\overline{C(w_0)}^{-1}\right)+O(\epsilon^{\frac{2}{5}})\end{aligned}\tag{5.110}$$

If we only need the correction up to the $\epsilon^{\frac{1}{5}}$ term, then the first iteration is sufficient, because the second iteration will only show up in $\epsilon^{\frac{2}{5}}$ power.

We recover the solution to sine-Gordon for the fluxon condensate from the expansion coefficients of the solution of the Riemann–Hilbert problem at 0 (2.23). Therefore, we define the evaluation of $\mathcal{E}^{(1)}(w)$ at 0 as $\mathcal{E}^{(1)}$,

$$\begin{aligned}\mathcal{E}^{(1)} =&\mathbb{I}+\epsilon^{\frac{1}{5}}\left(\frac{1}{-z_0}\frac{1}{2z_0W'(w_0)}C(w_0)\begin{bmatrix}0&H\\0&0\end{bmatrix}C(w_0)^{-1}\right.\\ &+\frac{1}{-z_0^*}\frac{1}{2z_0^*W'(w_0)^*}\sigma_2\overline{C(w_0)}\begin{bmatrix}0&H^*\\0&0\end{bmatrix}\overline{C(w_0)}^{-1}\sigma_2\\ &-\frac{1}{z_0}\frac{1}{2z_0W'(w_0)}\sigma_2C(w_0)\begin{bmatrix}0&H\\0&0\end{bmatrix}C(w_0)^{-1}\sigma_2\\ &\left.-\frac{1}{z_0^*}\frac{1}{2z_0^*W'(w_0)^*}C(w_0)^*\begin{bmatrix}0&H^*\\0&0\end{bmatrix}\overline{C(w_0)}^{-1}\right)+\mathcal{O}(\epsilon^{\frac{2}{5}})\end{aligned}\tag{5.111}$$

Recall that the global parametrix and the matrix function $\mathbf{O}$ differ by the error matrix. To obtain an asymptotic expansion in ϵ of $\mathbf{O}(w)$ at 0

$$\begin{aligned}\mathbf{O}(0) =&\mathcal{E}(0)\dot{\mathbf{O}}(0)\\ =&(\mathbb{I}+\epsilon^{\frac{1}{5}}\mathcal{E}^{(1)}+\mathcal{O}(\epsilon^{\frac{2}{5}}))\begin{bmatrix}\dot{C}&-\dot{S}\\\dot{S}&\dot{C}\end{bmatrix}.\end{aligned}\tag{5.112}$$

Furthermore, in the $\mathcal{O}(\epsilon^{\frac{4}{5}})$ neighbourhood under consideration, w_0, w_1 and $\mathbf{C}(w)$ are all

slow varying functions that depend on independent or parametric variables (x,t). This means that we can expand them near the gradient catastrophe point. This expansion produces errors of size $\mathcal{O}(\epsilon^{\frac{4}{5}})$ or smaller, which will not affect the first correction term of size $\epsilon^{\frac{1}{5}}$. Therefore, in $\mathcal{E}^{(1)}$, we can replace these values by the evaluation at the gradient catastrophe point.

$$\begin{aligned}\mathcal{E}^{(1)} =&\epsilon^{\frac{1}{5}}\frac{1}{-z_{\rm gc}}\frac{1}{2z_{\rm gc}W'(w_{\rm gc})}C(w_{\rm gc})\begin{bmatrix}0 & H\\ 0 & 0\end{bmatrix}C(w_0)^{-1}\\ &+\frac{1}{-z^*_{\rm gc}}\frac{1}{2z^*_{\rm gc}W'(w_{\rm gc})^*}\sigma_2 C(w_{\rm gc})^*\begin{bmatrix}0 & H^*\\ 0 & 0\end{bmatrix}C(w_{\rm gc})^{*-1}\sigma_2\\ &-\frac{1}{z_{\rm gc}}\frac{1}{2z_{\rm gc}W'(w_{\rm gc})}\sigma_2 C(w_{\rm gc})\begin{bmatrix}0 & H\\ 0 & 0\end{bmatrix}C(w_{\rm gc})^{-1}\sigma_2\\ &-\frac{1}{z^*_{\rm gc}}\frac{1}{2z^*_{\rm gc}W'(w_{\rm gc})^*}C(w_{\rm gc})^*\begin{bmatrix}0 & H^*\\ 0 & 0\end{bmatrix}C(w_{\rm gc})^{*-1}\end{aligned} \tag{5.113}$$

Assembling the pieces together, we have proved theorem 1.5.1.

Chapter 6

Theorem 2: near the poles

6.1 Statement of theorem 2

In this chapter we prove the second main theorem.

Theorem 1.5.2 (Rational solutions emerging at the poles of the tritronquée solution]). *Under the same assumptions as in theorem 1.5.1, suppose that ν_p is a pole of the tritronquée solution. There $\exists M$, when $|\nu|< M$ and $H(\nu)/(\nu-\nu_p) > M\epsilon^{-\frac{1}{5}}$, such that the corresponding (x,t) neighbourhood of (x_p,t_p), where $\nu_p = s(x_p,t_p)/\epsilon^{\frac{4}{5}}$ and $\nu = s(x,t)/\epsilon^{\frac{4}{5}}$, has a universal leading asymptotic behaviour (we call them local structures), described by a special soliton solution of sG, given by*

$$\begin{aligned} \sin(\tfrac{1}{2}u_N) &= \mathbf{G}_{11}^{\text{out}}\dot{C} + \mathbf{G}_{12}^{\text{out}}\dot{S} + \mathcal{O}(\epsilon^{\frac{1}{5}}), \\ \cos(\tfrac{1}{2}u_N) &= \mathbf{G}_{21}^{\text{out}}\dot{C} + \mathbf{G}_{22}^{\text{out}}\dot{S} + \mathcal{O}(\epsilon^{\frac{1}{5}}), \end{aligned} \tag{6.1}$$

$$\mathbf{G}^{\text{out}} = \mathbb{I} - \frac{\mathbf{G}_0}{\sqrt{w_0^{\text{gc}}}} - \frac{\sigma_2\mathbf{G}_0^*\sigma_2}{\sqrt{w_0^{\text{gc}*}}} - \frac{\sigma_2\mathbf{G}_0\sigma_2}{\sqrt{w_0^{\text{gc}}}} - \frac{\mathbf{G}_0^*}{\sqrt{w_0^{\text{gc}*}}}, \tag{6.2}$$

where

$$\mathbf{G}_0 = \begin{bmatrix} a \\ b \end{bmatrix} \begin{bmatrix} C_{0,21}^{\text{gc}} & -C_{0,11}^{\text{gc}} \end{bmatrix}. \tag{6.3}$$

and $C_{0,ij}^{\text{gc}}$ is the (i,j) element of the matrix $\mathbf{C}(w_0)$ evaluated at the gradient catastrophe point. The coefficients (a,b) solve a 4×4 linear system with $\epsilon^{-\frac{1}{5}}\frac{1}{H(\nu)}$ in the coefficients. The solution exists for every (x,t) in the area we consider.

6.2 Modifying the inner parametrix

6.2.1 Schlesinger transformation

Due to the blowing up of H, the estimate (5.2) clearly fails near the poles. To fix the problem, we seek a different parametrix to replace the Painlevé-I parametrix. Apply the Schlesinger transformation to the Painlevé-I parametrix. We want to new parametrix to have a different local behaviour.

Originally the inner parametrix $\mathbf{T}$ has an Laurent expansion

$$\mathbf{T}\mathbf{M}\zeta^{\frac{\sigma_3}{4}} = \mathbb{I} + \mathcal{O}(\zeta^{-1}) \tag{6.4}$$

when $\zeta \to \infty$. Now we seek a new matrix that has same jump condition as $\mathbf{T}$ but behaves like

$$\widetilde{\mathbf{T}}\mathbf{M}\zeta^{-\frac{3\sigma_3}{4}} = \mathbb{I} + \mathcal{O}(\zeta^{-1}). \tag{6.5}$$

Because the matrix $\widetilde{\mathbf{T}}\mathbf{T}^{-1}$ has no jump and goes to $\mathbb{I}$ at infinity, it is necessarily a meromorphic function with poles only at the origin. Suppose $\widetilde{\mathbf{T}}$ is obtained by the Schlesinger transformation

$$\widetilde{\mathbf{T}} = (\mathbf{P}\zeta + \mathbf{B})\mathbf{T}. \tag{6.6}$$

with $\mathbf{P} = \begin{bmatrix} P_{11} & P_{12} \\ P_{21} & P_{22} \end{bmatrix}$ and $\mathbf{B} = \begin{bmatrix} B_{11} & B_{12} \\ B_{21} & B_{22} \end{bmatrix}$. Note that this is equivalent to assume $\widetilde{\mathbf{T}}\mathbf{T}^{-1}$ is the simplest possible analytic function: a linear function.

Recall from section 5.2.11, we know some information about coefficients in the expansion in (6.4)

$$\mathbf{T}\mathbf{M}\xi^{\frac{\sigma_3}{4}} = \mathbb{I} + \frac{\mathbf{T}_1}{\zeta} + \frac{\mathbf{T}_2}{\zeta^2} + \frac{\mathbf{T}_3}{\zeta^3} + \cdots \tag{6.7}$$

Plug this expansion into (6.6), we obtain

$$\begin{aligned} \widetilde{\mathbf{T}}\mathbf{M}\xi^{-\frac{3\sigma_3}{4}} &= (\mathbf{P}\zeta + \mathbf{B})\mathbf{T}\mathbf{M}\xi^{\frac{\sigma_3}{4}}\xi^{-\sigma_3} \\ &= (\mathbf{P}\zeta + \mathbf{B})\left(\mathbb{I} + \frac{\mathbf{T}_1}{\zeta} + \frac{\mathbf{T}_2}{\zeta^2} + \frac{\mathbf{T}_3}{\zeta^3} + \cdots\right)\zeta^{-\sigma_3}. \end{aligned} \tag{6.8}$$

We also know that $\widetilde{\mathbf{T}}\mathbf{M}\xi^{-\frac{3\sigma}{4}}$ itself has a power expansion at infinity. Denote it by

$$\widetilde{\mathbf{T}}\mathbf{M}\xi^{-\frac{3\sigma}{4}} = \mathbb{I} + \frac{\widetilde{\mathbf{T}}_1}{\zeta} + \frac{\widetilde{\mathbf{T}}_2}{\zeta^2} + \frac{\widetilde{\mathbf{T}}_3}{\zeta^3} + \cdots. \tag{6.9}$$

Comparing (6.8) and (6.9), it is necessarily true that the following conditions hold

$$\begin{aligned} &P_{11} = 1,\ P_{12} = P_{21} = P_{22} = 0, \\ &B_{22} = 0,\ B_{12} = -T_{1,12},\ \mathbf{B}_{21} = \frac{1}{T_{1,12}},\ \mathbf{B}_{11} = T_{1,22} - \frac{T_{2,12}}{T_{1,12}}. \end{aligned} \tag{6.10}$$

Recall that the $\mathbf{T}_k$ is related to a linear system that involves Painlevé I equations. In particular, $T_{1,12} = H$.

Using the information we obtained about $\mathbf{P}$ and $\mathbf{B}$ in (6.10), the expansion (6.9) becomes

$$\widetilde{\mathbf{T}}\mathbf{M}\zeta^{-\frac{3\sigma}{4}} = \mathbb{I} + \frac{1}{\zeta}\begin{bmatrix} -\frac{T_{2,12}}{T_{1,12}} & -T_{1,11}T_{2,12} - \frac{(T_{2,12})^2}{T_{1,12}} - T_{1,12}T_{2,22} + T_{2,12} \\ \frac{1}{T_{1,12}} & \frac{T_{2,12}}{T_{1,12}} \end{bmatrix} + \mathcal{O}(\zeta^{-2}). \tag{6.11}$$

6.2.2 $\widetilde{\mathbf{T}}\mathbf{M}\zeta^{-3\frac{\sigma_3}{4}}$ is regular near the poles

Recall from the derivation of the Painlevé I parametrix in section 5.2, when we are not at the poles of the Painlevé I equation, the coefficients $\mathbf{T}_k$ in (6.4) are related to P_I in the following way:

$$\begin{aligned} T_{1,12} =& H, \\ T_{1,11} - T_{1,22} =& y + H^2, \\ z =& 2Hy + 2H(H^2 + y) + 2T_{1,21} - 2T_{2,12}, \end{aligned} \tag{6.12}$$

while y, z, H satisfy the following system of differential equations (5.54).

Standard ODE theory tells us that the solution y, z and H admits the following expansion near a pole ν_0,

$$\begin{aligned} y =& -\frac{1}{(\nu-\nu_0)^2} - \frac{\nu_0}{10}(\nu-\nu_0)^2 - \frac{1}{6}(\nu-\nu_0)^3 - \frac{\nu_0^2}{300}(\nu-\nu_0)^6 - \frac{\nu_0}{150}(\nu-\nu_0)^7 + \mathcal{O}\left((\nu-\nu_0)^8\right) \\ z =& \frac{2}{(\nu-\nu_0)^3} - \frac{1}{5}\nu_0(\nu-\nu_0) - \frac{1}{2}(\nu-\nu_0)^2 - \frac{1}{50}\nu_0^2(\nu-\nu_0)^5 - \frac{7}{150}\nu_0(\nu-\nu_0)^6 + \mathcal{O}\left((\nu-\nu_0)^7\right) \\ H =& \frac{1}{\nu-\nu_0} - \frac{1}{30}\nu_0(\nu-\nu_0)^3 + \mathcal{O}\left((\nu-\nu_0)^4\right) \end{aligned} \tag{6.13}$$

Next we will show that the expansion (6.9) is indeed a Laurent expansion when ν is near the poles of PI, i.e. all the coefficients are regular.

Plug the expansions (6.13), combined with (6.12), into (6.11), we can show

$$\widetilde{\mathbf{T}}\mathbf{M}\xi^{-\frac{3\sigma}{4}} = \mathbb{I} + \frac{1}{\zeta}\begin{bmatrix} -\frac{T_{2,12}}{H} & O(1) \\ \frac{1}{H} & \frac{T_{2,12}}{H} \end{bmatrix} + \mathcal{O}(\zeta^{-2}). \tag{6.14}$$

In particular, T_{12}^2 regular can be derived from equation (5.42) and (5.50).

The expansion of H near ν_0 tells us $\frac{1}{H}$ is regular. Thus we have shown that $\widetilde{\mathbf{T}}\mathbf{M}\zeta^{-3\frac{\sigma_3}{4}}$ is regular near the poles and $\widetilde{\mathbf{T}}$ is indeed a good candidate for the inner parametrix.

6.3 Bäcklund transformation, modifying the outer parametrix

The strategy is the same as in Chapter 5. In order to obtain information on the asymptotics of the solution of a Riemann–Hilbert problem we try to construct a small norm problem to do the asymptotic expansion.

6.3.1 Error matrix

The setup for the error matrix is very similar to what we have done in Chapter 5 away from the poles. As explained in section 5.3.2, when we are seeking a small-norm problem, it is best to consider the z variable instead of w, so we do not have to deal with a constant jump on the $\mathbb{R}_+$.

So assume $\mathbf{P}$ is the unfolded versions of $\mathbf{O}$, as well as $\dot{\mathbf{P}}$, $\dot{\mathbf{P}}^{\text{out}}$, $\dot{\mathbf{P}}^{\text{in}}$ for $\dot{\mathbf{O}}$, $\dot{\mathbf{O}}^{\text{out}}$ and $\dot{\mathbf{O}}^{\text{in}}$ respectively. The original error matrix we are considering is

$$\mathbf{E} = \mathbf{O}\dot{\mathbf{O}}^{-1}, \tag{6.15}$$

which has a jump across $\mathbb{R}$. Instead we consider

$$\mathbf{F} = \mathbf{P}\dot{\mathbf{P}}^{-1} = \begin{cases} \mathbf{E}(z^2) & \operatorname{Im}(z) > 0 \\ \sigma_2\mathbf{E}(z^2)\sigma_2 & \operatorname{Im}(z) < 0 \end{cases}, \tag{6.16}$$

which has no jump on the real axis.

Jump for $\mathbf{F}$

The jump contour for $\mathbf{F}$ has been shown in figure 5.6. As explained in section 5.3.2, w_0 and w_1, the endpoints of β, are now mapped to four symmetrical points in four quadrants. Endpoint $z_0 = \sqrt{w_0}$ is in the first quadrant. Suppose $\dot{\mathbf{P}}^{\text{in}}$ is defined in four symmetrical

$\mathcal{O}(1)$ disks around $\pm z_0$ and $\pm z_0^*$. Label the four disks by the quadrants they are in, namely U_I, U_{II}, U_{III} and U_{IV}, as shown in figure 6.1 below. The global parametrix is defined as

$$\dot{\mathbf{P}} = \begin{cases} \dot{\mathbf{P}}^{\text{in}} & z \in U_{I,II,III,IV}, \\ \dot{\mathbf{P}}^{\text{out}} & \text{otherwise} \end{cases}. \tag{6.17}$$

Figure 6.1: $\mathbf{F}$ has more significant jump on the boundary of the four disks

As explained in Chapter 5, $\mathbf{F}$ has exponentially small jumps except on the boundary of the disks.

Due to the symmetries, we only need to study one quadrant. Let's focus on the first quadrant, i.e. z_0 and U_I. Assuming clockwise orientation, the relationship between $\mathbf{F}$ outside of the disk and inside the disk is given by

$$\mathbf{F}_+ = \mathbf{P}\left(\dot{\mathbf{P}}^{\text{out}}\right)^{-1} = \mathbf{P}\left(\dot{\mathbf{P}}^{\text{in}}\right)^{-1}\dot{\mathbf{P}}^{\text{in}}\left(\dot{\mathbf{P}}^{\text{out}}\right)^{-1} = \mathbf{F}_-\dot{\mathbf{P}}^{\text{in}}\left(\dot{\mathbf{P}}^{\text{out}}\right)^{-1}. \tag{6.18}$$

Therefore, the jump matrix along the circles are

$$\mathbf{V}_U = \dot{\mathbf{P}}^{\text{in}}\left(\dot{\mathbf{P}}^{\text{out}}\right)^{-1}. \tag{6.19}$$

By assumption , The center z_0 of disk U_I lies in the first quadrant, so U_1 is completely in the upper half plane. $\dot{\mathbf{P}}^{\text{in}}$ is the same as $\dot{\mathbf{O}}^{\text{in}}(z^2)$. From section 6.2, $\dot{\mathbf{O}}^{\text{in}}$ is necessarily in

the following form:

$$\dot{\mathbf{O}}^{\text{in}} = \mathbf{H}(w)\widetilde{\mathbf{T}}e^{\frac{i\Phi}{2\epsilon}\sigma_3} = \hat{\mathbf{G}}(w)\left(\mathbb{I} + \frac{1}{\zeta(w)}\begin{bmatrix} -\frac{T_{2,12}}{H} & O(1) \\ \frac{1}{H} & \frac{T_{2,12}}{H}\end{bmatrix} + \mathcal{O}(\zeta^{-2})\right)\zeta(w)^{\frac{3}{4}\sigma_3}\mathbf{M}^{-1}e^{\frac{i\Phi}{2\epsilon}\kappa\sigma_3}, \tag{6.20}$$

$\hat{\mathbf{G}}(w)$ is a holomorphic function inside the disk. Restricting our attention to a neighbourhood of size $\mathcal{O}\left(\epsilon^{\frac{1}{5}}\right)$ near the pole.

In the upper-half plane, $\dot{\mathbf{P}}^{\text{in}}$ is obtained simply by replacing w by z^2.

$$\dot{\mathbf{P}}^{\text{in}} = \hat{\mathbf{G}}(w)\left(\mathbb{I} + \frac{1}{\zeta(w)}\begin{bmatrix} -\frac{T_{2,12}}{H} & O(1) \\ \frac{1}{H} & \frac{T_{2,12}}{H}\end{bmatrix} + \mathcal{O}(\zeta^{-2})\right)\zeta(w)^{\frac{3}{4}\sigma_3}\mathbf{M}^{-1}e^{\frac{i\Phi}{2\epsilon}\kappa\sigma_3}, \tag{6.21}$$

here all w should be seen as z^2.

Suppose that $\frac{1}{H}$ is bounded, by (6.19),

$$\begin{aligned}\mathbf{V}_{U_I} =& \hat{\mathbf{G}}(w)\left(\mathbb{I} + \frac{1}{\zeta(w)}\begin{bmatrix} -\frac{T_{2,12}}{H} & O(1) \\ \frac{1}{H} & \frac{T_{2,12}}{H}\end{bmatrix} + \mathcal{O}(\zeta^{-2})\right)\zeta(w)^{\frac{3}{4}\sigma_3}\mathbf{M}^{-1}e^{\frac{i\Phi}{2\epsilon}\kappa\sigma_3}\left(\dot{\mathbf{P}}^{\text{out}}\right)^{-1} \\ =& \hat{\mathbf{G}}(w)\left(\mathbb{I} + \frac{\epsilon^{\frac{2}{5}}}{W(w)}\begin{bmatrix} -\frac{T_{2,12}}{H} & O(1) \\ \frac{1}{H} & \frac{T_{2,12}}{H}\end{bmatrix} + \mathcal{O}(\epsilon^{\frac{4}{5}})\right)\epsilon^{\frac{1}{10}\sigma_3}W(w)^{\sigma_3}W(w)^{-\frac{1}{4}\sigma_3}\mathbf{M}^{-1}e^{i\nu\sigma_3}\left(\dot{\mathbf{O}}^{\text{out}}\right)^{-1},\end{aligned} \tag{6.22}$$

We have seen in (5.95) $\mathbf{C} = \dot{\mathbf{O}}^{\text{out}}e^{-i\kappa\sigma_3}\mathbf{M}W(w)^{\frac{1}{4}\sigma_3}$ is analytic inside the disk. In the last equation, notice the last factors are nothing but $\mathbf{C}^{-1}$. Because we are looking for a jump that is close to identity, we put the inverse of these factors along with the $\epsilon^{\frac{1}{10}\sigma_3}$ in $\hat{\mathbf{G}}$

$$\hat{\mathbf{G}}(w) = \mathbf{G}^{\text{in}}(z)\mathbf{C}(w)\epsilon^{-\frac{1}{10}\sigma_3}. \tag{6.23}$$

Here the notation $\mathbf{G}^{\text{in}}$ means the function is only defined inside the disk.

Thus, the jump becomes

$$\mathbf{V}_{U_I} = \mathbf{G}\mathbf{C}\left(W(w)^{\sigma_3} + \epsilon^{-\frac{1}{5}}\begin{bmatrix} 0 & 0 \\ \frac{1}{H} & 0\end{bmatrix} + \frac{\epsilon^{\frac{1}{5}}}{W(w)}\begin{bmatrix} 0 & 0 \\ \mathcal{O}(1) & 0\end{bmatrix} + \mathcal{O}(\epsilon^{\frac{2}{5}})\right)\mathbf{C}^{-1}. \tag{6.24}$$

It is clear that this cannot be a small-norm problem, because of the negative power in $\epsilon^{-\frac{1}{5}}$. We have to modify the outer parametrix, too.

6.3.2 Riemann–Hilbert problem for $\mathbf{G}$

Suppose the new outer parametrix is

$$\widetilde{\mathbf{P}}^{\text{out}}(z) = \mathbf{G}^{\text{out}}(z)\dot{\mathbf{P}}^{\text{out}}(z). \tag{6.25}$$

And define

$$\mathbf{G}(z) = \begin{cases} \mathbf{G}^{\text{in}}, & z \in U_{I,II,III,IV}, \\ \mathbf{G}^{\text{out}}, & \text{otherwise.} \end{cases} \tag{6.26}$$

Furthermore, assume that $\mathbf{G}$ solves a Riemann–Hilbert problem with jump on the boundaries on the disks,

$$\mathbf{G}_+ = \mathbf{G}_-\mathbf{C}\left(W(w)^{\sigma_3} + \epsilon^{-\frac{1}{5}}\begin{bmatrix} 0 & 0 \\ \frac{1}{H} & 0 \end{bmatrix})\right)\mathbf{C}^{-1}. \tag{6.27}$$

Then the new jump for the error matrix in the first quadrant becomes

$$\begin{aligned} \mathbf{V}_{U_I} =& \mathbf{G}^{\text{in}}\mathbf{C}\left(W(w)^{\sigma_3} + \epsilon^{-\frac{1}{5}}\begin{bmatrix} 0 & 0 \\ \frac{1}{H} & 0 \end{bmatrix} + \frac{\epsilon^{\frac{1}{5}}}{W(w)}\begin{bmatrix} 0 & 0 \\ \mathcal{O}(1) & 0 \end{bmatrix} + \mathcal{O}(\epsilon^{\frac{2}{5}})\right)\mathbf{C}^{-1}\left(\mathbf{G}^{\text{out}}\right)^{-1} \\ =& \mathbf{G}^{\text{in}}\mathbf{C}\left(W(w)^{\sigma_3} + \epsilon^{-\frac{1}{5}}\begin{bmatrix} 0 & 0 \\ \frac{1}{H} & 0 \end{bmatrix} + \frac{\epsilon^{\frac{1}{5}}}{W(w)}\begin{bmatrix} 0 & 0 \\ \mathcal{O}(1) & 0 \end{bmatrix} + \mathcal{O}(\epsilon^{\frac{2}{5}})\right)\mathbf{C}^{-1}\mathbf{V}_G^{-1}\left(\mathbf{G}^{\text{in}}\right)^{-1} \\ =& \mathbf{G}^{\text{in}}\mathbf{C}\left(W(w)^{\sigma_3} + \epsilon^{-\frac{1}{5}}\begin{bmatrix} 0 & 0 \\ \frac{1}{H} & 0 \end{bmatrix} + \frac{\epsilon^{\frac{1}{5}}}{W(w)}\begin{bmatrix} 0 & 0 \\ \mathcal{O}(1) & 0 \end{bmatrix} + \mathcal{O}(\epsilon^{\frac{2}{5}})\right) \\ & \left(W(w)^{-\sigma_3} - \epsilon^{-\frac{1}{5}}\begin{bmatrix} 0 & 0 \\ \frac{1}{H} & 0 \end{bmatrix}\right)\mathbf{C}^{-1}\mathbf{G}^{\text{in}} \\ =& \mathbf{G}^{\text{in}}\mathbf{C}\left(\mathbb{I} + \mathcal{O}(\epsilon^{\frac{1}{5}}\right)\mathbf{C}^{-1}\mathbf{G}^{\text{in}}. \end{aligned} \tag{6.28}$$

Since $\mathbf{G}^{\text{in}}$ is analytic in the disk and since $\det(\mathbf{G}^{\text{in}}) = 1$, this is indeed a small-norm problem. We conclude that we can use the new parametrix $\widetilde{\mathbf{P}}$ to approximate $\mathbf{P}$ and hence $\mathbf{O}$.

6.3.3 Scaling near the poles

Before we go on to prove the existence of such a $\mathbf{G}$, let's first look at in what neighbourhood can we use this modification of the outer parametrix. The scaling assumption we used is that $\epsilon^{-\frac{1}{5}}\frac{1}{H}$ is bounded. The expansion of H tells us that, if ν_0 is a pole of the tritronquée solution

which we used in the tritronquée parametrix, then near this pole, $\epsilon^{-\frac{1}{5}}\frac{1}{H}$ has expansion

$$\epsilon^{-\frac{1}{5}}\frac{1}{H} \sim \epsilon^{-\frac{1}{5}}(\nu - \nu_0) = \epsilon^{-1}(s - s_0). \tag{6.29}$$

Since s_x and s_t are finite and nonzero, the modified outer parametrix will give a good approximation in a neighbourhood of size $\mathcal{O}(\epsilon)$. This implies the local structures we are going to describe in more detail next will have size $\mathcal{O}(\epsilon)$.

6.3.4 Riemann–Hilbert problem for $\mathbf{G}$

Therefore, finding the leading approximation of the local structures (rogue wave like) near the poles of the Painlevé-I equation boils down to whether we can solve the Riemann–Hilbert problem for $\mathbf{G}$, where the jump contour is the four circles clockwise, the same as in figure 6.1. The jump condition is

Riemann-Hilbert Problem 3

$$\mathbf{G}_+ = \mathbf{G}_-\mathbf{V}_\mathbf{G}, \qquad z \in \partial U_{I,II,III,IV}, \tag{6.30}$$

and $\lim_{z\to\infty} \mathbf{G} = \mathbb{I}$.

$\mathbf{G}$ and the jump matrices $\mathbf{V}_G$ have the same symmetry we established in the section 5.3.2. In the first quadrant, $\mathbf{V}_G$ is given by

$$\mathbf{V}_{\mathbf{G}_I} = \mathbf{C}(z^2)\left(W(z^2)^{\sigma_3} + \epsilon^{-\frac{1}{5}}\begin{bmatrix} 0 & 0 \\ \frac{1}{H} & 0 \end{bmatrix}\right)\mathbf{C}^{-1} \tag{6.31}$$

while the other three quadrants can be determined by the symmetry of $\mathbf{G}$.

6.3.5 Fredholm theory, vanishing lemma and the existence of the solution to Riemann–Hilbert problem 3

From [41], we know that suppose in a Riemann–Hilbert problem the jump matrix on the jump contour Σ is Hölder continuous with Hölder exponent μ, then the RHP is equivalent to solving the singular integral equation:

$$(\mathcal{I} - C_\mathbf{W})\mathbf{X} = \mathbb{I} \in H^\nu(\Sigma) \tag{6.32}$$

where $\nu \leq \mu$.

Definition 6.3.1. A bounded linear operator $\mathcal{A} : B \to B$ on a Banach space B is a **Fredholm operator** if the dimension of both the kernel and cokernel of $\mathcal{A}$, $\dim(\ker(\mathcal{A}))$ and $\dim(\text{coker}(\mathcal{A}))$ are finite. The Fredholm index of $\mathcal{A}$ is $\text{ind}(\mathcal{A}) := \dim(\ker(\mathcal{A})) - \dim(\text{coker}(\mathcal{A}))$.

It can be easily shown that $\mathcal{I} - C_{\mathbf{W}}$ is a Fredholm operator on $H^{\nu}(\Sigma)$. The reader may find details in [14]. Furthermore, Zhou's Index Theorem [48] indicates that $\text{ind}(\mathcal{I} - C_{\mathbf{W}}) = 0$. Therefore, as long as we can show the RHP does not have a nontrivial kernel, we automatically show that the RHP has a solution.

To show the RHP does not have a nontrivial kernel, we use Zhou's vanishing lemma [48].

Lemma 6.3.1. (Zhou's vanishing lemma)*: Let Σ be a complete contour in the z-plane that is Schwarz-symmetric (invariant under reflection through the real axis, including orientation). Let $\mathbf{V}$ be an admissible jump matrix on Σ that satisfies*

$$\mathbf{V}(z^*) = \mathbf{V}(z)^{\dagger}, \quad z \in \Sigma \backslash \mathbb{R}. \tag{6.33}$$

Then the only matrix function $\mathbf{M}_0$ analytic for $z \in \mathbb{C}\backslash\Sigma$ and continuous up to the boundary with $\mathbf{M}_{0+} = \mathbf{M}_{0-}\mathbf{V}$ for $z \in \Sigma^0$, and that satisfies $\mathbf{M}_0(z) = \mathcal{O}\left(z^{-(1+\epsilon)/2}\right)$ as $z \to \infty$ for any $\epsilon > 0$ is $\mathbf{M}_0(z) \equiv 0$.

We verifying the assymptions in the vanishing lemma. We have

$$\mathbf{V}_{\mathbf{G}} = \mathbf{G}_-^{-1}\mathbf{G}_+. \tag{6.34}$$

From the symmetry in section 5.3.2, in the lower half plane the jump matrix is related to its reflection in the upper half plane. Notice here we changed the orientation so the contour has Schwarz-symmetry (as in the vanishing lemma).

$$\begin{aligned} \mathbf{V}_{\mathbf{G}}(z^*) =& \mathbf{G}_-^{-1}(z^*)\mathbf{G}_+(z^*) = \left(\overline{\mathbf{G}_+(-z)}\right)^{-1} \overline{\mathbf{G}_-(-z)} = \sigma_2 \overline{(\mathbf{G}_+(z))^{-1}\, \mathbf{G}_-(z)} \sigma_2 \\ =& \sigma_2 \overline{\mathbf{V}_{\mathbf{G}}^{-1}} \sigma_2 = \mathbf{V}_{\mathbf{G}}^{\dagger}(z). \end{aligned} \tag{6.35}$$

The last equality uses $\det \mathbf{V} = 1$.

Therefore, the assumption of Zhou's Vanishing lemma is satisfied. Now we can show that the solution for Riemann–Hilbert Problem 3 exists.

Proof. By Zhou's vanishing lemma, the kernel of the equivalent operator for the RHP is 0. Since the operator is of Fredholm index 0, it is also surjective. Therefore a solution must exist. □

6.4 Shape of local structures, solution near the poles

6.4.1 Solving $\mathbf{G}$, shape of local structures

Take $\mathbf{F}$ outside the disk to be a rational function with only simple poles at the end of $\widetilde{\beta}$, i.e. z_0 and its symmetric points. Due to symmetry and normalization at infinity (5.88), $\mathbf{G}_+ = \mathbf{G}^{\text{out}}$ necessarily has the form

$$\mathbf{G}^{\text{out}} = \mathbb{I} + \frac{\mathbf{G}_0}{z - z_0} + \frac{\sigma_2 \mathbf{G}_0^* \sigma_2}{z - z_0^*} - \frac{\sigma_2 \mathbf{G}_0 \sigma_2}{z + z_0} - \frac{\mathbf{G}_0^*}{z + z_0^*} \tag{6.36}$$

While $\mathbf{G}_-$ is holomorphic inside the disk U_0. Using jump condition (6.31),

$$\mathbf{G}_- = \mathbf{G}_+ \mathbf{C} \left(W(z^2)^{-\sigma_3} - \epsilon^{-\frac{1}{5}} \begin{bmatrix} 0 & 0 \\ \frac{1}{H} & 0 \end{bmatrix} \right) \mathbf{C}^{-1} \tag{6.37}$$

has no pole at z_0.

Expanding $\mathbf{C}$ at w_0,

$$\mathbf{C}(w) = \mathbf{C}_0 + \mathbf{C}_1 (w - w_0) + \mathcal{O}((w - w_0)^2). \tag{6.38}$$

Since we are looking for the poles in z-plane, we will substitute z for w. Here because we are considering the pole at z_0 which is lying in the first quadrant, we can assume $w = z^2$.

$$\mathbf{C}(w) = \mathbf{C}_0 + 2 z_0 \mathbf{C}_1 (z - z_0) + \mathcal{O}((z - z_0)^2). \tag{6.39}$$

$\mathbf{G}^{\text{out}}$ has one simple pole at z_0, while $W(w)^{-\sigma_3}$ also has a simple pole. The coefficients of the double pole and the simple pole must be zero. In order to find the coefficients for $(z - z_0)^{-1}$, note that

$$W(w) = W'(w_0)(w - w_0) + \mathcal{O}((w - w_0)^2) = 2 z_0 W'(w_0)(z - z_0) + \mathcal{O}((z - z_0)^2) \tag{6.40}$$

So the expansion of $W(w)^{-1}$ is

$$\frac{1}{W(w)} = \frac{1}{W'(w_0)} \frac{1}{w - w_0} + \mathcal{O}(1) = \frac{1}{2 z_0 W'(w_0)} \frac{1}{z - z_0} + \mathcal{O}(1). \tag{6.41}$$

Now look at expansion of (6.37),

$$\mathbf{G}^{\text{in}} = \left(\frac{\mathbf{G}_0}{z-z_0} + \mathbb{I} + \frac{\sigma_2 \mathbf{G}_0^* \sigma_2}{z_0 - z_0^*} - \frac{\sigma_2 \mathbf{G}_0 \sigma_2}{2z_0} - \frac{\mathbf{G}_0^*}{z_0 + z_0^*} + \mathcal{O}(z-z_0) \right) \left(\mathbf{C}_0 + 2z_0 \mathbf{C}_1 (z-z_0) \right.$$
$$\left. + \mathcal{O}((z-z_0)^2) \right) \left(\frac{1}{z-z_0} \begin{bmatrix} \frac{1}{2z_0 W'(w_0)} & 0 \\ 0 & 0 \end{bmatrix} + \begin{bmatrix} \mathcal{O}(1) & 0 \\ 0 & 0 \end{bmatrix} - \epsilon^{-\frac{1}{5}} \begin{bmatrix} 0 & 0 \\ \frac{1}{H} & 0 \end{bmatrix} \right.$$
$$\left. + \mathcal{O}(z-z_0) \right) \left(\mathbf{C}_0^{-1} + \mathcal{O}(z-z_0) \right) \tag{6.42}$$

The coefficients of the poles must be 0, thus we obtain two equations, with (-2). double pole:

$$\frac{1}{(z-z_0)^2} \mathbf{G}_0 \mathbf{C}_0 \begin{bmatrix} \frac{1}{2z_0 W'(w_0)} & 0 \\ 0 & 0 \end{bmatrix} \mathbf{C}_0^{-1} = 0 \tag{6.43}$$

(-1). simple pole:

$$\begin{aligned} &\frac{1}{z-z_0} \left(\mathbf{G}_0 \mathbf{C}_0 \begin{bmatrix} \mathcal{O}(1) & 0 \\ -\epsilon^{\frac{1}{5}} \frac{1}{H} & 0 \end{bmatrix} + \mathbf{G}_0 \mathbf{C}_1 \begin{bmatrix} \frac{1}{W'(w_0)} & 0 \\ 0 & 0 \end{bmatrix} \right. \\ &\left. + \left(\mathbb{I} + \frac{\sigma_2 \mathbf{G}_0^* \sigma_2}{z_0 - z_0^*} - \frac{\sigma_2 \mathbf{G}_0 \sigma_2}{2z_0} - \frac{\mathbf{G}_0^*}{z_0 + z_0^*} \right) \mathbf{C}_0 \begin{bmatrix} \frac{1}{2z_0 W'(w_0)} & 0 \\ 0 & 0 \end{bmatrix} \right) \mathbf{C}_0^{-1} \\ &+ \frac{1}{(z-z_0)^2} \mathbf{G}_0 \mathbf{C}_0 \begin{bmatrix} \frac{1}{2z_0 W'(w_0)} & 0 \\ 0 & 0 \end{bmatrix} \mathcal{O}(z-z_0) = 0 \end{aligned} \tag{6.44}$$

Since $\det(\mathbf{C}) = 1$ for any z, we can deduce that $\det(\mathbf{C}_0) = 1$, too. Therefore, (6.43) is equivalent to

$$\mathbf{G}_0 \mathbf{C}_0 \begin{bmatrix} 1 \\ 0 \end{bmatrix} = 0 \tag{6.45}$$

Using this relation in equation (6.44) to eliminate the undetermined $\mathcal{O}(1)$ and $\mathcal{O}(z-z_0)$ terms. We get

$$\mathbf{G}_0 \mathbf{C}_0 \begin{bmatrix} 0 \\ -\epsilon^{\frac{1}{5}} \frac{1}{H} \end{bmatrix} + \mathbf{G}_0 \mathbf{C}_1 \begin{bmatrix} \frac{1}{W'(w_0)} \\ 0 \end{bmatrix} + \left(\mathbb{I} + \frac{\sigma_2 \mathbf{G}_0^* \sigma_2}{z_0 - z_0^*} - \frac{\sigma_2 \mathbf{G}_0 \sigma_2}{2z_0} - \frac{\mathbf{G}_0^*}{z_0 + z_0^*} \right) \mathbf{C}_0 \begin{bmatrix} \frac{1}{2z_0 W'(w_0)} \\ 0 \end{bmatrix} = 0. \tag{6.46}$$

Denote

$$\mathbf{C}_0 = \begin{bmatrix} C_{0,11} & C_{0,12} \\ C_{0,21} & C_{0,22} \end{bmatrix}, \qquad \mathbf{C}_0 = \begin{bmatrix} C_{1,11} & * \\ C_{1,21} & * \end{bmatrix}. \tag{6.47}$$

The relation (6.45) tells us that $\mathbf{G}_0$ is of rank 1, and we can simplify the expression as two unknown variables

$$\mathbf{G}_0 = \begin{bmatrix} a \\ b \end{bmatrix} \begin{bmatrix} C_{0,21} & -C_{0,11} \end{bmatrix} \tag{6.48}$$

Rearranging terms in equation (6.46),

$$\begin{aligned}
\mathbf{G}_0\mathbf{C}_0 \begin{bmatrix} 0 \\ -\epsilon^{\frac{1}{5}}\frac{1}{H} \end{bmatrix} =& -\epsilon^{\frac{1}{5}}\frac{1}{H}\begin{bmatrix} a \\ b \end{bmatrix}(C_{0,21}C_{0,12} - C_{0,11}C_{0,22}) = -\epsilon^{\frac{1}{5}}\frac{1}{H}\begin{bmatrix} a \\ b \end{bmatrix}(-\det(\mathbf{C}_0)) \\
=& \epsilon^{\frac{1}{5}}\frac{1}{H}\begin{bmatrix} a \\ b \end{bmatrix}, \\
\mathbf{G}_0\mathbf{C}_1 \begin{bmatrix} \frac{1}{W'(w_0)} \\ 0 \end{bmatrix} =& \frac{C_{0,21}C_{1,11} - C_{0,11}C_{1,21}}{W'(w_0)}\begin{bmatrix} a \\ b \end{bmatrix},
\end{aligned}$$

and finally,

$$\begin{aligned}
\mathbf{G}_0 &= \begin{bmatrix} a \\ b \end{bmatrix}\begin{bmatrix} C_{0,21} & -C_{0,11} \end{bmatrix}, \qquad \sigma_2\mathbf{G}_0\sigma_2 = \begin{bmatrix} b \\ -a \end{bmatrix}\begin{bmatrix} C_{0,11} & C_{0,21} \end{bmatrix}, \\
\mathbf{G}_0^* &= \begin{bmatrix} a^* \\ b^* \end{bmatrix}\begin{bmatrix} C_{0,21}^* & -C_{0,11}^* \end{bmatrix}, \qquad \sigma_2\mathbf{G}_0^*\sigma_2 = \begin{bmatrix} b^* \\ -a^* \end{bmatrix}\begin{bmatrix} C_{0,11}^* & C_{0,21}^* \end{bmatrix},
\end{aligned}$$

so

$$\begin{aligned}
&\left(\mathbb{I} + \frac{\sigma_2\mathbf{G}_0^*\sigma_2}{z_0 - z_0^*} - \frac{\sigma_2\mathbf{G}_0\sigma_2}{2z_0} - \frac{\mathbf{G}_0^*}{z_0 + z_0^*}\right)\mathbf{C}_0\begin{bmatrix} \frac{1}{2z_0W'(w_0)} \\ 0 \end{bmatrix} = \frac{1}{2z_0W'(w_0)}\left(\begin{bmatrix} C_{0,11} \\ C_{0,21} \end{bmatrix}\right. \\
&\left. + \frac{1}{z_0 - z_0^*}\begin{bmatrix} b^* \\ -a^* \end{bmatrix}(|C_{0,11}|^2 + |C_{0,21}|^2) - \frac{1}{2z_0}\begin{bmatrix} b \\ -a \end{bmatrix}(C_{0,11}^2 + C_{0,21}^2) - \frac{1}{z_0 + z_0^*}\begin{bmatrix} a^* \\ b^* \end{bmatrix}(C_{0,11}C_{0,21}^* - C_{0,11}^*C_{0,21})\right).
\end{aligned}$$

Assembling the equations together, and plug them into (6.46), the linear system for unknowns a and b is the following

$$\begin{aligned}
0 =& \epsilon^{-\frac{1}{5}}\frac{1}{H}\begin{bmatrix} a \\ b \end{bmatrix} + \frac{C_{0,21}C_{1,11} - C_{0,11}C_{1,21}}{W'(w_0)}\begin{bmatrix} a \\ b \end{bmatrix} + \frac{1}{2z_0W'(w_0)}\begin{bmatrix} C_{0,11} \\ C_{0,21} \end{bmatrix} \\
&+ \frac{1}{2z_0W'(w_0)}\frac{1}{z_0 - z_0^*}\begin{bmatrix} b^* \\ -a^* \end{bmatrix}(|C_{0,11}|^2 + |C_{0,21}|^2) - \frac{1}{2z_0W'(w_0)}\frac{1}{2z_0}\begin{bmatrix} b \\ -a \end{bmatrix}(C_{0,11}^2 + C_{0,21}^2) \\
&- \frac{1}{2z_0W'(w_0)}\frac{1}{z_0 + z_0^*}\begin{bmatrix} a^* \\ b^* \end{bmatrix}(C_{0,11}C_{0,21}^* - C_{0,11}^*C_{0,21}).
\end{aligned} \tag{6.49}$$

Notice that both a, b and their complex conjugates shows up in this system so there are actually 4 independent variables. We can take the complex conjugate of equation (6.49) to arrive at a 4×4 linear system,

$$\begin{aligned}
&\left(\epsilon^{-\frac{1}{5}}\frac{1}{H}+\frac{C_{0,21}C_{1,11}-C_{0,11}C_{1,21}}{W'(w_0)}\right)a-\frac{C_{0,11}^2+C_{0,21}^2}{2z_0W'(w_0)}b\\
&\quad-\frac{C_{0,11}C_{0,21}^*-C_{0,11}^*C_{0,21}}{2z_0W'(w_0)(z_0+z_0^*)}a^*+\frac{|C_{0,11}|^2+|C_{0,21}|^2}{2z_0W'(w_0)(z_0-z_0^*)}b^*=-\frac{1}{2z_0W'(w_0)}C_{0,11}\\
&\frac{C_{0,11}^2+C_{0,21}^2}{2z_0W'(w_0)}a+\left(\epsilon^{-\frac{1}{5}}\frac{1}{H}+\frac{C_{0,21}C_{1,11}-C_{0,11}C_{1,21}}{W'(w_0)}\right)b\\
&\quad-\frac{|C_{0,11}|^2+|C_{0,21}|^2}{2z_0W'(w_0)(z_0-z_0^*)}a^*-\frac{C_{0,11}C_{0,21}^*-C_{0,11}^*C_{0,21}}{2z_0W'(w_0)(z_0+z_0^*)}b^*=-\frac{1}{2z_0W'(w_0)}C_{0,21}\\
&\quad\frac{C_{0,11}C_{0,21}^*-C_{0,11}^*C_{0,21}}{2z_0^*W'(w_0)^*(z_0+z_0^*)}a-\frac{|C_{0,11}|^2+|C_{0,21}|^2}{2z_0^*W'(w_0)^*(z_0-z_0^*)}b\\
&\left(\epsilon^{-\frac{1}{5}}\frac{1}{H^*}+\frac{C_{0,21}^*C_{1,11}^*-C_{0,11}^*C_{1,21}^*}{W'(w_0)^*}\right)a^*-\frac{{C_{0,11}^*}^2+{C_{0,21}^*}^2}{2z_0^*W'(w_0)^*}b^*=-\frac{1}{2z_0^*W'(w_0)^*}C_{0,11}^*\\
&\quad\frac{|C_{0,11}|^2+|C_{0,21}|^2}{2z_0^*W'(w_0)^*(z_0-z_0^*)}a+\frac{C_{0,11}C_{0,21}^*-C_{0,11}^*C_{0,21}}{2z_0^*W'(w_0)^*(z_0+z_0^*)}b\\
&\frac{{C_{0,11}^*}^2+{C_{0,21}^*}^2}{2z_0^*W'(w_0)^*}a^*+\left(\epsilon^{-\frac{1}{5}}\frac{1}{H^*}+\frac{C_{0,21}^*C_{1,11}^*-C_{0,11}^*C_{1,21}^*}{W'(w_0)^*}\right)b^*=-\frac{1}{2z_0^*W'(w_0)^*}C_{0,21}^*
\end{aligned}\tag{6.50}$$

While it is not immediately clear that this linear system has to be solvable, we have shown that the underlying RHP where the linear equations arise from must have a solution. Therefore, we have shown that (6.50) must be solvable. By a similar argument in Chapter 5, even though this system is evaluating at $w_0(x,t)$ near $w_0(x_{\rm gc},t_{\rm gc})$, expanding w_0 at $(x_{\rm gc},t_{\rm gc})$ will produce an error that is smaller than $\epsilon^{\frac{1}{5}}$. Thus, for our purpose, evaluating the system (6.50) at the gradient catastrophe point will not affect the leading asymptotics. That way the coefficients all become constants and the only (x,t) dependence comes in from $\epsilon^{-\frac{1}{5}}\frac{1}{H(\nu(x,t))}$.

Furthermore, to help the reader see the structure of (6.50), we rewrite the system in the following way:

$$\begin{bmatrix}
\epsilon^{-\frac{1}{5}}\frac{1}{H}+A & B & C & D\\
-B & \epsilon^{-\frac{1}{5}}\frac{1}{H}+A & -D & C\\
C^* & -D^* & \epsilon^{-\frac{1}{5}}\frac{1}{H^*}+A^* & B^*\\
D^* & C^* & -B^* & \epsilon^{-\frac{1}{5}}\frac{1}{H^*}+A^*
\end{bmatrix}\begin{bmatrix}a\\b\\a^*\\b^*\end{bmatrix}=\begin{bmatrix}E\\F\\E^*\\F^*\end{bmatrix}.\tag{6.51}$$

In this linear system, only H depends on (x,t), every other coefficient, A, B, C, D, E and

F are all constants, given by

$$\begin{aligned}
A =& \frac{C^{\rm gc}_{0,21}C^{\rm gc}_{1,11} - C^{\rm gc}_{0,11}C^{\rm gc}_{1,21}}{W'_{\rm gc}(w^{\rm gc}_0)},\\
B =& -\frac{(C^{\rm gc}_{0,11})2 + (C^{\rm gc}_{0,21})^2}{2z^{\rm gc}_0 W'_{\rm gc}(w^{\rm gc}_0)},\\
C =& -\frac{C^{\rm gc}_{0,11}C^{\rm gc}_{0,21}{}^* - C^{\rm gc}_{0,11}{}^* C^{\rm gc}_{0,21}}{2z^{\rm gc}_0 W'_{\rm gc}(w^{\rm gc}_0)(z^{\rm gc}_0 + z^{\rm gc*}_0)},\\
D =& \frac{|C^{\rm gc}_{0,11}|^2 + |C^{\rm gc}_{0,21}|^2}{2z^{\rm gc}_0 W'_{\rm gc}(w^{\rm gc}_0)(z^{\rm gc}_0 - z^{\rm gc*}_0)},\\
E =& -\frac{1}{2z^{\rm gc}_0 W'_{\rm gc}(w^{\rm gc}_0)} C^{\rm gc}_{0,11},\\
F =& -\frac{1}{2z^{\rm gc}_0 W'_{\rm gc}(w^{\rm gc}_0)} C^{\rm gc}_{0,21}.
\end{aligned} \tag{6.52}$$

By the way, we have already proved the second main theorem in the last page. I just don't know how to close.

Chapter 7

Conclusion

7.1 Future work

We list some possible ways to extend the research on universality of the semi-classical sine-Gordon equation:

7.1.1 Soliton solution to the sine-Gordon equation at poles of the tritronquée solution

In [8] Bertola and Tovbis found that the Peregrine Breather describes the spikes for NLS near the gradient catastrophe. Likewise, it is most probable that the local structures of the solution to (1.2) is described by a documented soliton solution of the sine-Gordon equation. Grava pointed to me that the breather solution of NLS appears in a certain limiting regime where the associated genus 2 Riemann surface degenerates into genus 0, as in [6]. More recently Liming Ling suggested the special solution for the sine-Gordon equation should arise similar to the treatment of NLS in [45, 44] following HJ Shin.

The **goals** of this project are:

- Better understand the local structures as a special solution of the sine-Gordon equation by finding/verifying how it will show up in a different setting;
- Build the special solution algebraically;
- Analysis by comparing the numerical solutions to (1.2) and the special solution to the sine-Gordon equation.

7.1.2 Universality of the asymptotic profile at the first breaking curve for the semi-classical sine-Gordon equation

After [17], in [18] Claeys and Grava studied the asymptotics of the KdV equation in the oscillatory zone near the leading edge. Or, in closer analogy to the case of semi-classical sine-Gordon equation, Bertola and Tovbis in [7] studied the universality near the first breaking curve in the focusing NLS equation. One can try to answer the same question for the sine-Gordon equation:

• What is the universal behaviour near the first breaking curve in the suitable double-scaling limit?

7.1.3 Breaking curves, asymmetrical initial data

It is known for the NLS equation that multiple breaking curves can exist beyond the first phase transition. They correspond to changes in the genus of the hyperelliptic Riemann surface whose theta functions are used to describe the solution. From numerical simulations in [12] it appears that the second breaking also exists for the above-threshold initial data case in the sine-Gordon equation, although we have no direct evidence that indicate the second breaking for below-threshold initial data.

In my thesis we are taking the initial data to be an even function, in which case the solution, hence the breaking curve, is also an even function.The g-function analysis will be more difficult but also more interesting if the initial data is not even. Furthermore, due to a symmetry in the RHP that only exists for even initial data, the breaking curve, at least near small $|x|$, can be expressed as a simple integral function determined by the initial data.

Goals:

- Finding numerical evidence for whether there exist multiple breaking curves;
- Using Riemann-Hilbert analysis and other theoretical tools to study the breakings if they exist;
- Describe breaking behaviours for asymmetrical initial data;
- Analyze the universality for asymmetrical initial data .

Bibliography

[1] M. Ablowitz and H. Segur. *Solitons and the Inverse Scattering Transform*. Society for Industrial and Applied Mathematics, Philadelphia, Pensilvania, 1981.

[2] M. J. Ablowitz, D. J. Kaup, A. C. Newell, and H. Segur. Nonlinear-evolution equations of physical significance. *Physcal Review Letters*, 31:125–127, Jul 1973.

[3] J. Baik, T. Kriecherbauer, K. T.-R. McLaughlin, and P. D. Miller. *Discrete Orthogonal Polynomials: Asymptotics and Applications*, volume 164 of *Annals of Mathematics Studies*. Princeton University Press, Princeton, New Jersey, 2007.

[4] A. Barone, F. Esposito, C. J. Magee, and A. C. Scott. Theory and applications of the sine-Gordon equation. *La Rivista del Nuovo Cimento (1971-1977)*, 1(2):227–267, Apr 1971.

[5] R. Beals and R. R. Coifman. Scattering and inverse scattering for first order systems. *Communications on Pure and Applied Mathematics*, 37(1):39–90, 1984.

[6] M. Bertola and P. Giavedoni. A degeneration of two-phase solutions of the focusing nonlinear Schrödinger equation via Riemann-Hilbert problems. *Journal of Mathematical Physics*, 56(6):061507, 2015.

[7] M. Bertola and A. Tovbis. Universality in the profile of the semiclassical limit solutions to the focusing nonlinear Schrödinger equation at the first breaking curve. *International Mathematics Research Notices*, 2010(11):2119–2167, 2010.

[8] M. Bertola and A. Tovbis. Universality for the focusing nonlinear Schrödinger equation at the gradient catastrophe point: Rational breathers and poles of the tritronquée solution to Painlevé I. *Communications on Pure and Applied Mathematics*, 66(5):678–752, 2014.

[9] E. Bour. Théorie de la déformation des surfaces. *Journal de L'École Imperiale Polytechnique*, 22:1–148, 1862.

[10] R. Buckingham and P. D. Miller. Exact solutions of semiclassical non-characteristic Cauchy problems for the sine-Gordon equation. *Physica D: Nonlinear Phenomena*, 237:2296–2341, 9 2008.

[11] R. J. Buckingham, R. M. Jenkins, and P. D. Miller. Semiclassical soliton ensembles for the three-wave resonant interaction equations. *Communications in Mathematical Physics*, 354(3):1015–1100, Sep 2017.

[12] R. J. Buckingham and P. D. Miller. The sine-Gordon equation in the semiclassical limit: Critical behavior near a separatrix. *Journal d'Analyse Mathématique*, 118(2):397–492, Nov 2012.

[13] R. J. Buckingham and P. D. Miller. The sine-Gordon equation in the semiclassical limit: dynamics of fluxon condensates. *Memoirs of the AMS*, 225(1059):(i)–(v) and 1–136, 2013.

[14] R. J. Buckingham and P. D. Miller. Large-degree asymptotics of rational Painlevé-II functions: noncritical behaviour. *Nonlinearity*, 27(10):2489, 2014.

[15] R. J. Buckingham and P. D. Miller. Large-degree asymptotics of rational Painlevé-II functions: critical behaviour. *Nonlinearity*, 28(6):1539, 2015.

[16] C. Chester, B. Friedman, and F. Ursell. An extension of the method of steepest descents. *Mathematical Proceedings of the Cambridge Philosophical Society*, 53(3):599–611, 1957.

[17] T. Claeys and T. Grava. Universality of the break-up profile for the KdV equation in the small dispersion limit using the Riemann-Hilbert approach. *Communications in Mathematical Physics*, 286(3):979, Nov 2008.

[18] T. Claeys and T. Grava. Painlevé II asymptotics near the leading edge of the oscillatory zone for the Korteweg–de Vries equation in the small dispersion limit. *Communications on Pure and Applied Mathematics*, 63(2):203–232, 2010.

[19] S. Coleman. Quantum sine-Gordon equation as the massive Thirring model. *Physical Review D*, 11:2088–2097, Apr 1975.

[20] O. Costin, M. Huang, and S. Tanveer. Proof of the Dubrovin conjecture and analysis of the tritronquée solutions of P_I. *Duke Mathematical Journal*, 163(4):665–704, 03 2014.

[21] J. Cuevas-Maraver, P. Kevrekidis, and F. Williams, editors. *The Sine-Gordon Model and Its Applications*, volume 10 of *Nonlinear Systems and Complexity*. Springer International Publishing, Cham, Germany, 2014.

[22] P. Deift and X. Zhou. A steepest descent method for oscillatory Riemann–Hilbert problems. Asymptotics for the MKdV equation. *Annals of Mathematics*, 137(2):295–368, 1993.

[23] P. A. Deift and X. Zhou. Asymptotics for the Painlevé II equation. *Communications on Pure and Applied Mathematics*, 48(3):277–337, 1995.

[24] *NIST Digital Library of Mathematical Functions*. http://dlmf.nist.gov/, Release 1.0.19 of 2018-06-22. F. W. J. Olver, A. B. Olde Daalhuis, D. W. Lozier, B. I. Schneider, R. F. Boisvert, C. W. Clark, B. R. Miller and B. V. Saunders, eds.

[25] B. Dubrovin. On Hamiltonian perturbations of hyperbolic systems of conservation laws, II: Universality of critical behaviour. *Communications in Mathematical Physics*, 267(1):117–139, Oct 2006.

[26] B. Dubrovin, T. Grava, and C. Klein. On universality of critical behavior in the focusing nonlinear Schrödinger equation, elliptic umbilic catastrophe and the tritronquée solution to the Painlevé-I equation. *Journal of Nonlinear Science*, 19(1):57–94, Feb 2009.

[27] B. Dubrovin, T. Grava, C. Klein, and A. Moro. On critical behaviour in systems of Hamiltonian partial differential equations. *Journal of Nonlinear Science*, 25(3):631–707, 2015.

[28] B. A. Dubrovin. Theta functions and non-linear equations. *Russian Mathematical Surveys*, 36(2(218)):11–92, 1982.

[29] L. D. Faddeev, L. A. Takhtajan, and V. E. Zakharov. Complete description of solutions of the sine-Gordon equation. *Doklady Akademii Nauk Series Fiziki*, 219:1334–1337, 1974. [Sov. Phys. Dokl.19,824(1975)].

[30] A. S. Fokas, A. R. Its, A. A. Kapaev, and V. Y. Novokshenov. *Painlevé Transcendents: The Riemann–Hilbert Approach*, volume 128 of *Mathematical Surveys and Monographs*. American Mathematics Society, Providence, Rhode Island, 2006.

[31] B. Fornberg and J. Weideman. A numerical methodology for the Painlevé equations. *Journal of Computational Physics*, 230(15):5957 – 5973, 2011.

[32] J. Frenkel and T. Kontorova. On the theory of plastic deformation and twinning. *Journal of Physics USSR*, l:137, 1939.

[33] S. Kamvissis, K. McLaughlin, and P. Miller. *Semiclassical Soliton Ensembles for the Focusing Nonlinear Schrödinger Equation*, volume 154 of *Annals of Mathematics Studies*. Princeton University Press, Princeton, New Jersey, 2003.

[34] A. A. Kapaev. Quasi-linear Stokes phenomenon for the Painlevé first equation. *Journal of Physics A: Mathematical and General*, 37(46):11149, 2004.

[35] D. J. Kaup. Method for solving the sine-Gordon equation in laboratory coordinates. *Studies in Applied Mathematics*, 54(2):165–179, June 1975.

[36] M. Klaus and J. K. Shaw. Purely imaginary eigenvalues of Zakharov-Shabat systems. *Physical Review E*, 65, February 2002.

[37] P. D. Lax and C. D. Levermore. The small dispersion limit for the Korteweg-de Vries equation. I., II., III. *Communications on Pure and Applied Mathematics*, 36:253–290, 571–593, 809–829, 1983.

[38] G. D. Lyng and P. D. Miller. The n-soliton of the focusing nonlinear Schrödinger equation for n large. *Communications on Pure and Applied Mathematics*, (7):951–1026, 2007.

[39] P. D. Miller and Z. Xu. On the zero-dispersion limit of the Benjamin-Ono Cauchy problem for positive initial data. *Communication on Pure and Applied Mathematics*, 64:205–270, 2011.

[40] P. D. Miller and Z. Xu. The Benjamin-Ono hierarchy with asymptotically reflectionless initial data in the zero-dispersion limit. *Communication in Mathematical Sciences*, 10:117–130, 2012.

[41] N. Muskhelishvili. *Singular Integral Equations*. Dover Publications, New York, translated from the second (1946) Russian edition. corrected reprint of the 1953 English translation edition, 1992.

[42] J. Satsuma and N. Yajima. Initial value problems of one-dimensional self-modulation of nonlinear waves in dispersive media. *Progress of Theoretical Physics Supplement*, 55:284–306, 1974.

[43] A. C. Scott, F. Y. F. Chu, and S. A. Reible. Magnetic-flux propagation on a Josephson transmission line. *Journal of Applied Physics*, 47(7):3272–3286, 1976.

[44] H. J. Shin. Soliton dynamics in phase-modulated lattices. *Journal of Physics A: Mathematical and Theoretical*, 45(25):255206, 2012.

[45] H. J. Shin. Deformation of a Peregrine soliton by fluctuating backgrounds. *Physical Review E*, 88:032919, Sep 2013.

[46] G. B. Whitham. *Linear and Nonlinear Waves*. John Wiley & Sons, Inc., New York, 1999.

[47] L. V. Yakushevich. *Nonlinear Physics of DNA, Second Edition*. Wiley-VCH Verlag GmbH & Co. KGaA, Weinheim, June 2005.

[48] X. Zhou. The Riemann–Hilbert problem and inverse scattering. *SIAM Journal on Mathematical Analysis*, 20(4):966–986, 1989.